THESIS

Submitted to The University Louis Pasteur of Strasbourg
in fulfilment of the requirements for the degree of

DOCTOR of PHILOSOPHY

Discipline: chemical science

Christian TOCK

Towards dynamic multirotaxanes:

A nanopress to mimic the activity of molecular chaperones

Defended in public on October 5th, 2007, in front of the following jury:

Prof. Mir Wais HOSSEINI	President
Prof. Olivia REINAUD	External referee
Prof. Peter BELSER	External referee
Dr. Jean-Pierre SAUVAGE	Supervisor
Dr. Jean-Paul COLLIN	Supervisor

In collaboration with Dr. Julien Frey and Dr. Valérie Heitz

THESE

présentée pour obtenir le grade de

DOCTEUR DE L'UNIVERSITE LOUIS PASTEUR

DE STRASBOURG

par

Christian TOCK

Vers des multirotaxanes dynamiques:

Vers une nano-presse pour mimer les chaperons moléculaires

Soutenue publiquement le 5 octobre 2007 devant la commission d'examen :

Prof. Mir Wais HOSSEINI	Président du jury
Prof. Olivia REINAUD	Rapporteur
Prof. Peter BELSER	Rapporteur
Dr. Jean-Pierre SAUVAGE	Directeur de Thèse
Dr. Jean-Paul COLLIN	Directeur de Thèse

En collaboration avec Dr. Julien Frey et Dr. Valérie Heitz

Der Mima Elsi

Dem Georges B.

Remerciements
(Acknowledgements)

Abstract

The work presented in this thesis belongs to the field of chemical topology as well as nanotechnology, more precisely the domain of molecular machines. The project is based on the synthesis of 4,7-phenanthroline based bis-bipyridine ligands, used as bis-chelate ligands for two copper(I) metal centres. Major problems related to the very poor solubility of this compounds could be overcome by adding ethyl groups to the molecules.

These ligands were used as threads to assemble catenanes and rotaxanes in combination with bis-macrocycles, synthesised by Julien Frey and Valérie Heitz and which contain a 1,10-phenanthroline chelate in each ring. By taking advantage of the gathering and threading effect of copper(I), we obtained a [4]pseudorotaxane containing four copper(I) centres, two threads and two bis-macrocycles as proven by its crystal structure. The two threads were then functionalized with triethyleneglycol chains bearing an allyl group. After a similar threading reaction with two bis-macrocycles, the threads were linked by Ring Closing Metathesis with a first generation Grubbs catalyst, thus representing one huge macrocycle. The resulting [3]catenane was examined in its metallated and demetallated form. Unfortunately up to this date, it could not be obtained in an entirely pure form.

The bis-bipyridine thread was also used as an axle for a molecular press. It was threaded through two macrocylces, each one attached to a Zn(II)-porphyrin (Julien Frey, Valérie Heitz), using the copper(I) template effect. Bulky groups were then added to the endings of the axle by the "Meldal-Sharpless" click reaction. This stoppering leads to a [3]rotaxane (molecular press), that was studied in its metallated (contracted) form and in its demetallated (relaxed) situation, in which the macrocycles and hence the porphyrins are free to move on the axle. A 1,10-di-4-pyridyldecane guest molecule was synthesised and its interactions with the porphyrins of the [3]rotaxane host, metallated and demetallated, were studied in detail.

Different tridentate terpyridines were synthesised in order to be linked to the endings of the bis-bipyridine axle. This should allow us to move the macrocycles, hence the porphyrins, in a controlled manner from the inside of the axle to its outsides by taking advantage of the different coordination requirements of copper (Cu(I) tetracoordinated and Cu(II) pentacoordinated). Work on this more sophisticated molecular press is still underway.

Keywords

Contents

List of Figures

(Schemes, Tables and Figures)

Figure 1. The giant mining excavator, Bagger 288, built by Krupp.

Figure 2. Muslce myosin :a) catalytic core (blue), b) lever arm (yellow), c) thick filament, d) coiled coil, e) binding site (green), f) actin (thin filament)

Figure 3: Muscle myosin at work. The catalytic head binds to actin (2), releasing Pi, performing the resulting power stroke (3), before releasing ADP and binding ATP, and detaching from actin (4). Then the ATP hydrolysis provokes the backstroke and the head returns to the ADP-Pi bond state starting position (1). Scale bar: 60 Å.

Figure 4. Schematic drawing and structure of a complex between GroES (blue) and GroEL (green), including a cross-section through the GroEL part

Figure 5. The GroE chaperone cycle (D = ADP, T=ATP). Two cavities are involved in the process, but description will be limited to the bottom one (lilac) for clarity. During the first step, the hydrophilic protein enters the polar cavity of GroEL, such being prevented from aggregation. Binding of GroES and ATP (step 2) induces structural changes that will liberate the protein inside the cavity (red) where it starts to fold. The following hydrolyzes of the ATP triggers new conformational changes that will allow the second cavity (lilac) to bind a protein and start a new cycle. This second cavity will bind GroES and ATP (step2), this will detach GroES of the first cavity (orange) and liberate the folded protein so far trapped inside.

Figure 6. A type of a ratchet mechanism, able to transport a particle along a potential-energy surface. a) The particle is in equilibrium between the potential minima A and B, moving back and forth, powered by Brownian motion. Potential maximum C avoiding any further motion to potential minimum D. b) If the particle is in the potential minimum B, rising potential A and lowering potential C allows the trapping of the particle between B and C. No backwards motion to A is possible anymore. By continuous variation of the potential-energy surface, one can thus move the particle in a unidirectional way.

Figure 7: Representation of a a) catenane, b) rotaxane.

Figure 8. Schematic drawing of an elementary muscle unit.

Figure 9. Reversible chemically controlled motion between the extended and the contracted position.

Figure 10. Structural drawing of the rotaxane containing a $[Ru(bipy)_3]^{2+}$ station P^{2+}, a spacer **S**, 2 electron acceptor stations A_1^{2+} and A_2^{2+}, a bulky stopper **T** and an electron donor macrocycle **R**.

Figure 11. The light-powered nanomotor: A) photoexcitation of P^{2+}, followed by electron transfer to A_1^{2+}, B) shuttling of the macrocycle to A_2^{2+}, C) electron back transfer from A_1^+ to P^{3+}, and final D) reset to the starting situation by motion back to A_2^{2+} of the ring.

Figure 12. A DNA walker, based on a walking unit, a track with different docking stations,

Figure 13. Structure of the dynamic [3]rotaxane. TTF stations (green), NP stations (red), $CBPQT^{4+}$ rings (blue)

Figure 14. Bending and relaxing of a cantilever beam by oxidising and reducing a [3]rotaxane.

Scheme 2.9. By mixing the thread, the m-30, and copper(I) in a 1:2:2 ratio, the easily accessible and therefore kinetically stable grid (a) forms first. This situation is thermodynamically unstable because the remaining half of the copper(I) ions are coordinated to only one m-30 chelate (b), and half of the m-30 macrocycles are left uncoordinated (c). Due to the steric hindrance of the ring, two macrocycles can not coordinate the same copper ion, therefore the system will evolve to form the thermodynamically favoured [3]pseudorotaxane situation.

Scheme 2.10. Threading reaction with two m-30 macrocycles using the Cu(I) template effect.

Scheme 2.11. m-30 based bis-macrocycle, attached "back to back" with a pyrazine spacer.

Scheme 2.12. Quantitative synthesis of a [4]pseudorotaxane **12**.

Crystal structure 2.1. Crystal structure of [4]pseudorotaxane **12**. Hydrogen atoms are omitted for clarity.

Crystal Structure 2.2. *Zoom on one of the Cu(I) coordination spheres of compound 12*

Table 2.1. Geometrical features of the [4]pseudorotaxane **12**.

Table 2.2. ^{1}H-NMR data for the free ligands **9**, **11** and the pseudorotaxane **12** (spectrum shown).

Scheme 3.1. Synthesis of the iodo-thread **13.**

Scheme 3.2. Very poorly soluble phenol compound **14**.

Scheme 3.3. Synthesis of 2,5-diphenyl-4-trimathylsillyl-phenylboronic acid **18**.

Scheme 3.4. Synthesis of the thread core, containing ethyl solubilizing chains.

Scheme 3.5. Threading m-30 macrocycles on an ethyl group containing thread using the Cu(I) template effect.

Scheme 4.1. Topological isomers: trefoil knot enantiomers (left and middle) and torus right.

Scheme 4.2. 2D-drawings of topologically a) trivial torus and b) non-trivial trefoil knot.

Figure 4.1. Three topologically identical items, a stone with a hole (left), a doughnut (middle) and a coffee cup (right).

Scheme 4.3. (a) [4]pseudorotaxane, (b) [3]catenane formed by linking the threads together to form a macrocycle (red).

Scheme 4.4. Elongated thread **30**, able to undergo ring closing metathesis.

Scheme 4.5. Preparing the axle for further Suzuki coupling by changing the TMS to Iodine.

Scheme 4.6. Synthesis of 4-(tetrahydro-2H-pyran-2-yloxy)phenylboronic acid **23.**

Scheme 4.7. Synthesis of the thread **25**, able to undergo Williamson type reactions.

Scheme 4.8. Syntesis of the bromo-polyethylenglycol chain with an allyl ending **29**.

Scheme 4.9. Synthesis of the polyethyleneglycol thread **30** by a Williamson type reactions.

Scheme 4.10. [4]pseudorotaxane obtained form bis-macrocylces **11** and thread **30**.

Scheme 4.11. RCM reaction of compound **31** with 1st generation Grubbs catalyst to give **32**.

Nomenclature

ATP	-	Adenosine TriPhosphate
ADP	-	Adenosine DiPhosphate
δ	-	chemical shift (ppm)
Bipy	-	bipyridine
BuLi	-	n-buthyllithium
CBPQT	-	CycloBis(ParaQuat-para-phenylene)
CPK	-	Corey-Pauling-Koltun (models)
CV	-	CycloVoltammetry
D	-	Diffusion coefficient ($\mu m^2.s^{-1}$)
dabco	-	1,4-diazabicyclo[2.2.2]octane
DCM	-	dichloromethane
DMF	-	*N,N*-dimethylformamide
DNA	-	DeoxyriboNucleic Acid
dppf	-	dichloro[1,1'-bis(diphenylphosphino)ferrocene]
COSY	-	COrrelation SpectroscopY
DOSY	-	Diffusion-Ordered SpectroscopY
ε	-	Molar extinction coefficient ($L.mol^{-1}.cm^{-1}$)
ES-MS	-	ElectroSpray Mass Spectroscopy
HMBC	-	Heteronuclear Multiple Bond Correlation
HMQC	-	Heteronuclear Multiple Quantum Correlation
HR ES-MS	-	High resolution ES-MS
J	-	coupling constant (Hz)
LC	-	Liquid Crystals
λ	-	wavelength (nm)
MALDI	-	Matrix Assisted Laser Desorption Ionization
m/z	-	mass-to-charge ratio ($g.mol^{-1}.z^{-1}$)
MeCN	-	acetonitrile
MeOH	-	methanol
MLCT	-	Metal to Ligand Charge Transfer
NMR	-	Nuclear Magnetic Resonance (spectroscopy)
NOESY	-	Nuclear Overhauser Effect SpectroscopY
NP	-	NaPhtalene
Phen	-	phenanthroline
Pi	-	inorganic Phosphate
ppm	-	Parts Per Million
phen	-	1,10-phenanthroline or 4,7-phenanthroline
RCM	-	Ring Closing Metathesis (reaction)
ROESY	-	Rotating frame Overhause Effect SpectroscopY
SCE	-	Saturated Calomel electrode
terpy	-	2,2':6',2"-terpyridine
Terpy	-	Terpyridine
THF	-	TetraHydroFuran
THP	-	TetraHydroPyran
TLC	-	Thin Layer Chromatography
TMS	-	TriMethylSilyl
TOF	-	Time Of Flight
TTF	-	TetraThiaFulvalene

General Introduction

About nanoscale machines

I. Setting in motion.

About 5000 years ago, with the invention of wedges, wheels and levers, human mankind started to build machines. Devices designed to make everyday life easier and achieve tasks that were so far unthinkable. At first the driving force was only human or animal strength and the machines thus constrained in size and work capacity. The ingenuity of engineers all through human history, allowed the developing of first steam, then fossil-fueled or electric engines. These new power sources permitted the building of big and even bigger machines, such as the 45500 tons Bagger 288 (figure 1), built by Krupp in 1978, which is the biggest moving machine ever built[1].

Figure 1. The giant mining excavator, Bagger 288, built by Krupp[2]

It seems that there is no limit in size for even larger, more colossal mobile constructions, but what about the other end of the scale? In the last decades an enormous effort has been made to make devices, such as cell phones or computers, smaller and smaller. As basic pieces of equipment have to be reduced more and more in size, the top-down approach, consisting of scaling down classical transistors or other key parts, starts to reach its feasible limits. A solution might be the bottom-up approach which, instead of reducing existing systems in size, builds up new ones by starting from the elementary chemical brick, the atom, assembled to molecules, themselves put together as molecular machines. This domain of nanotechnology is still a very young, but fast growing field of research with a multitude of possible future applications. Nature, having chosen the bottom up approach since the beginning of life, and using very sophisticated molecular machines, is a strong source of inspiration and encouragement for molecular machinery engineers.

II. Natural molecular machines

II.1.Muscle fibers

Nature has a head start of millions of years as far as synthesizing molecular machines goes, hence its devices are of a much higher complexity then what synthetic chemists even dare to think of.
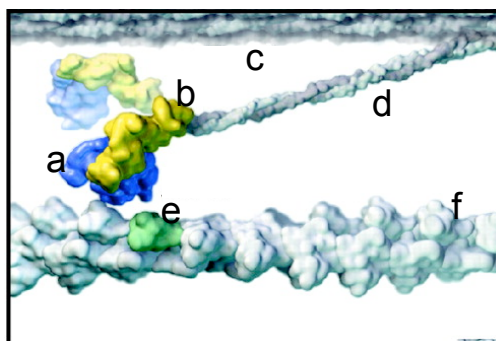
Figure 2. Muslce myosin :*a) catalytic core (blue), b) lever arm (yellow), c) thick filament, d) coiled coil, e) binding site (green), f) actin (thin filament)*

One example of such a machine working in our bodies is myosin, an actin-based motor, which is, among other tasks,[3] also responsible for muscle contraction. Muscle myosin is a dimer containing two identical heads, each composed of a catalytic core and a lever arm. These two entities are anchored to the thick filament by a coiled coil. The heads are in reach of the binding sites of the actin filament (figure 2).[4]

The two heads work independently, when ADP-Pi is bound to the catalytic core, one of them docks to the actin-binding site. This weak interaction causes the release of Pi (inorganic phosphate) from the active site (figure 3, frame 2), before the stroke of the lever arms results in a 100 Å move of actin, leading to the ADP bound state (figure 3, frame 3). The ADP then leaves the active site, and ATP binds to it (figure 3 frame 4), weakening the bond between head and actin, which finally causes the separation of the two units (figure 3, frame 1).
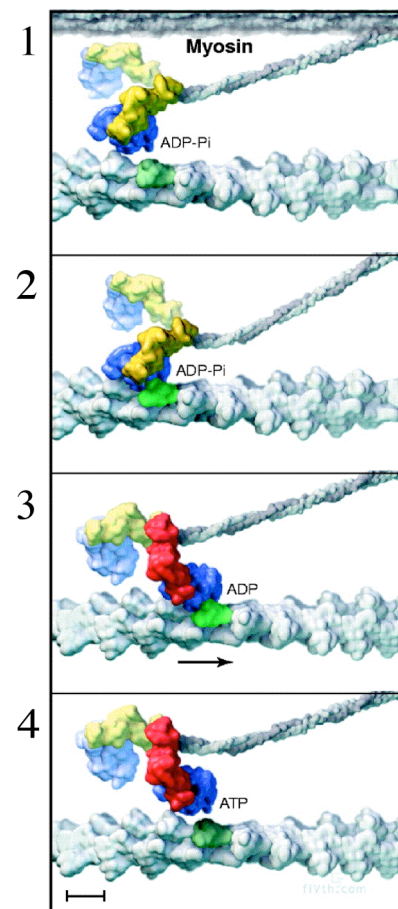
Figure 3:[4] *Muscle myosin at work. The catalytic head binds to actin (2), releasing Pi, performing the resulting power stroke (3), before releasing ADP and binding ATP, and detaching from actin (4). Then the ATP hydrolysis provokes the backstroke and the head returns to the ADP-Pi bond state starting position (1). Scale bar: 60 Å.*

The hydrolysis of ATP, yielding in ADP-Pi, allows the backstroke of the lever, thus returning to the initial state. Because the head unbinds from actin after one single stroke, it cannot move continuously along a track, in difference to kinesin,[4] which is able to perform long-range transport of proteins for example.

Obviously the contraction of an entire muscle cannot be achieved by a single stroke of a single head. Millions of these entities performing each one a little stroke in a disordered way, causes actin to move in one direction, "gliding" between the thick filaments, thus contracting the muscle. This system might be comparable to a large number of sailors pulling together on a rope. Even if at a given time, some don't participate at all, and even if their strokes are not simultaneous, the all over motion of the rope will be possible and unidirectional. One of Nature's ways to deal with the problem of imperfections, such as non-participating myosin heads, is to bundle a huge number of active sites together and thus compensating the defects.

II.2.Chaperones

Proteins need to adopt a unique three-dimensional structure to be able to function correctly in the cell. The information for the folding of the proteins is encoded in the protein itself, thus permitting their autonomous *in vitro* folding process, without any additional factors. Although this has been proven by Christian Anfinsen, which awarded him the Nobel prize in 1972,[5] *in vivo* conditions, such as dilution or pH, are different and the proteins need to be prevented from unfolding or aggregating. This task is carried out by the molecular chaperons which, like their human counterparts, avoid unwanted interactions between their immature clients.

The proteins are surrounded by a polar media, thus they tend to fold in a way to accumulate the hydrophobic amino acids close to their core, whereas the outer shell is mainly composed of hydrophilic groups. A polypeptide that is not, or only partially folded will still expose some of its hydrophobic parts on the outside. This characteristic is essential for the trapping mechanism by the chaperones. Indeed the chaperones contain a hydrophobic cavity, offering a "friendly" environment to the immature proteins, which will be isolated in this pocket and thus, prevented from any outside interaction, will fold to reach their functional tertiary structure. After this process totally or partially completed, the chaperon will release its guest and prepare for the next polypeptide. The whole process can be divided in three basic steps: capture, folding and release.

Part of the most studied molecular chaperones are the GroE proteins of the E.coli bacterium. This example, based on a very simplified mechanism, allows having a closer look on how these molecular machines work.[6]

The GroE chaperone is composed of the GroEL subunits, themselves devided into three subunits, and the GroES co-chaperones. The GroEL is basically shaped like an open barrel, separated in the middle into two cavities. The area close to the middle on each side is responsible for binding and hydrolyzing ATP, whereas the two cavities on the outside accommodate the proteins. The GroES co-chaperone can be viewed as a cover unit, used to close the "barrel" on each side (figure 4).
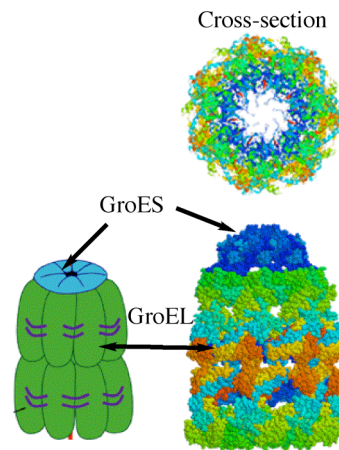
Figure 4.[7] *Schematic drawing and structure of a complex between GroES (blue) and GroEL (green), including a cross-section through the GroEL part.*

Each cavity of the chaperones is able to adapt to proteins of different size and shape because its own structure can be readily modified to optimize the binding surface for individual substrates. Once the polypeptide has entered the chaperone, the binding of ATP and the GroES subunit closes the cavity and leads to major structural changes in the GroEL particle. The hydrophobic inside of the cavity, to which the protein is bound, changes into a polar environment, thus setting the protein free inside its host. The capsule will also grow in size, allowing the protein to rearrange in order to reach its active conformation, a process that is encouraged by the hydrophilic environment. To be able to set the now correctly shaped molecule free, the strongly bound GroES moiety has to detach from the cavity. This should not happen to early nor to late, in order to avoid premature releasing of the protein and inefficient, excessively time-consuming working of the chaperone. To overcome this problem, nature has included a timer. The seven ATP molecules bound at the same time than the GroES entity are hydrolysed at a rate of 0.25-0.5 min^{-1}. This process induces a conformational change that increases the affinity of the second cavity (now also incorporating an immature protein) for ATP. The binding of ATP and a GroES unit to the second cavity,

inducing structural changes, release the GroES and the functional protein from the first cavity. The hole process is based on the two cavities, if one is binding GroES and ATP, the structural changes will release its protein inside the cavity and at the same time they will open the other side of the "barrel", releasing the protein (figure 5). The input of energy, produced by ATP hydrolyzes, is necessary to compensate the energy loss of the exergonic binding of the polypeptide, the ATP and the GroES moiety. Since the starting situation is identical to the end situation, there must be an energy input to be in agreement with the second law of thermodynamics.
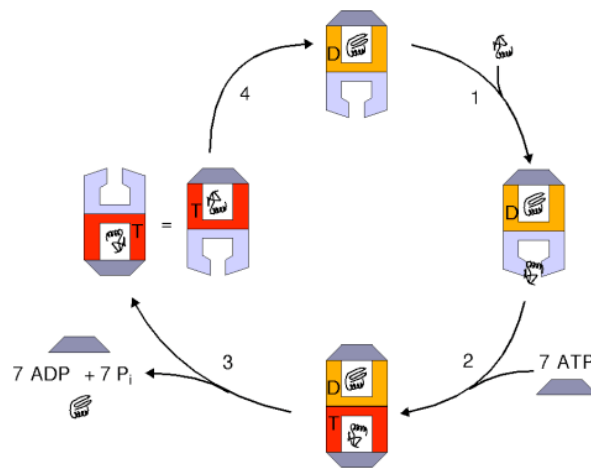
Figure 5.[6] *The GroE chaperone cycle (D = ADP, T=ATP). Two cavities are involved in the process, but description will be limited to the bottom one (lilac) for clarity. During the first step, the hydrophilic protein enters the polar cavity of GroEL, such being prevented from aggregation. Binding of GroES and ATP (step 2) induces structural changes that will liberate the protein inside the cavity (red) where it starts to fold. The following hydrolyzes of the ATP triggers new conformational changes that will allow the second cavity (lilac) to bind a protein and start a new cycle. This second cavity will bind GroES and ATP (step2), this will detach GroES of the first cavity (orange) and liberate the folded protein so far trapped inside.*

Natural selection has chosen to widely use molecular machines to perform tasks in living organisms, thus proving that they can be synthesized and that they are working effectively.

III. How to design machines the size of a molecule

III.1. General definition

The definition of the Oxford American dictionaries for machine is as follows:

machine
noun
an apparatus using or applying mechanical power and having several parts, each with a definite function and together performing a particular task[8]

Whereas in the macroscopic world, the definition of a machine does not leave a lot of space for subjective interpretation; there is no general consensus to define a molecular machine and what makes it different from any other molecular device. Initially molecules were compared to machines because their structure "looked" like pieces of machines, or because they carried out a task that would require a machine in the macroscopic world. Host-guest chemistry driven by external stimuli was often compared to pistons or other parts of machinery, even though their actual effects on their environment have little in common with those of their macroscopic counterparts. If we choose the word "machine" to qualify these molecules, there should be a strong similitude with the definition of our every day life machines, as there is a net task performed by a large amplitude, unidirectional, controlled mechanical motion of one component relative to another, triggered by an external stimuli.[9] Hence the challenge for scientists is to build molecules composed of different interconnected mobile parts and, even more important, to control their relative position and movement.

Before designing molecular machines, one has to consider that large machines and very small ones do not work under the same constrains. In the macroscopic sense,

machines are plunged into a vertical gravitational field that drives all motions towards the bottom, and inertia is a basic mechanical rule that machines are build to cope with. In the nanoscopic world, electromagnetic forces dominate over gravity and inertia is negligible compared to thermal agitation.

III.1.1 The Brownian motion

A particle, the size of a molecule, undergoes tempestuous bombardment from every side, like standing in the middle of a storm coming from each side with hundreds of huge hailstones striking every second.[10] In 1827, Robert Brown observed floating pollen grains moving as if alive[11] due to the thermal motion of the surrounding fluid molecules, which in his honor was named Brownian Motion. This phenomenon was explained in 1905 with Einstein's theory of "brownian motion",[12] proven experimentally by Jean-Baptiste Perrin[13] who won the Nobel prize in physics in 1926.

At equilibrium the effect of thermal motion is symmetric, even in an anisotropic medium. Single elementary motion units may occur pushing the molecule or one of its constituents either in one or in the other direction, but in average, they neutralize themselves and thus no unidirectional motion will occur. Compared to macroscopic machines, the problem we are facing in the nanoworld is not how to set molecular machines in motion, because they are moving already, but how to make them move into the right direction. Like natural molecular machines based on the brownian ratchet mechanism,[11] any molecular machine will have to face brownian motion, working against or with it.

Structural features alone such as breaking the symmetry of the molecule cannot induce motion in one preferential direction if only equilibrium fluctuations are at work.[14] Otherwise this device would constitute a Maxwell-demon[15] type perpetuum mobile, which is in contradiction to the second law of thermodynamics. This principal is illustrated by Feynman and his "ratchet and pawl" [16] as well as by Smoluchowski with a "trapdoor" system.[17]

To push molecules into the right direction, the system has to be driven away from its equilibrium, by changing the potential-energy surface using an external trigger. (figure 6).
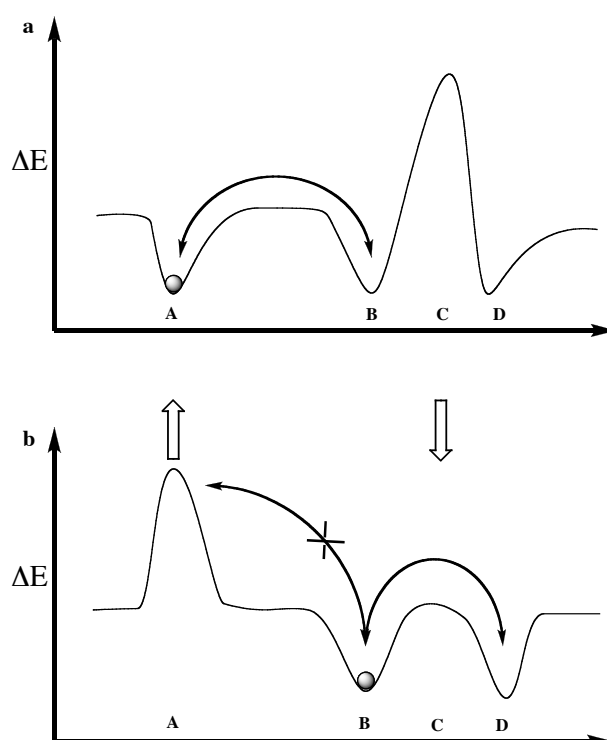
Figure 6. A type of a ratchet mechanism, able to transport a particle along a potential-energy surface. a) *The particle is in equilibrium between the potential minima A and B, moving back and forth, powered by Brownian motion. Potential maximum C avoiding any further motion to potential minimum D.* b) *If the particle is in the potential minimum B, rising potential A and lowering potential C allows the trapping of the particle between B and C. No backwards motion to A is possible anymore. By continuous variation of the potential-energy surface, one can thus move the particle in a unidirectional way.*

A particle in equilibrium between two different situations, moving back and forth thus making no unidirectional movement will still undergo single unidirectional motion on a short time scale (moving from A to B). As the molecule takes one step forward, the potential energy-surface can be changed by rising the potential in its "back", hence rendering impossible the backwards step. Lowering the potential in front of the particle will permit the next step forward. By repetitively changing the equilibrium conditions by an external trigger, a particle can be moved forward. Even though it might take steps into the wrong direction, the all-over motion will be unidirectional. The here shown illustration is only one simple example among others,[14, 18] containing three potential minima, of how a molecular machine can be driven by influencing the potential-energy surface.

III.1.2 External stimuli to control molecular motion

Thermal diffusion leading to motion cannot be considered as an external stimulus, as well as a statistical distribution of a molecular system between several states is not to be considered as a controlled motion. The external stimulus has to have a macroscopic influence so that the actual change occurring on the nanoscale can be experimentally proven.

Four different types of external signals have been used:

  • Chemical signal: Addition or withdrawal of metal ions,[19, 20] the introduction of an oxidizing or reducing agent,[21] or a change in pH can trigger motion.[22-24]

  • An electrochemical signal: oxidation or reduction at the electrode provokes motion.[25, 26]

•A photochemical signal: light triggers the motion, but a chemical sacrificial agent is needed to drive the system.[25, 27, 28]

• A photonic signal: light is the only triggering signal inducing the process, but thermal energy might be needed to complete the movement.[29-32]

Macroscopic tools, such as pH, light, heat or electric potential, allow us to influence the equilibrium of a nanosized object.

III.2. Catenanes and Rotaxanes

A particular approach to build molecular machines is to use catenanes or rotaxanes[33] (figure 7). A catenane is composed of at least two interlocked rings, therefore the only way of separating them is to break one of the rings. Its topology is non trivial as it cannot be drawn in a two-dimensional plane without avoiding crossing of the lines.

A rotaxane has a similar structure, containing at least on ring on an axle that is terminated with a sterically hindering group, avoiding the ring to come off the axle. Although one can consider the axle with the "stoppers" as an infinitely large ring, thus being similar to a catenane, strictly speaking, the rotaxane has a trivial topology, as the stoppers can be reduced in size, hence the ring can leave the thread.
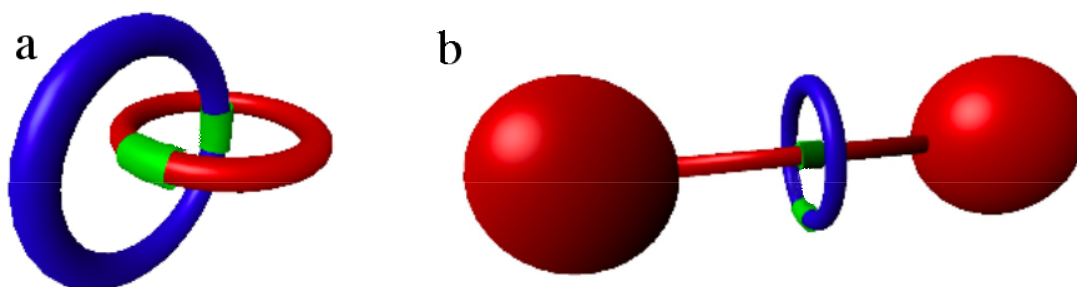
Figure 7: *Representation of a a) catenane, b) rotaxane.*

Even though the first catenanes and rotaxanes have been synthesized decades ago,[34, 35] they were considered as being curiosities with no further applications. It was only since 1983, when the first templated synthesis[36] was carried out, that the field started to grow rapidly. Pre-organizing the different constituents makes it possible to obtain these structures with very good, and even quantitative yields. Before the actual formation of a catenane or rotaxane, the two rings or the thread and the ring are already linked by different kind of interactions, as there are:

- coordination metals[26, 33, 37]

- hydrophobic effects[38]

- hydrogen bonds[39-42]

- charge transfer interactions[43, 44]

- covalent bonds[35, 45]

Once the synthesis is accomplished, the weak interactions between the different parts can be even weakened by demetallation or pH change for example. Therefore the constituents will be able to move, either by gliding or rotating, relative one to another, hence defining rotaxanes and catenanes as potential molecular machines.

IV. Examples of artificial molecular machines

Even though the molecular machine engineering domain has grown rapidly during the last decades, the synthetic tools that scientists dispose of are by far not powerful enough to achieve the synthesis of such complicated machines as used by Nature. Chemists try to reach their goal with "simple" molecules, by defining basic functions like controlled unidirectional translation or rotation. The following examples of

molecular machine prototypes were selected arbitrarily to illustrate possible approaches to the subject; they are by far not an exhaustive list.

IV.1. Molecular muscle, a dynamic linear rotaxane dimer

A schematic representation of how a muscle works is shown in figure 8, basically the thin filament and the myosin head covered thick filament glide along each other in opposite directions. The so induced shortening of the system corresponds to the contracted muscle state; by moving back to the extended situation the muscle relaxes.
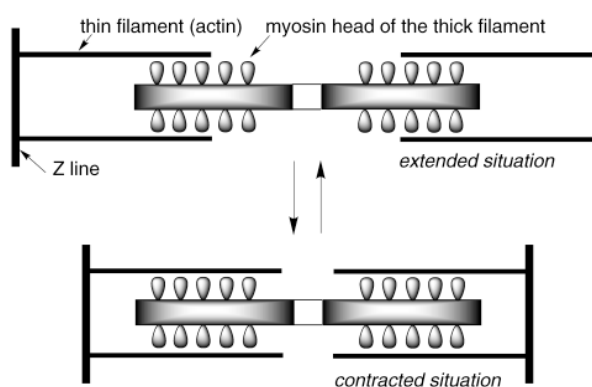
Figure 8.[19] *Schematic drawing of an elementary muscle unit.*

Maria Consuelo Jiminez-Molero *et al.* published a muscle mimicking device in 2002,[19] based on a linear rotaxane dimer, each entity being composed of a macrocycle containing an phenanthroline chelate, to which is attached a linear thread with a bidentate phenanthroline unit and a tridentate terpyridine entity. The dimer is formed by threading the linear part of one molecule into the macrocycle of the other participant by using the copper(I) template effect, as shown in figure 9a. The grey spheres on each side of the axle symbolise bulky groups that prevent the system from dethreading. Initially the external trigger for this system was supposed to be electrochemical oxidation of the copper (I) centres to copper (II), which in difference to the tetracoordinated mono-oxidized species prefers higher coordination numbers

and thus was expected to form a new pentacoordinated complex with the phenanthroline unit from the macrocycle and the terpyridine of the thread. To attain the required proximity between these two ligands, the two components would have to glide one along the other, hence reducing the all-over length of the system.
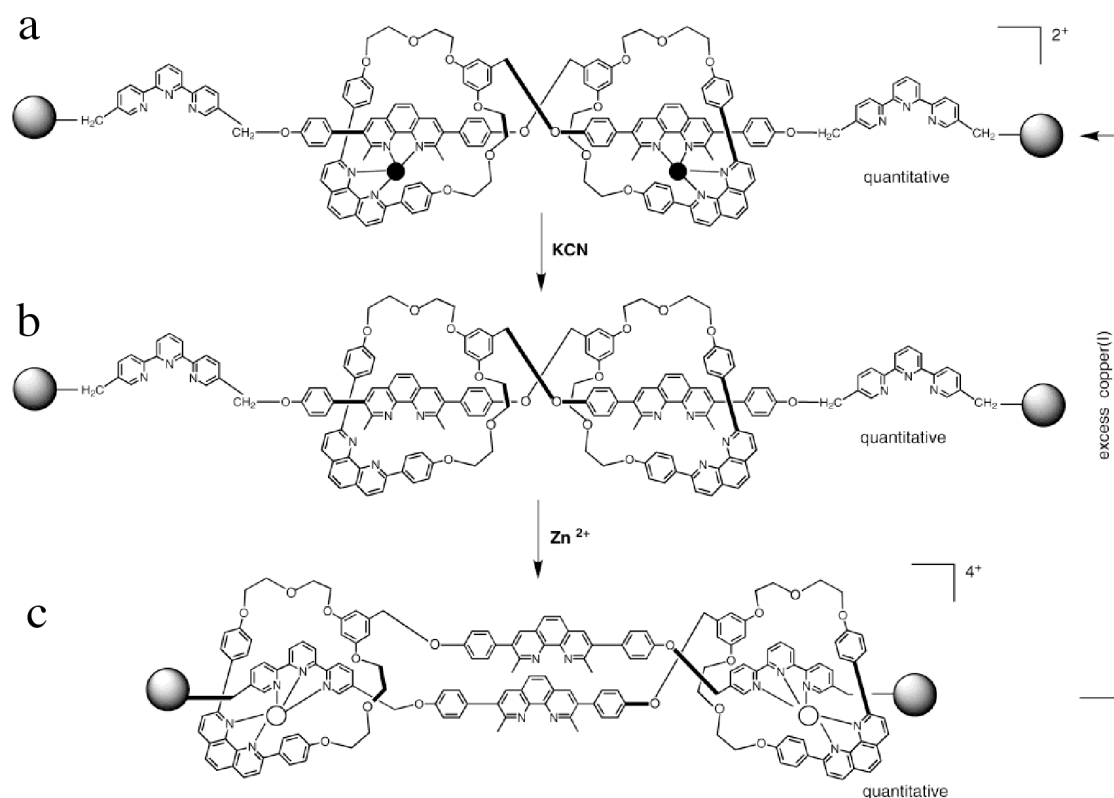
Figure 9. *Reversible chemically controlled motion between the extended and the contracted position.*

Unfortunately the expected motion upon oxidation did not occur. But after demetallation (figure 9b) and remetallation with zinc(II) ions, the system moved to its contracted conformation (figure 9c). By adding excess copper (I), the dimer relaxed again and returned to the starting situation. This molecular machine was the first "unimolecular" linear array able to be contracted and stretched at will by a chemical stimulus, reducing its length by 18 Å while moving from the extended (83Å) to the compressed (65Å) position, according to CPK model approximation[19].

IV.2. Autonomous artificial nanomotor triggered by sunlight

Credi *et al.* recently published a remarkable artificial nanomotor, based on a rotaxane structure and set to motion only by the influence of visible light.[28] Indeed the here presented machine features an autonomous behavior, absence of waste products, stability for at least 10^3 cycles while it can be driven at a frequency of 1kHz in a mild environment.

The system shown in figure 10 is composed of 6 parts, a $[Ru(bpy)_3]^{2+}$-type photosensitizer **P** connected to a spacer **S** separating it from a first electron accepting station, a 3,3'-dimethyl-4,4'-bipyridinium unit $\mathbf{A_2}$. The thread is continued by a second electron accepting 4,4'-bipyridinium $\mathbf{A_1}$ station and ends with a bulky stopper group **T**, which together with **P** prevents the electron donor macrocycle **R** from dethreading.
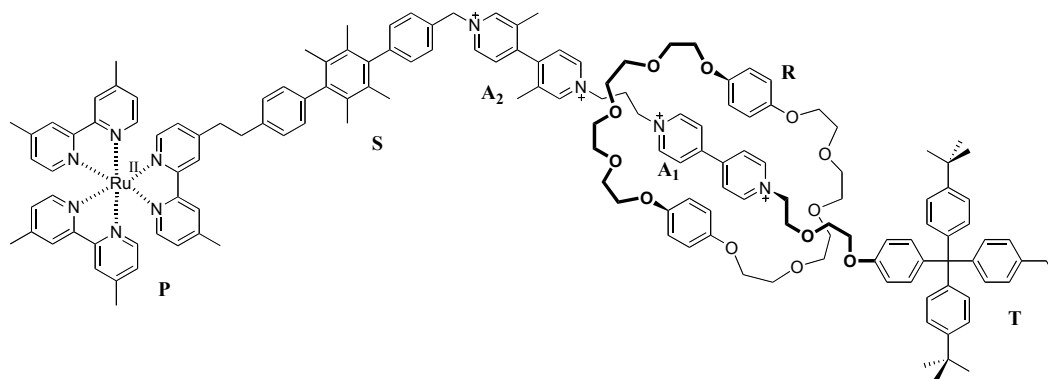
Figure 10. *Structural drawing of the rotaxane containing a $[Ru(bipy)_3]^{2+}$ station $\mathbf{P^{2+}}$, a spacer $\mathbf{S}$, 2 electron acceptor stations $\mathbf{A_1^{2+}}$ and $\mathbf{A_2^{2+}}$, a bulky stopper $\mathbf{T}$ and an electron donor macrocycle $\mathbf{R}$.*

In the absence of light, the stable conformation of the rotaxane is the one shown in figure 11A: the macrocycle is mainly localised on the more electron accepting station

A_1^{2+}, in other words, the local potential minimum shown on the potential-energy surface is lower than for A_1^{2+} then for A_2^{2+}.
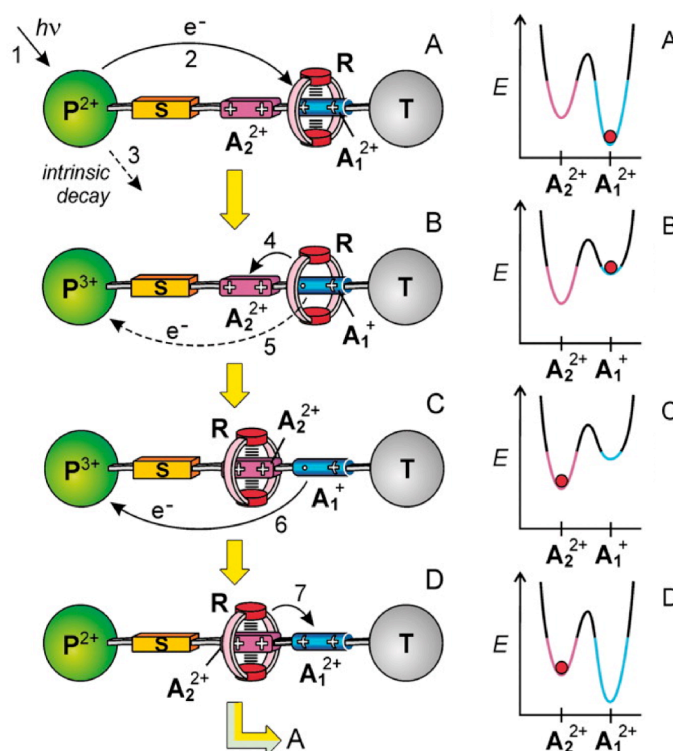
Figure 11. *The light-powered nanomotor: A) photoexcitation of P^{2+}, followed by electron transfer to A_1^{2+}, B) shuttling of the macrocycle to A_2^{2+}, C) electron back transfer from A_1^+ to P^{3+}, and final D) reset to the starting situation by motion back to A_2^{2+} of the ring.*

Light excitation of the photoactive station P^{2+} to $*P^{2+}$(1), followed by electron transfer to station A_1^{2+}(2), rises the local potential for this station above the one of the A_2^{2+}, thus inducing a Brownian motion driven shuttling of the ring **R** from A_1^+ to A_2^{2+}(4) (figure 11B). Two competing steps are interfering with this mechanism, the intrinsic decay of the photoexcited $*P^{2+}$ excited state (3) and the back electron transfer from A_1^+ to P^{3+}(5). Back electron transfer from A_1^+ to P^{3+} (6) after

shutteling, resets the energy-potential surface to its initial shape, the thus favoured $\mathbf{R}$ - $\mathbf{A_1}^{2+}$ interaction compared to the $\mathbf{R} - \mathbf{A_2}^{2+}$ interaction induces backwards motion (7) of the ring to the $\mathbf{A_1}^{2+}$ station.

A comparison with the four steps of a classical car engine turnover cycle is in a kind acceptable, fuel injection and combustion (A), piston displacement (B), exhaust removal (C) and piston replacement (D). The major drawback of the system is its inefficiency, indeed the quantum yield (number of ring shuttling events divided by number of absorbed photons) is only 2%. This is mainly due to the competition of step 4 with step 5, at 303K the rate constant for step 5 (back electron transfer without shuttling of the ring) is 7 times higher the for step 4 (ring displacement). The figures are even worse for lower temperatures (step 5 is 170 times faster then step 4 at 284 K), as step 4 is powered by Brownian motion and as such strongly temperature depended, whereas step 5 is almost independent from temperature. When electron transfer occurs before shuttling of the ring, the situation is equivalent to removing the fuel before combustion.

 The quantum yield can be increased to 12% by using an electron relay (phenothiazine), quenching step 5, thus leaving the ring more time to be displaced. Despite the low efficiency, this stable nanomotor working on free fuel (sunlight) at the single molecular level is an attractive and encouraging molecular machine.

Catenanes and rotaxanes are predisposed to be functionalized as molecular machines. They are composed of at least two entities, that are able to move one relative to another, but because they are "mechanically" linked, the different parts cannot be pulled apart. This feature gives these interlocked systems enough freedom to perform work, but at the same time defines clear limitations to the motion, restricting it to intramolecular movements. The system can therefore be more easily defined and controlled at a single molecular level then for systems with intermolecular motion and exchange. Nevertheless, natural as well as synthetic machines use other systems based on several, at least temporarily disconnected entities do carry out multiple tasks.
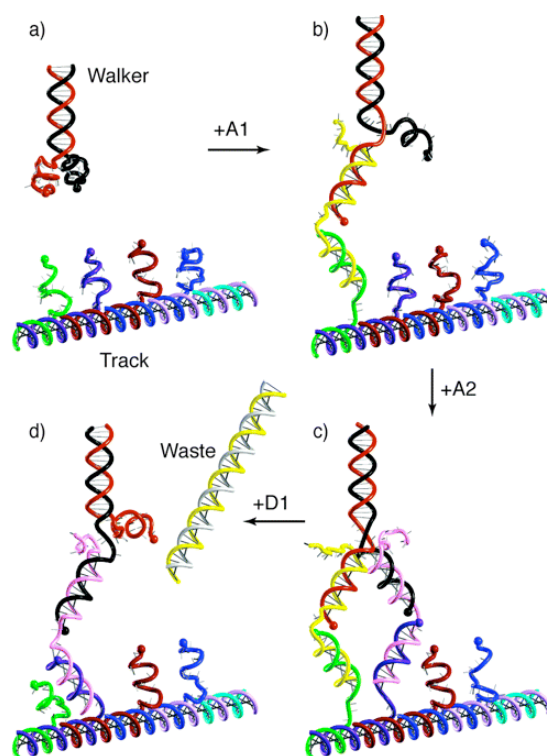
Figure 12. *A DNA walker, based on a walking unit, a track with different docking stations, attachment strands (A1, A2) and detachment strands (D1).*

One example is the DNA walker published by Jong-Shik Shin and Niles A. Pierce in 2004.[46] This kinesin[4]-mimicking device is based on different DNA strands and their matching or mismatching base pairs (bp). The mobile unit is composed of two 23bp oligonucléotides, that form a double stranded DNA helix with a little miss-match at one extremity, thus leaving the ending bases unpaired. These ends can be considered as being the legs of the walker. The track along which the machine will walk is composed of six oligonucleotides assembled in a way that the end of each strands point out of the track, thus being docking stations able to be connected to the unpaired strands of the walker unit. As shown in figure 12, a first attachment strand **A1** will join one of the walker's legs to the first docking station on the track, as well as a second strand **A2** will bind the second leg to the following station. The attachment strands are not completely paired at the ends, as well as in between the walker and the track. This last miss-match ensures the flexibility of the device by acting as a hinge. In presence of its perfectly matching detachment fuel strand **D1**, **A1** frees the leg from the track by forming a waste double strand with **D1**. The now free leg of the walker can bind to the third docking station of the track with the appropriate attachment strand, thus "taking one step forward". By repeating the process alternatively for both legs, the walker can move up and down the track in a unidirectional way, each step being about 5 nm long.

V. Nanomachines at work

Even though a large number of molecular machines and switches have been developed in recent years, those who can actually perform work or induce a macroscopic change by acting on a single molecular level are still rare.[47-50]

V.1. Bending a microcantilever beam

J. Fraser Stoddart *et al.* published a rotaxane-based molecular machine, which is able to bend a microcantilever beams in a skeletal muscle mimicking way[51]. The system is based on a [3]rotaxane, composed of a linear axle containing two outer tetrathiafulvalene (TTF) stations and two inner naphthalene (NP) stations, on which two cyclobis(paraquat-para-phenylene) ($CBPQT^{4+}$) units are threaded, such as shown in figure 13. A disulfide tether is grafted to each $CBPQT^{4+}$ ring to subsequent attachment of the rotaxane on a gold-coated silicon cantilever.

The $CBPQT^{4+}$ affinity for the TTF station due to donor acceptor (π-π stacking) interactions is dramatically greater than for the NP stations, hence the ring is largely located on the TTF stations. One or two electron oxidisation of the neutral TTF entities, resulting in the charged TTF^{2+} cation, induces shuttling of the ring to the NP stations due to the columbic repulsion between the TTF^{2+} station and the $CBPQT^{4+}$.
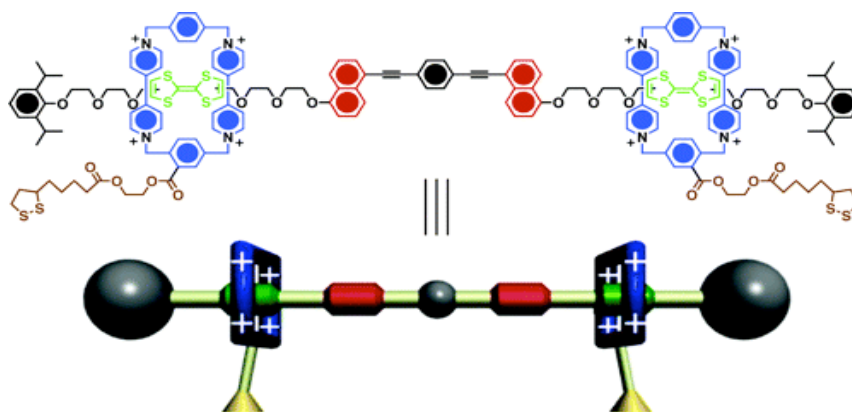
Figure 13. *Structure of the dynamic [3]rotaxane. TTF stations (green), NP stations (red), $CBPQT^{4+}$ rings (blue)*

Reduction of the TTF^{2+} to neutral TTF allows the ring to return to its original thermodynamically favoured position. Every $CBPQT^{4+}$ unit moves about 1,4 nm during this shuttling, meaning that the inter-ring distance change is 2,8 nm, which represents a 67% mechanical strain.

These rotaxanes (6 billions per beam) were deposited in random orientations on a silicon cantilever beam (500 x 100 x 1 μm) coated on its topside with a 20 nm thin layer of gold. The system was then placed in a fluid cell, and alternative flows of $Fe(ClO_4)_3$ (oxidant) and ascorbic acid (reductant) solutions were used to achieve oxidation and reduction of the TTF and TTF^{2+} units respectively. The shuttling triggered by these stimuli, and the resulting mechanical strain due to the variation of inter-ring distance, were able to bend and relax the cantilever beam upward and downwards by ca. 35 nm (figure 14).
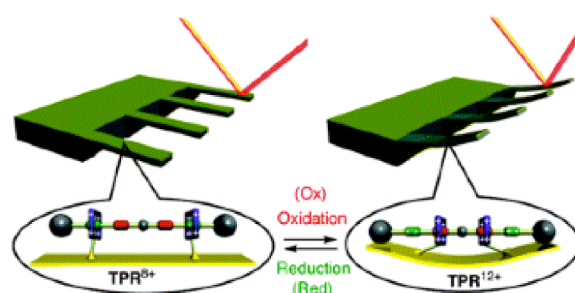
Figure 14. *Bending and relaxing of a cantilever beam by oxidising and reducing a [3]rotaxane.*

V.2.Molecular machines in liquid crystals

Liquid Crystals (LC) form a unique state of matter. They have a higher degree of organization than liquids, but a lower than crystalline solids. This allows a certain dynamic behaviour that can be triggered by external stimuli such as temperature, electric or magnetic fields, but also by non-mesogenic molecules dissolved in their matrix (the dopant). In a cholesteric (or chiral nematic) liquid crystalline phase the molecule orientating director changes its direction in a helical fashion throughout the sample, resulting in a supramolecular chirality characterised by its pitch (p) (distance in the material across which the director rotates 360°). Cholesteric liquid crystals

show selective reflection of light when the length of their pitch is of the same order of magnitude as the wavelength of visible light. As the pitch is dependent on the properties of the chiral dopant, the colour of a doped LC can be influenced by changing the concentration, enantiomeric excess or helical twisting power (β) of the dopant. Feringa *et al*. used a molecular machine as dopant, which features a large change in helical twisting powers when triggered by UV light or thermal energy,[52] thus having an influence on the pitch (figure 15) and colour of the LC .
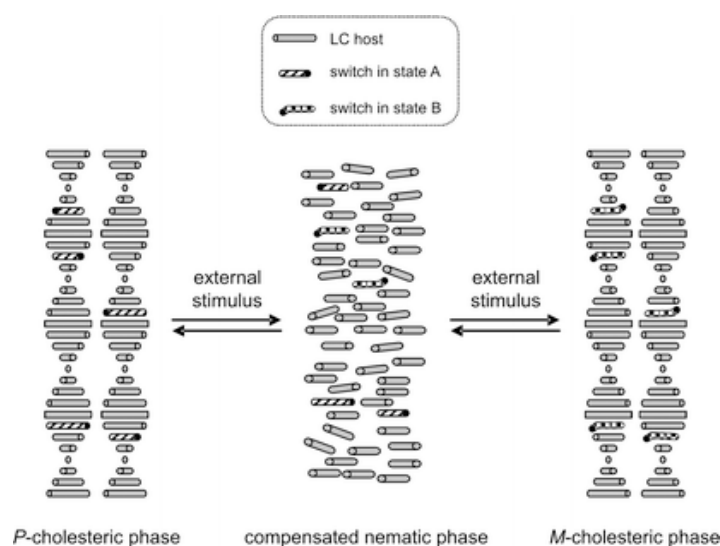
Figure 15.[52] *Schematic representation of the switching of the chirality of a doped cholesteric liquid crystal.*

 Important design features of this nanomachine (figure 16), are a P-helical structure, a single stereogenic centre in the upper part, a central carbon-carbon double bond that functions as axes of rotation and a symmetrical lower part, that resembles the biphenyl host compound E7 to facilitate its incorporation in the LC phase.
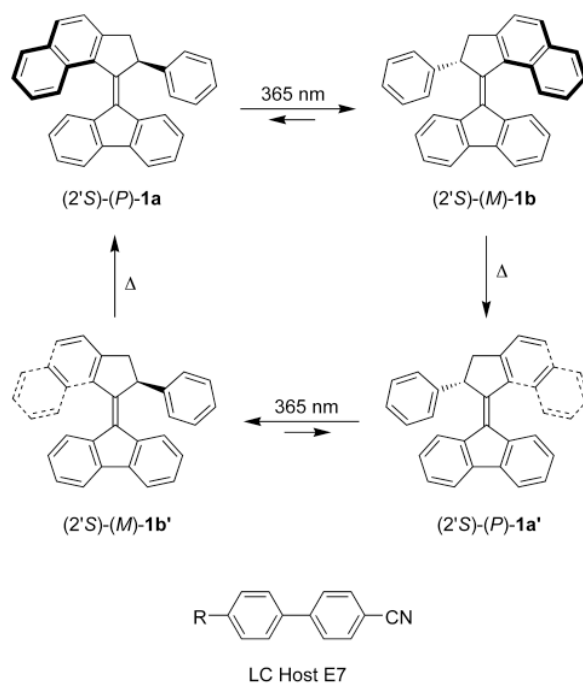
Figure 16.[30] *Chiral molecular motor **1** and the structure of E7 (R=nC$_5$H$_{11}$, nC$_7$H$_{15}$, nC$_8$H$_{17}$O, 4-nC$_5$H$_{11}$C$_6$H$_4$).*

In its stable form **1a**, the phenyl substitutent adopts a pseudoaxial orientation to avoid steric repulsion with the fluorene lower half. Upon irradiation with UV light (365 nm), a photochemical isomerization around the central double bond occurs with inversion of the helicity of the molecule ((**P**)-**1a** to (**M**)-**1b**). Simultaneously, the exocyclic phenyl substituent is forced to adopt a strained pseudoequatorial orientation due to a change in conformation of the five-membered ring. A subsequent thermal helix inversion (**MP**), governed by release of this strain, occurs readily at room temperature (t$_{1/2}$ = 9.9 min in toluene), leading to stable (**P**)-**1a**. Since **1a** and **1a'** are degenerate forms, this sequence can be considered as the first 180° part of the rotary cycle.

By including 6.8 wt % of this motor as a chiral switchable dopant in LC host E7, and triggering its isomerization by UV-light or heat, thus changing its helical twisting power and hence the pitch of the cholesteric phase, Ferniga *et al.* could address all colours in the visible spectrum.

Besides changes in colour, modification of the pitch also leads to rotational reorganization of the LC films, which is proposed to be the easiest mechanism for the cholesteric phase to increase or decrease its pitch.[53, 54] The fingerprint resembling lines (figure 17b) of the polygonal texture of the LC phase, corresponding to a half pitch, are able to take several turns, and eventually fade out ($\beta = 0$, $p = \infty$). A 5.0 x 28.4 μm glass rod, placed on top of the liquid crystalline film could be set in motion, following the rotation of the film on which it was placed (figure 17).

The here presented remarkable molecular motor system operating at a nanoscopic scale is able to influence the macroscopic world in two different ways, by changing the colour of its host LC film and by setting in motion microscale objects.
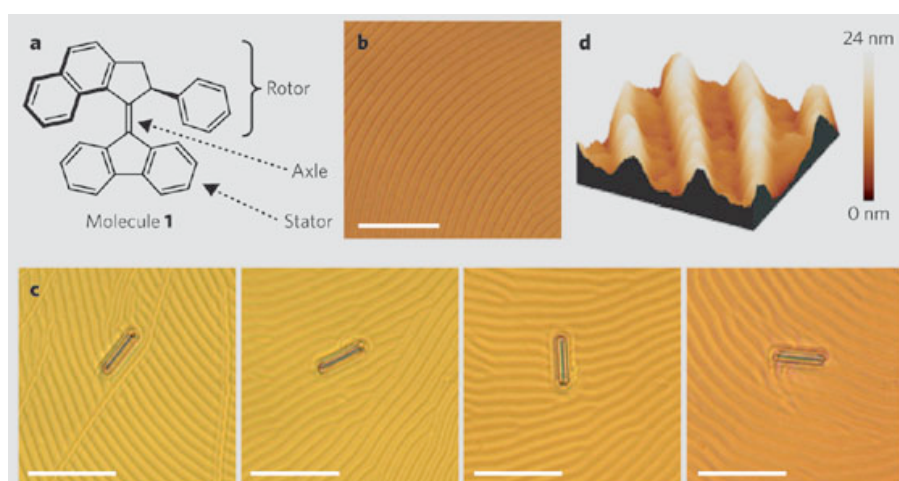
Figure 17.[54] a) Structure of the motor. B) Polygonal texture of a liquid-crystal film doped with molecule **1** (1% by weight) resembling fingerprints. C) Glass rod rotating on the liquid crystal during irradiation with ultraviolet light. Scale bars, 50 microm. d) Surface structure of the liquid-crystal film (atomic force microscopy image; 15 μm^2).

Chapter 1

Towards a molecular chaperones-mimicking nanopress

I. Mimicking Nature

I.1.Cavitand-based systems

Molecular chaperones play an important role in biological systems; they help proteins in acquiring their functional three-dimensional structure (as described in General Introduction section II.2.). To do so, they carry out three major tasks, capture, folding and release of their guest molecules. Synthetic molecular devices can be used to mimic this simplified view of their activities.

Alkenes adopt extended conformations to minimize the steric interactions, in a hydrophilic solution however they can be forced to fold inside hydrophobic cavitands, in order to reduce contact with the solvent.[55-57]

Figure 1.1. *Top) Tetraimide cavitand 1, the dimeric capsule 1.1 and its cartoon representation. (Bottom) alkanes inside 1.1: (right) decane is accommodated in its fully extended, anti conformation; (left) the longer tetradecane coils into a helical conformation. Peripheral alkyl groups and some capsule "walls" have been removed for viewing clarity.*
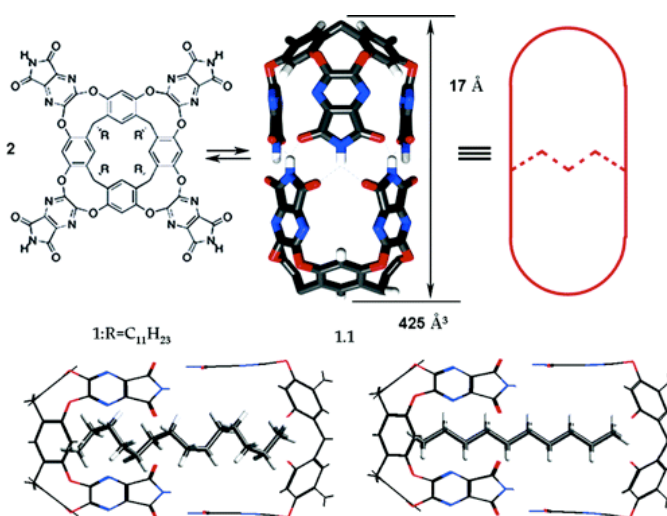
Julius Rebek Jr. *et al.*[58] synthesised hydrophobic pockets that can be modulated in size, thus offering more or less space to its guest. The cavity is formed by two identical molecules shown in figure 1.1, it is large enough two host a decane (C_{10}) without contracting it, whereas the tetradecane C_{14} is folded to fit into the given space.

In the presence of a protonated glycoluril derivative, which will enter the space between the two host entities, the cavity is enlarged, thus offering enough space for the C_{14} molecule to expand to its full size. Lowering the pH induces deprotonation of the glycoluril molecules, which then precipitate, thus the initial small cavity is formed and the C_{14} contracts again (figure 1.2). The system can be compared to the chaperones, because it is able to capture, fold, and release (in hydrophobic solvents) a guest molecule.
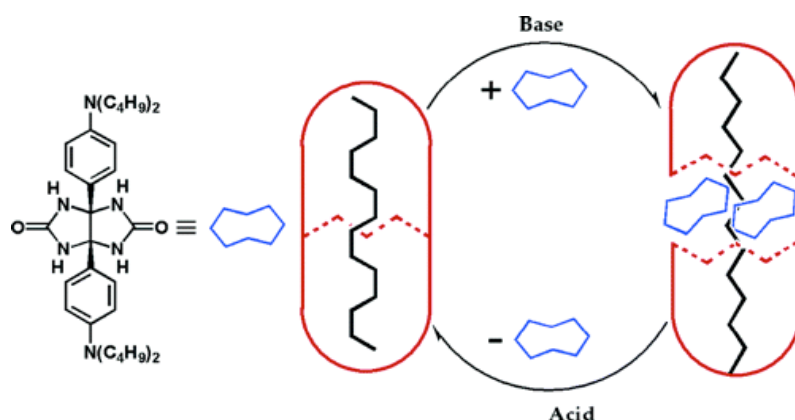
Figure 1.2. *Schematic representation of the coiling/uncoiling cycles of tetradecane, $C_{14}H_{30}$. The C_{14} is encapsulated as a helical coil in **1.1**. Addition of spacer (left) to the solution generates the longer assembly and the C_{14} guest relaxes to an extended conformation. Addition of HCl protonates the aniline sites of the spacer and causes precipitation of the spacer as its dihydrochloride salt; the system reverts to coiled C_{14} in the original capsule **1.1**. Addition of triethyl amine to the mixture releases the spacer into solution where it inserts and generates the longer assembly with extended C_{14} inside.*

Fujita *et al.* proposed a similar system based on transition metal based bowls, which formed dimeric capsules, able to accommodate a nine-residue peptide and thus stabilizing its α-helical conformation.[59]

I.2. Rotaxane-based systems: our project

The [3]rotaxane system is composed of two macrocycles containing two guest molecule docking stations, that can be moved towards or away from each other on a thread, thus folding and elongating a molecule trapped between the moving parts, as shown in figure 1.3.
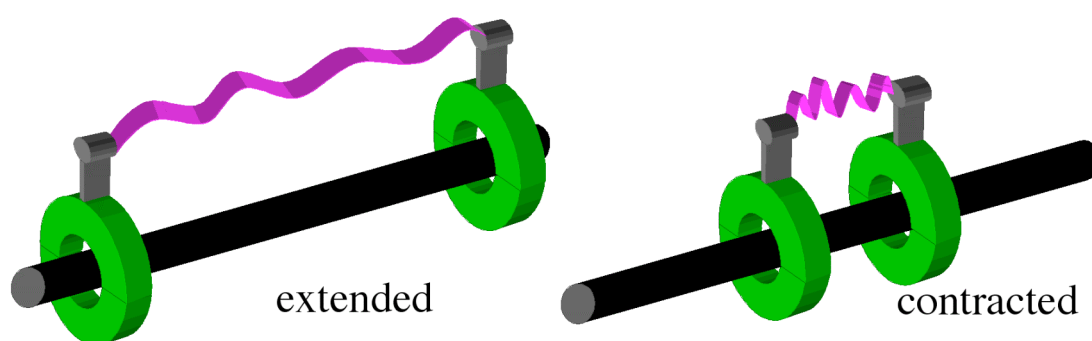
Figure 1.3. *A nano-press, based on a pseudo-rotaxane containing a thread (black), two macrocycles (green), two docking stations (grey) and a guest molecule (pink)*

To switch between the two situations at will, we developed a system based on the different coordination preferences of Cu(I) and Cu(II). Indeed, Cu(I) prefers tetracoordinating sites whereas Cu(II) prefers penta- or hexacoordinating sites[60, 61]. The macrocycles that are used for these systems are derivatives of the m-30 ring (figure 1.4), synthesized in the laboratory for the first time in 1983 by Christiane Dietrich-Buchecker *et al.,*[62] containing a phenanthroline (phen) chelate.
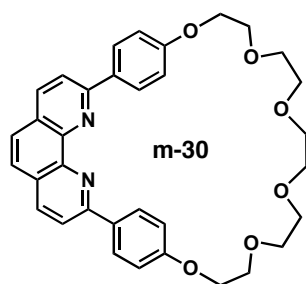
Figure 1.4: Macrocycle m-30, containing a 1,10-phenanthroline bidentate ligand

If this bidentate macrocycle is threaded by an axle containing a bidentate (2,2'-bipyridine) and a tridentate (2,2',6',2''-terpyridine) station, motion can be induced by an electrochemical stimulus.

In the presence of Cu(I), the ring will mainly sit on the bipyridine (bipy) station of the thread, because it offers a four coordinating environment to the metal centre. In presence of Cu(II) however, the ring will be localised on the tridentate terpyridine (terpy) station to create a five coordinating site. By oxidizing Cu(I) to Cu(II) we can trigger the motion of the ring from the bipy to the terpy, whereas reduction causes the movement in the opposite direction. Gaviña *et al.* were the first to report such a system based on terpy and phen moieties[19, 63, 64] (figure 1.5).
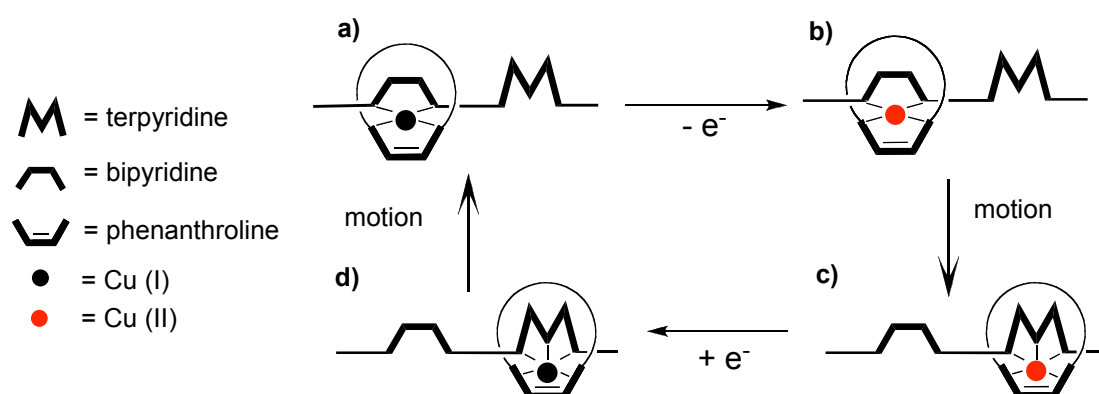
Figure 1.5. *Schematic drawing of the motion cycle of a Cu based rotaxane: a) Cu(I) in a stable tetracoordinated complex b) oxidization of Cu(I) to Cu(II), affording a metastable tetracoordinated Cu(II) complex c) after gliding of the macrocycle to the terpyridine to offer a pentacoordinating site to the Cu(II) d) reduction of Cu(II) to Cu(I) leads to the pentacoordinated Cu(II) intermediate before reorganisation brings the ring back to the starting position.*

The system presented in figure 1.5, and already synthesized in the laboratory,[64] represents only half the system we need to move two rings towards and away from each other. The chaperons-mimicking system requires a thread featuring two bidentate (bipy type) ligands in its centre and two tridentate (terpy) ligands on its outside, as shown in figure 1.6.
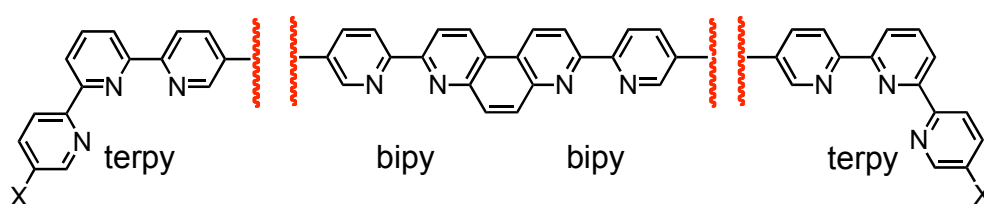
Figure 1.6. *The core and extremity ligands of the thread (X = bulky stoppers)*

To be able to exploit this motion as a nanopress, the phenanthroline of the macrocycle is functionalized on its ethenyl bridge (carbon 5 and 6) in order to graft the molecular host units for the guest molecules, which is attached either to one ring or between two rings. In the latter case, the system needs two "rails" to glide on. As shown in figure 1.7, the rings to which the host units are attached are threaded on the rail, on which they can be moved towards another (Cu(I)-bipy situation) or away from each other (Cu(II)-terpy situation), thus elongating or contracting the guest molecule. Zn(II) porphyrins are possible hosting units, by taking advantage of the free coordination site on the Zn.
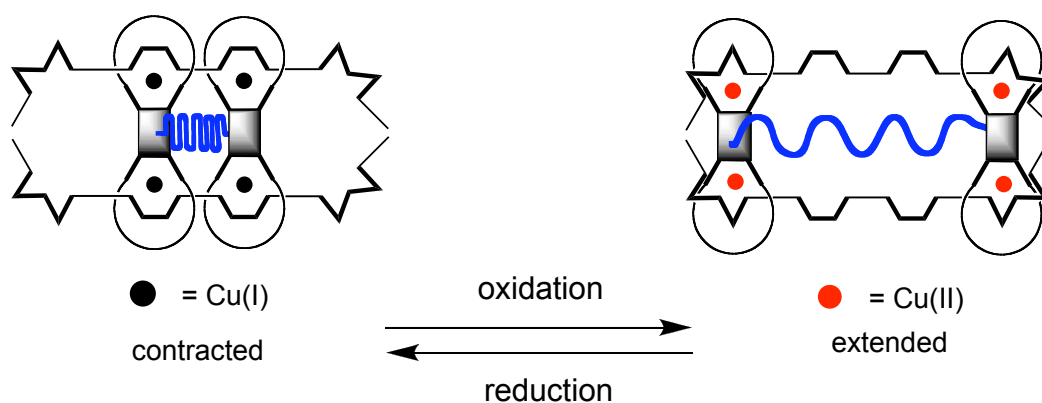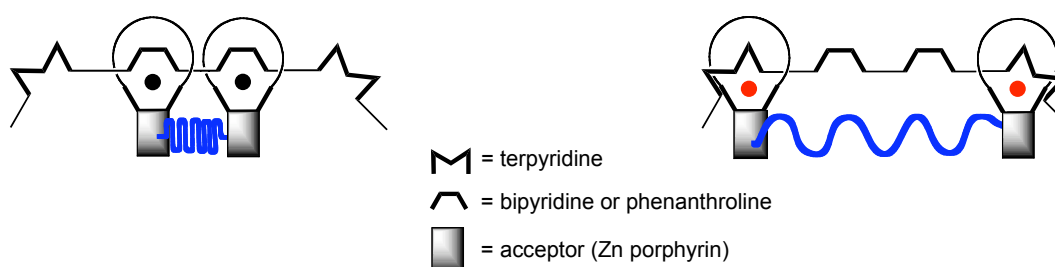
Figure 1.7. *The two possible nanopress models, with either bis-macrocycle units (top) or single macrocycle units (bottom). The driving force is the same in both cases, Cu(I) favours the bidentate bipyridine station whereas Cu(II) prefers the tridentate terpyridine station on the thread. The bulky stoppers are omitted for clarity.*

Another possible function of the system is the trapping of molecules.

    - Large rigid molecules could be hosted by the porphyrin moieties in the "open", extended, situation of the press. However, in its contracted, "closed", situation, the rigid molecule will no longer fit between the porphyrins. Depending on the association constant of the guest molecule to the host the guest might then be released.

    - Small molecules can be trapped in the closed form of the press and be released upon switching to the extended form.

Chapter 2

The central part of the thread and first pseudorotaxanes

I. The heart of the thread

I.1 The choice of the bidentate ligands

As already discussed before, the centre of the thread is composed of two bidentate ligands, the two bipys. To make sure that both metals will later on bind on the same side of the thread, thus ensuring alignment of the acceptor units, we have to orientate the bipys in the same direction. Therefore, we started the synthesis with the commercially available 4,7-phenanthroline (phen), which is basically a 4,7-bipyridine unit with a ethenyl bridge, preventing the heterocycles from turning one relative to the other, thus keeping the coordinating nitrogen atoms on the same side of the future thread.
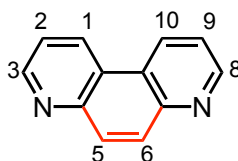
Scheme 2.1. *4,7-phenanthroline (ethenyl bridge = red).*

By attaching a pyridyl group on each side (3 and 8) of the phen, we obtain two bidentate bipy sites, which upon coordination to a transition metal will have to follow

the preorganisation of the rigid phen, and thus bind the metal centres on the same side.
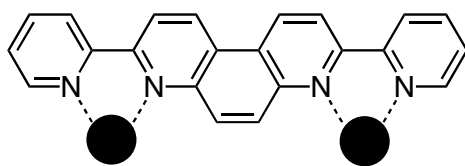
Scheme 2.2. *Bis-bipyridine coordinated to two metal centres (black spheres).*

Preliminary experiments were carried out by Evelina Sakelariou to make sure that Cu(I) bound to the m-30 macrocycle prefers a bipyridine and not a terpyridine as second ligand. To mimic the bipyridine entity of the thread, the pyridyl quinoline was synthesized and ^{1}H-NMR showed that even in presence of terpyridine, the pyridyl quinoline binds to the Cu(I)-m-30 complex (scheme 2.3).
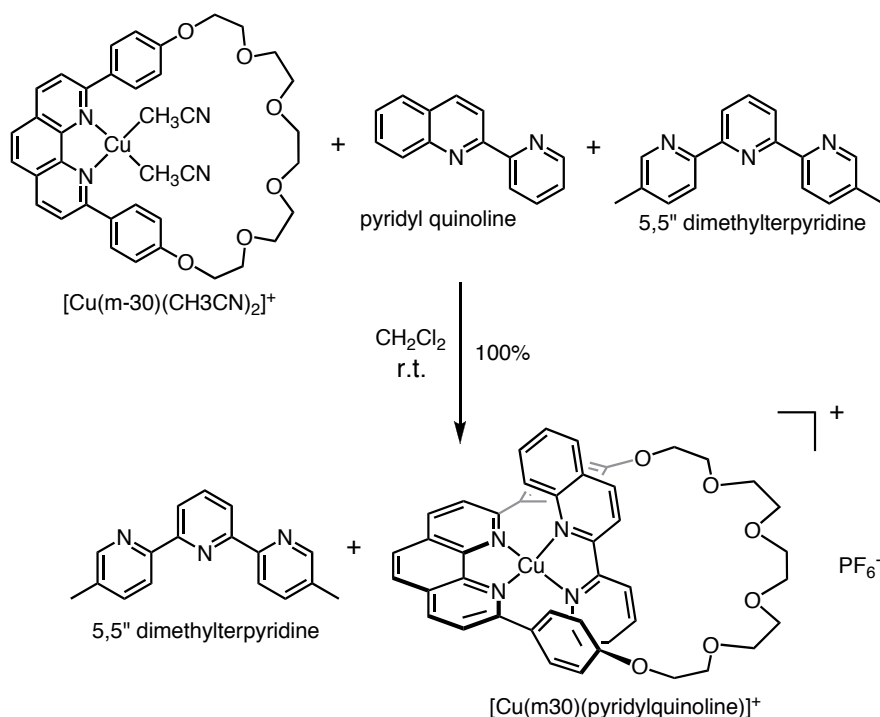
Scheme 2.3. *Terpy versus bipy binding test with the m-30 macrocycle and Cu(I).*

To allow further functionalization of the bis-bipy ligand, we synthesized ligand **7,** by modification of the literature procedure,[65] with bromine atoms at each end (scheme 2.4).
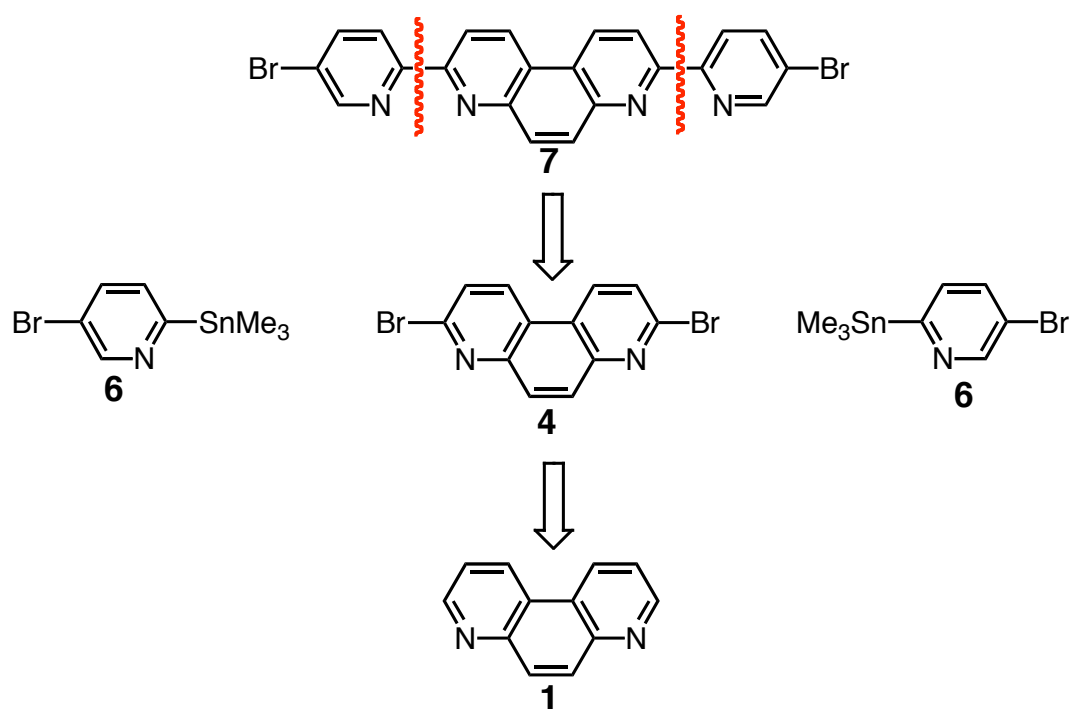
Scheme 2.4. *Retrosynthesis of bis-bidentate ligand **7**.*

►   *3,8-dibromo-4,7-phenanthroline (4):*
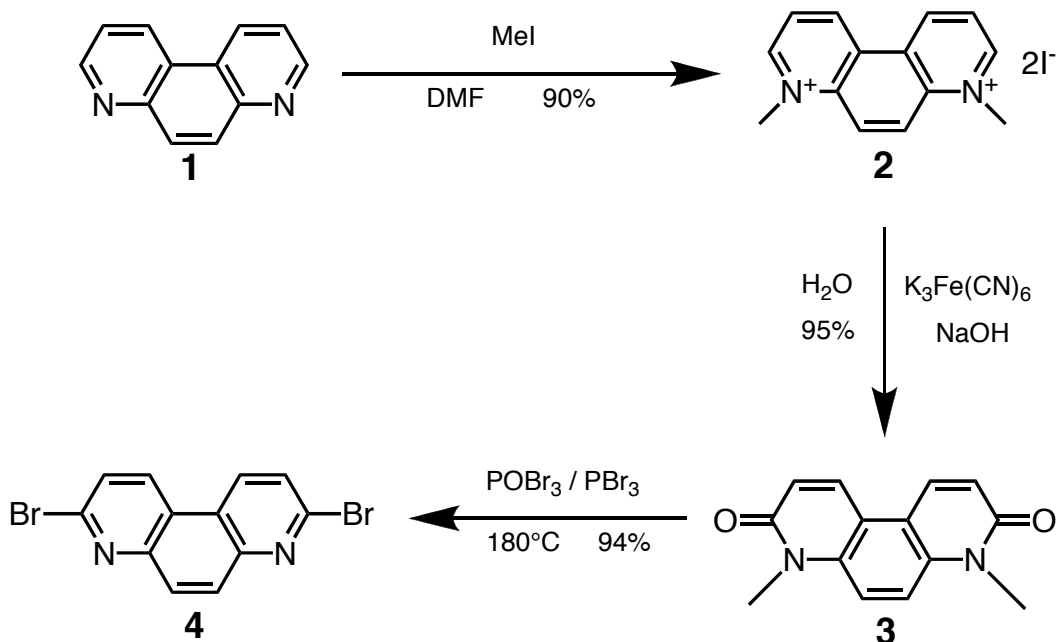
Scheme 2.5. *Three-step synthesis of the 3,8-dibromo-4,7-phenanthroline 4.*

To activate the α-positions (3 and 8) of the commercially availabe 4,7-phenanthroline **1**, we proceed to a methylation of the pyridyl heterocycles with methyliodide. A further consequence of this methylation is the protection of the nitrogen atoms towards oxidation. Although the reaction is nearly quantitative, a large excess of methylation agent has to be used to prepare the bright orange product **2** in gram quantities.

The oxidation of **2** to the corresponding dione **3** is achieved by using $K_3Fe(CN)_6$ as oxidant in an alkaline environment. Mesomeric and induction effects are responsible for a strong regioselective oxidation of the partially charged carbons in position 3 and 8 of the phenanthroline. After 5 hours, the brown product **3** is extracted with CH_2Cl_2 in 95 % yield.

Bromination of the 4,7-phenanthroline dione **3** is achieved in harsh conditions by a mixture of POBr$_3$ (30 eq.) and PBr$_3$ (5 eq.) at 180°C. In these conditions, beside bromination, the nitrogen atoms are demethylated and the aromaticity of the compound is regenerated. The work-up for this product is very tedious and time-consuming, because the major part agglomerates and is trapped in the celite, used for filtering the compound. Therefore the celite was washed with CH$_2$Cl$_2$ to remove the more soluble impurities, and then extracted about 15 times with boiling CHCl$_3$ after sonication of the suspension. Soxlet extraction did not work; the product is so strongly stuck to itself and the celite, that sonication is absolutely necessary to render it slightly soluble. Nevertheless, the pure compound **4** could be obtained in 94% yield.

▶ *5-bromo-2-trimethystannylpyridine (6):*
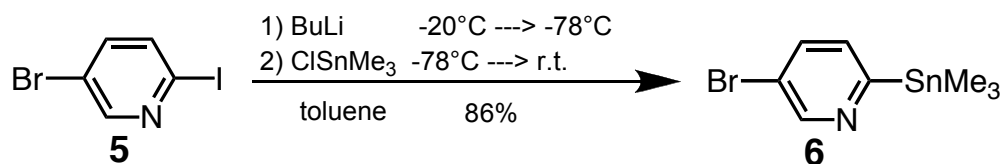
Scheme 2.6. *Preparation of the 5-bromo-2-trimethylstannylpyridine (6).*

Compound **6** is synthesized by starting from the commercially available 5-bromo-2-iodopyridine **5**, which is reacted with BuLi, then quenched with ClSnMe$_3$. The iodide vs. bromide selectivity in the interconversion with BuLi as well as the nature of the solvent,[66] which determines the regioselectivity, afforded **6** in 86% yield.

To synthesize the bis-bipy ligand core, molecules **4** and **6** are linked by Stille coupling (scheme 2.7).

▶ *3,8-bis(5-bromo-2'-pyridyl)-4,7-phenanthroline (5):*
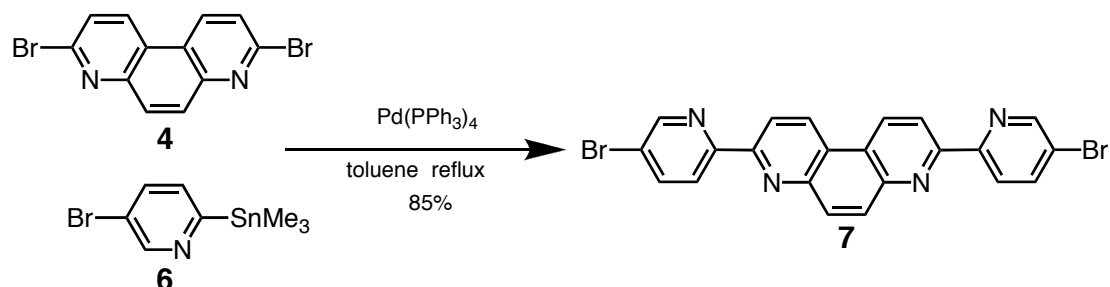
Scheme 2.7. *Stille coupling between **4** and **6** to afford the bis-bidentate ligand **7**.*

During this Stille coupling reaction,[67, 68] oxidative addition on the palladium catalyst is possible on two different bromo-aryl sites. The 85% yield for compound **7** shows that it is much more likely to happen on the phenanthroline than on the pyridine moiety. This can be explained by a higher net charge (+0.075) on the activated carbon in ortho position than in the meta position (-0,004) on the pyridyl heterocycle. Hence the more polarized C-Br bond in the ortho position is more reactive towards oxidative addition, and the homocoupling between two pyridine heterocycles is not observed. Compound **7** is even more insoluble than the phenanthroline **4**, and could only be purified in the same way, by extracting it, after sonication, from celite with boiling chloroform.

In order to make the first threading tests with m-30 or m-30-like macrocycles, the axle is elongated by Suzuki coupling[69, 70] with 4-(trimethylsilyl)phenylboronic acid and 4-methoxyphenylboronic acid, which are both commercially available. These boronic acids are chosen because they permit further functionalization. The trimethylsilyl

(TMS) can easily be substituted by an iodide, thus allowing further coupling reactions, whereas deprotection of the methoxyphenyl results in a phenol, able to undergo Williamson reactions (scheme 2.8).
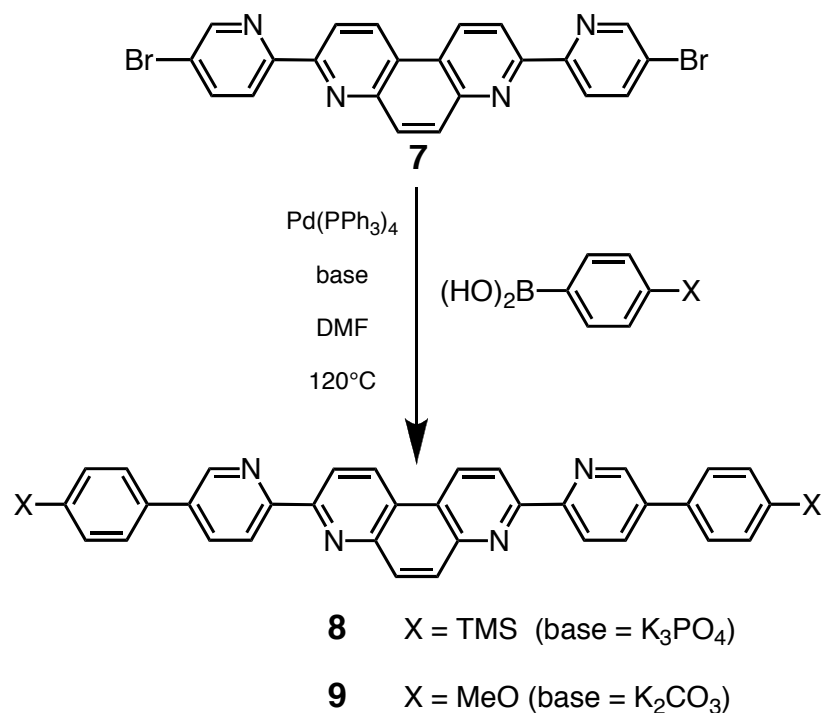
Scheme 2.8. *Synthesis of the functionalized thread by Suzuki coupling.*

Compounds, **8** and **9**, obtained in 66% and 82% yield respectively, are the first important fragments towards the construction of a longer thread, but they are also interesting by themselves, as they can be used to assemble several multicomponent systems. It is worth noticing that compound **9** is even less soluble than compound **7**, due to additional anisyl groups, elongating the delocalized system. To be able to carry out proper ^{1}H-NMR spectroscopy in CDCl$_3$, we are forced to add a small amount of TFA (trifluoroacetic acid), thus protonating the bipyridines, and rendering the compound slightly more soluble. Compound **8** benefits of the TMS groups as solubilising agents and is slightly easier to handle.

II. The first pseudo-rotaxanes

II.1. [3]pseudorotaxane

A first test-reaction, to make sure that the double threading induced by the Cu(I) template effect will occur efficiently, was carried out using the TMS thread **8** and two m-30 macrocycles. Even though the Cu(I) metal centres can coordinate to different ligands on the ring or the thread, the thermodynamically favoured compound is rotaxane **10**. Indeed in presence of the thread, m-30 and Cu(I) in a 1:2:2 ratio, **10** represents the only molecule that can offer two bidentate ligands to the Cu(I) centres, because two m-30 coordinated to one Cu(I) is a sterically impossible situation. Even though the thread can form grid-like assemblies, this situation is thermodynamically not favoured because it leaves the remaining Cu(I) bound only to one chelate inside the m-30 macrocycle (scheme 2.9).

After three days, the different kinetically favoured structures have re-arranged to give only the [3]pseudorotaxane **10**. Unfortunately some impurities were noticeable on the ^{1}H-NMR spectra. Usually such threading reactions are quantitative, therefore it is most likely that the observed impurities do not come from the actual threading reaction, but might have been present in the m-30 starting material. Column chromatography finally gave us the pure product in 50% yield. Even though this is a very poor yield for a supposed quantitative reaction, it shows that compound **10** is quite stable to dethreading and oxidation of Cu(I) during column chromatography, because 50% of the compound "survived" this treatment.
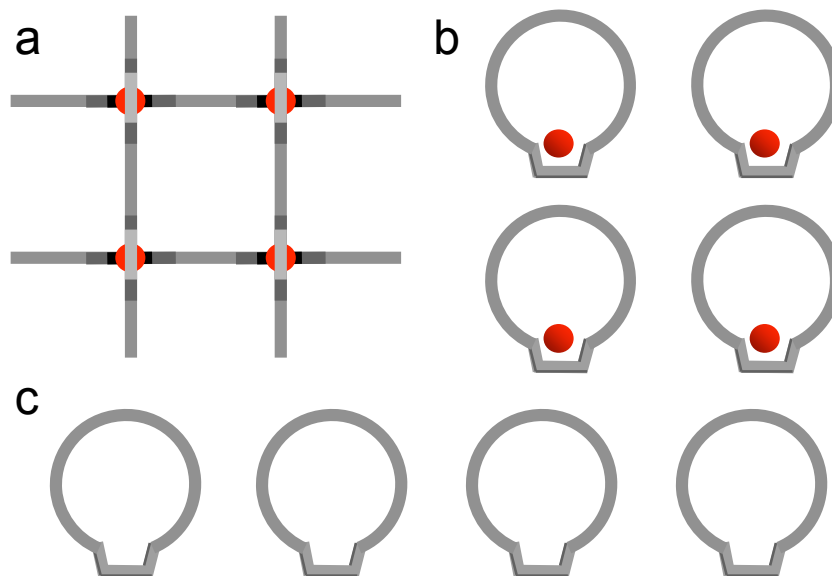
Scheme 2.9. *By mixing the thread, the m-30, and copper(I) in a 1:2:2 ratio, the easily accessible and therefore kinetically stable grid (a) forms first. This situation is thermodynamically unstable because the remaining half of the copper(I) ions are coordinated to only one m-30 chelate (b), and half of the m-30 macrocycles are left uncoordinated (c). Due to the steric hindrance of the ring, two macrocycles can not coordinate the same copper ion, therefore the system will evolve to form the thermodynamically favoured [3]pseudorotaxane situation.*

Compound **10** is a **2+** charged [3]pseudorotaxane with 2 PF_6^- counterions. ^{1}H-NMR peak integrations clearly show that the obtained product is composed of one axle with two macrocycles. Shifts of 0.1 up to 1.2 ppm are observed compared to the free ligands, especially the *o* and *m* hydrogens of the macrocycle are strongly shifted up-field, due to their proximity to the bipyridine units of the axle. Moreover, Noesy NMR shows correlation spots between H_o and $H_{6'}$, as well as for H_o and $H_{5'}$. UV/vis-spectra reveals two absorption bands at 346 and 418 nm with absorption coefficients of 5×10^4 and 3×10^3 $mol^{-1}.L.cm^{-1}$ respectively which is typically in the range of a tetracoordinated Cu(I) complex.[71]
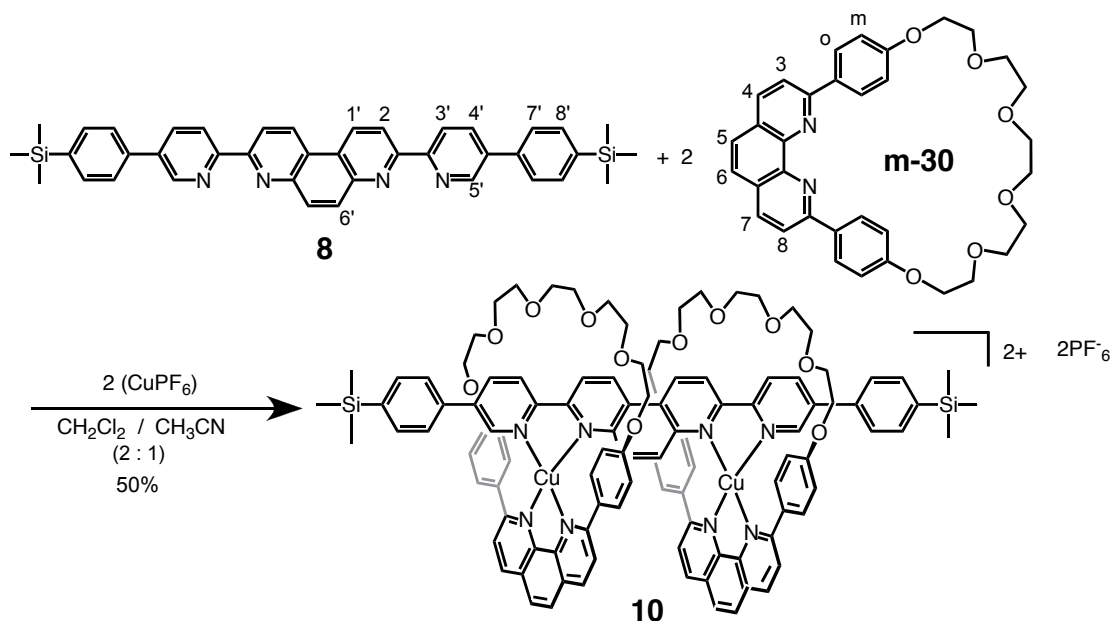
Scheme 2.10. *Threading reaction with two m-30 macrocycles using the Cu(I) template effect.*

Electrochemical investigations, carried out in acetonitrile, showed a redox signal, from which we can determine slightly different oxidation potentials for the two Cu(I) centres. The first oxidation takes place at 0.56 V and the second at 0.63 V versus SCE electrode, which indicates a weak interaction between the two copper centres. We determine a 70 mV difference between the two potentials,[72] not enough to oxidize one copper after another, which was proven to be possible in previous papers.[73] The threading test being a success, the next step is the functionalization of the thread to be able to graft stoppers and/or terpyridine moieties on each end.

II.2. [4]pseudorotaxane

As mentioned above, the m-30 macrocycle can be funcionalized on the ethenyl bridge, thus allowing us to synthesize a bis-macrocycle, composed of two m-30 rings, attached together "back-to-back" with a pyrazine spacer. Julien Frey and Valérie Heitz synthesized bis-macrocycle **11**[74], during his Ph.D thesis in our laboratory (scheme 2.11).
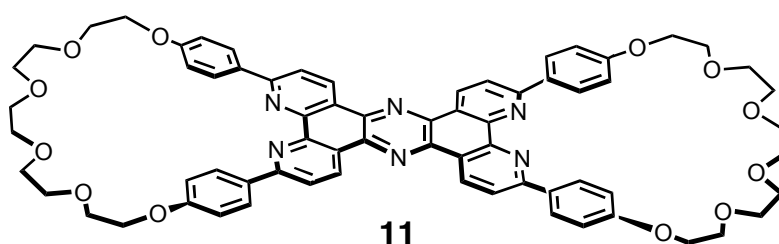
Scheme 2.11. *m-30 based bis-macrocycle, attached "back to back" with a pyrazine spacer.*

In order to check the threading reaction with four metal centres, we use two bis-macrocycles **11**, and two threads **9** in presence of 4 equivalent of Cu(I). The methoxyphenyl thread is chosen, because we plan to use it together with the bis-macrocycle to synthesize a [3]catenane later on *via* Williamson reaction after preparation of the corresponding bis-phenol.
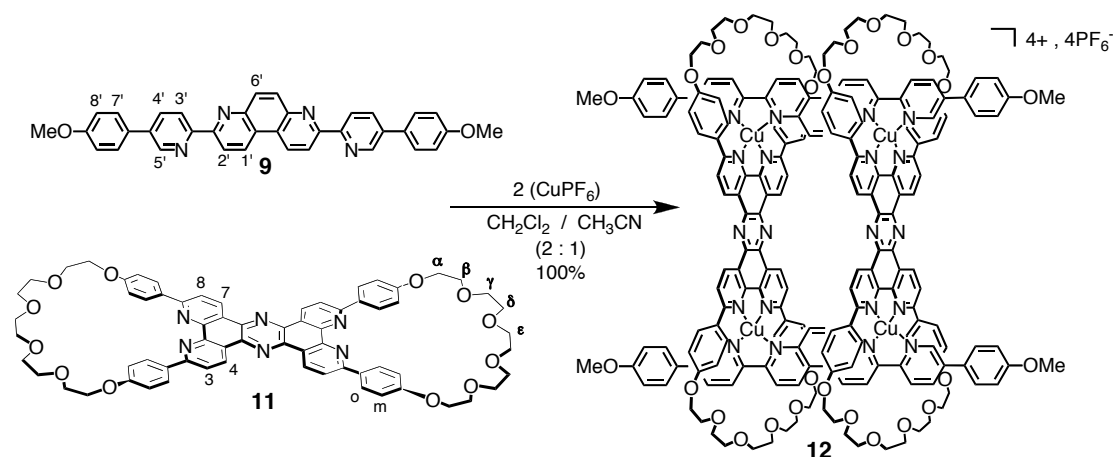
Scheme 2.12. *Quantitative synthesis of a [4]pseudorotaxane 12.*

The [4]pseudorotaxane **12** is obtained quantitatively after 7 days at room temperature (scheme 2.12). Even though the starting materials, the thread as well as the bis-macrocycle, are of very low solubility, the template effect of Cu(I) is strong enough to assemble the thermodynamically favoured compound if it is given the appropriate amount of time. This demonstrates the power of coordination chemistry, and in particular the efficiency of copper (I) acting as a "gathering and threading" element. Furthermore, the final [4]pseudorotaxane is well soluble and crystals of the [4]pseudorotaxane $(PF_6^-)_4$ could be grown from slow diffusion of THF into DCM. The crystal structure was solved by Professeur Kari Rissanen from the Nanoscience Centre of Jyväskylä University in Finland. Some relevant geometrical features of the [4]pseudorotaxane **12** are given in table 2.1.
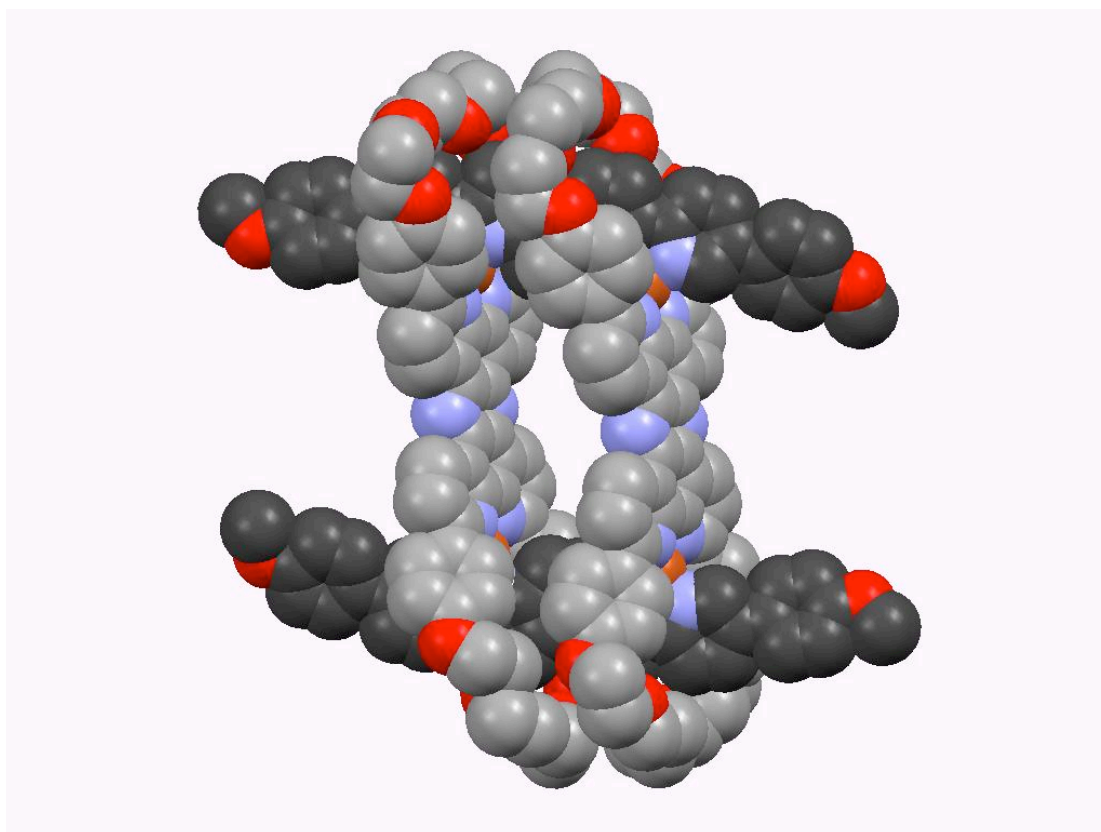
Crystal structure 2.1. *Crystal structure of [4]pseudorotaxane **12**. Hydrogen atoms are omitted for clarity.*

Distances:			
Cu – Cu			
	On one thread :	7.803 Å	
	On one bis-macrocycle :	12.663 Å	
Cu – N			
	Cu – N$_{thread}$:	2.007 – 2.045 Å	
	Cu – N$_{macrocycle}$:	2.031 – 2.048 Å	
Pyrazine – Pyrazine	(pyrazine spacer of the two bis-macrocycles)		8.394 Å
Angles:			
Phen (macrocycle) – bipy (thread) distortion angles		59.12°	61.16°
		59.14°	61.14°
N – Cu – N			
	phen (macrocycle) bite angles:	81.61° - 82.40°	
	bipy (thread) bite angles:	81.89° - 82.07°	

Table 2.1. *Geometrical features of the [4]pseudorotaxane **12**.*

It is noticeable that the spacers of the bis-macrocycles are slightly bent away from each other, thus increasing the distance between them to 8.395 Å, compared to 7.803 Å for the copper – copper distances. The threads on the other hand are bent about 13° towards the copper centres.

The geometry of the bipy-phen environment around the metal centres is a distorted tetrahedron. In fact the bipy and the phen are not orthogonal to each other, their dihedral distortion angle is only about 59° - 60° instead of the required 90° for a perfect tetrahedron. This "flattening" of the geometry brings the phenyl groups in the 2 and 9 positions of the macrocycle phenanthrolines closer to the thread (see crystal structure 2.2).
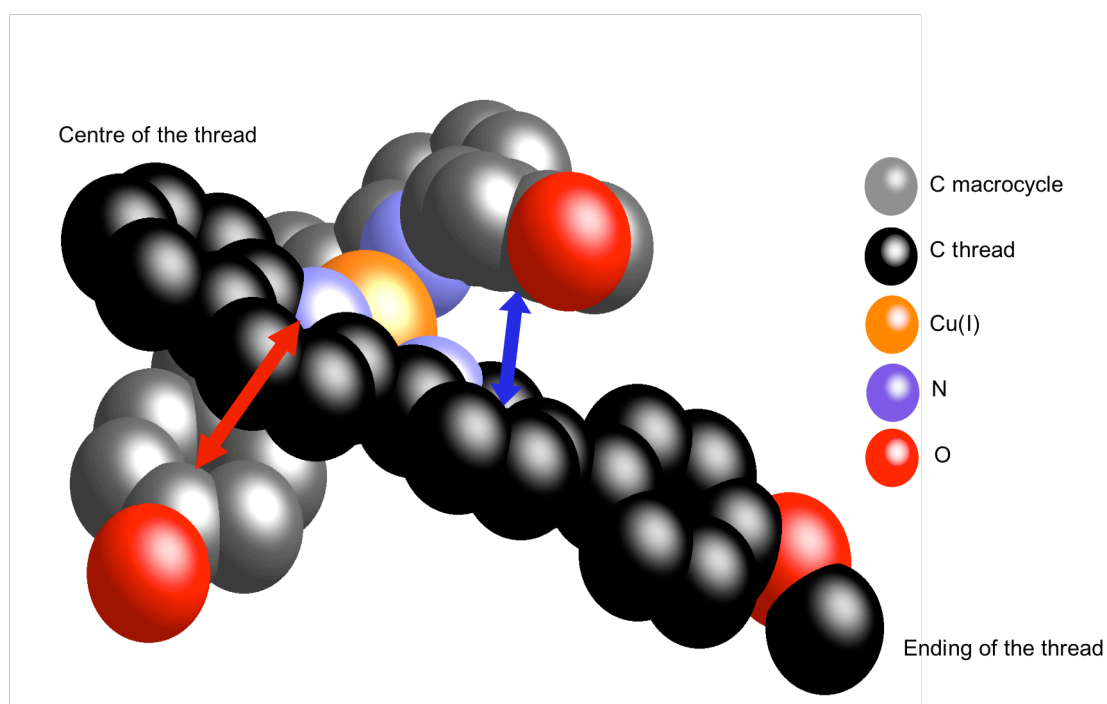
Crystal Structure 2.2. *Zoom on one of the Cu(I) coordination spheres of compound **12**.*

For each macrocycle, one of the two phenyl moieties approaches an external pyridyl heterocycle of the bis-bipy ligand of the thread (blue arrow). The distance between the centroids of these two cycles is 3.724 Å. The second phenyl moiety of the

macrocycles approaches the central phen of the thread either at the ethenyl-bridge (distance 6' to centroid = 3.453 Å) or at one of the pyridyl heterocycles (distance centroid to centroid = 3.701 Å) (red arrow). These distances do allow π-π interactions and also explain why the proton in the 6' position has the most dramatically shifted resonance in the ^{1}H-NMR spectrum upon coordination of the macrocycles to the threads (see table 2.2). Indeed it finds itself situated in the de-shielding cone of the phenyl rings.

	H-4,7	H-1'	H-2'	H-3'	H-4'	H-5'	H-3,8	H-7'	H-6'	H-o	H-8'	H-m
12	10.02	9.54	8.76	8.61	8.33	8.27	8.24	7.57	7.43	7.34	7.06	6.10
9		9.44	8.56	8.56	8.56	9.13		7.71	8.75		7.15	
11	10.19						8.72			8.28		7.36
Δδ [c]	-0.17	0.10	0.20	0.05	-0.13	-0.86	-0.48	-0.14	-1.32	-0.94	-0.06	-1.26

Table 2.2. ^{1}*H-NMR data for the free ligands* **9**, **11** *and the pseudorotaxane* **12** *(spectrum shown).* [a] The very poor solubility of **9** and **11** in normal organic solvents did not allow NMR studies without protonating these ligands so as to dissolve them.[b] Solvent: CD_2Cl_2 + 3% TFA for **9** and **11**, CD_2Cl_2 for **12**.[c] $\Delta\delta = \delta(\textbf{12}) - \delta(\textbf{9}$ or $\textbf{11})$.

Compound **12** contains four identical Cu(I) centres, each one being coordinated to 1,10-phenanthroline and 2,2'-bipyridine type ligands. Each metal centre is roughly in a tetrahedral environment and hence the Cu(I) state is strongly stabilised. The electronic properties of the compound are in perfect agreement with its structure. Three different absorption bands are observed in the UV region ($\lambda_{max} \sim 240$ nm, $\varepsilon \sim 1.03$ x 10^6 Lmol^{-1}cm^{-1}, $\lambda_{max} \sim 263$ nm, $\varepsilon \sim 9.36$ x 10^5 Lmol^{-1}cm^{-1} and $\lambda_{max} \sim 355$ nm, $\varepsilon \sim 1.35$ x 10^6 Lmol^{-1}cm^{-1}), which correspond to ligand-localised transitions. A much less intense band, which is very likely to correspond to the Metal-to-Ligand Charge Transfer (MLCT) transition, is observed in the visible region ($\lambda_{max} \sim 585$ nm, $\varepsilon \sim$

5900 Lmol^{-1}cm^{-1}). The MLCT band appears at unusually low energy for bis-diimine copper(I) complexes, which is in agreement with the strong π-accepting nature of the organic ligands used, in agreement with previous observations made on copper(I) complexes with related ligands. Cyclic voltammetry shows that the Cu^{II}/Cu^{I} couple has a redox potential around 0.6 V *vs*. SCE in acetonitrile, in accordance with previously reported values for similar systems[75].

Chapter 3

Solubility problems and how to solve them

I. Solubility problems

After the threading reactions were accomplished with success, we went on with the elongation of the thread, in order to add functional groups at the endings.

In regards of further coupling of the terpyridine and the thread, either by Stille or Suzuki coupling,[67, 68] the TMS-thread **8** is converted into the iodo-thread **13** with ICl as shown in scheme 3.1.
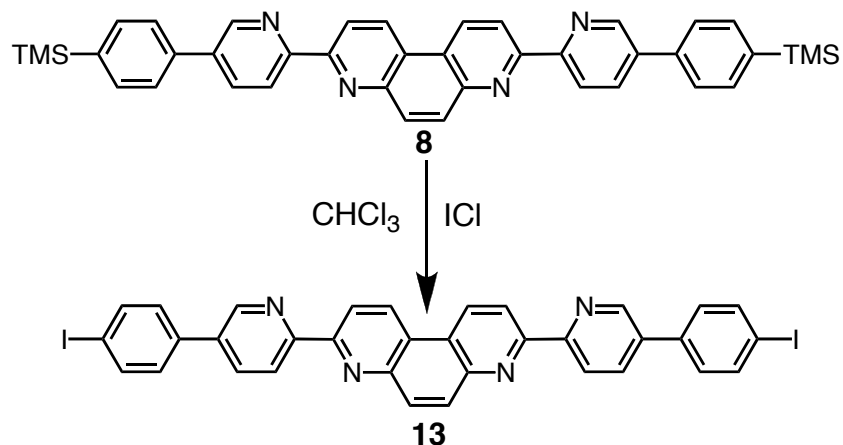
Scheme 3.1. *Synthesis of the iodo-thread 13.*

Even though the product could be obtained, as proven by microTOF mass spectrometry, it is of limited solubility. Even by adding TFA to $CDCl_3$, thus

protonating the pyridyl heterocycles, only very small peaks could be observed on the ¹H-NMR spectra. We can prove that the compound exists and that all the starting materials have been consumed, but we have no trustful indication about the purity of compound **13**. Even though coupling reactions on poorly soluble compounds are possible, adding terpyridines to a yet insoluble central part of the thread seems to be a hopeless task. Furthermore, the resulting bis-bipyridines-terpyridines thread would be absolutely insoluble, thus rendering further handling and purification very difficult, if not impossible.

Unfortunately these were not the only solubility problems we were facing. As mentioned above, the anisyl-thread **9** is of poor solubility too. After its microwave deprotection with pyridinium chloride, the obtained phenol **14** is even less soluble. Again only addition of TFA to CDCl₃ enabled us to carry out ¹H-NMR, which together with microTOF mass spectrometry proves that compound **14** had formed.

14
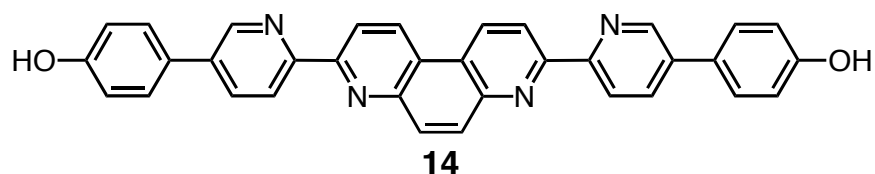
Scheme 3.2. *Very poorly soluble phenol compound 14.*

Nevertheless, we went on with the further functionalization of this thread, counting on the Cu(I) template effect to solubilize it for the threading reaction. We added polyethyleneglycol chains with allyl endings to perform later ring closing metathesis, as will be discussed later (chapter 4). By doing so, we added solubilizing groups to the thread, which nevertheless stayed poorly soluble. After threading reactions with bis-macrocycle **11**, which afforded a completely soluble mixture of products, and the following work-up, we realized that the deprotection of compound **9** to compound **14**

had been incomplete. Indeed, now that ^{1}H-NMR spectroscopy and mass spectrometry were readily accessible for this totally soluble mixture, we found that the thread we used was a mixture threads end-functionalised by either anisyl, phenol and also polyethyleneglycol. Due to its tragic poor solubility, we were forced to deal with very bad quality ^{1}HNMR spectra until the threading step. Even though the products seemed to be pure, unavoidable filtration before NMR spectroscopy might have removed the more insoluble impurities.

II. Ruthenium complex as a possible solution

Finishing the project based on such poorly soluble compounds seemed very ambitious, even hopeless, but if we could increase solubility, at least temporarily, the final threading reaction should be a reachable task.

The thread is a bis-bidentate ligand, therefore an evident solution seems to be the formation of a metal complex that could be decomplexed after all the necessary reaction steps are completed. Photoinduced decoordination of bipyridine derivatives in a $[Ru(II)(phen)_2(bipy)]^{2+}$ complex has been studied by Etienne Baranoff[76] and recently used in the laboratory by Pierre Mobian to synthesize light-driven machine prototypes.[31] Based on these results, we synthesized a $[(Ru(phen)_2)_2(\mathbf{7})]^{4+}$ complex, and investigated the photoinduced decoordination of the thread. This would have been a very elegant solution to the problem. Indeed we were able to synthesis the complex, but unfortunately photoinduced decoordination did not occur in an exploitable manner.

III. Small but powerful ethyl chains

In order to render our molecules more soluble, we decided to add alkyl chains to the thread. The synthesis of the bis-bipy core of the axle is well known, and its behaviour towards the m-30 macrocycle has been studied, (scheme 2.3, 2.10 and 2.11). Therefore we decided that this part of the molecule should be kept, and diethylphenyl units were attached at each end of the thread **7**. As a consequence of the position of the alkyl chains in-between the bipy and terpy stations, we had to limit their size to ethyl groups. Indeed, according to CPK models, longer groups would obstruct the gliding of the macrocycles on the axle; ethyl groups however are small enough to permit the free motion of the rings, even though it might be slightly slower than with no substituents. The needed diethyl-phenyl boronic acid is prepared similarly to comparable molecules in literature.[77, 78] starting from the commercially available 1,4-diethylbenzene **15** (scheme 3.3).
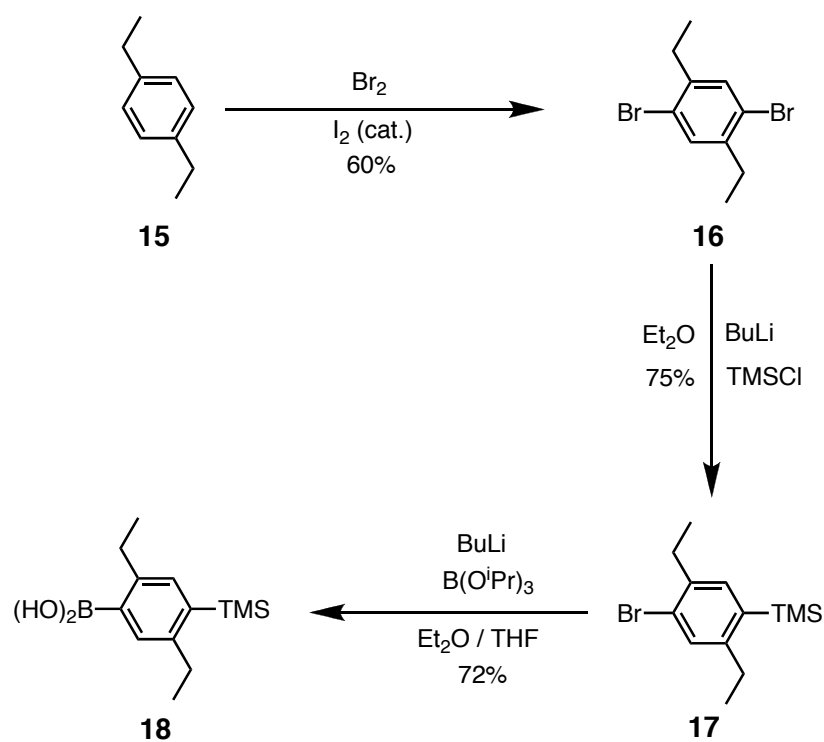
Scheme 3.3. *Synthesis of 2,5-diphenyl-4-trimathylsillyl-phenylboronic acid **18**.*

After dibromination of compound **15** to give 2,5-diethyl-1,4-dibromobenzene **16**, a first bromine atom is replaced by a TMS group upon reaction with BuLi and TMSCl to yield compound **17**. Finally the required boronic acid is obtained by reacting **17** with first BuLi, then B(O^{i}Pr)$_3$ and, subsequent, hydrolysis. The TMS group is added so as to be converted later on to an iodide and hence allow further coupling reactions. Suzuki coupling between the thus obtained boronic acid **18** and axle **7**, as shown in scheme 3.4, generates bis-bipy ligand **19**.
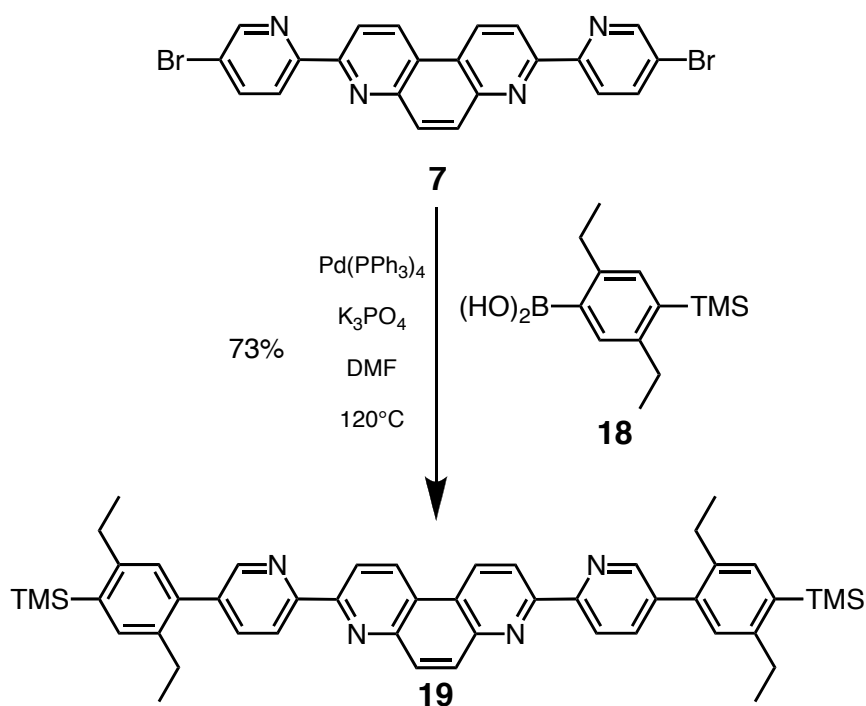
Scheme 3.4. *Synthesis of the thread core, containing ethyl solubilizing chains.*

This new compound is now readily soluble in classic solvents such as dichloromethane or chloroform, although the TMS entities add also some solubility; the short ethyl groups are very effective solubilizing agents. Even after substitution of the TMS groups by less soluble moieties, as iodo or phenolic groups, the thread stays

soluble enough to carry out effective chemistry in solution and allow easy handling of the molecule. The solubility enhancement surely results from the hydrophobic character of the alkyl chains, but it might also by partially due to the steric hindrance they induce. The co-planarity of the phenyl entities allows a large delocalization of the electron density all over the molecule, decreasing its solubility. The ethyl chains are probably forcing the phenyl ring to which they are attached to adopt a less coplanar conformation relative to the adjacent pyridyl heterocycle, the delocalization thus being less important than for the poorly soluble molecules **8**, **13** and **14**.

Having in hands a soluble molecule, a first test, to see whether the ethyl groups interfere with the threading of the macrocycles, was carried out on the axle **19**, the ring **m-30** and [Cu(CH₃CN)₄]PF₆. Using the same reaction conditions as for pseudorotaxane **10**, the threading reaction is slower but successful, giving [3]pseudorotaxane **20**, after 5 days at room temperature, which was fully characterized by mass spectrometry as well as by COESY and ROESY ¹HNMR.
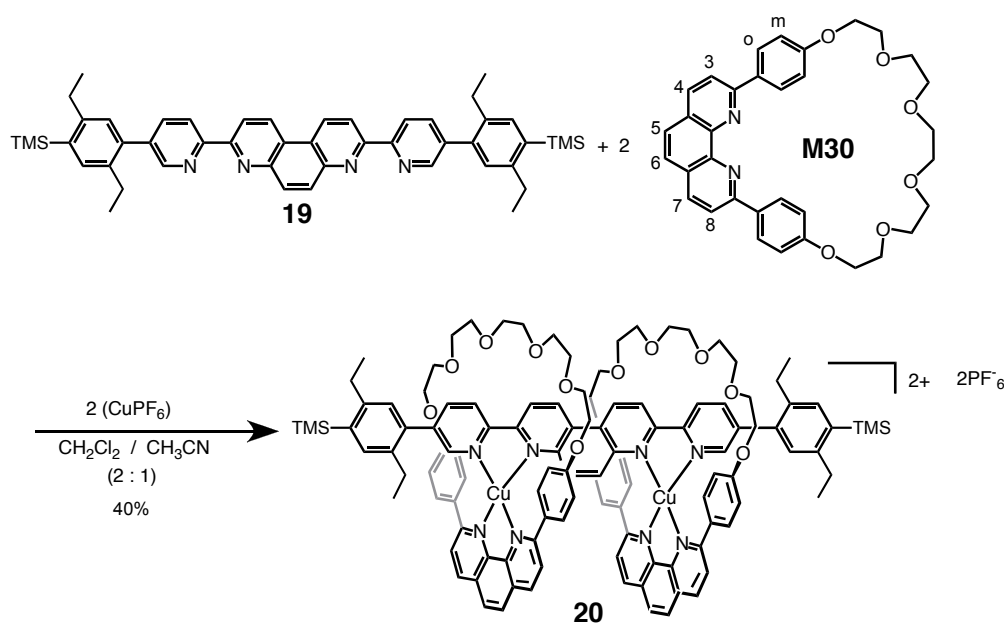
Scheme 3.5. *Threading m-30 macrocycles on an ethyl group containing thread using the Cu(I) template effect.*

The solubility problems being now solved by the ethyl groups, we can go on with further functionalization of the thread in order to add tridentate ligands, bulky stoppering groups or polyethylene glycol chains with an allyl ending, in order to synthesize a catenane.

A four copper centre [3]catenane obtained by Ring Closing Metathesis

I. Topology

"A Topologist is a person who cannot tell a coffee cup from a doughnut..."[79]

The structure of a molecule is normally described by the atoms it contains as well as by how they are connected to each other, by the nature of the bonds between the atoms and also by the arrangement around rigid centres (asymmetric centres, double bonds etc.). For most molecules, these characterizations leave no ambiguity. In some cases nevertheless, they are not sufficient as can be most easily explained by an example.

A linear, flexible molecule can form for example a torus (scheme 4.1 right), or a trefoil knot (scheme 4.1 left and middle), if both ends are linked together. According to the characteristics mentioned above, these molecules would be strictly identical, but it is impossible to switch from one conformation to another without breaking bonds, hence they are topological isomers.
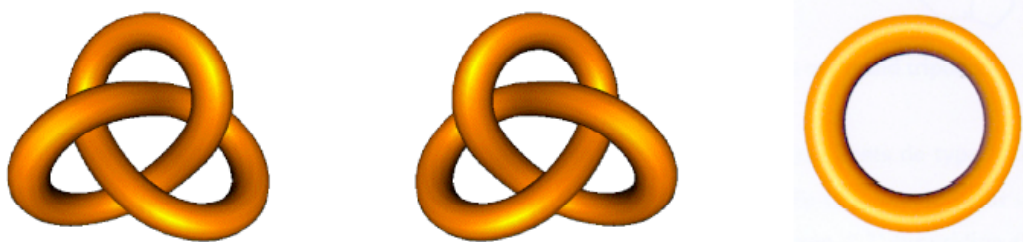
Scheme 4.1. *Topological isomers: trefoil knot enantiomers (left and middle) and torus (right).*

In the knot theory, the torus is an unknot, the simplest element of the knot family, it can be easily drawn on a two dimensional surface. The trefoil knot is topologically less trivial, it is a three-dimensional object, for which the cross-overs have to be stylised to permit a two dimensional drawing (scheme 4.2).

a

b
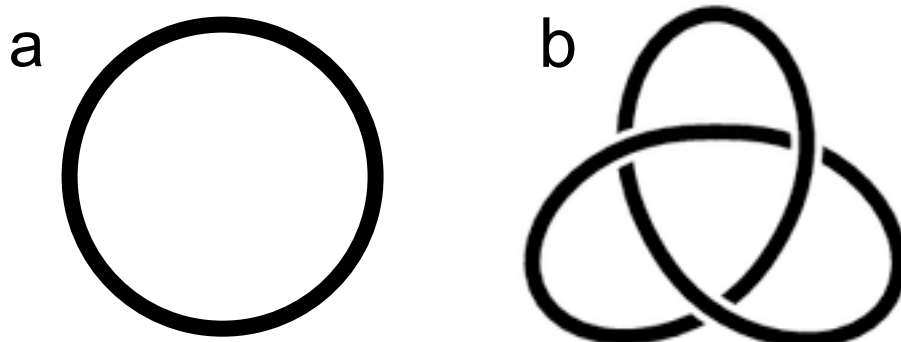
Scheme 4.2. *2D-drawings of topologically a) trivial ring and b) non-trivial trefoil knot.*

Topologically, two objects are identical if they can be transformed into one another in a continuous fashion by elongation or deformation, as long as nothing is broken and no holes are punched through during the process. Following this rule, a random stone with a hole in it, a coffee cup and a doughnut are topologically the same as a torus, they are identical topological items.

Figure 4.1. *Three topologically identical items, a stone with a hole (left), a doughnut (middle) and a coffee cup (right).*

Topological chemistry started with the stochastic synthesis of the first catenane in 1961 by Wassermann *et al.*,[80] later Schill and Lüttringhaus published[35] the first directed catenane synthesis in 1964. But it was only since the Cu(I) template based high-yield catenane synthesis by Sauvage *et al.*[36] in 1983 that the field of chemical topology grew rapidly and led to multiple topologically interesting molecules like the trefoil knot by Christiane Dietrich-Buchecker,[81] the multicatenane of Böhmer *et al.*[82] or the molecular Borromean rings published by Stoddart *et al.*[83]

II. A [3]catenane

II.1. From a rotaxane to a catenane

Based on the previously shown [4]pseudorotaxane **12** (2.II.2.), which upon demetallation would simply fall apart, we decided to synthesize a topologically interesting [3]catenane. To do so, we have to link the threads together at each end of the pseudorotaxane, as shown in scheme 4.3.
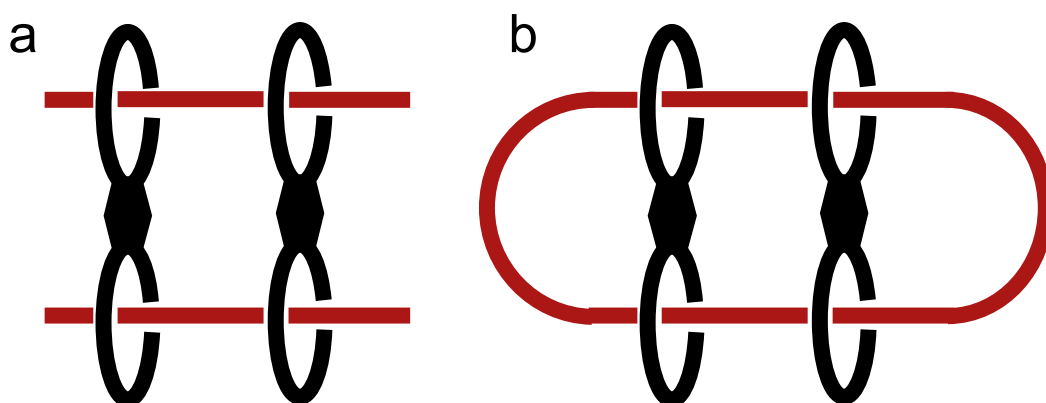
Scheme 4.3. *(a) [4]pseudorotaxane, (b) [3]catenane formed by linking the threads together to form a macrocycle (red).*

The [3]catenane (scheme 4.3 (b)) is composed by a large macrocyle, formed by the previously independent threads linked to each other at their ends, and the two bis-macrocycles. One can argue about the terminology used. The catenane is composed of three different entities, two bis-macrocycles (black), and one large macrocycle (red), therefore it is a [3]catenane (3 components). But on the other hand, if we consider the rings that are part of the catenane, (four on the two bis-macrocycles, and one large macrocycle), then we should call it a [5]catenane (5 rings). The latter terminology has been used by Böhmer et al.,[82] when they described their [8]catenane. Both nomenclatures are inefficient and give only ambiguous descriptions of the compounds. To our knowledge, no general consensus has been found yet. The synthesis of the multiple catenane, that we chose to call [3]catenane, was carried out as described below.

II.2. Synthesis

To reach our goal, the thread has to be elongated and functionalized at their endings so that they can be connected. This can be achieved by the means of polyethyleneglycol chains with allyl endings, attached on each side of the thread by a Williamson type reaction. Subsequent Ring Closing Metathesis (RCM) between two of these threads should lead to the formation of the large macrocycle.
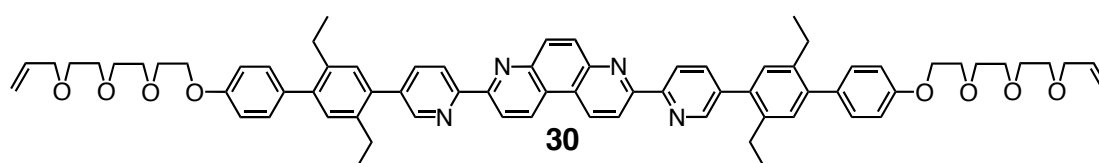
Scheme 4.4. *Elongated thread 30, able to undergo ring closing metathesis.*

To perform a Williamson type reaction on the central part of the thread, phenol groups are needed on both ends; they can be added by Suzuki coupling after the TMS groups have been changed to iodine (scheme 4.5).
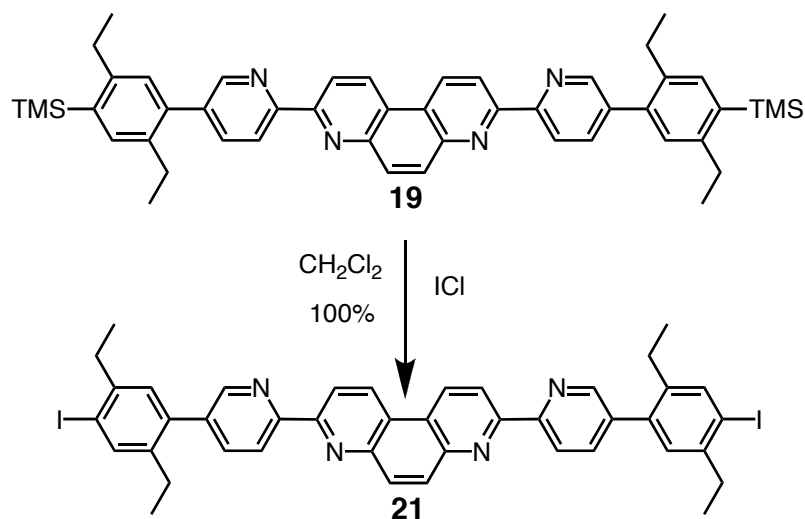
Scheme 4.5. *Preparing the axle for further Suzuki coupling by changing the TMS to Iodine.*

The commercially available THP protected *para*-bromophenol, 2-(4-bromophenoxy)tetrahydro-2H-pyran **22**, is transformed into its corresponding boronic acid **23**.
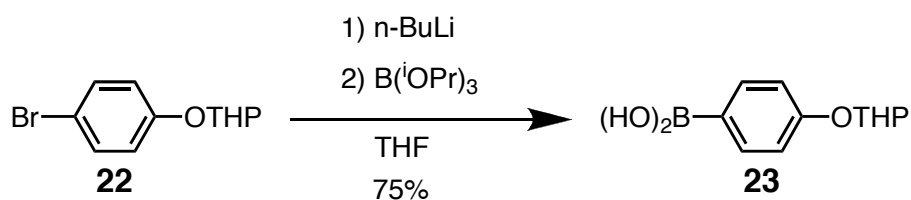
Scheme 4.6. *Synthesis of 4-(tetrahydro-2H-pyran-2-yloxy)phenylboronic acid 23.*

The THP protected boronic acid **23** is connected by Suzuki coupling to the iodo-thread **21**, to give the slightly elongated thread **24**. A satisfying yield of 75% for a double coupling reaction is an indication that the steric hindrance imposed by the ethyl groups close to the iodide do not interfere with the Suzuki coupling reaction. After deprotection of the OTHP groups, the diphenol thread **25** is obtained in a nearly quantitative yield. The thread now contains eight aromatic cycles. Despite the presence of phenol moieties at each end of molecule **25**, it can be readily manipulated and analyzed by ^{1}H-NMR. The four ethyl groups are really powerful solubilizing agents rendering the work with these molecules a feasible task.
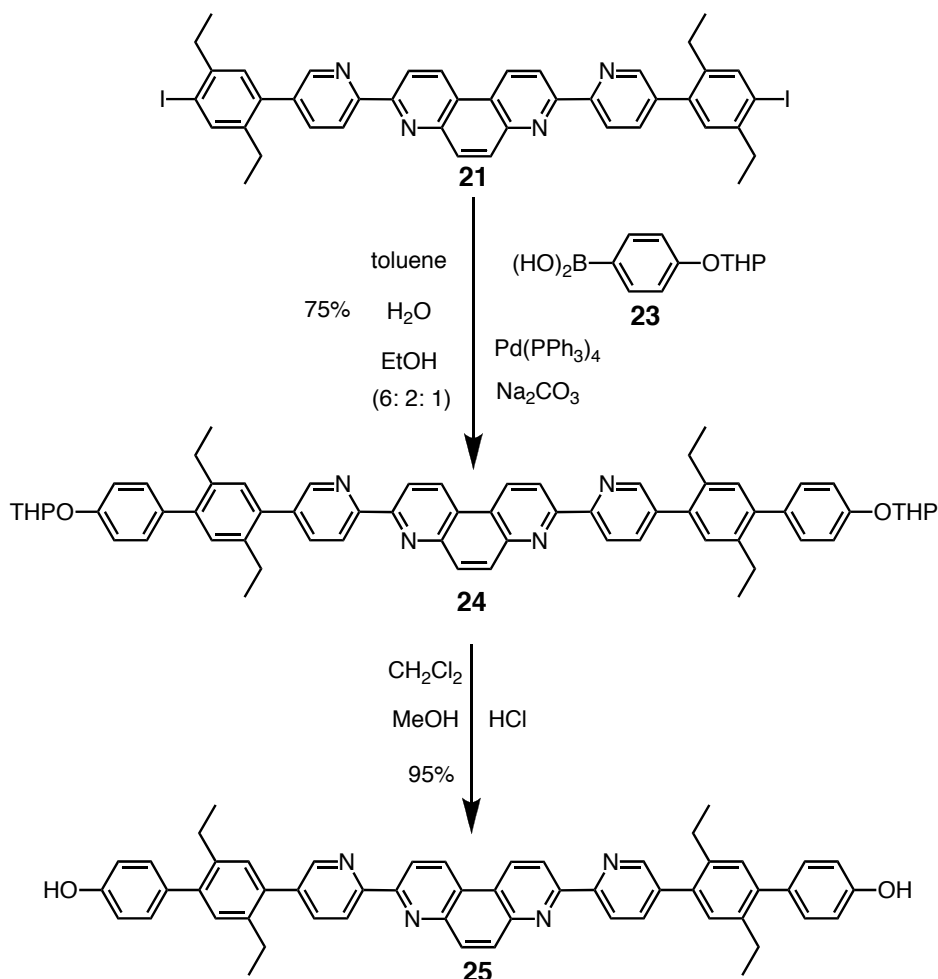
Scheme 4.7. *Synthesis of the thread 25, able to undergo Williamson type reactions.*

The polyethyleneglycol chains are prepared as shown in scheme 4.8, starting from the commercially available triethyleneglycol **26**.
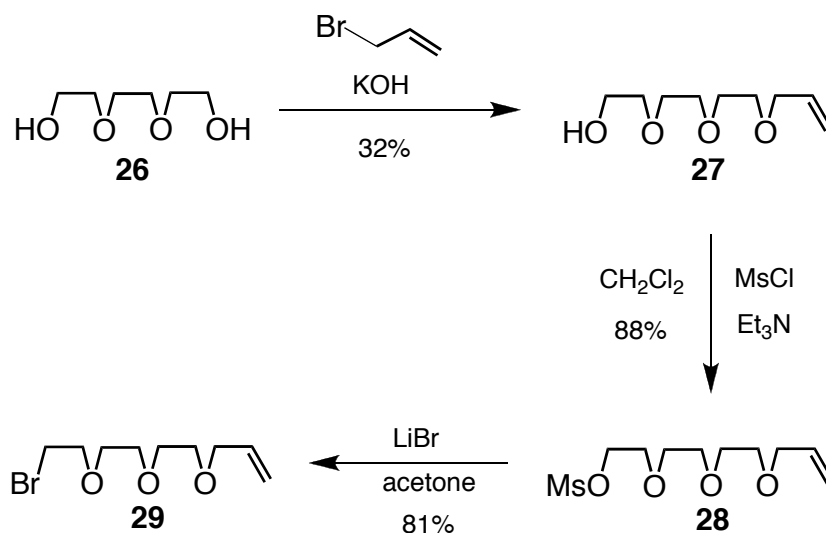
Scheme 4.8. *Syntesis of the bromo-polyethyleneglycol chain with an allyl ending 29.*

A statistical reaction with bromoallyl is carried out on the triethyleneglycol **26**, to give compound **27** in 32% yield after separation of the different products. After mesylation of the remaining alcohol group and subsequent bromination with LiBr, the final compound **29** is obtained in 81% yield. This polyethyleneglycol chain **29** is then attached to the thread **25**, by a Williamson type reaction as shown in scheme 4.9. The thus obtained thread **30** is now ready for a threading reaction with the bis-macrocycle **11**. The length of the polyethylene glycol chains has been determined by CPK modelling. Indeed, on one hand they have to be long enough, so that the two threads can be linked, once the bis-macrocycles are threaded, but on the other hand they have to be short enough to avoid RCM between two allyls of the same thread. Furthermore, the shorter the chains are, the less freedom of motion they have and the closer they are in space, thus favouring the intramolecular reactions over the intermolecular ones.

Compound **30** fulfils these conditions (Scheme 4.9). Furthermore, polyethyleneglycol chains are preferred over alkanes for several reasons:

1) they are more flexible than their alkane analogues, which should facilitate the cyclization.

2) they are most of the time readily accessible compounds.

3) they simplify ^{1}H-NMR assignations since they display several sets of signals.
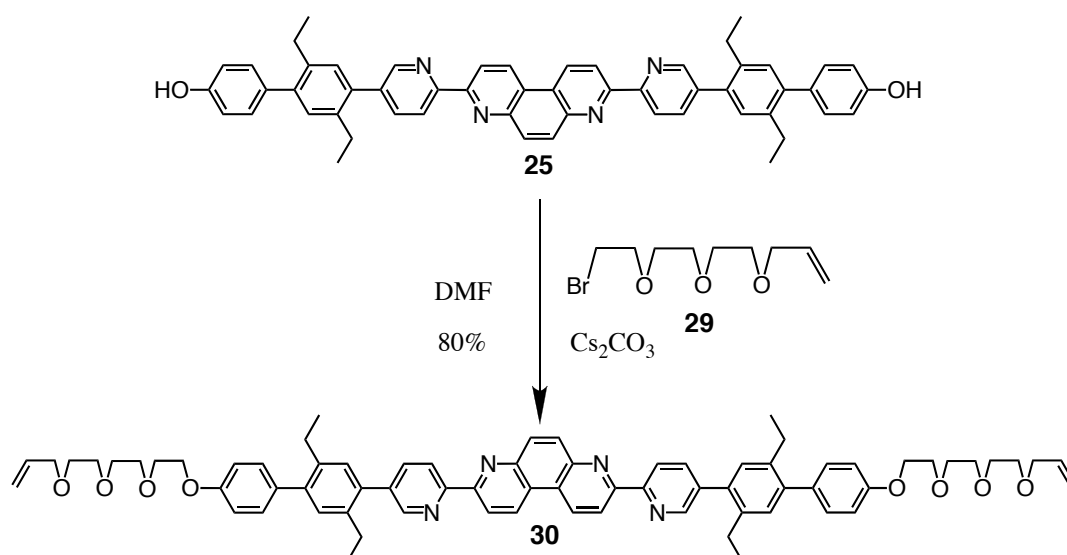
Scheme 4.9. *Synthesis of the polyethyleneglycol thread 30 by a Williamson type reactions.*

The axle **30** and two bis-macrocycles **11** are reacted with [Cu(CH$_3$CN)$_4$]PF$_6$ in typical threading reaction conditions, CH$_2$Cl$_2$ / MeCN at room temperature, to obtain the [4]pseudorotaxane **31** after 7 days in 98% yield.

$4+$, $4PF_6^-$

31
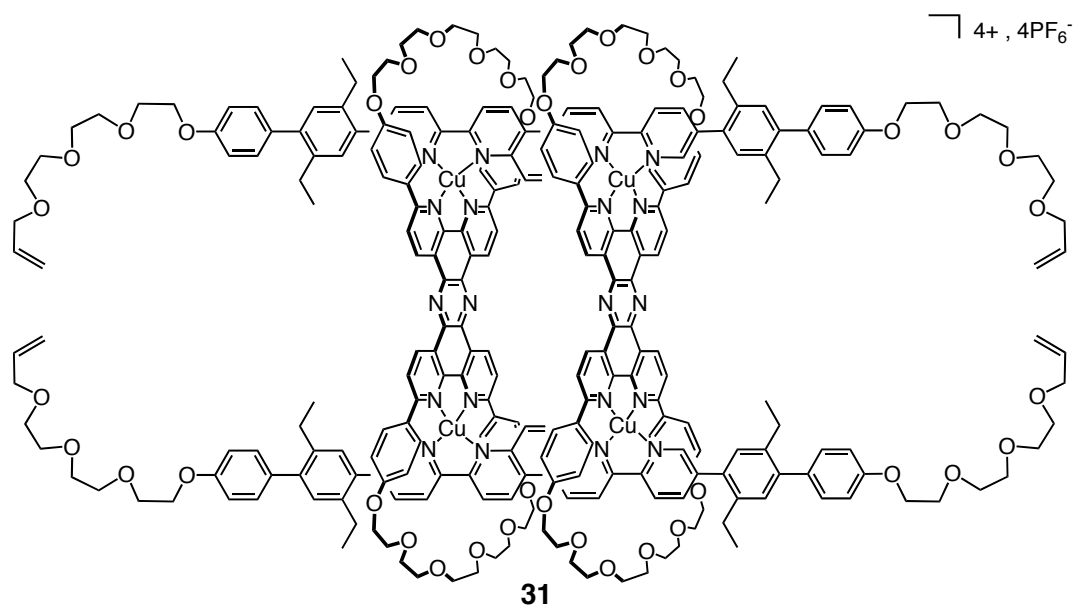
Scheme 4.10. *[4]pseudorotaxane obtained from bis-macrocycles 11 and thread 30.*

Compound **31** was characterized by ^{1}H-NMR, COESY, ROESY and mass spectrometry. The connections between the two threads is achieved by RCM reaction using a first generation Grubbs catalyst, namely [Bis(tricyclohexylphosphine)benzyilidine Ru(IV) dichloride] as shown in scheme 4.11.

Compound **31** and Grubbs' first generation catalyst (10% per pairs of olefins) were degassed with argon. The solids were dissolved in freshly distilled CH_2Cl_2 (so as to get a 10^{-3} M solution). ^{1}H-NMR monitored the disappearance of olefins signals. The reaction seemed to have come to an end after 10 days. An aqueous saturated KPF_6 solution was added until the brown material precipitates and the crude product was collected by filtration.
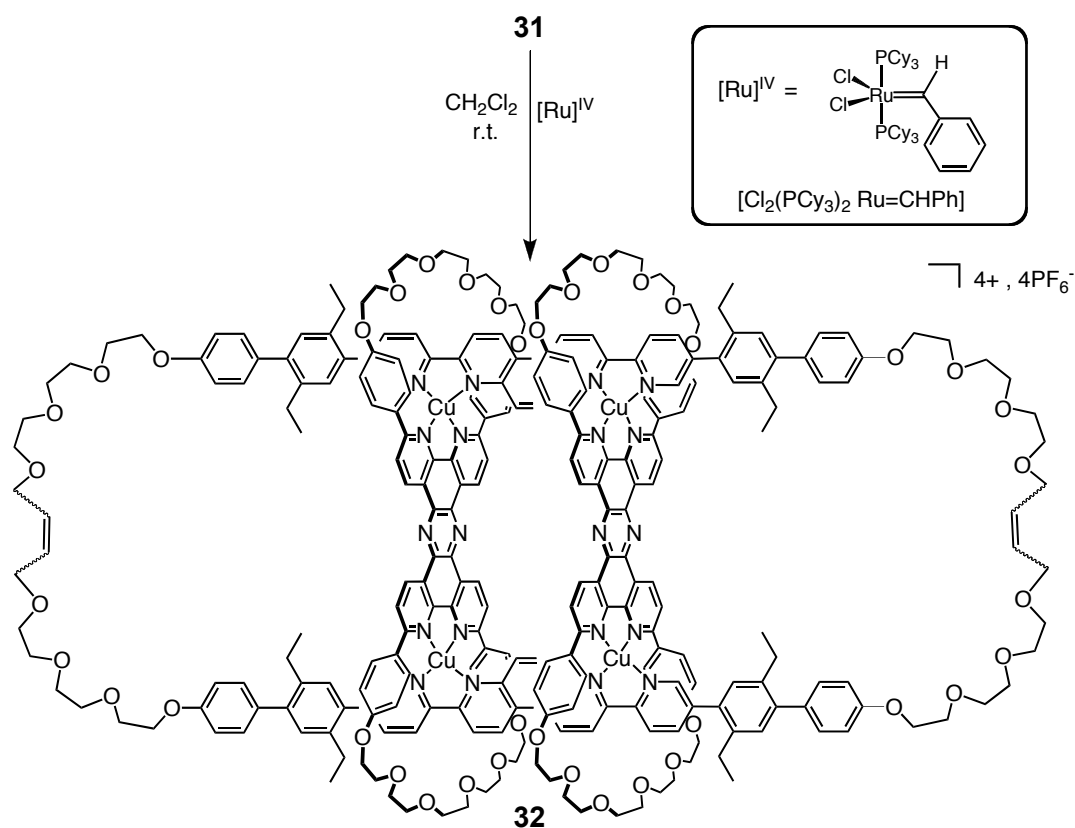
Scheme 4.11. *RCM reaction of compound 31 with 1st generation Grubbs catalyst to give 32.*

II.3. *Impossible purification of the [3]catenane?*

The first precipitation only permits to replace potential chlorine anions from the complex. The crude product was then filtered over alumina so as to remove the rest of the catalyst (ruthenium salts and phosphines) and the bis-macrocycle. In fact, during the RCM, a yellow precipitates appears (namely, compound **11**) originating from dethreading reactions.

The remaining solid was then subjected to several chromatographies (silica, gradient elution CHCl₃/MeOH from 0 to 3%). However, compound **32** could not be isolated pure, even by using other solvent mixtures as eluent. Nevertheless, the impure compound **32** was characterized by mass spectrometry and by ¹H-NMR.

We then decided to remove the Cu(I) centres, hoping that the demetallated compound would be easier to purify (Figure 4.12). Impure **32** was stirred in presence of KCN (2:1:1 mixture of CH$_2$Cl$_2$/MeCN/H$_2$O as solvent). After 1 hour, the brown colour completely disappeared; the remaining bright yellow solution was abundantly washed with water, organic layers were separated and evaporated to dryness giving impure **33**.

32

CH$_2$Cl$_2$ / MeCN / H$_2$O
(2:1:1)   KCN

33
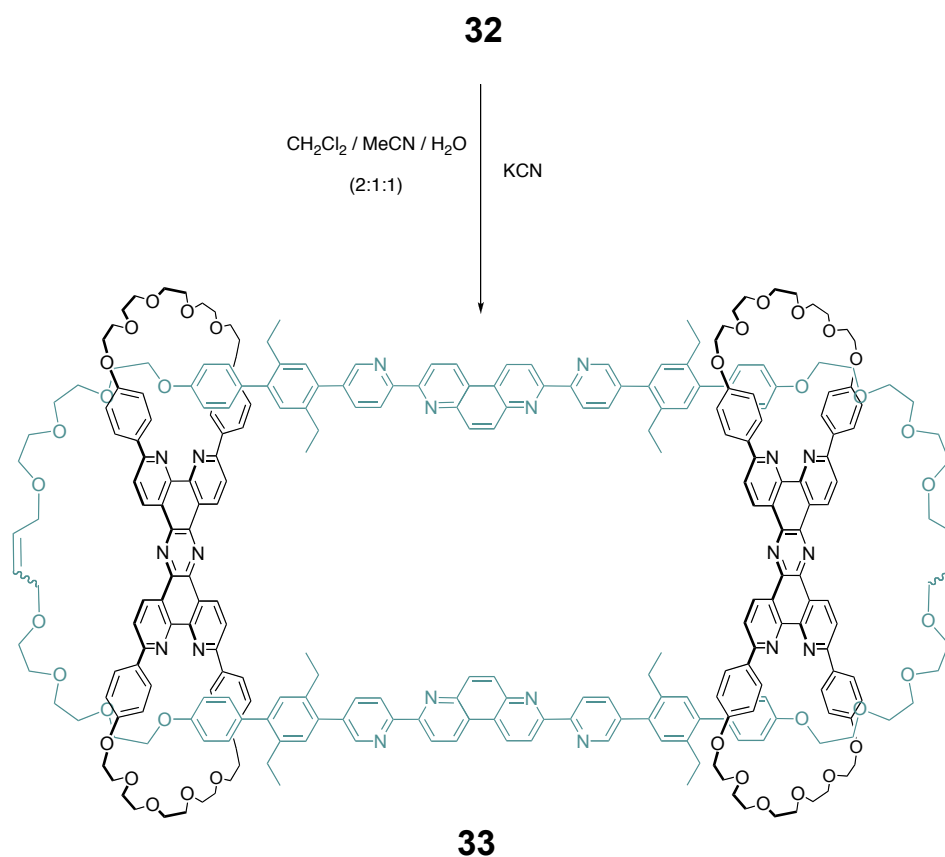
Scheme 4.12. *Demetallation of impure [3]catenane 32 leading to free [3]catenane 33.*

This second crude mixture showed to be also highly contaminated by the bis-macrocycle **11**, which points out that the cyclization is inefficient despite the clear modifications of the olefins, observed by ^{1}H-NMR. However, we have no precise idea about the nature of these "open" impurities, hence it is difficult to foresee what kind of improvement(s) could be propose for this procedure.

Anyway, the retention factor of **33** compared to the one of the side-products leaves hope for a better separation on chromatography. Unfortunately the problem is only delayed, the demetallated compound sticks very strongly to the support (alumina or silica) and thus gives rise to inhomogeneous progression while eluting. At this stage, the only "valuable" method is the use of preparative TLC (silica – thickness: 2 mm). After several elutions (with $CHCl_3$ / MeOH 96:4), a large band can be separated from the bulk impurits bands (Figure 4.13). But even this nice looking product is not totally pure on TLC and according to mass spectrometry.
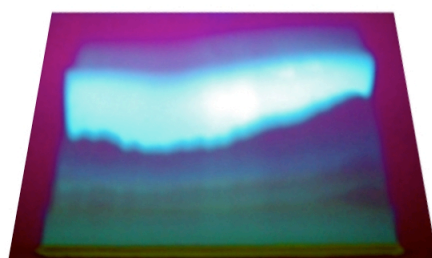
Figure 4.2. *Picture of the preparative TLC during the purification of the [3]catenane 33 (UV irradiation at 365 nm). The large blue band contains the desired compound.*

These failures of our purification attempts might be explained by the kinetic lability of the copper(I) complexes; this dynamic character could allow interactions between the ligands (a dianisyl-phenanthroline and a bipyridine) and the catalyst, thus causing the degradation of the latter. The equilibrium between the ligands and the Cu(I) centres can also be affected due to the presence of excess metal centres (Ru) to which the thread or the macrocycles can bind.

Despite their high activity and functional group tolerance,[84-86] one of the major limitations for the use of ruthenium carbene catalysts is their lifetime and efficiency. As a result, the ring-closing metathesis of large rings (116 atoms in the present case) requires increased catalysts loading in relatively diluted media. Furthermore, catalyst

degradation sometimes leads to unwanted side reactions, such as olefin isomerizations.[87-89]

Nevertheless, the existence of demetalatted catenane **33** is proven by HR ES-MS analysis. Two peaks can be observed at m/z ratio of 1505.3518 and 2257.5153 corresponding to [**33** + 3H]$^{3+}$ and [**33** + 2H]$^{2+}$, respectively. Unfortunately, the purity of the compound is still not satisfying. With only 3 mg of the compound left, we will probably not be able to isolate the [3]catenane in its pure form.

However we succeeded in the synthesis of the metallated [3]catenane **32** as well as of its demetallated counterpart **33**. Unfortunately, despite all our efforts, we could not isolate them in their pure form. This drawback is mostly related to the previously discussed problems with ring closing metathesis reaction (RCM), leading to several impurities that we were unable to remove.

Nevertheless, the precursor for these catenanes, namely the [4]pseudorotaxane **31** was obtained in its pure form and fully characterized. This compound constitutes in itself a non-trivial 4 metal centre assembly, that was obtained nearly quantitatively by taking advantage of the powerful gathering and threading effect of Cu(I). These results, combined with those from the [4]pseudorotaxane **12** (see chapter 2.II.2) show that such two dimensional devices can be obtained in very good yields by starting from well pre-organized ligands.

The threading itself being very successful, one can imagine using different threads, with different functional groups at their ends. We can think of using azide endings to attach bulky groups on each end by using the "Meldal-Sharpless" reaction (discussed later in section 5.II.2). This feature could then lead to a topologically interesting demetallated [4]rotaxane with two macrocycles and two "stoppered" threads.

Chapter 5

A first simplified press based on a [3]rotaxane

I. The system

A next step towards the final press containing four anchoring stations on the thread is a simplified model with only two ligands on the thread part. Indeed, one can imagine a press based on the bis-bidentate thread and two macrocycles containing a capture unit for a guest molecule. When the system is in a Cu(I) complex form, it is the metal centre that determines the position of the macrocycles on the thread, the phen of the m-30-like macrocycle sits over the bipy of the thread to offer a four coordination environment to the Cu(I). When the structure is demetallated, the rings are more or less free to move on the thread, in this case, it is the guest molecule that imposes the distance between the two rings, provided the guest remains attached to the capture units. Remetallation brings the rings back to the bipy stations and the guest molecule will have to accommodate to the offered space. Thus one can imagine elongating and contracting a molecule as shown in scheme 5.1.

Rigid guest molecules can be trapped inside the press in the extended state, and released by switching to the contracted situation, which does not offer enough space to the unbendable molecule. Smaller rigid molecules can also fit inside the contracted press and be released once the press is opened.
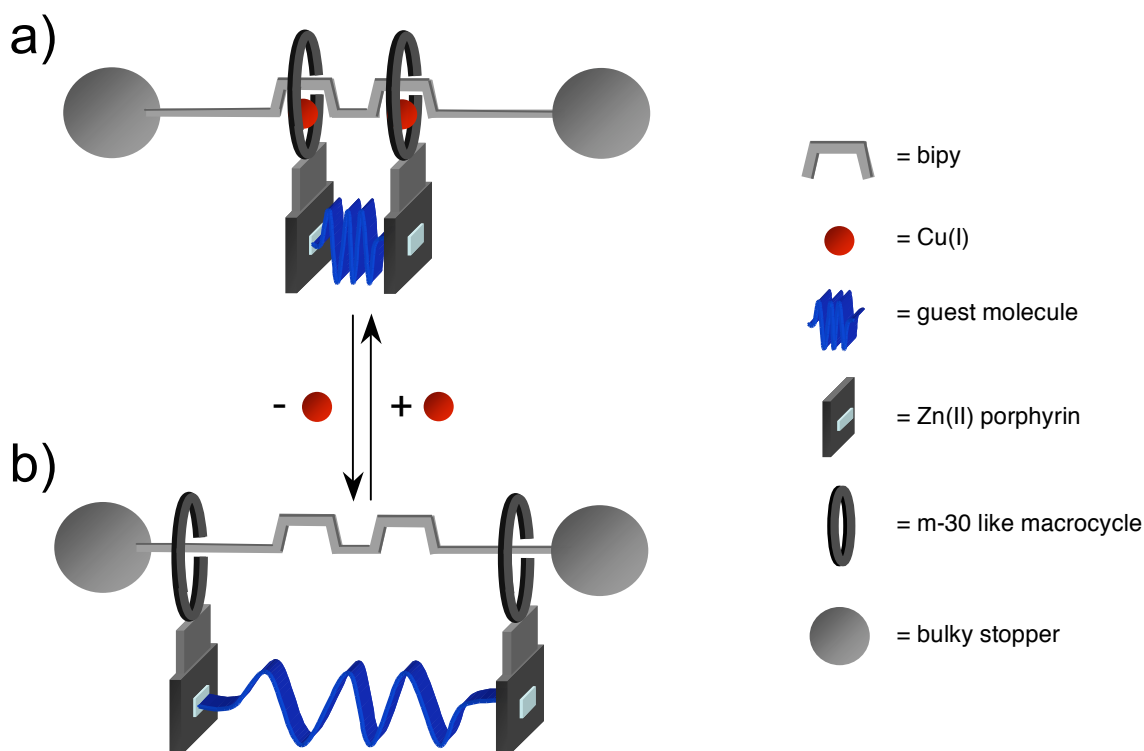
Scheme 5.1. *A two chelating site based nano-press a) in its contracted situation the Cu(I) metal centres determine the position of the macrocycles on the thread, the phen of the ring sits on the bipy of the thread, thus offering a tetracoordination site to the Cu(I), the guest molecule has to adopt its conformation to the offered space and is hence folded. b) After demetallation, the macrocycles are free to glide on the thread and the guest molecule can extend itself to its preferred conformation and thus determines the position of the rings.*

All this mechanism depends obviously on the binding constants of the guest molecule to the acceptor units. This is even more true because the guest molecules can also bind on the "outside" of the capturing units. These parts of the press are Zn(II) porphyrin, which can use the free fifth Zn(II) binding site (in light blue on scheme 5.1) either on one side of the porphyrin or the other. Nevertheless, if the guest molecule has two coordination sites and is short and/or rigid enough, it can only bind to two porphyrins of the same press if it is on the inside. This binding mode should be

thermodynamically preferred over the simple binding or the double outside binding to two different presses.

The bulky stoppering groups on each side of the thread, which make it a real [3]rotaxane, are necessary to avoid dethreading of the rings once the system is demetalated.

To build such a press, we designed a system based on a porphyrin, attached to an m-30-like macrocycle **34**, synthesized by Julien Frey in the laboratory[90], and the existing bis-bipy thread **25**.
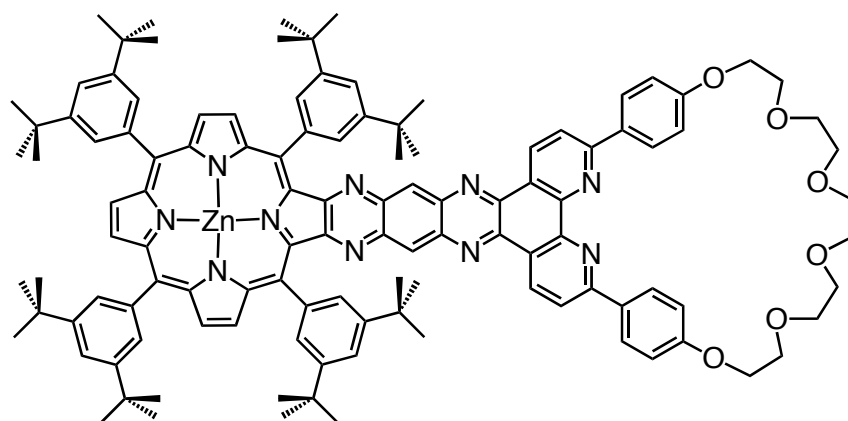
34

Scheme 5.2. *Compound 34, a Zn(II) porphyrin attached to a **m-30** like macrocycle by a tetraazaanthracene spacer.*

m-30-like macrocycle **34** is connected on the phenanthroline "back" by a tetraazaanthracene unit to a Zn(II) pophyrin. The porphyrin contains four di-tertiobutylphenyl units in the meso positions, which act as solubilizing groups. As mentioned before, the Zn(II) is tetracoordinated to the porphyrin, thus leaving one binding site free to be used as a docking station for the guest molecule.

II. The synthesis

At first the unstoppered pseudorotaxane is obtained by threading the macrocycle **34** on the phenol ending thread **25**. As for other pseudorotaxanes described above, the threading reaction was carried out, in presence of $[Cu(CH_3CN)_4]PF_6$ in CH_2Cl_2 / MeCN (2:1) at room temperature in absence of oxygen and light for 5 days. Monitoring the reaction progress and the purity of the final compound by TLC is a tricky task, indeed dethreading occurs while the complex migrates on silica or alumina plates. It is only after ^{1}H-NMR spectroscopy, that we can tell for sure whether the reaction is complete or not. We have to deal with the same problem whenever column chromatography on such complexes is to be monitored by TLC. Nevertheless, if the reaction mixture is left long enough to allow rearrangement of the different transition species formed, the thermodynamically favoured pseudorotaxane **35** is obtained quantitatively and fully characterized.
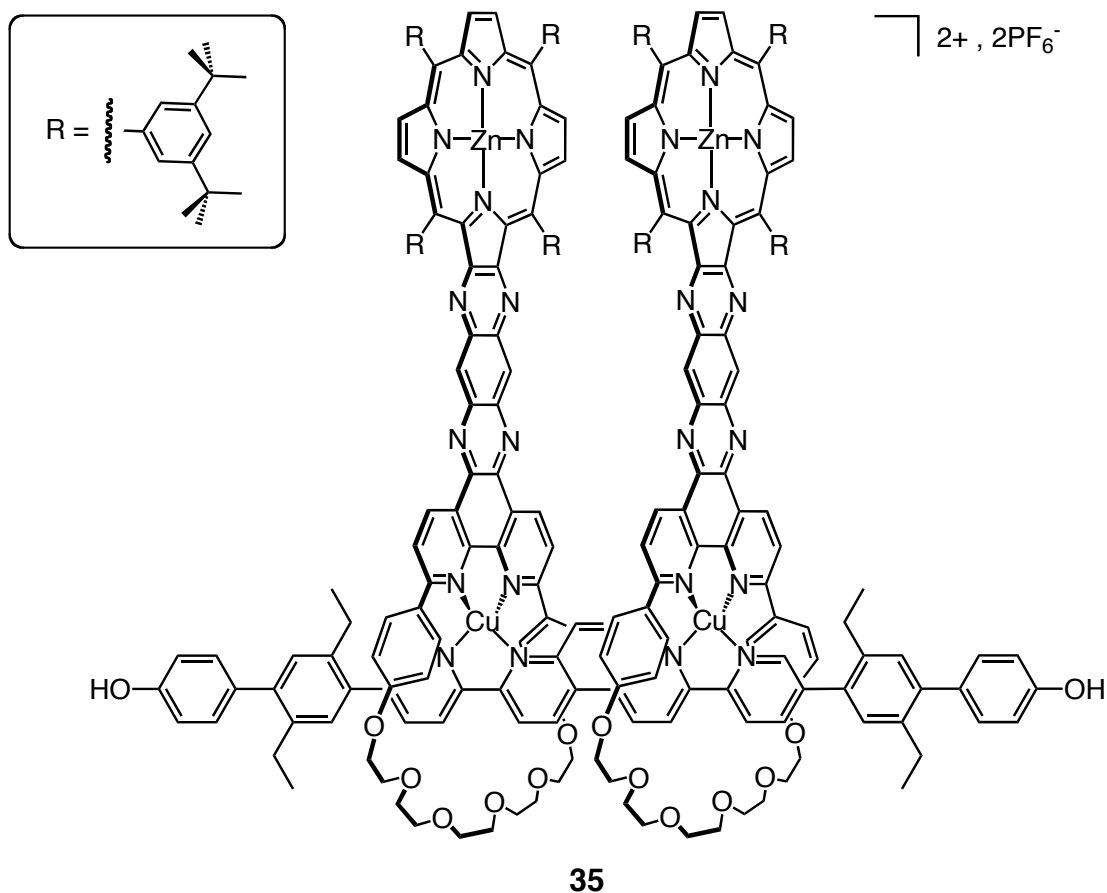
Scheme 5.3. *[4]pseudorotaxane 35 with two phenol endings on the thread.*

II.1. Williamson reaction

The phenol thread is chosen for this pseudorotaxane because it enables us to "stopper" the system by adding bulky groups *via* a Williamson type reaction. This synthetic path for rotaxane formation has been used several times in our laboratory.[63, 91] A first attempt to add bulky groups to the thread is carried out with "stopper" **36**, taken from a stock left in the laboratory by Jean-Claude Chambron.[92]

36
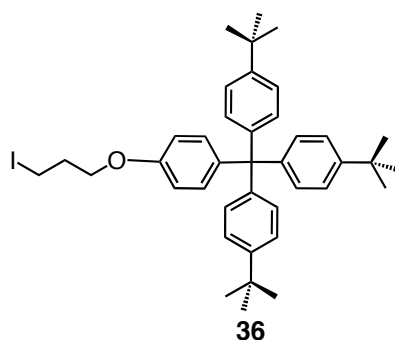
Scheme 5.4. *Bulky stoppering group able to undergo Williamson-type reactions.*

Williamson-type reactions are carried out in basic solutions with little heating (40-60°C). Under these conditions, dethreading of the system is quite likely to happen because they destabilize the Cu(I) complex more or less, depending on the ligands. On one hand the macrocycle is based on a diphenylphenanthroline, which has shielding phenyl units that protect the Cu(I) metal centre. The ligand on the thread on the other hand is basically a simple bipyridine, which is known to render the complex vulnerable to dethreading because of its lower stability towards the reaction conditions. To avoid this unwanted decomposition of compound **35**, special precautions are taken during the synthesis.

- The heating is limited to 40°C

Lower temperatures reduce the dethreading risk, but also slow down the Williamson raction.

- Cs$_2$CO$_3$ is used as a base

The bulky cesium cation enhances the nucleophilicity of the phenolate formed, thus accelerating the stoppering reaction, leaving less time to the decomposition.

- Base and stopper are added bit by bit[19, 92]

A fifth of the total amount of Cs$_2$CO$_3$ is added, followed by a fifth of the stopper, then after one hour of stirring, the same amounts are added. This cycle is repeated until addition of the reagents is completed. By doing so, we hope to limit the amount of free base in the solution, thus reduce the basicity of the reaction mixture and render the conditions less hostile for the pseudorotaxane.

Despite all these precautions, the final product is a mixture containing among others, the monostoppered pseudorotaxane, with one or two macrocycles still on the thread. The thread with two stoppers was also observed, but only one ring was present on the thread. Even though the target compound was present, the yield was very bad, and purification impossible. Therefore we decided to try another Williamson reaction using this time stopper **38**. We thought that the drawback from the first reaction was mainly due to the stopper. Indeed the iodopropyl part of the stopper **36** is able to undergo elimination reactions in alkaline media, thus rendering it inactive towards Williamson reactions. The bromobenzyl ending of stopper **38** on the contrary is known in the laboratory to have a good reactivity towards this kind of reactions[19] and undergoes less elimination side-reactions. It was synthesized according to literature[93] starting from the phenol stopper **37** taken from the laboratory stock, which was then reacted with bromoxylene (scheme 5.5).
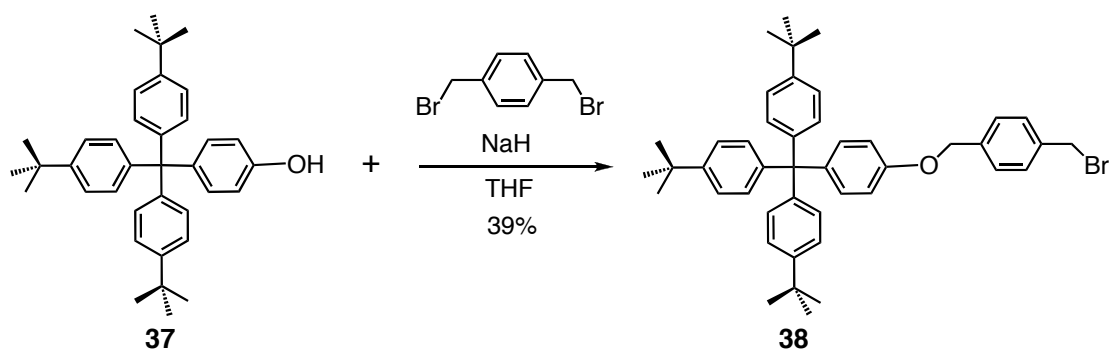
Scheme 5.5. *Synthesis of bromobenzyl-ending stopper 38 by Williamson reaction.*

Unfortunately, the results were very similar to those we observed the first time. Although a lot of effort was put into the separation and purification of the different compounds, no satisfying results could be obtained. It seems that under the Williamson reaction conditions, the Cu(I) complex is too unstable, and dethreading occurs before the two stoppers can be grafted on the thread. Having two rings that can undergo dethreading obviously worsens the situation. We tried to stabilize the complex by adding one equivalent of dabco (1,4-diazabicyclo[2.2.2]octane), which (as shown by ^{1}H-NMR spectroscopy) is located between the two Zn(II) porphyrins, and bound to both of them. The so formed connection between the two entities should help keeping the macrocycles on the thread, but unfortunately no improvement can be observed in Williamson conditions. After a third failure, this time with a terpyridine-containing stopper, (which will be discussed in chapter 6), we decided to give up the Williamson-type reaction and to search for another solution.

Recently in our laboratory, a double stoppering reaction has been carried out on a very labile Cu(I) complex by Pierre Mobian.[94] The system is based on a 5,5'-diazidomethyl-2,2'-bipyridine as a thread, and a m-30 macrocycle. The coordination sphere of the Cu(I) centre is very similar to the one of our complex (bipy-phen), but the thread is much shorter, thus rendering the dethreading process even faster. The Huisgen reaction used for the stoppering of the pseudorotaxane was successful and gave the final rotaxane in 62% yield, (79% for one Huisgen reaction). Encouraged by these results, we decided to synthesize a bis-bipy thread able to undergo this kind of reactions to finally obtain the desired rotaxane.

II.2. Huisgen reaction[95, 96], "click"- chemistry

In 1960's Rolf Huisgen[97] systematically studied the general application of [1,3]-dipoles in organic chemistry, one of them being the cycloaddition of organic azides and alkynes to give [1,2,3]-triazoles. These reactions have high activation energies (24-26 kcal/mol) and are therefore very slow and need elevated temperatures. Moreover the final product is a mixture of different regioisomers.[98]

In 2002, Morten Meldal *et al.*[99] and, nearly simultaneously, Barry Sharpless *et al.*[100] published a regiospecific copper(I)-catalyzed [1,3]-dipolar cycloaddition between terminal alkynes and azides, that can be run at room temperature and under mild conditions, giving only the [1,4]-triazoles regioisomers. The stability of the azides towards H_2O, O_2 and the majority of organic synthesis conditions as well as the simple reaction procedure, have made this Cu(I)-catalyzed reaction a member of the "click"-chemistry family - a concept introduced by Barry Sharpless, which regroups reactions that have a wide scope, high yields, are easy to perform starting from readily available reagents and feature high selectivity.[101]
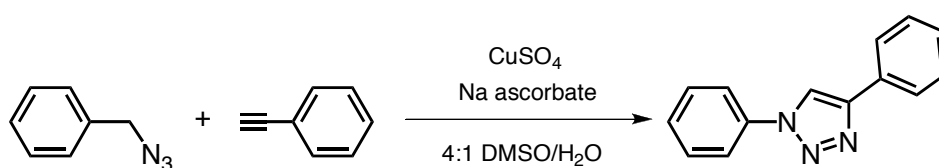
Scheme 5.6. *Example of a copper catalyst "Meldal-Sharpless" reaction*[102]

II.3 Synthesis

To be able to carry out this kind of "click"-chemistry reaction, we have to functionalize the thread with an azide at each end. The bis-bipy thread with the ethyl groups has been well characterized, its synthesis is well known and it has been used to

assemble rotaxanes and catenanes, therefore we decided to keep the trunk of the thread and to modify only the outer parts. This decision was supported by the fact that we can obtain the azide groups in a two-step synthesis starting from the phenol-thread **25**. The first step is a Williamson reaction between axle **25** and the commercially available α,α'-dibromo-*p*-xylene **39** (scheme 5.7).
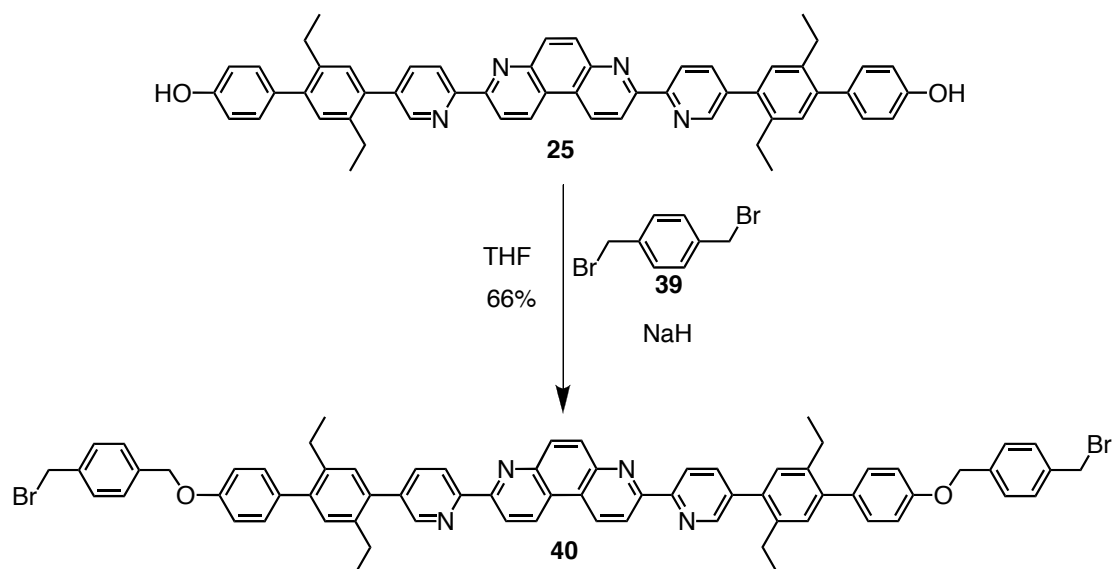
Scheme 5.7. *Synthesis of thread 40 by Williamson reaction with α,α'-dibromo-p-xylene 39.*

To avoid the formation of polymers, a large excess of α,α'-dibromo-*p*-xylene (15 equivalents) was used. The final compound **40** can be easily obtained upon simple washings with ethanol and water. The thus obtained bromobenzyl-thread is reacted with NaN$_3$ to obtain the azide-thread **41** in 60% yield (see scheme 5.8)
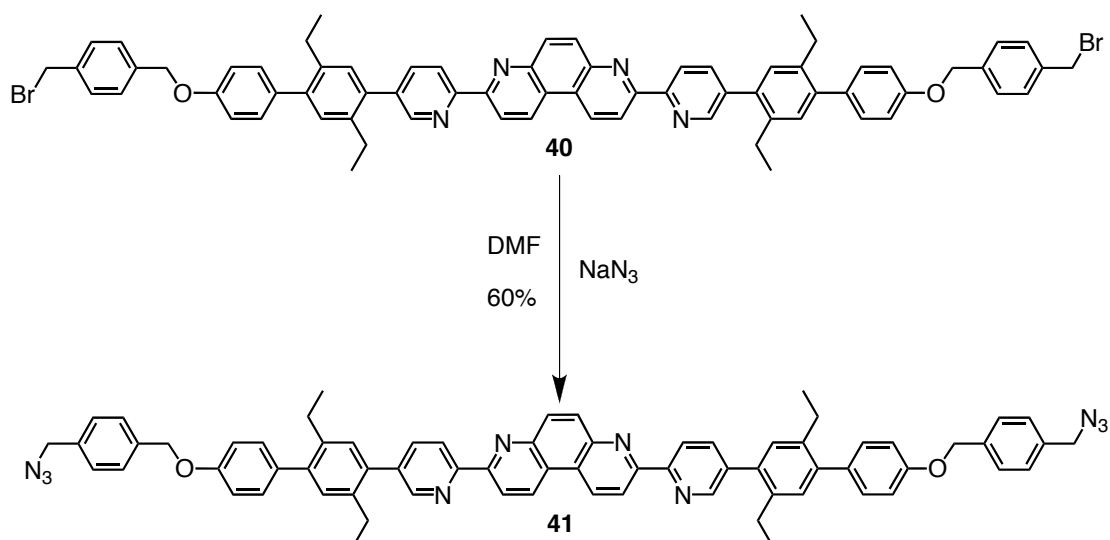
Scheme 5.8. *Synthesis of the azide-thread 41.*

The product was purified by column chromatography, which is essential towards the subsequent threading reaction. The thermodynamically favoured pseudorotaxane can only be obtained quantitatively if no impurities are present that could interfere with the equilibrium. Indeed respecting the stoichiometry is very important for this kind of reactions, and is obviously only possible if compounds of high purity are used.

The pseudrototaxane **42** is synthesized under the same conditions as all its predecessors by threading **41** into macrocycle **34**, using $[Cu(CH_3CN)_4]PF_6$ in a degassed solvent mixture of CH_2Cl_2 and MeCN (2:1), as shown in scheme 5.9. After 3 days at room temperature, in absence of light and oxygen, the [3]pseudorotaxane **42** is obtained in 100% yield and characterized by ^{1}H-NMR as well as by ES-MS.
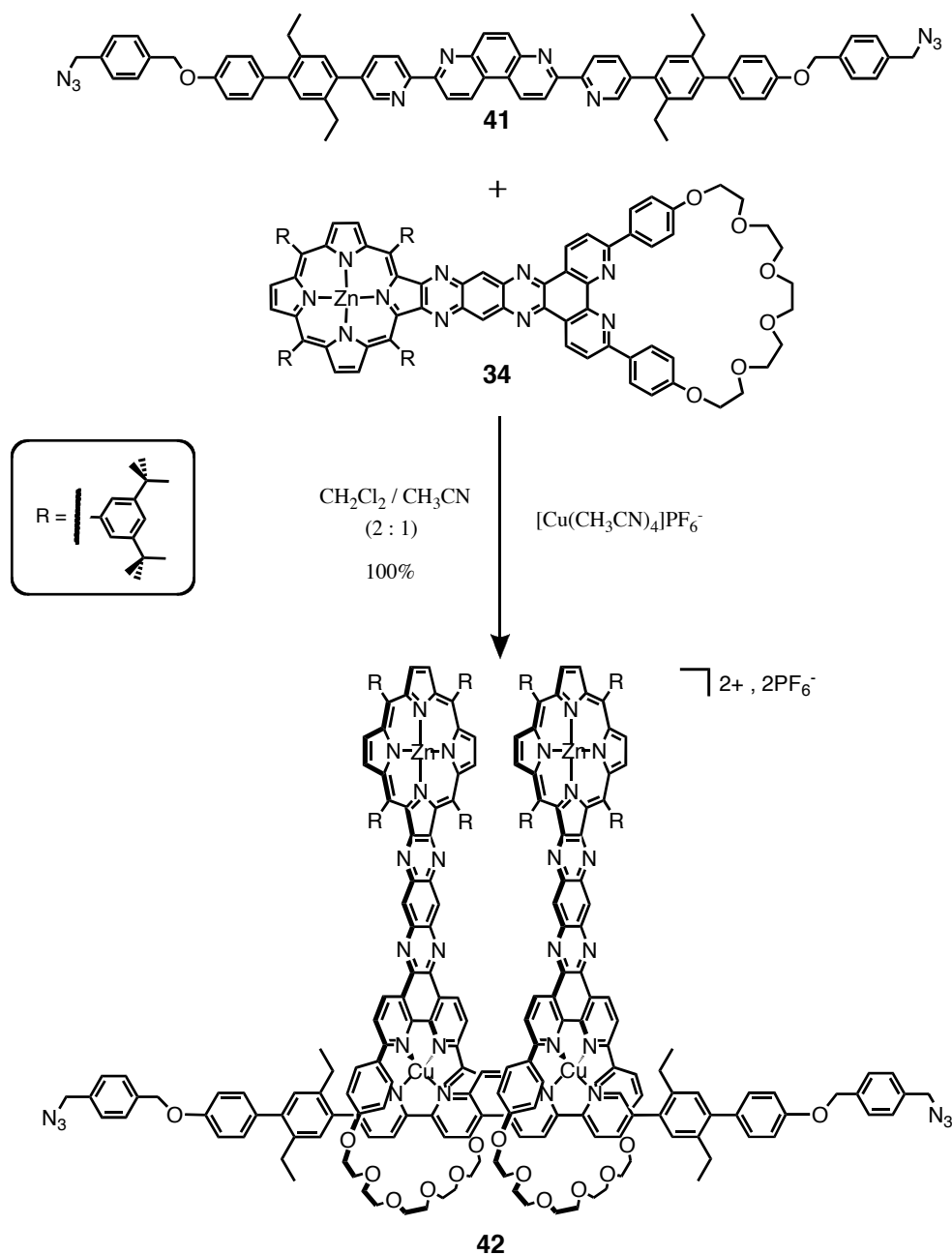
Scheme 5.9. *Threading reaction between azide-thread 41 and macrocycle 38 based on the Cu(I) template effect.*

The stopper **43** used to change the pseudorotaxane into a rotaxane is synthesized by Julien Frey according to literature[93, 94] starting from the phenol stopper **37**[93] (see scheme 5.10).
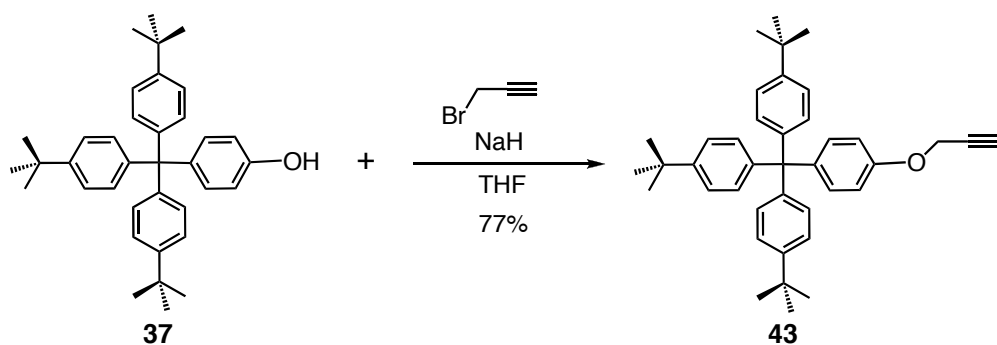
Scheme 5.10: Synthesis of the terminal alkyne stopper **43** starting from phenol-stopper **37**.

Now that all the starting materials for the Huisgen (or "click") reaction are available, we proceed to the stoppering of the pseudorotaxane. The conditions are, as mentioned already above, very mild. The catalyst that is used is Cu(I), the same metal ion around which the rotaxane complex is formed, therefore there should be no problem due to metal exchange reactions. Whereas up to 10 equivalents of base are used for a Williamson reaction, here we only use the "catalytic amount" of 40% (20% per azide) of sodium carbonate as a base. The solution is therefore much less alkaline and hence the dethreading side-reaction should be less important, even more so because no heating is necessary for this copper catalyst [1,3]-dipolar addition (see scheme 5.11).
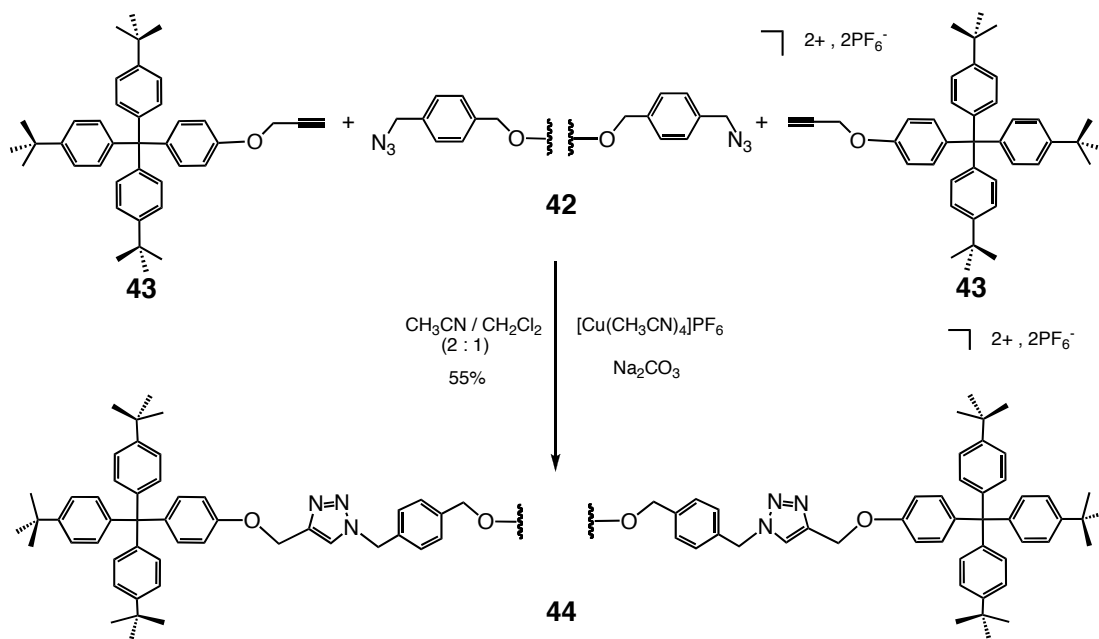
Scheme 5.11. *[1,3]-dipolar cycloaddition reaction giving rotaxane **44** (scheme 5.12).*

As foreseen, the decomposition of the complex is under these conditions less important, and rotaxane **44** (scheme 5.12) is obtained in 55% yield after purification by column chromatography on silica.

One can argue about the "click"-character of this reaction. The 55% yield as well as the time consuming and tedious purification of this compound, involving several column chromatographies (each lasting up to 5 days), is not in agreement with a supposed high yield and easy to perform reaction. But all this inconveniences are mainly related to the complexity of the rotaxane entity and not to the "Meldal-Sharpless" reaction itself. After washing the crude reaction mixture with H_2O, its ^{1}H-NMR spectrum leads to the assumption that the stoppering reaction itself was a success and might respect the click-reaction criteria (section II.2.1). This can be affirmed as being a general statement. The success of the stoppering reaction on rotaxanes of this kind depends mostly on the stability of the complex under the given

conditions rather than on the reaction efficiency itself. (See also chapter 6, scheme 6.9).

Whether this reaction can be considered as a click reaction or not is only of minor importance for our work. The [3]rotaxane **44** is finally obtained and fully characterized by cyclic voltammetry, UV/vis spectroscopy, mass spectrometry (ES-MS) as well as ^{1}H-NMR (1D, COESY, ROESY, DOSY).

Figure 5.1 shows the aromatic region of the 1D ^{1}H-NMR spectrum of rotaxane **44**, please see scheme 5.12 for the corresponding atom labels.
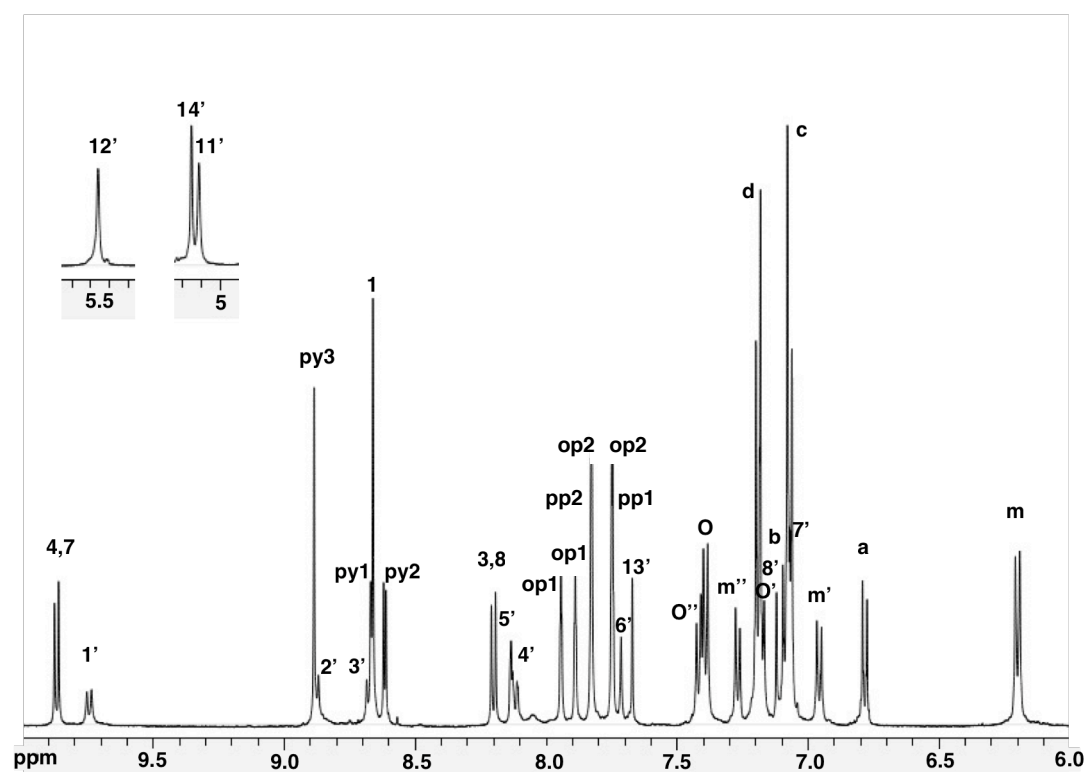
Figure 5.1. *^{1}HNMR (500MHz, CD$_2$Cl$_2$, 25°C) spectrum of rotaxane **44** displaying the peaks in the 5 to 10 ppm range. (See scheme 5.12 for atom labelling). Protons that are part of the thread are marked with a prime (').*

ROESY NMR coupling:

Thread		Macrocycles
$H_{6'}$	coupling with	H_o
$H_{7'}$	coupling with	H_m
$H_{8'}$	coupling with	H_m

Thread coupling with stopper

$H_{12'}$	coupling with	$H_{13'}$
$H_{13'}$	coupling with	$H_{14'}$
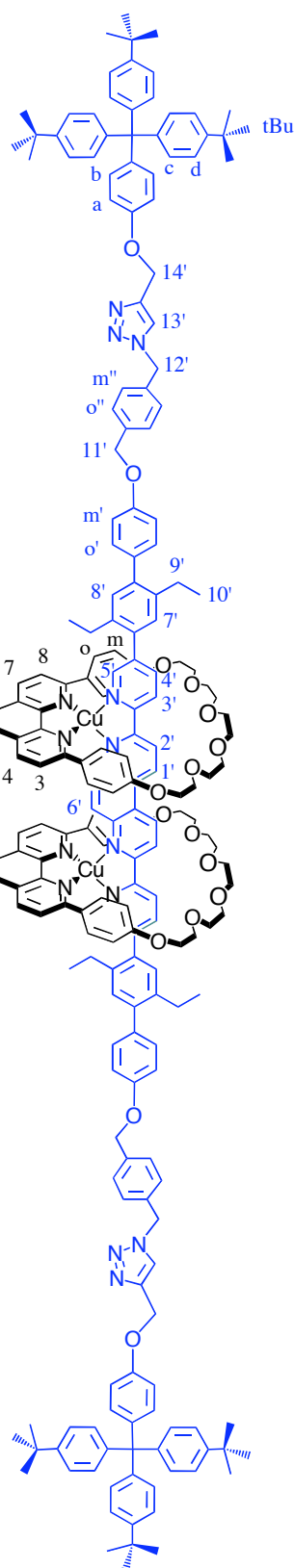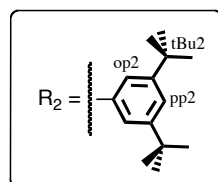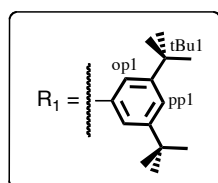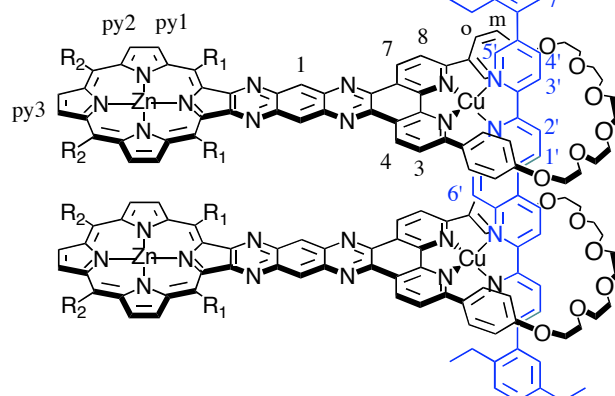
44

Scheme 5.12. *[3]rotaxane **44**.*

The protons that are labelled by **op1**, correspond to two different signals in the NMR spectrum of the metallated rotaxane **44**. This is due to the fact that the di-tertiobutylphenyl units attached to the porphyrin moiety are disposed orthogonally to the porphyrin itself. Free rotation is hindered by bulky ^{t}Bu groups. Therefore one **op1** proton points into the space between the two porphyrins and one "outside" the porphyrins, hence they correspond to two different peaks on the NMR spectrum. The same explanation applies to the proton groups labelled by **op2**, **tBu1** and **tBu2**.

ROESY NMR coupling between $H_{12'}$ of the thread part, $H_{13'}$ of the newly formed triazol unit and $H_{14'}$ of the stopper unit is clear evidence for the success of the stoppering reaction.

ROESY coupling is also observed between protons of the thread and protons of the macrocycles, thus leaving no doubt that the axle and the macrocycles are threaded. (See table 5.1 and scheme 5.12)

Thread		Macrocycles
$H_{6'}$	coupling with	H_o
$H_{7'}$	coupling with	H_m
$H_{8'}$	coupling with	H_m

Table 5.1: *ROESY NMR coupling between the thread and the macrocycles.*

Protons H_o and H_m of the macrocycles couple with $H_{6'}$, and $H_{7'}$, $H_{8'}$ respectively. Therefore we can assume, that one of the phenyl groups of each macrocycle is situated next to the ethyl bridge of the central 4,7-phenathroline unit ($H_{6'}$) of the thread, whereas the other one is in close proximity of the diethylphenyl moiety ($H_{7'}$, $H_{8'}$). This is a clear indication that the dihedral distortion angle between the

phenanthroline (macrocycle) and the bipyridine ligands (thread) of the Cu(I) metal centre is smaller than 90° as it would be for a perfect tetrahedral geometry, which is in agreement with the observations made for [4]pseudorotaxane **12** (see section 2.II.2). The macrocycles are not orthogonal to the thread, they rotate to bring their phenyl units closer to the thread, thus "flattening" the system.

Rotaxane **44** represents the molecular press in its contracted situation. To be able to study the press in its extended, relaxed position, we must first demetallate the complex to obtain the "real" rotaxane **45**, only kept together as an entity by mechanical links (the bulky stopper groups at each end of the thread), the macrocycles being thus able to glide on the axle. An excess of potassium cyanide, accomplishes the demetallation, as shown in scheme 5.13.
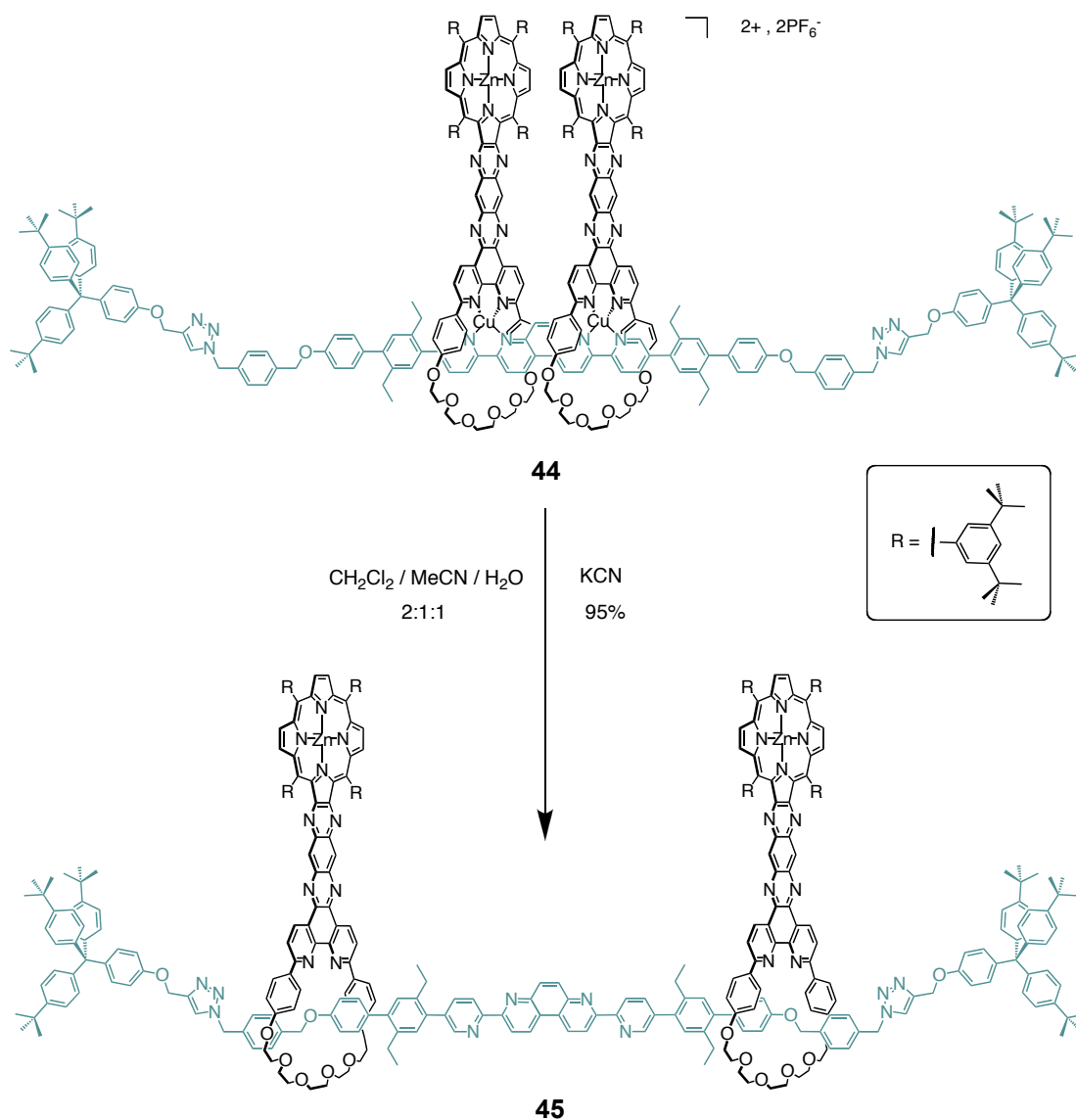
Scheme 5.13. *Demetallated [3]rotaxane **45**. The macrocycles are free to glide on and to turn around the thread; the here shown configuration is an arbitrary choice.*

Rotaxane **45** represents the press in its relaxed situation. The macrocycles and their attached porphyrin units can randomly glide and spin on the thread. Unfortunately these conformational changes do not allow us to characterize rotaxane **45** by ^{1}H-NMR. Even at low (-40°C) or high (80°C) temperatures, the peaks are too broad to be the subject of a detailed analysis. Nevertheless, the compound could unambiguously be identified by mass spectrometry (figure 5.2 and 5.3).
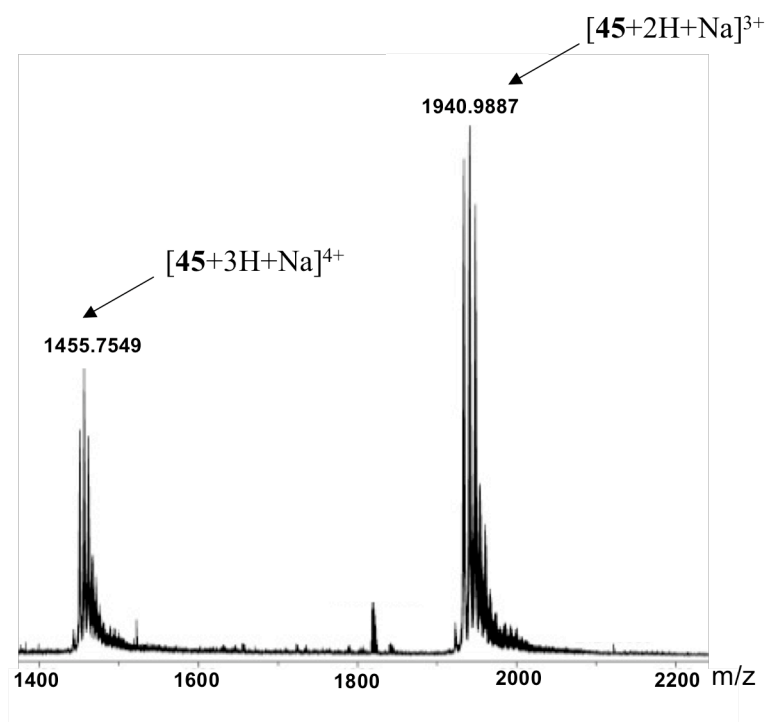
Figure 5.2. *ES mass spectrum spectrum of compound **45** (from m/z = 1400 to 2200)*
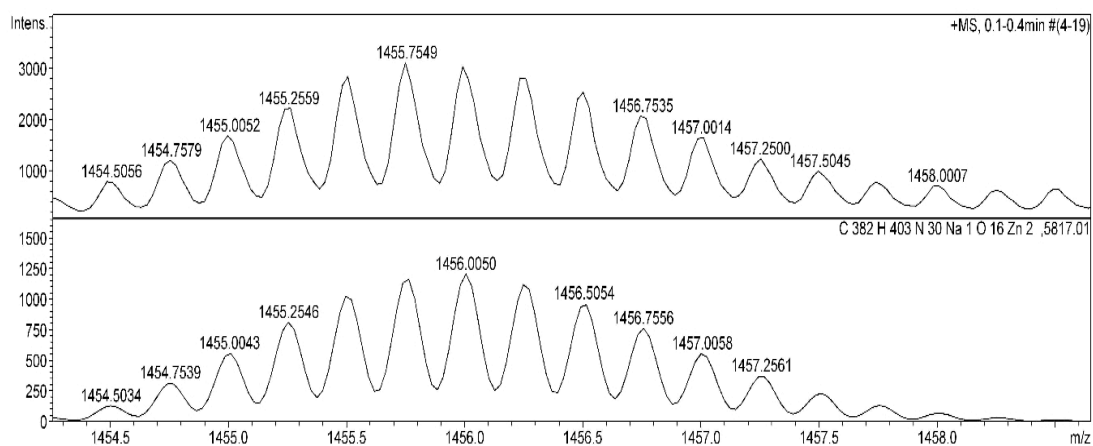
Figure 5.3. *Isotopic distribution pattern of compound 45 at m/z = 1455 (top) and the simulation (bottom).*
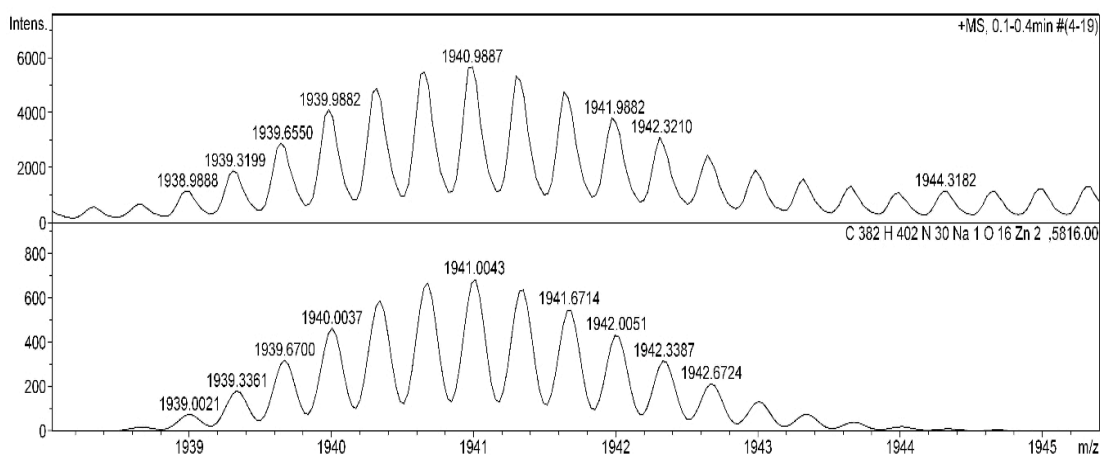
Figure 5.4. *Isotopic distribution pattern of compound 45 at m/z = 1940 (top) and the simulation (bottom).*

Furthermore, compounds **44** and **45** were studied and characterized by cyclic voltammetry and DOSY analysis, which will be discussed in the following paragraphs.

II.4. Cyclic voltammetry

The electrochemical experiments were carried out in freshly distilled and degassed dichloromethane with $^tBu_4NPF_6$ as supporting electrolyte salt. A silver wire is used as pseudo-reference electrode, a platinum wire as counter electrode and a platinum disk as working electrode. Ferrocene ($E° Fc^+/Fc = 0.56$ V vs SCE) was used as an internal reference, all redox potentials are given $versus$ SCE. The scan rate is 100 mV s^{-1}.

First we studied the macrocycle-Zn-porphyrin **34** by scanning the potential from +1.2 V to -1.2 V. Its cyclic voltammogram is displayed in Figure 5.5.
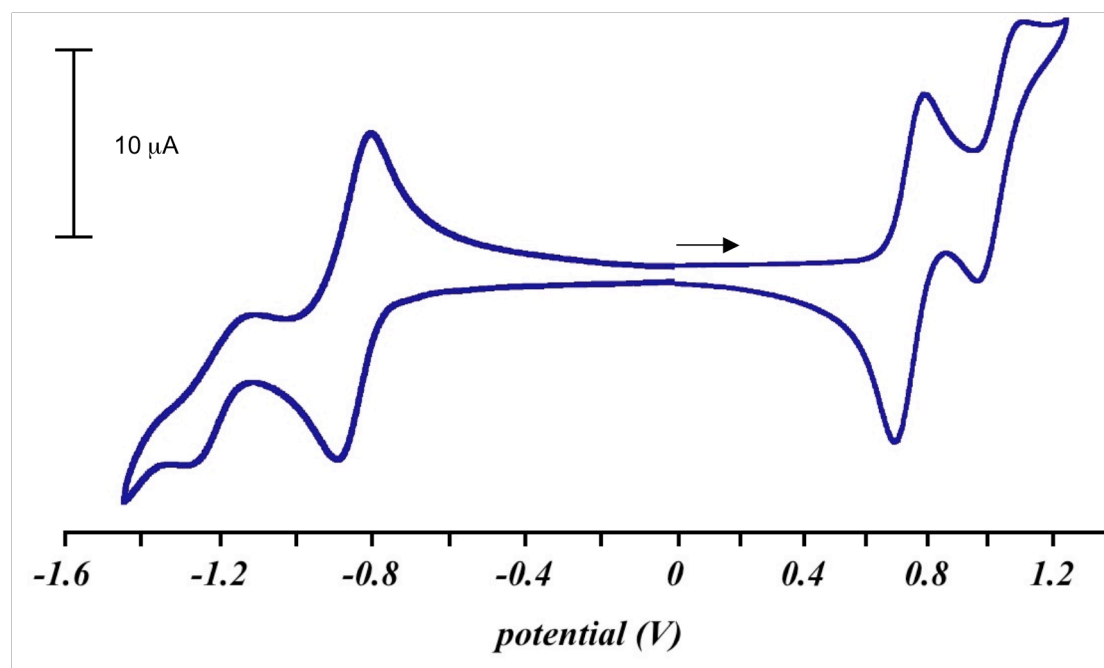
Figure 5.5. *Voltammogram of macrocycle-porphyrin 34.*

Upon reduction (left), one redox couple can be observed (-0.75 V, ΔE = 93 mV) which corresponds to the reduction of the tetra-azaanthracene bridging unit between the Zn-porphyrin part and the ring-unit of the macrocycle-Zn-porphyrin compound **34**. This assignment is in agreement with previously published studies on spatially separate pyrazines (-0.96 V).[103] A second, irreversible, redox couple is observed at -

1.14 V that might be a second reduction of the tetra-azaanthracene or the first reduction of the porphyrin moiety.

Upon oxidation two redox couples can be determined that correspond to the first (0.78 V, ΔE =117 mV) and the second (1.06 V, ΔE = 174 mV) oxidation of the Zn-porphyrin unit.[104]
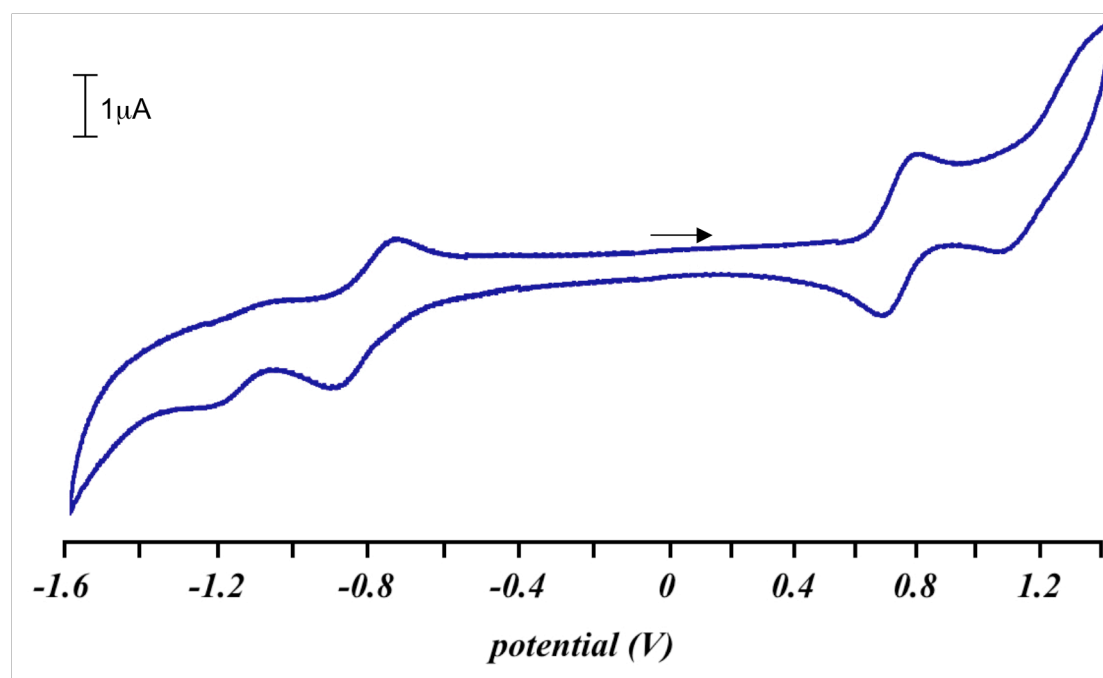
Figure 5.6. *Voltammogram of the demetallated rotaxane 45.*

The electrochemical behaviour of the demetallated rotaxane **45** is shown in Figure 5.6. The oxidation and reduction potentials of the two redox couples are similar to those observed for the macrocycle **34**, therefore we can presume that the dumbbell shaped thread does not, or only slightly, influence the redox potentials of the macrocycle **34**. As can be seen on Figure 5.6, the first oxidation peak and the reduction peak have the same intensity for the demetallated rotaxane **45**. Both correspond to a double one-electron exchange, one for each macrocycle (porphyrin unit (oxidation) and one for each tetra-azaanthracene unit (reduction)).

The metallated rotaxane **44** is expected to give a different result, due to its Cu(I) centres that are electrochemically active. Indeed we observed the same profile upon reduction, but the first oxidation signal is different. In the case of the metallated rotaxane, the intensity of the first oxidation peak is twice as high as the one of the reduction peak (Figure 5.7). Therefore we can assume that four electrons are involved in this oxidation, one for each of the two porphyrins and one for each of the two copper(I) centres. The observed redox couple (0.87 V, ΔE = 81mV) is the superposition of two different oxidations (porphyrins and Cu(I) centres).
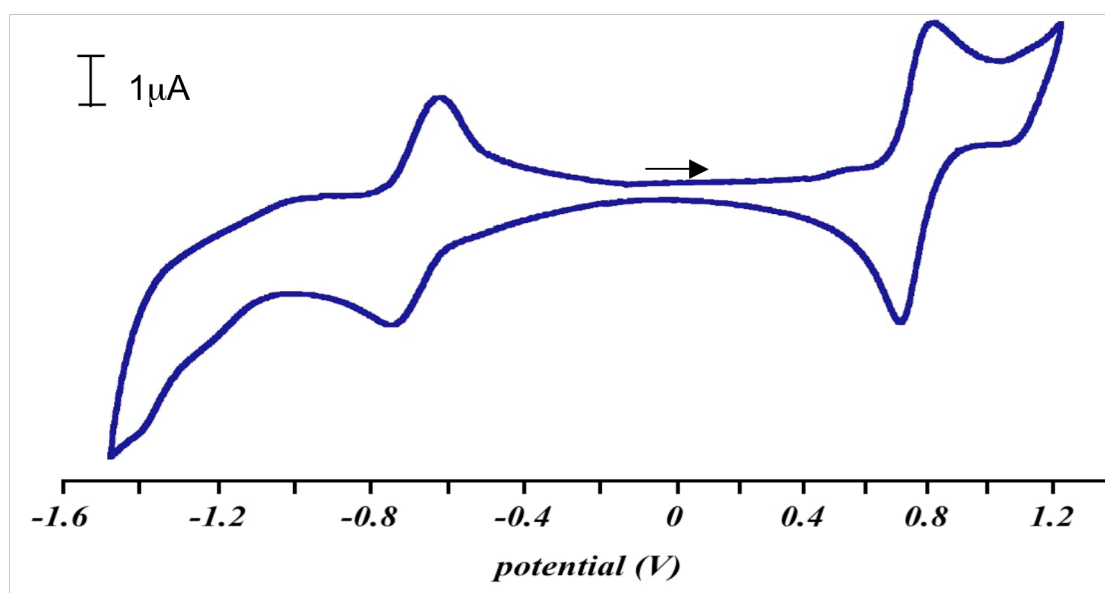
Figure 5.7. *Voltammogram of the metallated rotaxane 44.*

Since the oxidation of the porphyrin units and copper (I) centres occurs almost at the same potential, this electrochemical study shows no eventual coupling between the copper centres.

<u>II.5 DOSY NMR analysis</u>

All NMR experiments on a Bruker AVANCE 500 MHz machine, and especially the DOSY analysis, were carried out by Lionel Allouche of the "Service Commun de RMN de l'ULP Strasbourg".

Diffusion-ordered spectroscopy (DOSY) seeks to separate the NMR signals of different species according to their diffusion coefficient (D). This technique allows us to determine whether different species are present in the sample and to obtain information about their size. Indeed the diffusion coefficient of a molecule depends on its shape and dimensions. Once this coefficient has been determined, we can calculate the approximate size of the molecule using an ellipsoid as a model. The ellipsoidal model is based on three parameters: **a** (2a = length), **b** (2b = height) and **c** (2c = width) as shown in Figure 5.8.
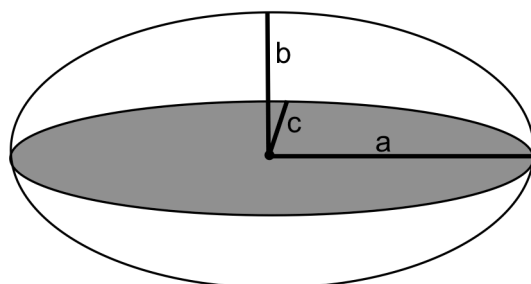
Figure 5.8. *Model of an ellipsoid with three parameters **a** (**2a** = length), **b** (**2b** = height) and **c** (**2c** = width).*

Unfortunately the simulation program does not allow to chose different values for **b** and **c**, therefore the theoretical ellipsoid has the same height and width.

A given diffusion coefficient can correspond to different ellipsoids. Indeed one can imagine increasing the value for parameter **a**, while decreasing **b** and **c**, thus lengthening the ellipsoid, or decreasing **a** while increasing **b** and **c**, thus shortening but widening the ellipsoid. These simultaneous changes can lead to different ellipsoids having the same diffusion coefficient D.

We must first examine the theoretical shapes of the two compounds. Whereas for the metallated rotaxane **44** the macrocycles are locked in the middle of the thread and are both pointing into the same direction, they are free to slide and twist around the thread in demetallated rotaxane **45**. They can point in opposite directions and occupy a larger average volume, and therefore we should expect to find a lower diffusion coefficient corresponding to a larger molecule (scheme 5.14).
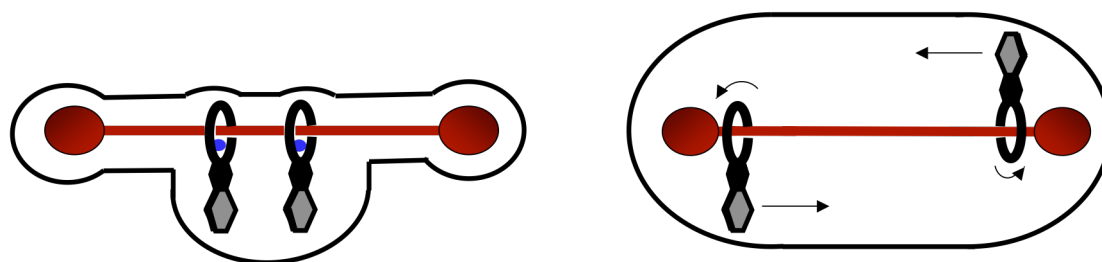
Scheme 5.14. *Schematic representation of metallated rotaxane **44** (left) and demetallated rotaxane **45** (right) with their respective average occupied volume (black line).*

A very simplified view of the average volume occupied by compound **44** (left) and **45** (right) can be seen in scheme 5.14. Even though our means do not allow us to know the exact dimensions of the two compounds, it seems obvious that demetallated rotaxane **45** occupies a bigger volume than its metallated counterpart **44**. The corresponding ellipsoid should therefore be larger, knowing that its length is the same.

To determine the approximate dimensions of the molecule we measured the length (**2a**) of the axle by means of a simulation of compound **44** on Hyperchem® by using MM2 energy minimization calculations. The axle is approximately 85 Å long (Figure 5.9).
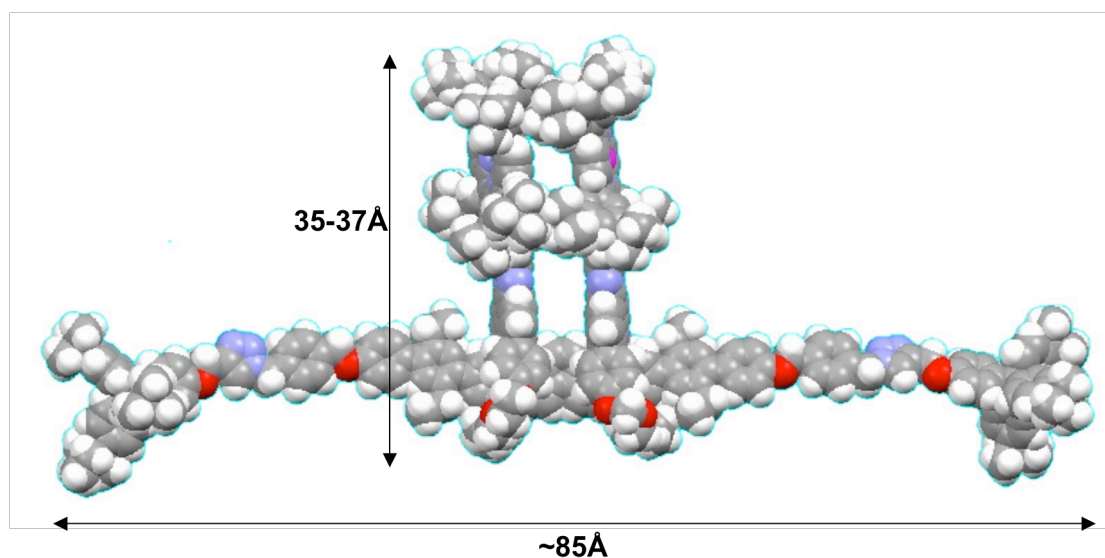
Figure 5.9. *Spacefilling Hyperchem® model of metallated rotaxane **44** after energy minimization by MM2 calculations.*

If we take into account the solvent sphere around the molecule, we can assume that the lengths of the ellipsoid that corresponds the best to our molecules should be in-between 85 and 90 Å (parameter **2a**).

The macrocycle-Zn-porphyrin has a length of about 35-37 Å. The average occupied volume of demetallated rotaxane **45** resembles very much an ellipsoid that has the length of the thread (85-90 Å) and the height and width of about twice the length of the macrocycle (70-80 Å). Therefore it is quite close to the theoretical ellipsoid model, especially because **b** and **c** have the same values.
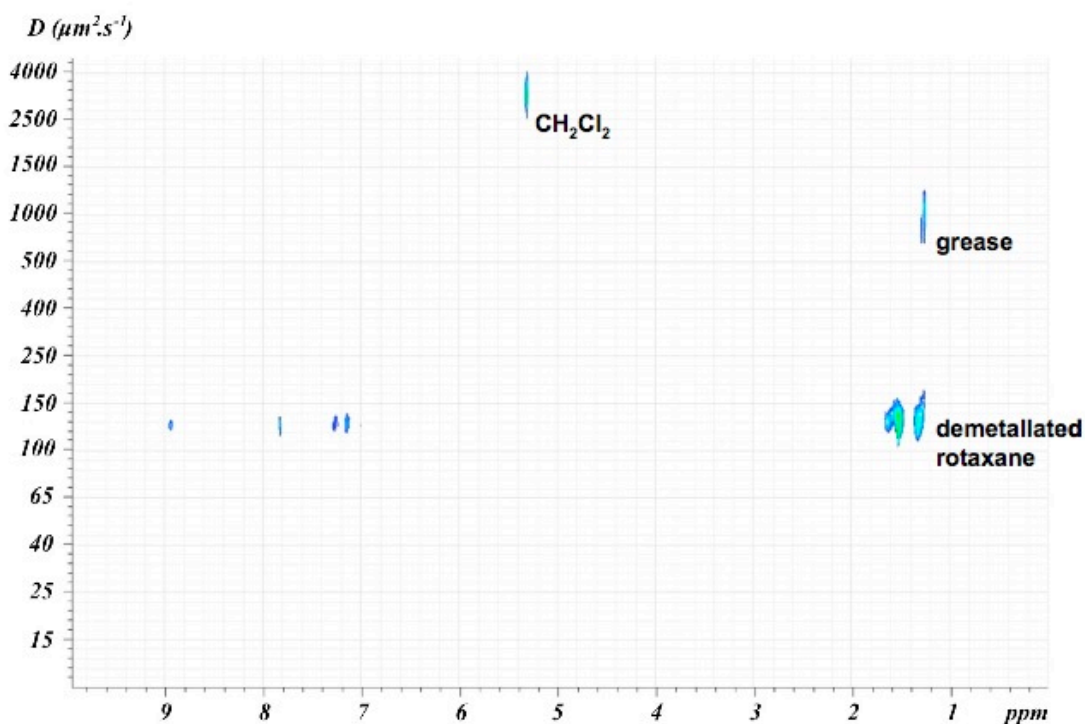
Figure 5.10. *DOSY spectrum of demetallated rotaxane **45**.*

The DOSY spectrum of demetallated rotaxane **45** (Figure 5.10), displays the diffusion coefficients on the vertical axes and the chemical shifts on the horizontal axes. All observable peaks (besides the solvent CD_2Cl_2 (5.3ppm), and a little bit of grease (1.1 ppm) appear with the same diffusion coefficient (*i.e.* a horizontal line can be traced from the y-axes through all the peaks). This indicates that only one species is present in solution (high purity), having a diffusion coefficient of 132 μm^2 s^{-1}.

Table 5.2. displays the dimensions for several possible ellipsoids that correspond to the found diffusion coefficient. According to our simulations, the length (2**a**) can be fixed at 85-90 Å; hence the height (2**b**) and width (2**c**) of the model ellipsoid are 75-77 Å.

2**a** (Å)	80	85	90	95	100
2**b**, 2**c** (Å)	80	77	75	73	71

Table 5.2. *Different values for parameters 2**a**, 2**b** and 2**c** that are in agreement with the diffusion coefficient of demetallated rotaxane **45**.*

The diffusion coefficient determined by the DOSY experiment and the corresponding calculations for the model ellipsoid are in good agreement with our predictions.

The volume occupied by metallated rotaxane **44** has not exactly what one would refer to as an ellipsoidal shape (scheme 5.14): **b** and **c** have not the same values at all, hence we can not correlate its dimensions directly to those of its ellipsoidal counterpart. Nevertheless, the occupied volume is smaller than for the demetallated rotaxane **45**, thus if we use the same length for both model ellipsoids (85-90 Å), we should find lower values for its width and height. The diffusion coefficient on the other hand should be higher, as the molecule is smaller. The DOSY analysis on the metallated rotaxane **44** is shown in Figure 5.11.
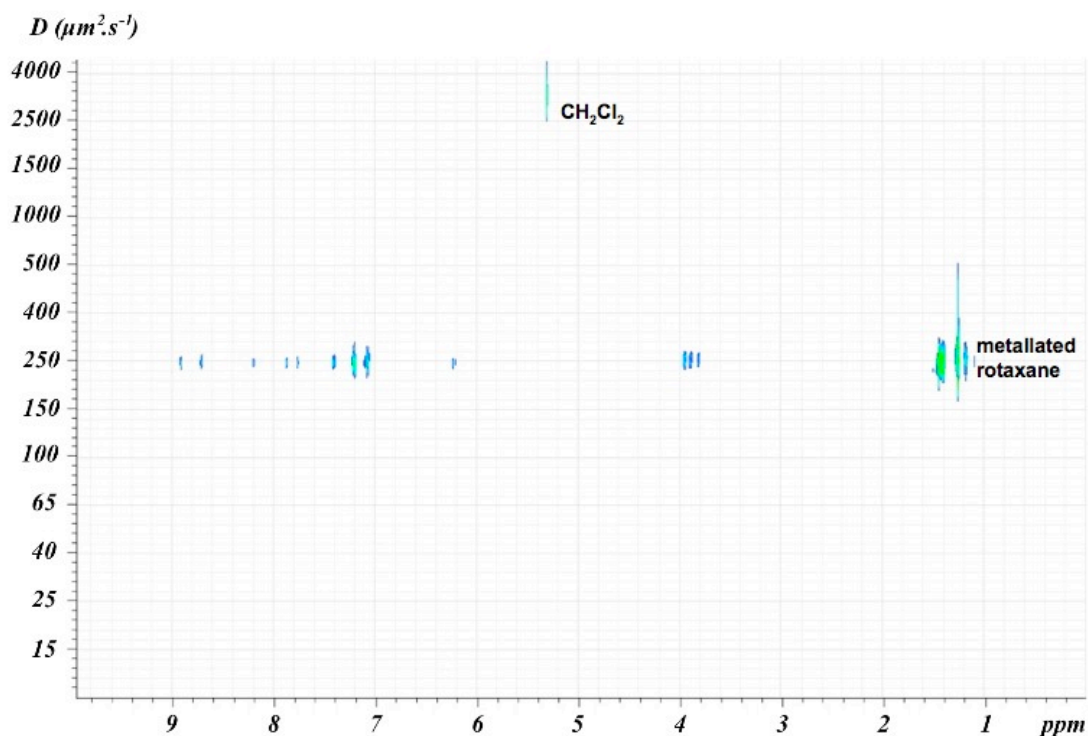
Figure 5.11. *DOSY spectrum of metallated rotaxane 44.*

96

Again only one species is observable on the spectrum. The pure product has a diffusion coefficient of 248 μm^2 s^{-1}, which corresponds to ellipsoids that have the dimensions given in table 5.3.

2a (Å)	75	80	85	90	95
2b, **2c** (Å)	28.5	26.5	25	23	21.5

Table 5.3. *Different, calculated values for parameters 2a, 2b and 2c that are in agreement with the diffusion coefficient of metallated rotaxane 44.*

It can be noticed that for the same length of the ellipsoid than for compound **45**, we observe a height and width of only 23-25 Å, which is three times less than for the demetallated rotaxane **45**. This is not surprising; as predicted before the fixed macrocyles occupy much less space than if they were free to move. It is worth noting that the ellipsoidal model is not really well adapted to metallated rotaxane **44**.

Even though an ellipsoid model is only an approximation, we can conclude from these results that demetallation of compound **44** was fully accomplished; that the free rotaxane **45** occupies a much larger average volume and therefore that the macrocycles are free to glide on and spin around the thread. For that reason the two porphyrins should be able to accommodate different guests of various sizes.

III. Host-guest Chemistry

Having this new tool in our hands, a molecular press, fully characterized in its relaxed as well as in its contracted situation, we now needed an appropriate guest molecule.

To be able to bind to the porphyrin receptors, the molecule will have a pyridine moiety at each end, whereas its middle part should be flexible so as to be compressed. We designed guest-molecule **46**, shown in scheme 5.15.

46
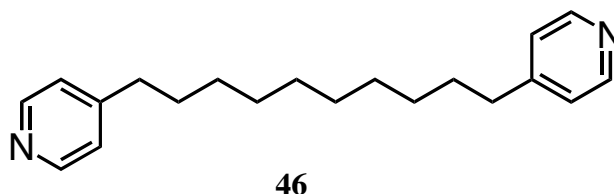
Scheme 5.15. Guest molecule **46**. A 4,4'-bipyridine separated by a C_{10} alkyl chain.

The spacer between the two pyridyl units is a $C_{10}H_{20}$ alkyl chain rather than a polyethyleneglycol one, because the host molecules contain already polyethyleneglycol moieties on the macrocycles and therefore the identification by NMR might be unnecessarily complicated by using the same kind of chains.

Guest **46** has to be long enough to be compressed, but not too long in order to avoid external-external or internal-external binding to the porphyrins as shown in Figure 5.15. By using a decane chain, only internal-internal binding is possible between host **44** and guest **46** according to CPK models.

external-external   external-internal   internal-internal
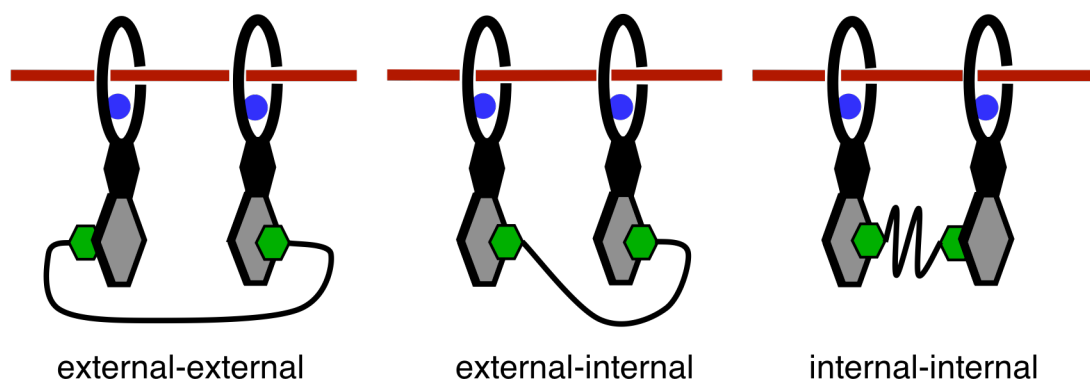
Scheme 5.16. *Different possible host-guest binding modes depending on the chain length of guest-molecule* **46**.

UV-titration experiments are carried out by adding either the guest **46** or plain

pyridine to a metallated rotaxane **44** or demetallated rotaxane **45** (1.725×10^{-6} mol L^{-1}).

Guest and host are in solution in freshly distilled and degassed toluene. Negligible

volumes (100 to 200 μL) of a guest-solution were added to the UV cuvette containing

the host-solution (3 mL). After each addition, the mixture was stirred until no more

changes were observed on the UV/vis spectrum. Neither the guest molecule **46** nor

pyridine do absorb in the Soret band region of the UV/visible spectra, therefore we

should be able to monitor the binding of the guest to the host by observing the 400-

500 nm region of the spectra, which contains a large absorption band, belonging to

the porphyrin moiety. The association constants were calculated according to the

following formula:[105, 106]

$$A = A_0 + \frac{\Delta A}{2S_0} \left\{ K_{dis} + X + S_0 - \left[(K_{dis} + X + S_0)^2 - 4XS_0 \right]^{\frac{1}{2}} \right\}$$

The meanings of the parameters are: A is the absorbance, S_0 is the concentration of the

host, X is the concentration of the guest. ΔA is the maximum variation of the

absorbance, A_0 = absorbance of the host without the guest and K_{dis} = $1/K_{ass}$, where

K_{ass} is the association constant.

It should be noted that the association constants presented here are only preliminary

results; future, more sophisticated analysis will give more accurate values.

III.1.1 Reference titration with plain pyridine

A first reference titration was carried out by adding plain pyridine to the demetallated

host **45** in solution in toluene. First we added the pyridine by 0.2 equivalents at a time,

but after 2 equivalents were added, no change could be observed on the UV/vis spectrum. Therefore we changed the amount of guest to 10 equivalents for each addition. The resulting spectrum is shown in Figure 5.12.
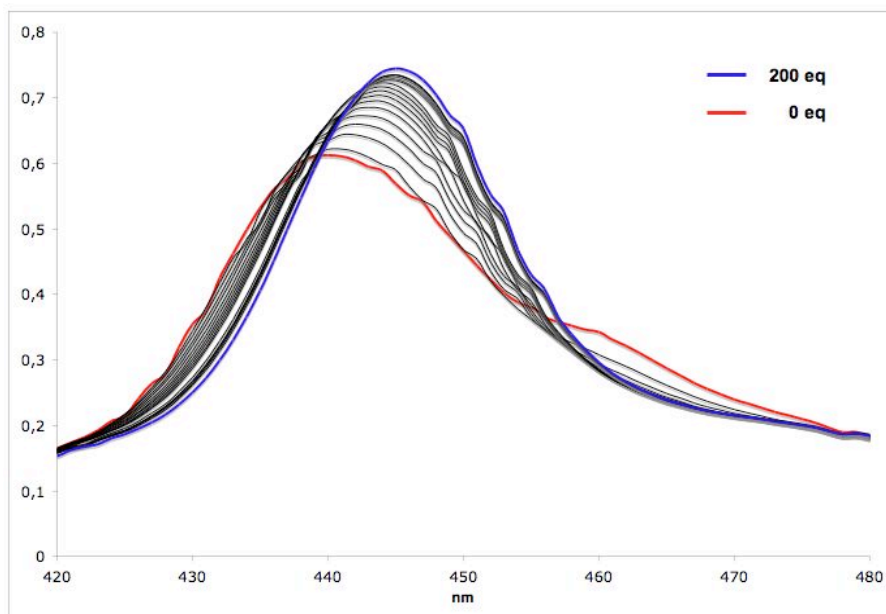
Figure 5.12. *UV/vis titration of demetallated rotaxane **45** with pyridine in toluene.*

At 0 equivalents (red curve) of pyridine added, λ_{max} equals 440 nm ($\varepsilon = 3.55 \times 10^5$ mol L^{-1} cm^{-1}). Upon addition of 200 equivalents (blue curve) of pyridine, λ_{max} has shifted to 445 nm ($\varepsilon = 4.32 \times 10^5$ mol L^{-1} cm^{-1}). The equilibrium involves the formation of two or several complexes (one or two guest molecules, internal or external binding); therefore it is not surprising that no isosbestic point can be observed. The association constant can be evaluated at about 10^4 M^{-2}, which is in agreement with similar pyridine-tetraarylporphyrin systems[107], if we assume that the two porphyrins can be seen as independent.
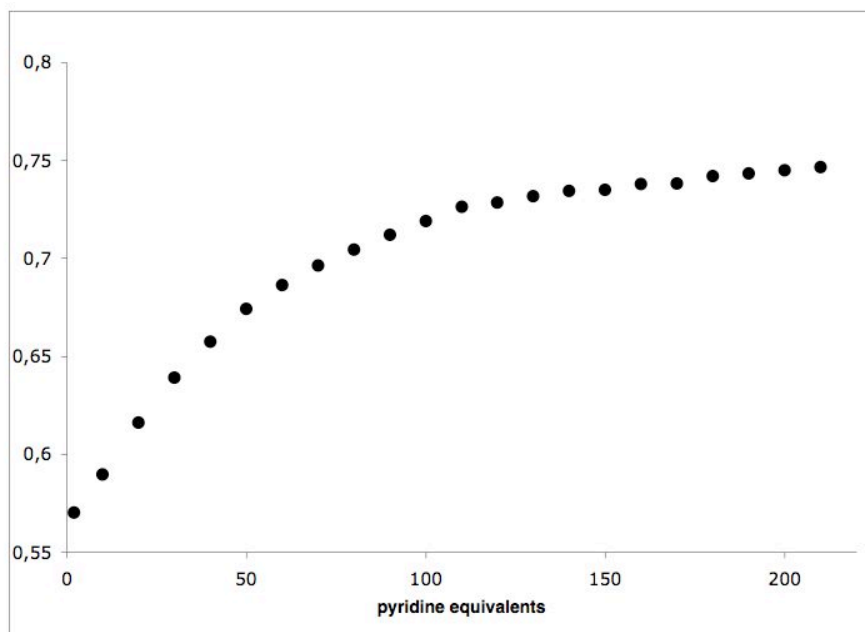
Figure 5.13. *Titration of host **45** with pyridine in toluene. Absorbance plotted against the added pyridine equivalents at λ_{max} = 445 nm.*

Figure 5.13 on which the absorbance at λ_{max} (445 nm) is plotted against the pyridine equivalents added to the host solution, shows that at approximately 150 equivalents are necessary to reach the absorbance maximum, showing that with such a large excess each Zn-porphyrin has accepted a pyridine.

III.1.2 Titration of demetallated rotaxane **45** with guest molecule **46**

To the solution of demetallated rotaxane **45** was added guest molecule **46**, 0.1 equivalents at a time. The resulting UV/vis spectrum is shown in Figure 5.14.
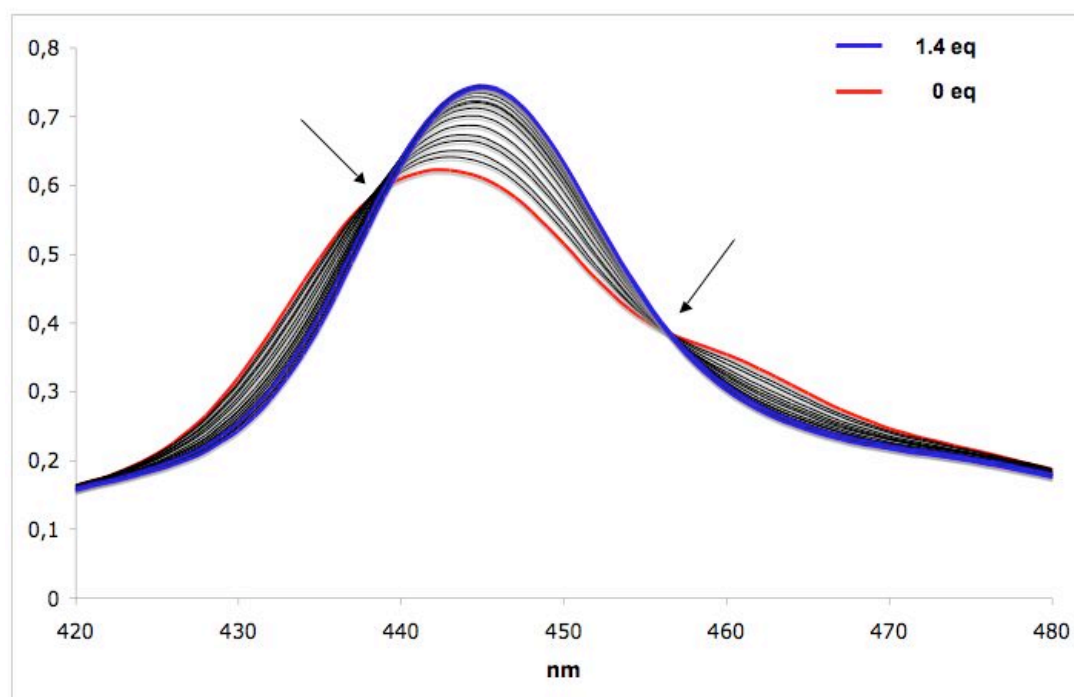
Figure 5.14. *UV/vis titration of demetallated rotaxane 45 with guest molecule 46.*

As for the titration with pyridine we observe a shift of λ_{max} from 442 nm ($\varepsilon = 3.60 \times 10^5$ mol L^{-1} cm^{-1}) at 0 equivalents of the guest molecule (red curve), to 445 nm ($\varepsilon = 4.30 \times 10^5$ mol L^{-1} cm^{-1}) at 1.4 equivalents (blue curve). However, we can clearly determine two isosbestic points at 439 and 457 nm (black arrows), showing the formation of a single well defined species. By plotting the absorbance against the number of equivalents added at $\lambda_{max} = 445$ nm (Figure 5.15), we notice that 1.2 equivalents are enough to make sure that each pyridine receptor is bound to one guest pyridyl unit (maximum absorbance), which is about 100 times less than for the plain pyridine ligand.
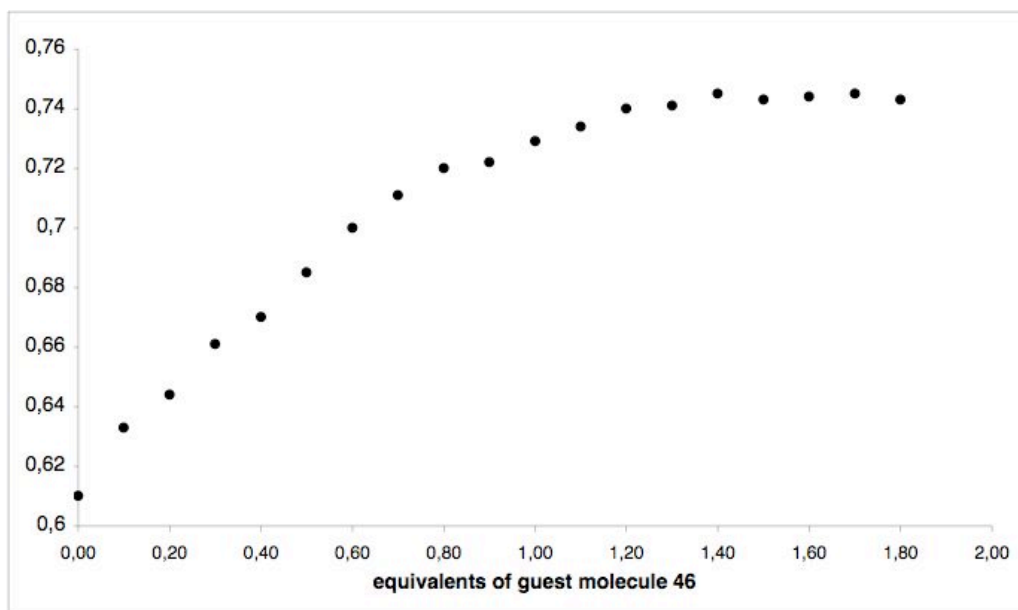
Figure 5.15. *Titration of host **45** with guest **46** in toluene. Absorbance plotted against the added pyridine equivalents at λ_{max} = 445 nm.*

The association constant between guest and host is about $10^8 \, M^{-1}$. These results can be explained by a cooperative binding effect. In the former example, two pyridines bind to one guest each one with one coordination bond. Here, one guest binds to one host on two different binding sites, making the link much stronger. After one pyridyl unit of the guest has bound to the first porphyrin unit of the host, the second one is obviously close to the second porphyrin unit, which accelerates its coordination to the same host rather then to a second one. These are the reasons why the association constant is much larger for the guest **46** than for simple pyridine[108-110].

III.1.3 Titration of metallated rotaxane **44** with guest molecule **46**.

Very similar results are obtained for metallated rotaxane **44** with guest **46**. Again λ_{max} is shifted from 442 nm ($\varepsilon = 6.76 \times 10^5$ mol L^{-1} cm^{-1}) at 0 equivalents (red curve) to 447 nm ($\varepsilon = 7.49 \times 10^5$ mol L^{-1} cm^{-1}) at 1.4 equivalents (blue curve). An isosbestic point (black arrow) is observed at 444 nm, showing that the association equilibrium takes place again between only two species, one rotaxane and one guest.
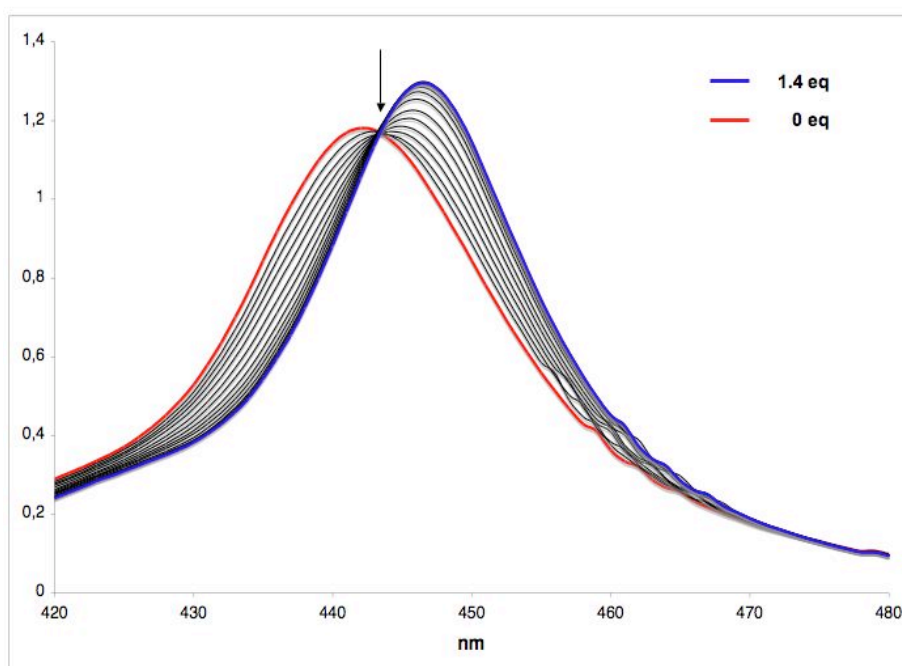
Figure 5.16. *UV/vis titration of metallated rotaxane **44** with guest molecule **46**.*

By plotting the absorbance against the added equivalents for $\lambda = 447$ nm (Figure 5.17), we observe that the absorbance maximum is reached earlier than for the demetallated rotaxane **45**. This is due to the fact that the two porphyrin receptors are kept in a fixed position by the Cu(I) centres, thus facing each other. This pre-organisation is favourable to a stronger binding of the guest to the hos, even though distortion of the Zn-porphyrin-macrocycle moieties (and/or the guest) is necessary to accommodate the guest molecule **46**.
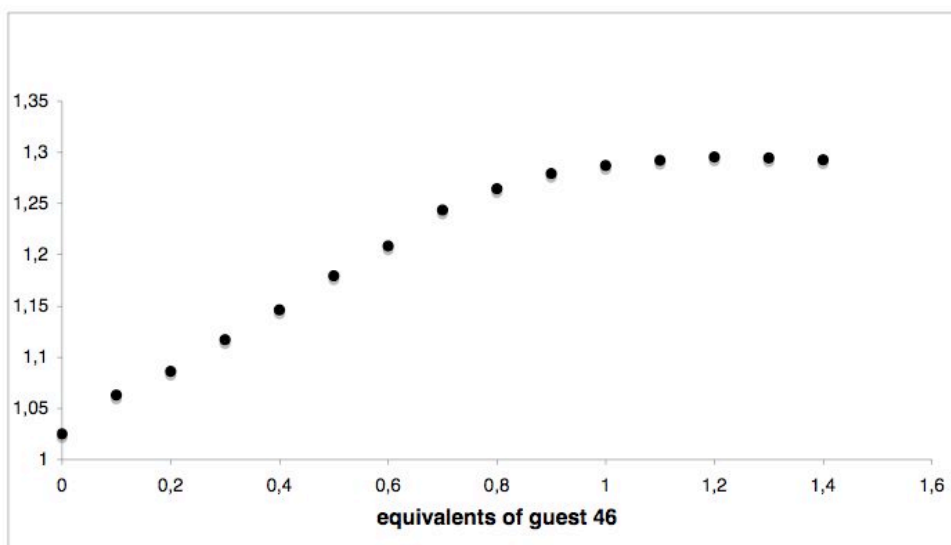
Figure 5.17. *Titration of host **44** with guest **46** in toluene. Absorbance plotted against the added pyridine equivalents at λ_{max} = 447 nm.*

The association constant between host **44** and guest **46** is determined as being 2×10^8 M^{-1}, which is in agreement with the one found for similar compounds.[107]

We can conclude from these results that there is a cooperative effect for the binding of the guest **46** to the rotaxanes **44** and **45**, due to which the binding constants are much higher than if we use pyridine as a guest. We can assume that one guest binds to one host, the metallated rotaxane being a better host for guest **46** due to its pre-organised porphyrin receptors.

The here presented results, together with the CPK models, leave no doubt to the intra-intra binding mode of the guest to the porphyrin units of the host.

Further confirmation for the formation of the host-guest complexes upon addition of the guest to the host in solution in dichloromethane or toluene, is ES-mass-spectrometry. Figures 5.18 and 5.19 show the corresponding spectra of the demetallated rotaxane **45** and metallated rotaxane **44** respectively, each one having accepted one guest molecule **46**.
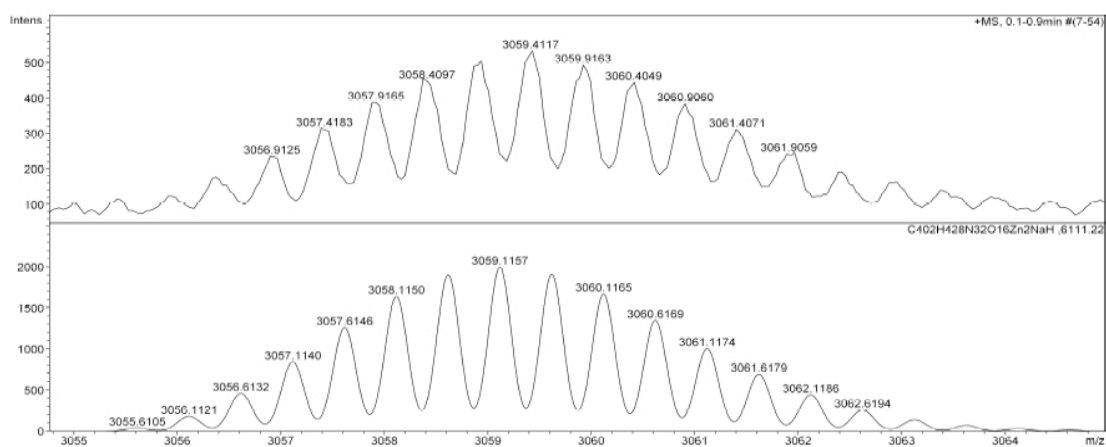
Figure 5.18. *Isotopic distribution pattern of [Host **45** – Guest **46** + Na + H]$^{2+}$ complex. Zoom on the m/z = 3059 region (top) and the simulation (bottom).*
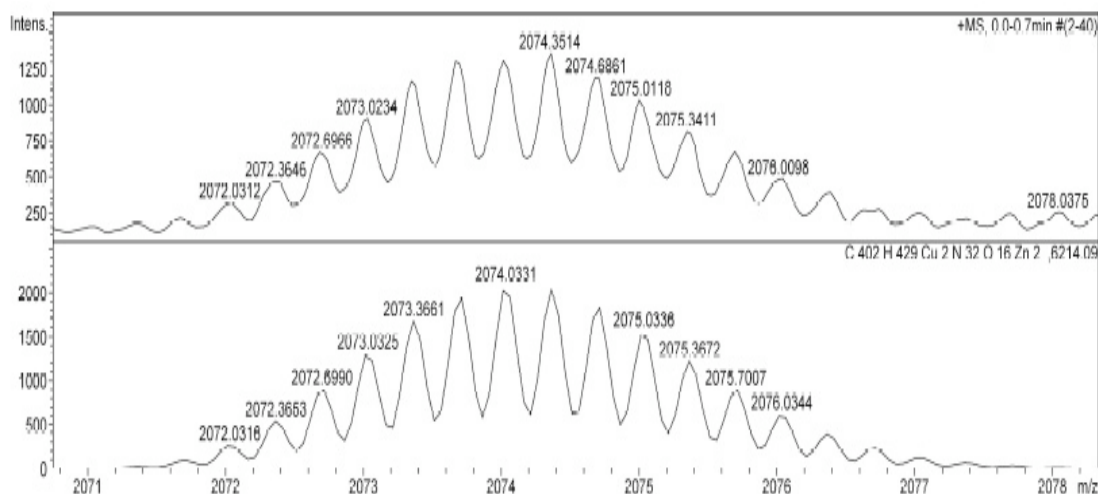
Figure 5.19. Isotopic patter of *[Host **44** – Guest **46** + H]$^{3+}$ complex. Zoom on the m/z = 2074 region (top) and the simulation (bottom).*

III.3. NMR analysis

III.3.1 Demetallated rotaxane **45** – guest **46** complex

The demetallated rotaxane **45** – guest **46** complex was obtained by adding one equivalent of the guest **46** to the host **45** in solution in dichloromethane.

As already discussed before, most NMR experiments on demetallated rotaxane **45** are not exploitable because slow conformational changes in the molecule render the observed peaks far too large. The only exploitable information was obtained by DOSY NMR. The diffusion coefficient of the host **45** – guest **46** complex was determined to be 240 μm^2 s^{-1}, which is a surprisingly high value compared to D = 132 μm^2 s^{-1} for the demetallated rotaxane **45**. Indeed it points out that the DOSY analysis of the host-guest complex and the metallated rotaxane **44** without a guest (248 μm^2 s^{-1}) are very similar. The sizes of the model ellipsoids for both molecules are therefore nearly the same and hence the host-guest moiety is occupying less space than the host molecule on its own. A possible explanation for this observation is the fact that the two macrocycles are no longer independent. Indeed they are linked by the guest molecule, and behave like one large bis-macrocycle. Even though the connection between the two macrocycles is quite flexible, this newly formed entity moves slower on the axle. The average occupied volume is therefore smaller and thus the diffusion coefficient is larger. By DOSY NMR we proved that the demetallated rotaxane **45** as such, is no longer present in solution. Upon addition of the guest molecule, a dramatic change is observed for its diffusion coefficient, which can be explained by a one-to-one binding between host and guest.

III.3.2 Metallated rotaxane **44** – guest **46** complex

The metallated rotaxane **44** – guest **46** complex is obtained in two different ways, both leading to the same compound:

1) Adding one equivalent of the guest **46** to a solution of host **44** in dichloromethane.

2) Adding two equivalents of Cu(I), more precisely ([Cu(MeCN)$_4$]PF$_6$), to the demetallated rotaxane **45** – guest **46** complex.

Whereas the first procedure is a host-guest interaction, the second one is featuring the press "at work". The guest is linked to the two porphyrin units in the extended form of the press, which is then forced into its contracted situation by formation of a Cu(I) complex. Whatever procedure we used, the resulting compound is the same.

The DOSY spectra for the metallated rotaxane **44** does not significantly change upon addition of the guest molecule **46**. The two macrocycles are already kept in a fixed position by the Cu(I) centres, the additional linkage by the guest molecule has no major consequences on the occupied average volume.

The host-guest complex was closely examined by 1D, COSY, ROESY, HMQC and HMBC NMR analysis. Unfortunately, despite all our efforts we were unable to assign the corresponding peaks to the guest molecule on the different spectra. The alkyl part of the guest can be monitored in the 1 ppm to 2 ppm region, but is only represented by broad peaks which do not allow further investigations. We therefore think that the guest molecule, once it is bound to the porphyrin units of its host, is subject to slow

conformational changes that render detailed NMR analysis impossible. Furthermore, due to the complexity of the molecule and its spectrum, superimposition of the peaks is most likely. Nevertheless, no free guest was observed and interesting shifts for the resonance corresponding to protons of the porphyrin units upon binding of the guest were identified (Figure 5.20).
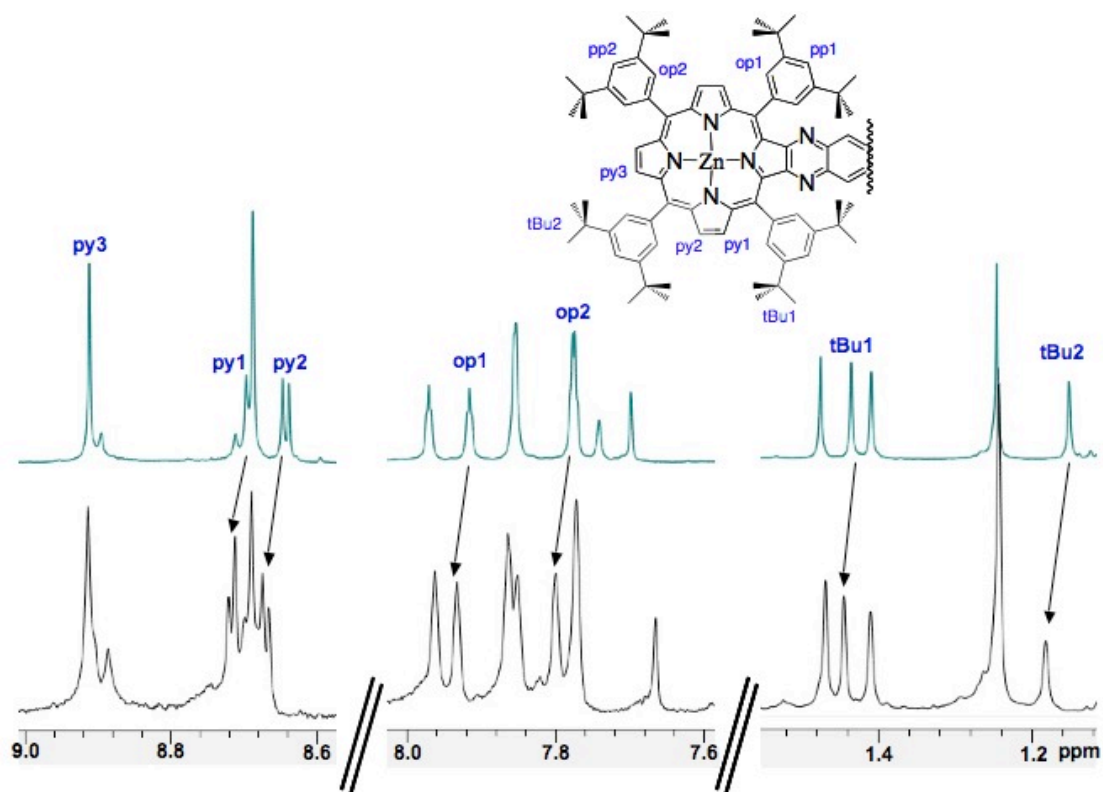
Figure 5.20. *Observed proton resonance shifts corresponding to the porphyrin moieties of the metallated rotaxane **44** (top) and the host **44** – guest **46** complex (bottom). In order to simplify the representation, the relative peak intensities for the different regions of the spectrum were altered.*

Even though the shifts are small (0.02 ppm to 0.03 ppm), they affect all the designated peaks in the same way, by moving them downfield. This is a clear indication that their environment has changed and therefore we can assume that the guest has bound to the porphyrins.

As discussed in section 5.II.3 (figure 5.1), the di-tertiobutylphenyl units are disposed orthogonally to the porphyrin moiety. As a consequence, one of the **op1**, **op2**, **tBu1** and **tBu2** proton groups points inside the space between the two porphyrins, whereas the other one is on the outside. For the simple metallated rotaxane **44** we were unable to determine which peak corresponds to the inside and which to the outside of the porphyrin. Now that the guest has bound to the host, we can observe that only one of the two peaks of each proton group is shifted. If we consider that the guest is bound in an internal-internal mode, we can assume that the observed shifts correspond to the protons situated at the inside of the cavity. This assumption is in agreement with the fact that the **pp1** and **pp2** signals are not altered upon addition of the guest molecule. The corresponding protons point into a co-planar direction of the porphyrin and are therefore not influenced by the binding of the guest molecule (see scheme 5.17).
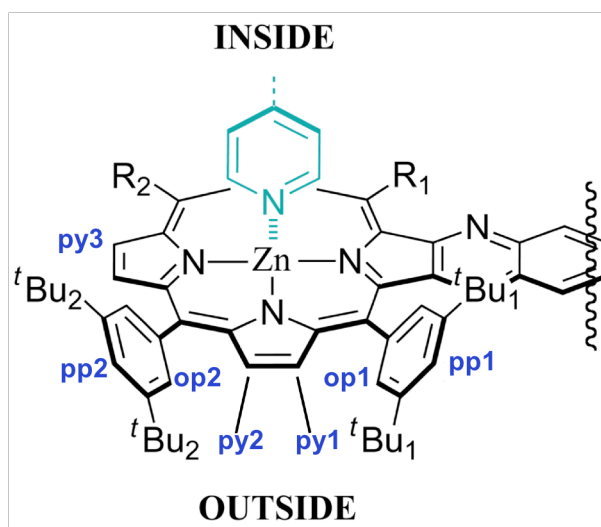
Scheme 5.17. *Explanatory scheme: concerning the inside or outside positioning of the **op1**, **op2**, **tBu1** and **tBu2** protons.*

Shifts can also be observed for the protons directly situated on the porphyrins, namely **py1**, **py2** and **py3** (for the latter one the shift is very small).

Furthermore, the signals we observe are the same for both porphyrins, this leads to the conclusion that they are equivalent; hence the binding mode of the guest is the same for both porphyrins. This observation shows that the guest is bound to the host in an internal – internal fashion, because CPK models exclude the possibility of external – external binding.

Even though we have no evidence that the guest molecule is compressed, several other facts have been proven.

The metallated and demetallated rotaxane **44** and **45** respectively were synthesized and characterized, leaving no doubt about their existence. They represent a molecular press in its extended, relaxed conformation and in its corresponding contracted one. UV/vis titration, mass spectrometry and NMR experiments clearly show that the guest molecule **46** binds to the porphyrin moieties of this press, whether it is extended or contracted. Upon addition of Cu(I), the press switches from its extended to its contracted situation without losing its guest molecule. Furthermore, we have strong indications that the binding between the host and guest takes place in an internal – internal fashion.

A major challenge for the future will be to prove that the guest molecule has actually been compressed, and thus to justify the label "molecular press". Therefore it is necessary to synthesis a different guest in the future. One could for instance think of using a fluorine-substituted molecule that could be monitored by ^{19}F NMR.

Another possible feature to be studied is the expulsion of a rigid guest molecule, which could fit in-between the two porphyrins in the extended press but would be too large for the contracted conformation.

Chapter 6

Towards a four station thread by adding terpyridines

I. Strategy and choice of the building block

As discussed already in section 1.I.2., the final goal of the project is the construction of a thread with four anchoring stations for the threaded rings, two bidentate ones in the middle (bipys), and two tridentate ones on the extremities (terpys).

The terpyridine core **48** (scheme 6.1), has been chosen for several reasons. It is functionalized in the 5,5" positions of the terpy, which, compared to a 6,6" functionalization, is less sterically hindering, thus allowing fast shuttling movement of the macrocycles. Moreover, this terpy core allows us to synthesize the thread in the most linear and rigid way. Indeed, two of the three pyridyl heterocycles will be perfectly aligned to the aryls of the thread centre, as shown in figure 1.6 (1.I.2.). In a second step, the terpy will have to be rendered dissymetric, so it can be attached to the thread core on one side, and later on "stoppered" on the other. Finally, the terpy **48** is well known to our laboratory[111], it has already been synthesized in good yield; hence it became the terpy of choice.

II. Synthesis

II.1. Dissymmetric terpyridine

Different terpyridines are synthesized in parallel to the thread. The middle part of the tridentate terpyridine is synthesized according to literature[111] as shown in scheme 6.1.
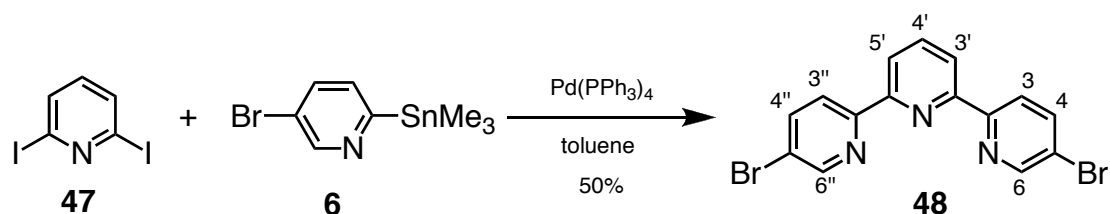
Scheme 6.1. *Synthesis of the 5,5"-dibromo-2,2':6',2"-terpyridine 48.*

The 2,6-diiodopyridine **47** was taken from a stock, prepared by Benoit X. Collasson by reacting commercially available 2,6-dibromopyridine with HI (57%) and NaI to obtain compound **47** in 70% yield. The 5,5"-dibromo-2,2':6',2"-terpyridine **48,** is prepared by a Stille cross-coupling reaction between the 2-trimethylstannyl-5-bromopyridine **6**, already used for the synthesis of the bis-bipyridine thread **7**, and the 2,6-diiodopyridine **47**. The higher reactivity of the carbon-iodine bond compared to the carbon-bromine bond, explains the very good yield of this Stille coupling reaction. After 7 hours, the reaction is stopped to avoid reduction that would lead to the plain pyridine.

The obtained dibromoterpyridine **48** has to be reacted further to obtain a dissymetric tridentate ligand, which is necessary to avoid the formation of oligomers during the

113

coupling reaction to the middle part of the thread. We decided to use the commercially available 4-methoxyphenylboronic acid **49** in a statistical Suzuki coupling reaction in order to break the symmetry of the terpy. Later on the anisyl group at the end of the thread can be deprotected and a stoppering reaction can be carried out.

The Suzuki cross-coupling reaction between compound **48** and **49** is performed in a toluene, water and ethanol mixture in a 6:2:1 ratio, the ethanol helping to solubilize the boronic acid (scheme 6.2).
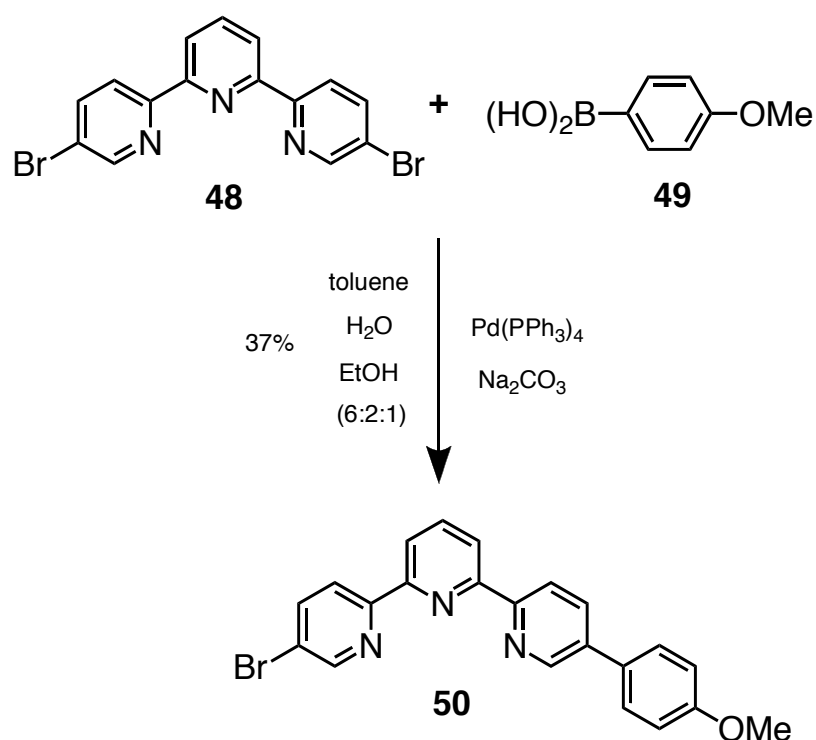
Scheme 6.2. *Statistical Suzuki cross-coupling to give dissymmetric terpy 50.*

This Suzuki coupling is a key step in the terpyridine synthesis. After several attempts varying the catalyst batch and most importantly the reaction time, we could finally obtain a yield of 37%, which is acceptable for a statistical reaction. The yield is optimized by using a commercially available Pd catalyst, one equivalent of boronic

acid, and by a reaction time of 3 hours. When left longer than 3 hours, the dissymmetric terpy **50** undergoes a reduction process, removing the bromine and replacing it by a hydrogen atom. The purification by column chromatography on alumina with pentane/ethyl acetate (96 : 4) of the final terpy is very tedious and time-consuming, the polarity of the elution gradient must be increased very slowly. The dianisyl-terpy waste product and the wanted monoanisyl-terpy are difficult to separate; both are streaking on the column, which is one of the reasons why we are unable to obtain the possible 50% yield. Nevertheless, the dissymetric terpy can be prepared and fully characterized.

II.2. Preparing the terpyridine for future coupling to the thread

To be able to graft this terpy to the bis-bipy thread, we tried to substitute the remaining bromine by a boronic acid, which could then be used in another Suzuki coupling with the thread having iodophenyl ending groups.

Functionalizing terpys with tin groups or boronic acids is not an easy task; as often observed in the laboratory, its coordination properties interfere with multiple reactions, such as lithiation reaction with *n*-BuLi or *ter*-BuLi, followed by a quenching with an electrophile, or deprotection of an anisyl group with BBr_3.

Benoit X. Colasson obtained the diboronic acid terpyridine starting from the dibromo-terpy **48**, using $Pd(dppf)Cl_2$, Bis(neopentyl glycolato)diboron and KOAc, in dioxane in 90% yield. This reaction worked only twice, it could later on never be reproduced. The reasons for this non-reproducibility are unknown.

Unfortunately our attempts in the same reaction conditions or using pinacolborane resulted, just as well as trying to add a trimethyltin group to the terpy, in failure.

Therefore we decided to avoid the direct formation of a boronic acid or a stannyl group in the β position of the nitrogens and to add a phenyl spacer on the terpy. The spacer was initially supposed to be added to the thread **7,** but according to the problems we were facing with the solubility of the bis-bipy thread and the functionalization of the terpy, it seemed a good alternative to add the spacer to the terpy, thus solving two problems at a time.

The dissymetric terpy **50** is therefore reacted with the commercially available 4-(trimethylsilyl)phenyl boronic acid **51** in a Suzuki cross-coupling reaction to afford terpy **52** in 70% yield. In this case, the coordination properties of the terpy do not interfere with the coupling reaction.
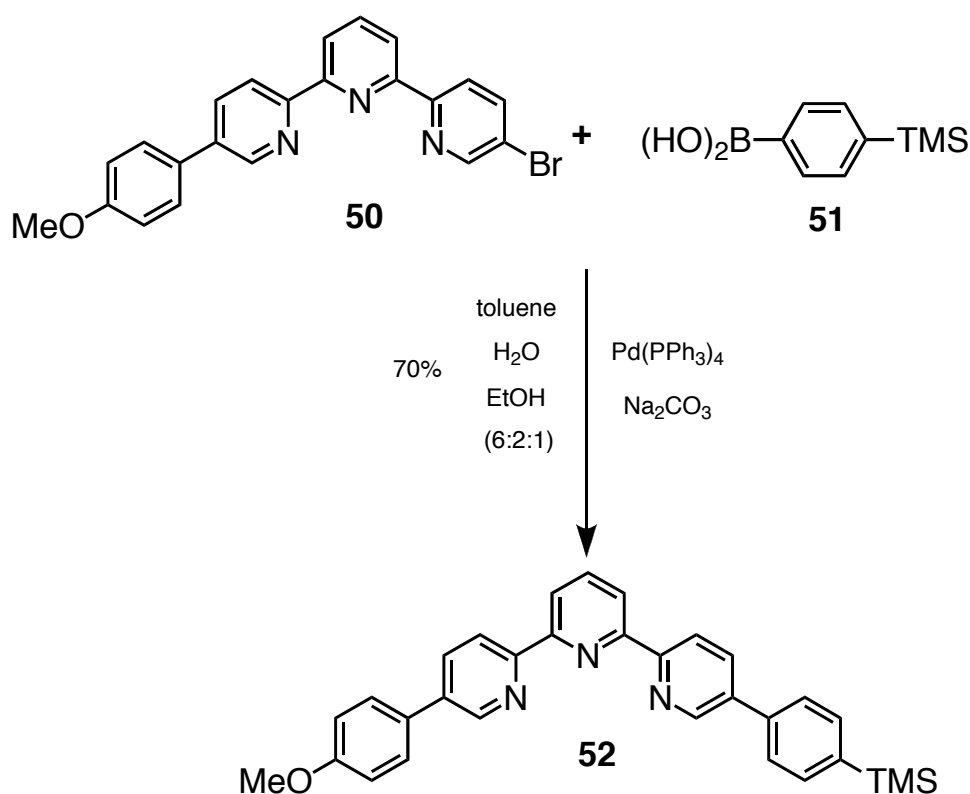
Scheme 6.3. *Synthesis of terpyridine* **52** *by Suzuki cross-coupling reaction.*

To be able to couple the terpy to either the bromo-thread **7** or the iodo-thread **21**, we need to have a stannyl or boronic acid group at one of its ends. To achieve this, we first substituted the TMS group by an iodo group in the same conditions used before to convert TMS-thread **19** to the iodo-thread **21**, using ICl (see scheme 6.4).
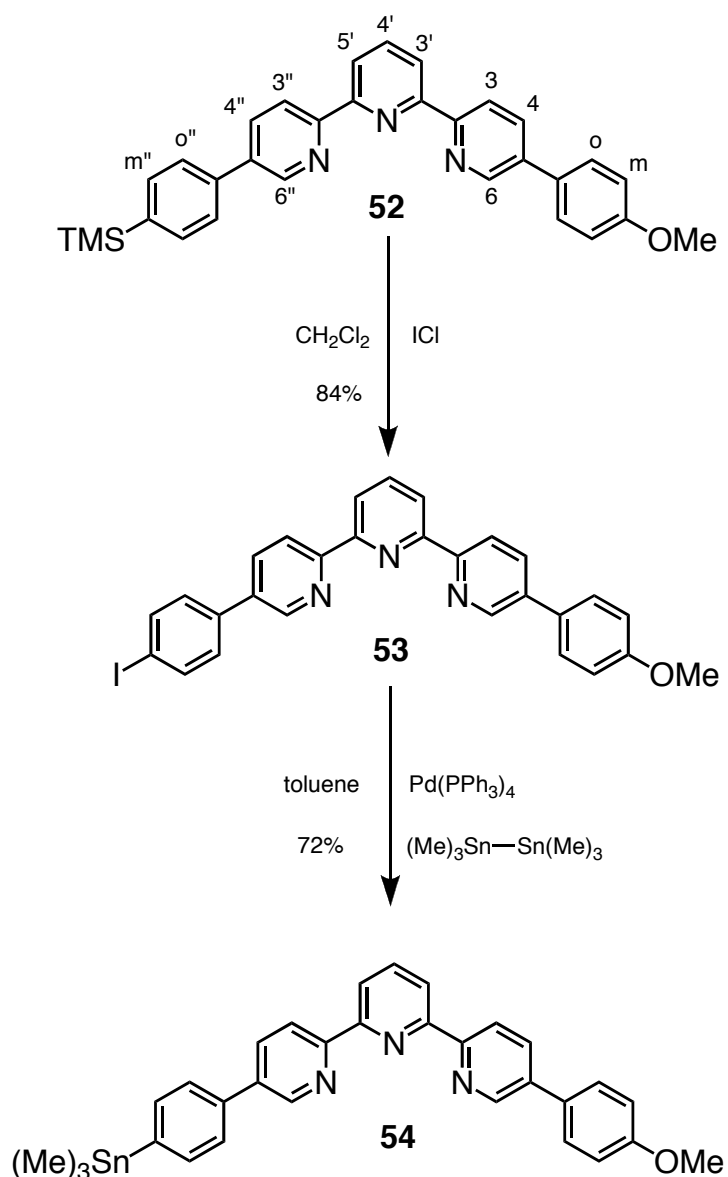
Scheme 6.4. *Synthesis of the stannyl-terpy 54 starting from compound 52.*

The formation of a boronic acid on the terpy was unsuccessful, but we succeeded in obtaining the stannyl compound **54**, by using the hexamethyl-ditin reagent and

Pd(PPh$_3$)$_4$ as a catalyst (see scheme 6.4). All compounds were fully characterized by ^{1}H-NMR and mass spectrometry (see scheme 6.5).
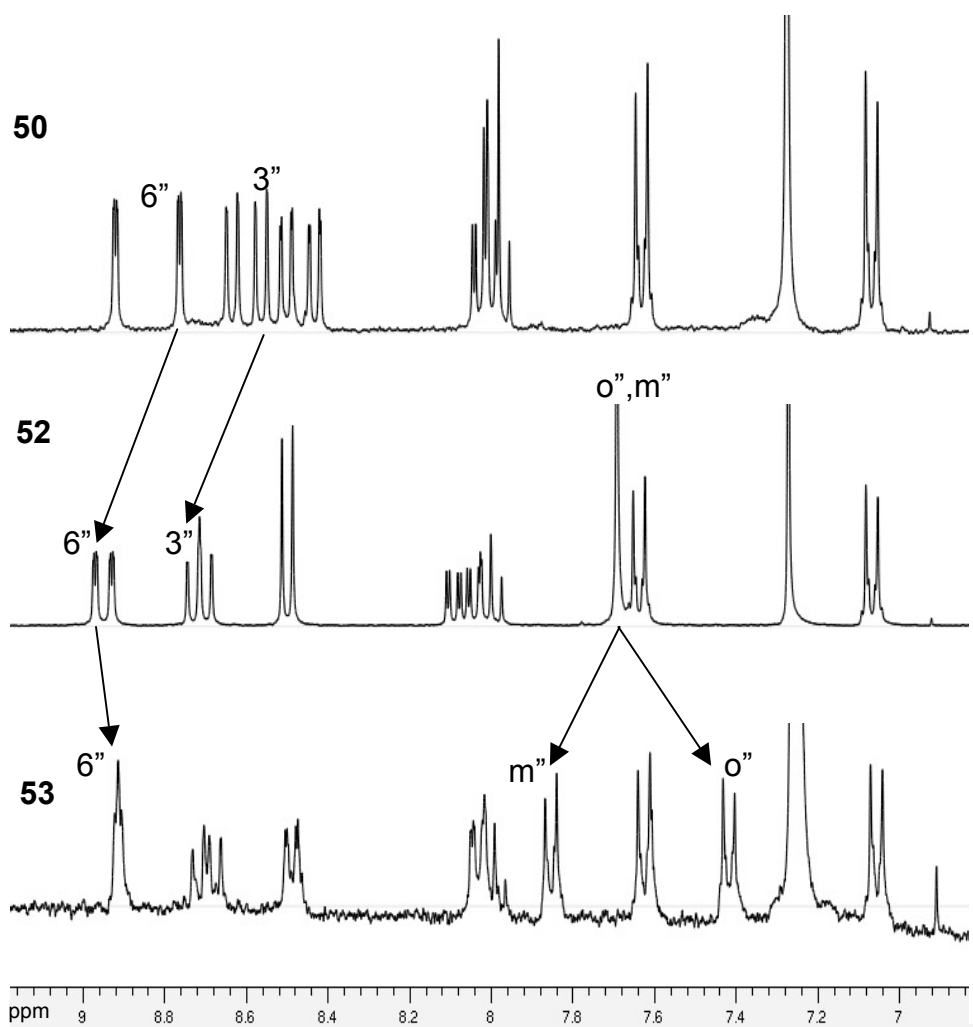
Scheme 6.5. *^{1}H-NMR (300MHz) aromatic region spectra of the terpys **50**, **52** and **53**. All the signals have been assigned. The most characteristic signals are indicated by arrows on the scheme 6.5. The signal of the H$_{6"}$ is particularly sensitive to substitution in terms of chemical shifts. It is worth noting that the spectra of terpy **52** and **54** are almost perfectly identical in the here presented region of the spectra.*

The obtained dissymetric stannyl-terpy was then used for Stille coupling reactions, first to the dibromo-thread **7**, and later also to the diiodo-thread **21**, in the latter case, two phenyl spacers would be between the bipy and the terpy.

Both reactions did not give satisfying results, the target molecules could only be observed as very minor products in mass-spectrometry. Especially for the more promising coupling reaction with the thread **21**, a lot of effort was put into purification to isolate the bis-bipy-bis-terpy thread, but no pure product could be obtained.
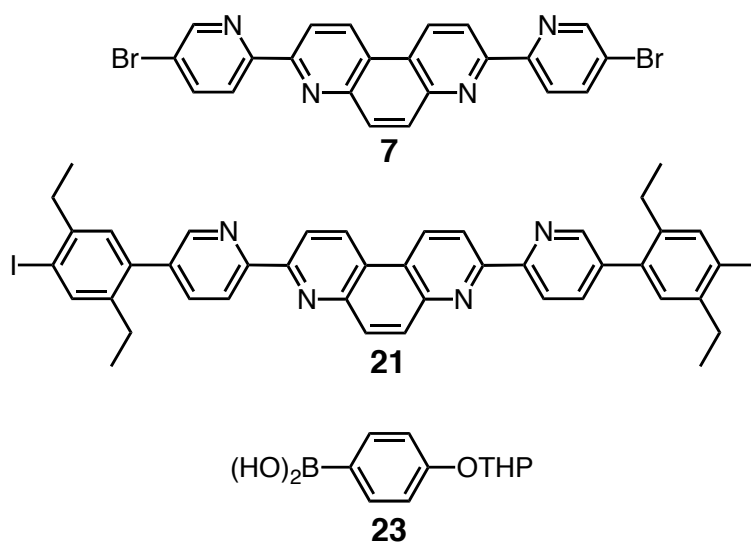
Scheme 6.6. *Reminder of the structures of thread 7 and 21 as well as of boronic acid 23.*

We think that the reasons for this failure are different in each case. The coupling to thread **7** is probably inhibited by its poor solubility as already discussed before. After a first coupling between the bis-bipy thread and the terpy, the resulting mono-terpy-

products should be even less soluble, which means it will precipitate out of the solution and thus not be able to undergo the second coupling reaction.

The soluble thread **21** on the other hand, even after the first coupling reaction, should be soluble enough to permit a second Stille reaction. Unfortunately the iodo group is in the sterically hindered α-position of the ethyl chains, which probably interferes with the Stille coupling reaction. For both reactions, the terpy, acting as a ligand towards the metals present in the reaction mixture is a possible reason for the failure. Being unable to couple terpy **54** to any of the threads, we thought that maybe we can reach our goal by synthesizing a thread with a boronic acid or a stannyl group, and then try Suzuki or Stille coupling with the bromo-terpy **50**. The substitution of the iodine by a boronic acid starting from the iodo-thread **21**, using diboronic ester or pinacolborane, Pd(dppf)Cl$_2$ and KOAc, failed. Even though the here described reaction is the formation of the boronic ester and not the Suzuki coupling in itself, the conditions under which the reaction is carried out are very similar. Suzuki coupling reactions are known to be less successful when carried out on sterically hindered aryl halide substrates.[112, 113] However, we carried out Suzuki coupling with thread **21** and the 4-(tetrahydro-2H-pyran-2-yloxy)phenylboronic acid **23** (see chapter 4.II.2) in a very good yield. Moreover, examples in literature show that even hexyl groups in α-position of either the boronic acid or the halide or even both do not inhibit the Suzuki coupling.[78, 114] The oxidative addition of the aryl halide to the Pd^0 occurs in both reactions, thus it should not be the cause of the failure. The critical step in the mechanism seems to be the transmetallation, which works out fine for an aryl boronic acid, but seems to be ineffective in the case of a diboronic ester or the pinacolborane. Literature is not providing a lot of information on this issue, because most of the

sterically hindered boronic acids are obtained using a BuLi involving synthesis, which, in our case, is not an option due to the presence of the two bipyridines units.

Although we did not succeed in obtaining the boronic acid-thread, we did manage to synthesize the trimethyltin compound **55** (see scheme 6.7). Starting from thread **21**, hexamethylditin, using [Pd(PPh₃)₄] as a catalyst in toluene, we obtained the target compound **55** in 60 % yield.
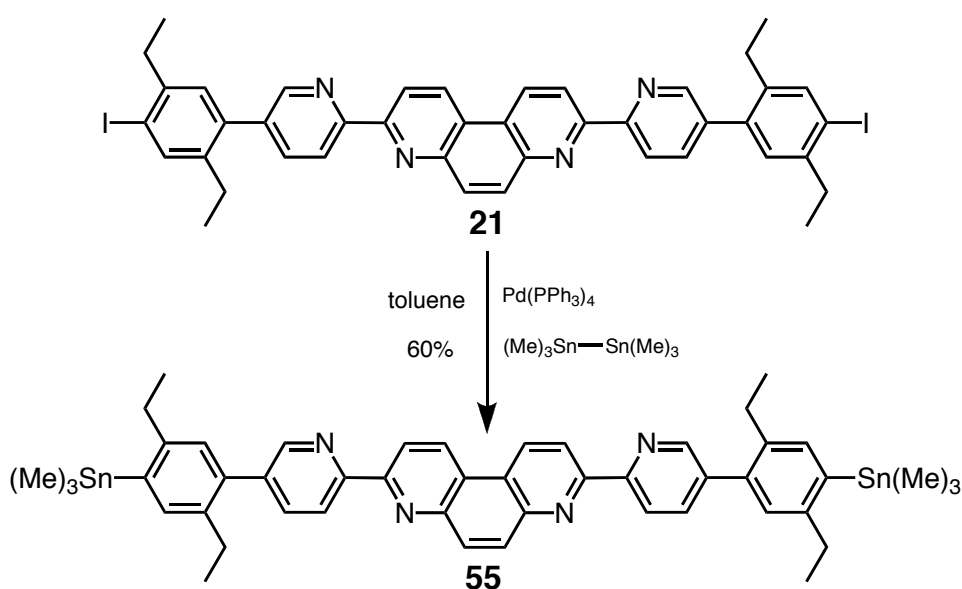
Scheme 6.7. *Synthesis of the stannyl-thread 55 starting from compound 21.*

Again we observe that a reaction process including an oxidative addition of thread **21** on Pd⁰ is a success, strengthening the hypothesis that it is the transmetallation step that causes problems in the formation of the boronic acid. The obtained thread **55** is reacted with the bromo-terpy **50** in Stille coupling conditions, but no linking of the two substrates could be observed. Possible reasons are the steric hindrance, or the

presence of the terpy, that is interfering with coupling reactions due to its coordinating properties as already discussed before.

II.4. Williamson reaction

After having tried several coupling reactions between the terpy and the bis-bipy thread, we decided to choose another synthetic route to reach our goal.

It should be mentioned that, encouraged by positive results obtained in the laboratory, we tried to add a terpy by Williamson reaction. The terpy we synthesized for this attempt is already described in literature: it is the mono-stopper terpy **56**, which was used in the synthesis of a molecular muscle prototype in our laboratory by Maria Consuelo Jimenez-Molero *et al.*[19]

56
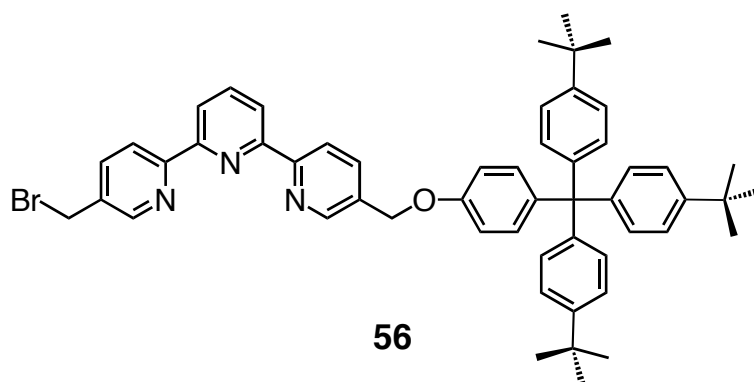
Scheme 6.8. *Terpyridine 56, a tridentate ligand with a stopper group on one side.*

Unfortunately, our Cu(I) complex is of a higher instability then the one mentioned above[19] and thus we are facing the same problems as for the previously discussed Williamson reactions. The chelate (bidentate) ligand in the molecular muscle prototype is a phenanthroline, which forms a more stable complex with Cu(I) than the bipyridine used in our case. Furthermore, as shown in scheme 6.9, in our system (a), both rings are independent. As soon as one copper coordination site is becoming

unstable, thus no longer linking the macrocycle to the thread, dethreading of the concerned macrocycle can occur. The situation is different for the molecular muscle dimer (b): both macrocycles are not independent, they are linked to the thread of the other macrocycle, hence both coordination sites have to be labile at the same time to allow dethreading.
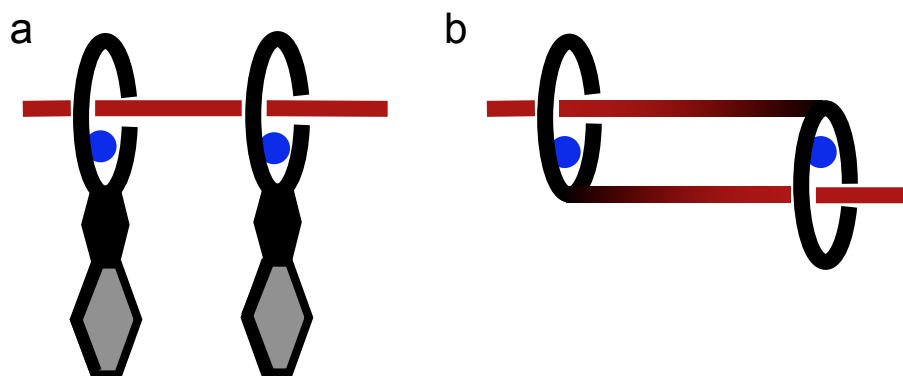
Scheme 6.9. *Schematic representation of the press-like complex (a) and the molecular muscle prototype (b).*

When pseudo-rotaxane **35** is reacted with the terpy **56** under Williamson reaction conditions (Cs_2CO_3, 45°C, DMF), dethreading of the thread and macrocycles occurred, and the final product could not be observed.

III. Conclusion and future prospective

A lot of effort was put in the synthesis of terpyridines able to undergo Suzuki or Stille coupling, or Williamson type reactions with the central bis-bipy-thread part, unfortunately until now, none of these attempts gave satisfying results.

Terpy	Thread	Reaction Conditions
X =	Y =	
—Sn(Me)$_3$	Br	Pd(PPh$_3$)$_2$Cl$_2$ DMF 100°C
		Pd(PPh$_3$)$_4$ DMF 100°C
—Sn(Me)$_3$		Pd(PPh$_3$)$_4$ DMF 100°C
Br	—Sn(Me)$_3$	Pd(PPh$_3$)$_4$ DMF 100°C
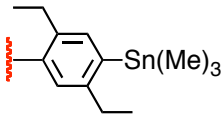
Table 6.1. *Attempts of Stille coupling reactions between the bis-bipy-thread and the terpy moieties.*

Table 6.1. gives an overview of the different threads and terpys that we synthesized and used in different coupling reactions (not including the Williamson reaction described here above).

The rigidity of the target thread imposed C-C coupling reactions as the first choice to graft a terpyridine on the bis-bipy thread. After several attempts with different substrates, it appears that Suzuki or Stille coupling reactions are not suitable for the synthesis of the "4-stations" thread we intended to synthesize. The rigidity of the thread has to be given up, and because Williamson type reactions did not give any satisfying results either, at this stage of the project we are investigating ester or peptide bonding in order to achieve the goal target.

General Conclusion

We have designed a molecular press prototype, based on the functions of the chaperone proteins, which should be able to capture, compress and release guest molecules. The work presented in this thesis has been accomplished while trying to reach this major goal.

The synthesised 4,7-phenanthroline based bis-bipyridine ligand is a crucial building block as it is the core of the threads used in the rotaxane and catenane synthesis. The rigidity that was required to ensure high geometrical control over the rings in the proposed press prototype was the origin of critical solubility problems. Fortunately, these complications could be overcome by adding ethyl groups to this molecule.

A collaboration within the laboratory with Julien Frey and Valérie Heitz led to topologically interesting two dimensional networks containing four copper(I) centres. Indeed, by taking advantage of the gathering and threading effect of copper(I), two bis-macrocycles and two threads have been assembled to form a [4]pseudorotaxane of which a crystal structure was obtained.

Further functionalisation was achieved by grafting polyethyleneglycol chains, bearing allyl groups, to the endings of the axle. After the bis-macrocycles were threaded, the two axles were combined by Ring Closing Metathesis to form one large ring. The resulting [3]catenane was characterized in its metallated as well as in its demetallated form.

Moreover, a first simplified press prototype was synthesised and studied. The thread in this case contains two bipyridine ligands to which two macrocycles can bind by means of a copper(I) metal centre, thus corresponding to the press in its contracted form. Upon demetallation, the rings are free to move on the thread between the two bulky stopper groups, the press then being in its relaxed form. Major problems with the stoppering reactions of this [3]rotaxane could be solved by using the "Meldal-Sharpless" reaction.

Finally, Zn(II)-porphyrins, which operate as captors for a guest molecule, were attached to the macrocycles. A pyridyl-based guest molecule was synthesised and its interaction with the contracted as well as with the relaxed press are studied. Moreover, the press was put to work; copper(I) was added to the demetallated rotaxane-guest complex, forcing the press in its contracted situation, probably compressing the guest.

In order to build a more sophisticated press, a lot of effort was put into the synthesis of dissymmetric terpyridine ligands that could be attached to the outsides of the thread. Several interesting terpyridines have been synthesized, while the junction between the bis-bidentate core-thread and the tridentate ligands is still under investigation.

Williamson as well as coupling reactions are not suited neither for the fixation of the terpyridines nor for the stoppering reactions. As a consequence, several other promising systems, such as peptide bonding or ester formation are currently investigated. We are confident that these new routes will lead us to the four-station molecular press prototype as it was imagined at the beginning of this project. Based on the encouraging results we obtained with the simplified model press, we expect the final press to be operational and we are looking forward to exploring its new features.

References

[1] Wikipedia, **http://en.wikipedia.org/wiki/Bagger_288**.

[2]Gizmodo,**http://gizmodo.com/gadgets/krupps/worlds-largest-digger-digs-potentially-destroys-world-215801.php**.

[3] V. Mermall, P. L. Post and M. S. Mooseker, *Science* **1998**, *279*, 527-533.

[4] R. D. Vale and R. A. Milligan, *Science* **2000**, *288*, 88-95.

[5] C. B. Anfinsen, *Nobel Lecture* (Stockholm) **1972**.

[6] S. Walter and J. Buchner, *Angewandte Chemie International Edition* **2002**, *41*, 1098-1113.

[7] J. C. Ranford, A. R. M. Coates and B. Henderson, *Expert Reviews in Molecular Medicine [online computer file]* **2000**, 1-17.

[8] Dictionary, *Oxford American* **2005**, *version 1.0.1*.

[9] E. R. Kay, D. A. Leigh and F. Zerbetto, *Angewandte Chemie International Edition* **2007**, *46*, 72-191.

[10] R. D. Astumian, *Scientific American* **2001**, *285*, 56-64.

[11] G. Oster, *Nature* **2002**, *417*, 25.

[12] A. Einstein, *Annalen der Physik* **1905**, *17*, 549.

[13] J.-B. Perrin, *Comptes rendus par l'Académie des Sciences* **1908**, *146*, 1500.

[14] P. Reimann and P. Hanggi, *Applied Physics A: Materials Science & Processing* **2002**, *75*, 169-178.

[15] J. C. Maxwell, *Longmans, Green and Co.* **1871**.

[16] R. P. Feynman, R. B. Leighton and M. Sands, *The Feynman lectures on Physics, Chap.46 (Addison-Wesley Reading)* **1963**, *1*.

[17] M. v. Smoluchowski, *Physikalische Zeit* **1912**, *13*, 1069.

[18] D. R. Astumian, *Science* **1997**, *276*, 917-922.

[19] M. C. Jiménez-Molero, C. Dietrich-Buchecker and J.-P. Sauvage, *Chemistry-- A European Journal* **2002**, *8*, 1456-1466.

[20] M. Barboiu, L. Prodi, M. Montalti, N. Zaccheroni, N. Kyritsakas and J.-M. Lehn, *Chem. Eur. J.* **2004**, *10*, 2953-2959.

[21] H.-R. Tseng, S. A. Vignon and J. F. Stoddart, *Angewandte Chemie, International Edition* **2003**, *42*, 1491-1495.

[22] V. A. Azov, A. Schlegel and F. Diederich, *Bulletin of the Chemical Society of Japan* **2006**, *79*, 1926-1940.

[23] J. D. Badjic, V. Balzani, A. Credi, S. Silvi and J. F. Stoddart, *Science* **2004**, *303*, 1845-1849.

[24] P. R. Ashton, R. Ballardini, V. Balzani, I. Baxter, A. Credi, M. C. T. Fyfe, M. T. Gandolfi, M. Gomez-Lopez, M. V. Martinez-Diaz, A. Piersanti, N. Spencer, J. F. Stoddart, M. Venturi, A. J. P. White and D. J. Williams, *Journal of the American Chemical Society* **1998**, *120*, 11932-11942.

[25] A. Livoreil, J.-P. Sauvage, N. Armaroli, V. Balzani, L. Flamigni and B. Ventura, *Journal of the American Chemical Society* **1997**, *119*, 12114-12124.

[26] B. Korybut-Daszkiewicz, A. Wieckowska, R. Bilewicz, S. Domagala and K. Wozniak, *Angewandte Chemie International Edition* **2004**, *43*, 1668-1672.

[27] A. M. Brouwer, C. Frochot, F. G. Gatti, D. A. Leigh, L. Mottier, F. Paolucci, S. Roffia and G. W. H. Wurpel, *Science* **2001**, *291*, 2124-2128.

[28] V. Balzani, M. Clemente-Leon, A. Credi, B. Ferrer, M. Venturi, A. H. Flood and J. F. Stoddart, *Proceedings of the National Academy of Sciences of the United States of America* **2006**, *103*, 1178-1183.

[29] S. Saha, L. E. Johansson, A. H. Flood, H.-R. Tseng, J. I. Zink and J. F. Stoddart, *Small* **2005**, *1*, 87-90.

[30] R. Eelkema and B. L. Feringa, *Chemistry--An Asian Journal* **2006**, *1*, 367-369.

[31] P. Mobian, J.-M. Kern and J.-P. Sauvage, *Angewandte Chemie International Edition* **2004**, *43*, 2392-2395.

[32] D. A. Leigh, J. K. Y. Wong, F. Dehez and F. Zerbetto, *Nature* **2003**, *424*, 174-179.

[33] C. Dietrich-Buchecker and J.-P. Sauvage, *Catenanes, Rotaxanes and Knots. A Journey Through the World of Molecular Topology*, Wiley-VCH, Weinheim, **1999**, p.

[34] G. Schill and H. Zollenkopf, *Justus Liebigs Annalen der Chemie* **1969**, *721*, 53-74.

[35] G. Schill and Lüttringhaus, *Angewandte Chemie* **1964**, *76*, 567-568.

[36] C. Dietrich-Buchecker, J.-P. Sauvage and J.-P. Kintzinger, *Tetrahedron Letters* **1983**, *24*, 5095-5098.

[37] L. Hogg, D. A. Leigh, P. J. Lusby, A. Morelli, S. Parsons and J. K. Y. Wong, *Angewandte Chemie International Edition* **2004**, *43*, 1218-1221.

[38] H. Ogino, *Journal of the American Chemical Society* **1981**, *103*, 1303-1304.

[39] W. Clegg, C. Gimenez-Saiz, D. A. Leigh, A. Murphy, A. M. Z. Slawin and S. J. Teat, *Journal of the American Chemical Society* **1999**, *121*, 4124-4129.

[40] P. R. Ashton, M. C. T. Fyfe, S. K. Hickingbottom, S. Menzer, J. F. Stoddart, A. J. P. White and D. J. Williams, *Chemistry--A European Journal* **1998**, *4*, 577-589.

[41] C. A. Hunter, *Journal of the American Chemical Society* **1992**, *114*, 5303-5311.

[42] A.-M. L. Fuller, D. A. Leigh and P. J. Lusby, *Angewandte Chemie International Edition* **2007**, *46*, 5015-5019.

[43] D. G. Hamilton, N. Feeder, L. Prodi, S. J. Teat, W. Clegg and J. K. M. Sanders, *Journal of the American Chemical Society* **1998**, *120*, 1096-1097.

[44] P. L. Anelli, P. R. Ashton, R. Ballerdini, V. Balzani, M. Delgado, M. T. Gandolfi, T. T. Goodnow, A. E. Kaifer, D. Philiè, M. Pietraszkiewicz, L. Prodi, M. V. Reddington, A. M. Z. Slawin, N. Spencer, J. F. Stoddart, C. Vincent and D. J. Williams, *Journal of the American Chemical Society* **1992**, *114*, 193-218.

[45] H. Kawai, T. Umehara, K. Fujiwara, T. Tsuji and T. Suzuki, *Angewandte Chemie, International Edition* **2006**, *45*, 4281-4286.

[46] J.-S. Shin and N. A. Pierce, *Journal of the American Chemical Society* **2004**, *126*, 10834-10835.

[47] K. Ichimura, S.-K. Oh and M. Nakagawa, *Science* **2000**, *288*, 1624-1626.

[48] J. Berna, D. A. Leigh, M. Lubowska, S. M. Mendoza, E. M. Pérez, P. Rudolf, G. Teobaldi and F. Zerbetto, *Nature Materials* **2005**, *4*, 704-710.

[49] E. Green Jonathan, W. Choi Jang, A. Boukai, Y. Bunimovich, E. Johnston-Halperin, E. DeIonno, Y. Luo, A. Sheriff Bonnie, K. Xu, S. Shin Young, H.-R. Tseng, J. F. Stoddart and R. Heath James, *Nature* **2007**, *445*, 414-417.

[50] T. D. Nguyen, Y. Liu, S. Saha, K. C.-F. Leung, J. F. Stoddart and J. I. Zink, *Journal of the American Chemical Society* **2007**, *129*, 626-634.

[51] Y. Liu, A. H. Flood, P. A. Bonvallet, S. A. Vignon, B. H. Northrop, H.-R. Tseng, J. O. Jeppesen, T. J. Huang, B. Brough, M. Baller, S. Magonov, S. D. Solares, W. A. Goddard, C.-M. Ho and J. F. Stoddart, *Journal of the American Chemical Society* **2005**, *127*, 9745-9759.

[52] R. Eelkema and B. L. Feringa, *Organic & Biomolecular Chemistry* **2006**, *4*, 3729-3745.

[53] R. Eelkema, M. M. Pollard, N. Katsonis, J. Vicario, D. J. Broer and B. L. Feringa, *Journal of the American Chemical Society* **2006**, *128*, 14397-14407.

[54] R. Eelkema, M. M. Pollard, J. Vicario, N. Katsonis, B. S. Ramon, C. W. M. Bastiaansen, D. J. Broer and B. L. Feringa, *Nature* **2006**, *440*, 163.

[55] L. C. Palmer and J. Rebek, Jr., *Organic Letters* **2005**, *7*, 787-789.

[56] O. Seneque, M.-N. Rager, M. Giorgi and O. Reinaud, *Journal of the American Chemical Society* **2000**, *122*, 6183-6189.

[57] L. Trembleau and J. Rebek, Jr., *Science* **2003**, *301*, 1219-1221.

[58] D. Ajami and J. J. Rebek, *Journal of the American Chemical Society* **2006**, *128*, 15038-15039.

[59] S. Tashiro, M. Tominaga, Y. Yamaguchi, K. Kato and M. Fujita, *Chemistry--A European Journal* **2006**, *12*, 3211-3217.

[60] V. Chaurin, E. C. Constable and C. E. Housecroft, *New Journal of Chemistry* **2006**, *30*, 1740-1744.

[61] J.-P. Collin, C. Dietrich-Buchecker, P. Gaviña, M. C. Jiménez-Molero and J.-P. Sauvage, *Accounts of Chemical Research* **2001**, *34*, 477-487.

[62] C. Dietrich-Buchecker and J.-P. Sauvage, *Tetrahedron Letters* **1983**, *24*, 5091-5094.

[63] N. Armaroli, V. Balzani, J.-P. Collin, P. Gaviña, J.-P. Sauvage and B. Ventura, *Journal of the American Chemical Society* **1999**, *121*, 4397-4408.

[64] J.-P. Collin, P. Gaviña and J.-P. Sauvage, *New Journal of Chemistry* **1997**, *21*, 525-528.

[65] P. N. W. Baxter, R. G. Khoury, J.-M. Lehn, G. Baum and D. Fenske, *Chemistry--A European Journal* **2000**, *6*, 4140-4148.

[66] X. Wang, P. Rabbat, P. O'Shea, R. Tillyer, E. J. J. Grabowski and P. J. Reider, *Tetrahedron Letters* **2000**, *41*, 4335-4338.

[67] K. C. Nicolaou, P. G. Bulger and D. Sarlah, *Angewandte Chemie, International Edition* **2005**, *44*, 4442-4489.

[68] S. P. Stanforth, *Tetrahedron* **1998**, *54*, 263-303.

[69] N. Miyaura, T. Yanagi and A. Suzuki, *Synthetic Communications* **1981**, *11*, 513-519.

[70] N. Miyaura and A. Suzuki, *Chemical Reviews* **1995**, *95*, 2457-2483.

[71] I. Poleschak, J.-M. Kern and J.-P. Sauvage, *Chemical Communications* **2004**, 474-476.

[72] D. E. Richardson and H. Taube, *Inorganic Chemistry* **1981**, *20*, 1278-1285.

[73] C. O. Dietrich-Buchecker, J.-P. Sauvage, A. De Cian and J. Fischer, *Journal of the Chemical Society, Chemical Communications* **1994**, 2231-2232.

[74] J. Frey, T. Kraus, V. Heitz and J.-P. Sauvage, *Chemical Communications* **2005**, 5310-5312.

[75] C. Dietrich-Buchecker, J.-P. Sauvage and J.-M. Kern, *Journal of the American Chemical Society* **1989**, *111*, 7791-7800.

[76] E. Baranoff, J.-P. Collin, J. Furusho, Y. Furusho, A.-C. Laemmel and J.-P. Sauvage, *Inorganic Chemistry* **2002**, *41*, 1215-1222.

[77] M. Rehahn, A. D. Schlueter and W. J. Feast, *Synthesis* **1988**, 386-388.

[78] V. Hensel and D. A. Schlüter, *Liebigs Annalen Recueil* **1997**, 303-309.

[79] A. Gorka in *Vol.* **http://www.math.clemson.edu/~agorka/topology.htm**.

[80] E. Wasserman, *Journal of the American Chemical Society* **1960**, *83*, 4433-4434.

[81] C. O. Dietrich-Buchecker, J. F. Nierengarten, J. P. Sauvage, N. Armaroli, V. Balzani and L. De Cola, *Journal of the American Chemical Society* **1993**, *115*, 11237-11244.

[82] L. Wang, M. O. Vysotsky, A. Bogdan, M. Bolte and V. Boehmer, *Science* **2004**, *304*, 1312-1314.

[83] K. S. Chichak, S. S. Cantrill, A. R. Pease, S.-H. Chiu, G. W. V. Cave, J. L. Atwood and J. F. Stoddart, *Science* **2004**, *304*, 1308-1312.

[84] T. M. Trnka and R. H. Grubbs, *Accounts of Chemical Research* **2001**, *34*, 18-29.

[85] A. Furstner, *Angewandte Chemie, International Edition* **2000**, *39*, 3012-3043.

[86] R. H. Grubbs, *Tetrahedron* **2004**, *60*, 7117-7140.

[87] Schmidt Bernd, *European Journal of Organic Chemistry* **2004**, *2004*, 1865-1880.

[88] S. H. Hong, D. P. Sanders, C. W. Lee and R. H. Grubbs, *Journal of the American Chemical Society* **2005**, *127*, 17160-17161.

[89] B. Alcaide and P. Almendros, *Chemistry--A European Journal* **2003**, *9*, 1258-1262.

[90] J. Frey, W. Dobbs, V. Heitz and J.-P. Sauvage, *European Journal of Inorganic Chemistry* **2007**, 2416-2419.

[91] L. Raehm, J.-M. Kern and J.-P. Sauvage, *Chemistry--A European Journal* **1999**, *5*, 3310-3317.

[92] J.-C. Chambron, J.-P. Sauvage, K. Mislow, A. De Cian and F. Jean, *Chemistry--A European Journal* **2001**, *7*, 4085-4096.

[93] H. W. Gibson, S. H. Lee, P. T. Engen, P. Lecavalier, J. Sze, Y. X. Shen and M. Bheda, *Journal of Organic Chemistry* **1993**, *58*, 3748-3756.

[94] P. Mobian, J.-P. Collin and J.-P. Sauvage, *Tetrahedron Letters* **2006**, *47*.

[95] K. V. Gothelf and K. A. Jorgensen, *Chemical Reviews* **1998**, *98*, 863-909.

[96] V. V. Rostovtsev, L. G. Green, V. V. Fokin and K. B. Sharpless, *Angewandte Chemie, International Edition* **2002**, *41*, 2596-2599.

[97] R. Huisgen, *Angewandte Chemie* **1963**, *75*, 604-637.

[98] L. Zhang, X. Chen, P. Xue, H. H. Y. Sun, I. D. Williams, K. B. Sharpless, V. V. Fokin and G. Jia, *Journal of the American Chemical Society* **2005**, *127*, 15998-15999.

[99] M. Meldal, C. Christensen and C. W. Tornoe, *Journal of Organic Chemistry* **2002**, *67*, 3057-3064.

[100] K. B. Sharpless, V. V. Fokin, L. G. Green and V. V. Rostovtsev, *Angewandte Chemie International Edition* **2002**, *41*, 2596-2599.

[101] H. C. Kolb, M. G. Finn and K. B. Sharpless, *Angewandte Chemie, International Edition* **2001**, *40*, 2004-2021.

[102] V. O. Rodionov, V. V. Fokin and M. G. Finn, *Angewandte Chemie International Edition* **2005**, *44*, 2210-2215.

[103] T. Kobayashi and S. Kobayashi, *European Journal of Organic Chemistry* **2002**, 2066-2073.

[104] K. M. Kadish, K. M. Smith and R. Guilard in *Database of redox potentials and binding constants*, *Vol. 9* (Ed. A. Press), **2000**.

[105] L. Flamigni, A. M. Talarico, F. Barigelletti and M. R. Johnston, *Photochemical and Photobiological Science* **2002**, *1*, 190-197.

[106] J. Bourson, J. Pouget and B. Valeur, *Journal of Physical Chemistry* **1993**, *97*, 4552-4557.

[107] A. Satake and Y. Kobuke, *Tetrahedron* **2005**, *61*, 13-41.

[108] E. Iengo, E. Zangrando, E. Alessio, J.-C. Chambron, V. Heitz, L. Flamigni and J.-P. Sauvage, *Chemistry--A European Journal* **2003**, *9*, 5879-5887.

[109] A. O. Pablo Ballester, Antoni Costa, Pere Deya, Antonio Frontera, Rosa Gomila, and Christopher Hunter, *J. Am. Chem. Soc.* **2006**, *128*, 5560-5569.

[110] J. K. M. Sanders, J. L. Atwood, E. D. Davis, D. D. M. Nicol and F. Vögtle in *Templated Chemistry of Porphyrin Oligomers*, *Vol. 9* Eds.: J.-P. Sauvage and M. W. Hosseini), Pergamon, **1996**, pp. 131-164.

[111] B. X. Colasson, C. Dietrich-Buchecker and J.-P. Sauvage, *Synlett* **2002**, *2*, 271-272.

[112] M. G. Johnson and R. J. Foglesong, *Tetrahedron Letters* **1997**, *38*, 7001-7002.

[113] H. Chaumeil, S. Signorella and C. Le Drian, *Tetrahedron* **2000**, *56*, 9655-9662.

[114] X. Deng, A. Mayeux and C. Cai, *Journal of Organic Chemistry* **2002**, *67*, 5279-5283.

[115] H. Gilman and F. K. Cartledge, *Journal of Organometallic Chemistry* **1964**, *2*, 447-454.

Experimental part

General points

Instrumentation

Nuclear Magnetic Resonance (NMR) spectra for ^{1}H and ^{13}C were acquired on either a Bruker AVANCE 300 (300 MHz) or a Bruker AVANCE 400 (400 MHz) or a Bruker AVANCE 500 (500 MHz) spectrometer. The spectra were referenced to residual proton-solvent references (^{1}H: CD$_2$Cl$_2$: 5.32 ppm, CDCl$_3$: 7.26 ppm; D$_2$O: 4.79ppm, DMSO-d$_6$: 2.50 ppm, ^{13}C: CD$_2$Cl$_2$: 53.7 ppm, CDCl$_3$: 77.1 ppm). In the assignments, the chemical shift (in ppm) is given first, followed, in brackets, by the multiplicity of the signal (s: singlet, d: doublet, t: triplet, dd: doublet doublet, tt: triplet triplet, dt: doublet triplet, m: multiplet), the value of the coupling constants in Hertz if applicable, the assignment and finally the number of protons implied.

Mass spectra were obtained by using a VG ZAB-HF (FAB) spectrometer, a VG-BIOQ triple quadrupole, positive mode, a Bruker MicroTOF spectrometer (ES-MS). MALDI analysis were performed on an Autoflex II TOF/TOF Bruker Daltronics spectrometer.

Cyclic voltammetry experiments were performed using an EG&G Princeton Applied Research 273A potentiostat, a Pt working electrode, a Pt counter electrode, a silver wire as a reference, and 0.1 M Bu$_4$NPF$_6$ as supporting electrolyte. Redox potential are given *versus* SCE.

UV-Visible absorption spectra were performed using a Kontron UVIKON 860 spectrophotometer. Wavelengths are given in nm and molar extinction coefficients (ε) are given in L.mol^{-1}.cm^{-1}.

Chromatographic supports

Thin-layer chromatography was performed using glass or plastic sheets coated with silica or neutral alumina. They were examined after dipping in an aqueous iron(II) solution (terpyridines), after oxidation with iodine (other organic compounds) or under the UV lamp. Column chromatography was carried out on silicagel (Kieselgel 60 (0.063-0.200 mm), Merck) or alumina (Aluminoxid 90 standardized (0.060-0.200mm), Merck). Automatic column chromatography was carried out on an Isco Combiflash Retrieve (205L20133) machine with pre-packed RediSep alumina (80g) or silica (45g) columns.

Some solvents were dried in the laboratory by distillation under argon, over the appropriate drying agent: tetrahydrofuran, toluene, diethylether and dioxane over sodium/benzophenone, dichloromethane over CaH_2. All other anhydrous solvents used are commercially available ("analytical grade").

All commercial chemicals were of the best commercially available grade, and were used without further purification, except *n*-BuLi, titrated using the double titration method described by H. Gilman *et al*[115].

Synthesis

N,N-dimethyl-4,7-phenanthrolinium diiodide (**2**):
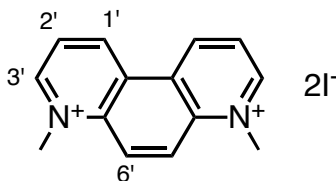
A large excess of MeI 20 mL (45.6g , 321.26 mmol) was added to a solution of 4,7-phenanthroline 1.7459 g (9.68 mmol) in DMF (240 mL) and the resulting reaction mixture was stirred at 20 ^{0}C for 41 h. The precipitate formed was collected by filtration, dried and its ^{1}H-NMR recorded (in order to see if the material was pure or a mixture of mono- and diiodo-derivatives was present). To the mother liquor more MeI (10ml) was added and the reaction further stirred for 24 h. The precipitate formed was again collected by filtration, dried and characterized by ^{1}H-NMR spectroscopy. Compound **2** was isolated as an orange crystalline solid in 90 % yield.

^{1}H-NMR (300 MHz, D_2O, 25 ^{0}C): δ = 10.07 (d, J = 8.2 Hz, $H_{3'}$, 2H), 9.49 (ddd, J_1 = 5.9 Hz, J_2 = 0.6 Hz, $H_{1'}$, 2H), 9.04 (s, $H_{6'}$,2H), 8.43 (ddd, J_1 = 8.7 Hz, J_2 = 5.9 Hz, $H_{2'}$, 2H), 4.80 (s,CH_3, 6H) ppm

MS (ES): *m/z* (%) = 195.0 (100) [**2** - 2I - Me]$^+$ (calcd: 195.0)

N,N-dimethyl-4,7-phenanthrolinium dione (**3**):
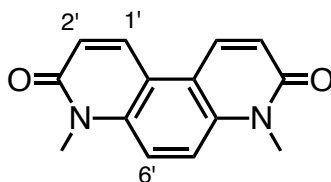
N,N-dimethyl-4,7-phenanthrolinium diiodide **2**, 3.652 g (7.87 mmol) was dissolved in hot distilled water (250 mL) and the solution allowed to cool to ambient temperature. Five drops of aq. NaOH (3.21g in 80 mL of dist. H_2O) were added followed by aq. $K_3Fe(CN)_6$, 127 mL (0.305 mol/L in dist. H_2O) added to the stirred solution drop by drop over a period of 1 h. Afterwards NaOH was added so to rise the pH from 6 to 9. The colour of the solution changed from yellow to orange-brown and a very fine precipitate formed. Another 6.75 g of NaOH were added as well as 72 mL of aq. $K_3Fe(CN)_6$ (0.305 mol/L in distilled H_2O) in order to precipitate more solid and the mixture further stirred for 4 h (pH = 9). The aqueous layer was in turn reduced to half of its original volume, and extracted with $CHCl_3$ (5 times 250 mL). The chloroform layer was then collected and evaporated to dryness and the brown product was isolated in 99% yield. Purity was checked by ^{1}H-NMR spectroscopy.

^{1}H-NMR (300 MHz, $CDCl_3$, 25 ^{0}C): δ = 8.25 (d, J = 9.8 Hz, H$_{1'}$, 2H), 7.65 (s, H$_{6'}$, 2H), 6.92 (d, J = 9.9 Hz, H$_{2'}$, 2H), 3.81 (s, CH_3, 6H) ppm

MS (FAB); *m/z* (%) = 241.0 (100) [**3** + H]$^+$ (calcd: 241.1)

3,8-dibromo-4,7-phenanthroline (**4**):
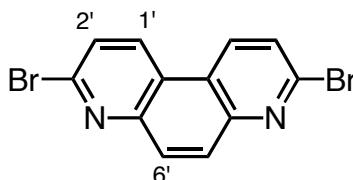
Compound **3** (1g, 4.16 mmol), POBr$_3$ (34.23 g, 120 mmol) and PBr$_3$ (5.84 g, 21.6 mmol) were placed in a round bottomed flask fitted with an air condenser under argon. The mixture was heated at 180 ^{0}C for 48 h. After cooling to about 60 ^{0}C, the black residue formed was added to excess ice/water (500 ml) and was vigorously stirred until hydrolysis of the remaining phosphorous halides was complete. Further ice was added and the mixture adjusted to pH 14 by dropwise addition of 20 % aq. NaOH. The final mixture was left to react further for 30 min and then cooled down in an ice bath. The precipitate formed was collected by filtration and washed with hot $CHCl_3$ (10x100 ml) while the aqueous layer was extracted with $CHCl_3$ (4 x 250 mL). The combined organic layers were in turn evaporated to afford a yellowish-white solid in 94% yield.

^{1}H-NMR (300 MHz, $CDCl_3$, 25 ^{0}C): δ = 8.68 (d, J = 8.7 Hz, H$_{1'}$, 2H), 8.21 (s, H$_{6'}$, 2H), 7.78 (d, J = 8.7 Hz, H$_{2'}$, 2H) ppm

MS (FAB): *m/z* (%) = 338.8 (100) [**4** + H]$^+$ (calcd: 338.9)

5-bromo-2-trimethylstannyl pyridine **(6)**:
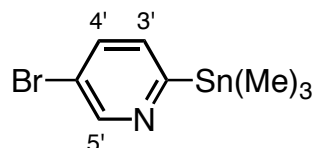
BuLi (9.2 mL of a 1.65 M solution in hexane) was added dropwise to a solution of 5-bromo-2-iodopyridine (4 g, 14.06 mmol) in dry toluene (130 mL) at -20 ^{0}C. During the addition, the temperature was progressively lowered to -76 ^{0}C. When all BuLi was added, the reaction mixture was further stirred for 2 h at -76 ^{0}C. To this, a solution of ClSnMe$_3$ (3.4 g, 16.8 mmol) in dry toluene (40 mL) was added and the resulting yellow solution stirred for an additional hour at -76 ^{0}C. It was then allowed to warm up to ambient temperature. Toluene was evaporated and the crude product taken up in CH$_2$Cl$_2$. Insoluble salts were filtered off and the filtrate evaporated to dryness. The resulting yellow oil was submitted to a very fast column (45 minutes, over 100 g of oven dried alumina, eluent Et$_2$O) to afford the stannyl compound **6** as yellow oil in 86%.

^{1}H-NMR (300 MHz, CDCl$_3$, 25 ^{0}C): δ = 8.80 (d, J = 2.3 Hz, H$_{5'}$, 1H), 7.64 (dd, J$_1$ = 7.9 Hz, J$_2$ = 2.3 Hz, H$_{4'}$, 1H), 7.32 (dd, J$_1$ = 7.9 Hz, J$_2$ = 0.7 Hz, H$_{3'}$, 1H), 0.33 (s, with Sn satellites, -CH$_3$, 9H) ppm

MS (EI): *m/z* (%) = 305.9 (100) [**6** - CH$_3$]$^+$ (calcd: 305.89).

3,8-bis(4-bromo-2'-pyridyl)-4,7-phenanthroline **(7)**:
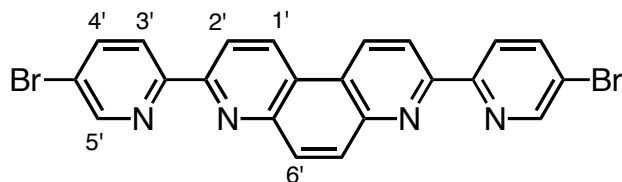
5-bromo-2-trimethylstannyl pyridine **6** (1.96 g, 6.05 mmol) and 3,8-dibromo-4,7-phenanthroline **4** (1 g, 2.96 mmol) were suspended in dry toluene (130 mL) and the mixture degassed for 5 minutes. To this, Pd[P(Ph$_3$)$_4$], (230 mg, 0.2 mmol) was added and the resulting reaction mixture further degassed for 5 minutes. It was then refluxed (140 ^{0}C) under argon atmosphere for 18 h. Another 160 mg of Pd[P(Ph$_3$)$_4$] were added and the reaction stirred for another 44 h under reflux. Evaporation of toluene afforded the crude product as a grey solid that was washed with MeOH (2 x150 mL) and Et$_2$O (2 x 150 mL). Compound **7** was extracted from the remaining solid by washing it with 5 times 150 mL of chloroform. After evaporating the chloroform an washing the grey solid again with MeOH and Et$_2$O, 1.26 g of a greyish yellow solid were obtained (85% yield).

^{1}H-NMR (300 MHz, CDCl$_3$, 25 ^{0}C): δ = 9.05 (d, J = 8.7 Hz, H$_{1'}$, 2H), 8.80 (d, J = 1.6 Hz, H$_{5'}$, 2H), 8.74 (d, J = 8.7 Hz, H$_{2'}$, 2H), 8.64 (d, J = 9.1 Hz, H$_{3'}$, 2H), 8.31 (s, H$_{6'}$, 2H), 8.03 (dd, J$_1$ = 8.4 Hz, J$_2$ = 2.3 Hz, H$_{4'}$, 2H) ppm

MS (FAB): *m/z* (%) = 493.0 (100) [**7** + H]$^+$ (calcd: 492.9)

3,8-bis(4-(4-trimethylsilylphenyl)-2'-pyridyl)-4,7-phenanthroline **(8)**:
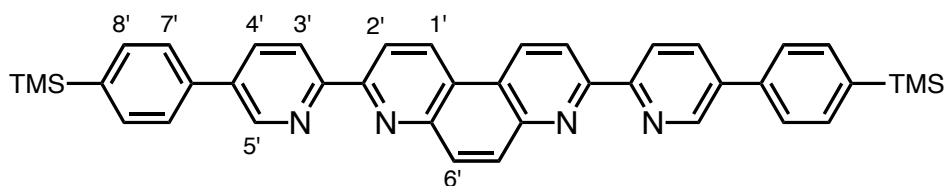
The following reactants were added under argon atmosphere with a little bit of DMF (25 mL all together) in the following order. After each adding; the reaction mixture was degassed. Compound **7** (200 mg, 0.4 mmol), $[Pd(PPh_3)_4]$ (46 mg, 0.04 mmol), K_3PO_4 (255 mg, 1.2 mmol), 4-(trimethylsilyl)phenylboronic acid (171mg, 0.88 mmol). The mixture was then heated to 100 °C and stirred for 28 h. After cooling down to room temperature, the solution was added to 250 mL of water. The formed precipitate was filtered off and washed with Et_2O (2 x 250 mL), EtOH (2 x 250 mL). The product was extracted from the remaining solid with chloroform (4 x 50 mL + 1 x 150 mL). The combined organic fractions were filtered over celite and evaporated to dryness. After recrystallizing the yellowish-white product in chloroform. The white product **8** was obtained in 66% yield.

^{1}H-NMR (300 MHz, CDCl$_3$, 25 ^{0}C): δ = 9.10 (d, J = 8.9 Hz, H$_{1'}$, 2H), 9.02(dd, J$_1$ = 1.6 Hz, J$_2$ = 0.75 Hz, H$_{11'}$, 2H) 8.83 (d, J = 8.5 Hz, H$_{2'}$, 2H), 8.81 (d, J = 7.5 Hz, H$_{13}$,H$_{13'}$, 2H), 8.37 (s, H$_{6'}$, 2H), 8.13 (dd, J$_1$ = 8.0 Hz, J$_2$ = 2.0 Hz, H$_{4'}$, 2H), 7.70 (s, H$_{7'}$, H$_{8'}$, 8H), 0.33 (s, -Si*(CH$_3$)$_3$*, 9H) ppm

MS (ES): *m/z* (%) = 631.3131 (100) [**8** + H]$^+$ (calcd: 631.2713)

3,8-bis(4-(4-methoxyphenyl)-2'-pyridyl)-4,7-phenanthroline **(9)**:
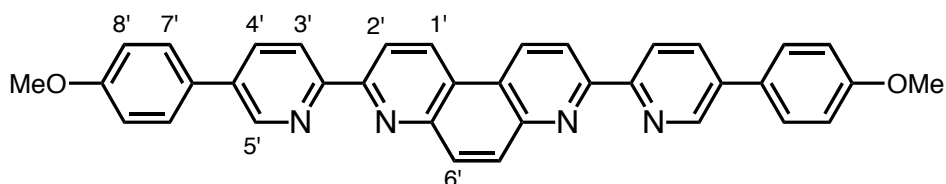
A solution of 3,8-bis(4-bromo-2'-pyridyl)-4,7-phenanthroline **7** (200 mg, 0.4 mmol), 4-methoxyphenylboronic acid (134 mg, 0.88 mmol) and potassium carbonate 425 mg (2 mmol) in 25 ml DMF was degassed (3 times vacuum/argon) before palladium tetratriphenylphospine (46 mg, 0.04 mmol, 10% mol) was added. The solution was then heated up to reflux (120 °C) under argon atmosphere and stirred for 3h, then15 mg of catalyst were added. After another 18 h of heating, the reaction mixture was cooled down to room temperature and poured into 250 mL of water. The product thus precipitated with impurities and was then filtered over celite and washed with EtOH and dichloromethane. The celite-product mixture was then extracted with boiling

137

chloroform. The organic fractions were collected and washed one more time with chloroform. Compound **9** is finally obtained in 88% yield.

¹H-NMR (300 MHz, CDCl$_3$, TFA(3%), 25 ^{0}C): δ = 9.42 (d, J$_1$ = 8.43 Hz, H$_{1'}$, 2H), 9.12 (s, H$_{5'}$,2H) 8.79 (dd, J$_1$ = 3.48 Hz, J$_4$ = 1.29 Hz, H$_{4'}$, 2H), 8.73 (d, J$_1$ = 8.22 Hz, H$_{2'}$, 2H), 8.57 (d, J$_1$ = 8.76 Hz, H$_{3'}$, 2H 7.70 (d, J$_1$ = 8.79 Hz, H$_{7'}$, 4H), 7.15 (d, J$_1$ = 8.97 Hz, H$_{8'}$, 4H), 3.99 (s, -O-CH$_3$, 4H) ppm

MS (ES): *m/z* (%) = 547.2161 (100) [**9** + H]$^+$ (calcd: 547.2129)

pseudo[3]rotaxane **(10)**:
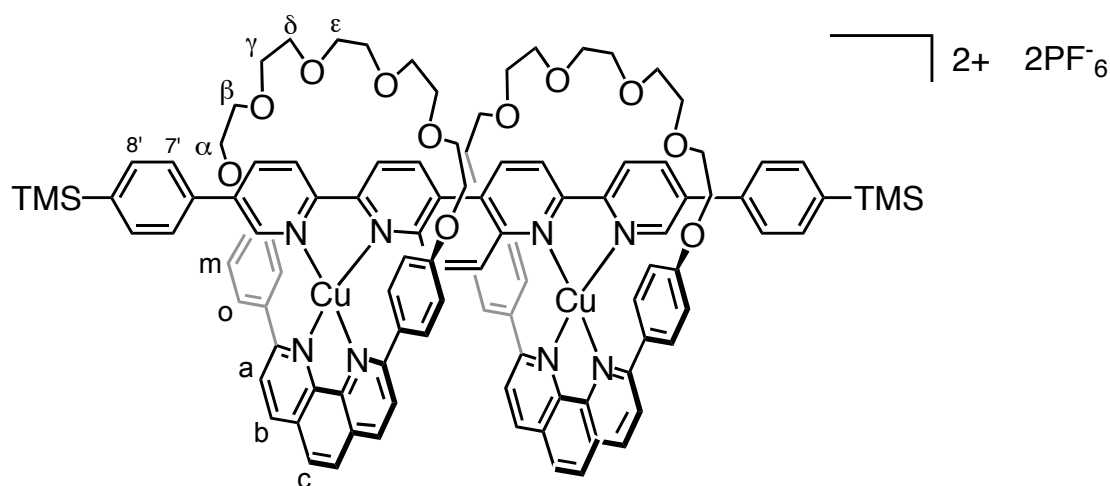
TMS-thread **8** (10 mg, 0.016 mmol), **m-30** (18.5 mg, 0.032 mmol), and [Cu(CH$_3$CN)$_4$]PF$_6$, (11.9 mg, 0.032 mmol), in 5 mL CH$_2$Cl$_2$, were stirred for 22 h under argon atmosphere. The solvent was then evaporated and the solid purified on a fast column (silica, MeOH 5%, CH$_2$Cl$_2$ 95%). The brownish red product was obtained in 50% yield.

¹H-NMR (300 MHz, CD$_2$Cl$_2$, MeOH-d$_3$, 25 ^{0}C): δ = 9.53 (d, J = 8.9 Hz, H$_{1'}$, 2H) 8.76 (d, J = 8.9 Hz, H$_{2'}$, 2H) 8.60 (d, J = 8.3 Hz, H$_b$,H$_{3'}$,6H) 8.32 (dd, J$_1$ = 8.3 Hz, J$_2$ = 2.1 Hz, H$_{4'}$, 2H) 8.24 (d, J$_1$=1.6 Hz, H$_{5'}$, 2H), 8.08 (s, H$_c$, 4H), 7.98 (d, J$_1$=8.3 Hz, H$_a$, 4H) 7.63 (d, J$_1$= 8.2 Hz, H$_{8'}$, 4H) 7.52 (d, J$_1$= 8.3 Hz, H$_{7'}$, 4H) 7.37 (s, H$_{6'}$, 2H) 7.21 (d, J$_1$= 8.7 Hz, H$_o$, 8H) 6.05(d, J$_1$= 8.7 Hz, H$_m$, 8H) 3.08 (m, -O-CH$_2$-CH$_2$-O-, 40H) 0.26 (s,-Si(CH$_3$)$_3$, 18H) ppm

MS (ES): *m/z* (%) = 945.23222 (100) [**10** – 2PF$_6$]$^{2+}$ (calcd: 945.3034)

UV/vis: λ$_{max}$ (ε in L.mol^{-1}.cm^{-1}) in acetonitrile: 346 (5 x 10^4), 418 (3 x 10^3)

[4]pseudorotaxane (**12**):
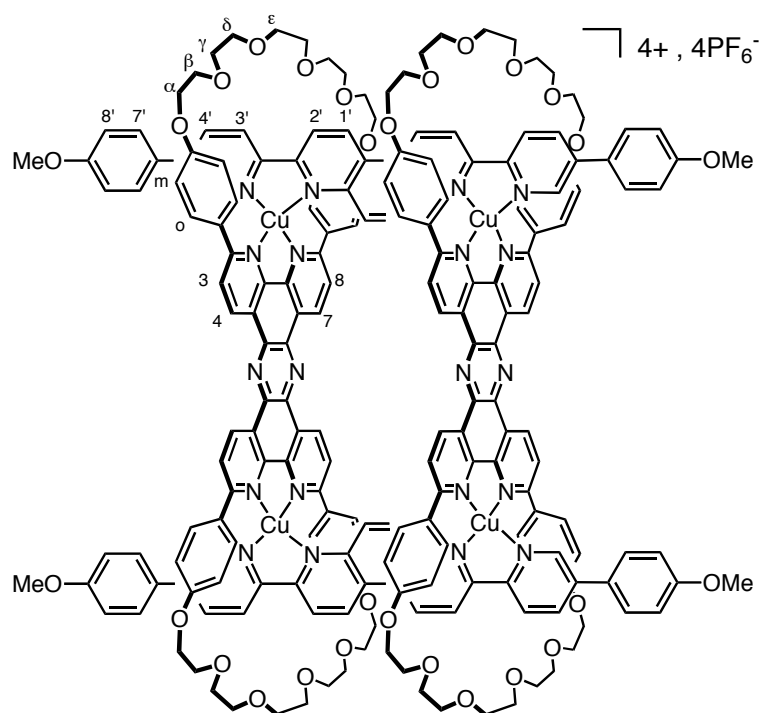
A solid-solid mixture of the bis-macrocycle **11** (50 mg, 4.32 x 10^{-5} mol) and the thread **9** (23.6 mg, 4.32 x 10^{-5} mol) is suspended in freshly distilled DCM (40 mL) under argon atmosphere. A degassed solution of MeCN containing [Cu(MeCN)$_4$](PF$_6$) (33.3 mg, 8.94 x 10^{-5} mol, 20 mL) was added *via* canula technique. The solution was stirred at room temperature avoiding light exposure. After 7 days, the mixture was homogeneous. The solvents were then evaporated and the product extracted from water with dichloromethane. After evaporation, the tetrameric pseudorotaxane [**12**$^{4+}$]4PF$_6^-$ was quantitatively obtained (98% yield).

^{1}H-NMR (CD$_2$Cl$_2$, 500 MHz, COSY, ROESY, 25°C): δ = 10.02 (d, J = 8.2 Hz, H$_4$,H$_7$, 8H) 9.54 (d, J = 8.9 Hz, 4H; H$_{1'}$, 4H) 8.76 (d, J = 9.0 Hz, 4H; H$_{2'}$, 4H) 8.61 (d, J = 8.6 Hz, 4H; H$_{3'}$, 4H) 8.33 (dd, J$_1$ = 8.6 Hz, J$_2$ = 2.2 Hz, H$_{4'}$, 4H) 8.27 (d, J = 1.8 Hz, H$_{5'}$, 4H) 8.24 (d, J = 8.2 Hz, H$_3$, H$_8$, 8H) 7.57 (m, ^{3}J = 9.1 Hz, H$_{7'}$ 8H) 7.43 (s, H$_{6'}$, 4H), 7.34 (m, J = 8.4 Hz, H$_o$, 8H), 7.06 (m, J = 9.1 Hz, H$_{8'}$, 8H), 6.10 (m, J = 8.5 Hz, H$_m$, 8H), 3.95-3.78 (m, H$_\alpha$, H$_\beta$, H$_\gamma$, H$_\delta$, H$_\varepsilon$,-OMe, 92H) ppm
MS (ES): *m/z(%)* = 915.2614 (100) [**12**]$^{4+}$ (calcd: 915.2621)

3,8-bis(4-(4-iodophenyl)-2'-pyridyl)-4,7-phenanthroline **(13)** :
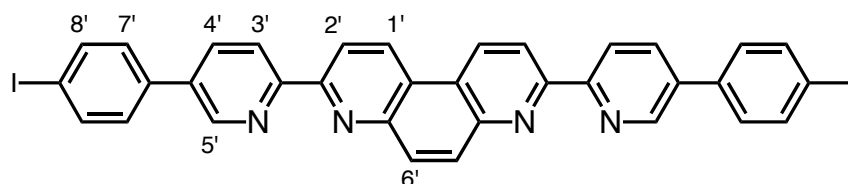
A solution of 3,8-bis(4-(4-trimethylsilylphenyl)-2'-pyridyl)-4,7-phenanthroline (20 mg, 3.17×10^{-5} mol) in 25 mL of chloroform was degassed (3 times vacuum/argon) before ICl was added (0.3 mL, 5.89 mmol). The mixture was heated up to 60 °C (reflux) for 48h. The reaction was quenched with a saturated solution of $Na_2S_2O_5$ (50 mL). The solvents were then evaporated and the obtained solid washed on Millipore filter with water (100 mL), pentane (20 mL) and toluene (120 mL). The final product was obtained in 57% yield.

We were not able to get an acceptable ^{1}H-NMR spectrum due to the insolubility of the product, even though the few visible peaks indicate that the reaction carried out was successful. The starting material is no longer present, and the mass spectrometry clearly indicates the formation of compound **13**.

MS (ES): *m/z* (%) = 738.9751 (100) $[13 + H]^+$ (calcd: 738.985)

3,8-bis(4-(4-hydroxyphenyl)-2'-pyridyl)-4,7-phenanthroline **(14)**:
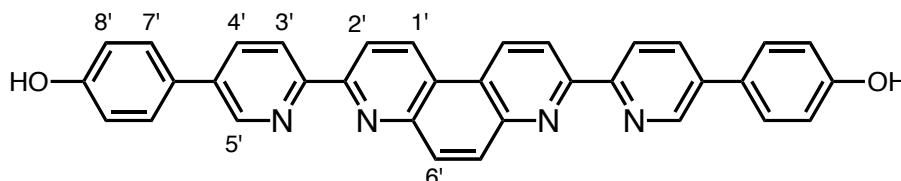
A 10 mL round bottom flask was loaded with 3,8-bis(4-(4-methoxyphenyl)-2'-pyridyl)-4,7-phenanthroline **(9)** (72 mg, 0.132 mmol) and pyridinium chloride (2 g). The mixture was then heated by microwave for 10 min (position 1). Another 2 g of pyridinium chloride were added and heated for another 10 min. The product was then poured in 200 mL water. This solution was brought to pH 8 by adding NaOH 1M . After cooling down the solution to 0°C, the product is filtered of on millipore filter and dried over night. The very poorly soluble compound **(14)** is obtained in 60% yield.

^{1}**H-NMR** (300 MHz, DMSO-d_6, 25 ^{0}C): δ = 9.48 (d, J_1 = 9.12 Hz, $H_{1'}$, 2H), 9.09 (s, $H_{5'}$, 2H) [8.72 (d, J = 8.4 Hz, 2H), 8.82 (d, J = 8.4 Hz, 2H), 8.29 (d, J = 8.04 Hz, 2H) $H_{2'}$, $H_{3'}$, $H_{4'}$,] 8.38 (s, $H_{6'}$, 2H), 7.73 (d, J = 8.61 Hz, $H_{7'}$, 4H), 6.97 (d, J = 8.61 Hz, $H_{8'}$, 4H) ppm

MS (ES): *m/z* (%) = 519.1795 (100) $[14 + H]^+$ (calcd: 519.1816)

1,4-dibromo-2,5-diethylbenzene **(16)**:
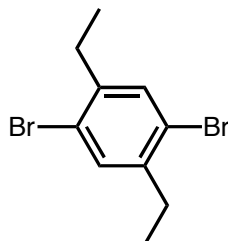
A 50mL three-necked round-bottom flask was loaded with 5 g of commercially available 1,4-diethylenbenzene (37.2 mmol) which was then cooled down to 0 °C. In the absence of light, 44 mg of I_2 (0.17 mmol) were added and the mixture stirred for 10 min at 0°C. Then Br_2 (12.19 g, 3,9 mL) was added in the dark with an ampoule over a period of 30 min. The ice-bath was removed and the reaction mixture left at room temperature for 1 day.

After 24 h, 30 mL of KOH (20% aqueous solution) were added to neutralize the excess of bromide. After the red colour had disappeared, the aqueous phase was removed and the crude product dissolved in 200 mL of hot EtOH. Then the EtOH was partly removed by evaporation till some crystals had formed. The mixture was allowed to cool down in the fridge over night. After filtration the white product was obtained in 60% yield.

^{1}H-NMR (300 MHz, CDCl$_3$, 25 ^{0}C): δ = 7.37 (s, H$_{aromatic}$, 2H), δ = 2.68 (q, J=7.50 Hz, -CH$_2$-, 4H), 1.20 (t, J$_1$ = 7.50 Hz, -CH$_3$- $_3$, 6H) ppm

^{13}C NMR (300 MHz, CD$_2$Cl$_2$, 25 ^{0}C): δ = 142.54 / 133.04 / 123.01 / 28.7 / 13.86 ppm

MS (ES): *m/z* (%) = 292.0 (100) [**16**]$^+$ (calcd: 291.93)

2,5-diethyl-4-trimethylsilyl-bromobenzene **(17)** :
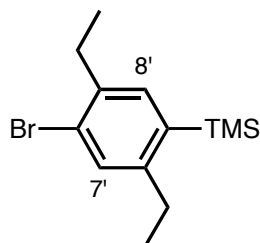
A three necked round bottom flask, previously dried in the oven was loaded under argon atmosphere with, (1 g, 3.42 mmol) of 1,4-dibromo-2,5-diethylbenzene **16**, and 20 mL of ether. After cooling down the solution to -78°C (acetone/CO$_2$), 3,35 mL of a solution of BuLi (4.45 mmol) in hexane (1.34 M) were added slowly drop by drop.

The mixture was then allowed to warm up to 0°C and then cooled down again to -78°C. Then 0.875 mL of trimethysilylchloride (6.84 mmol) were added drop by drop and mixture was allowed to warm up to room temperature and stirred for another 15 hours. 10 mL of water were then added and stirred for 10 minutes. The aqueous phase was extracted twice with 10 mL of ether. This organic was washed twice with 10 mL of water and then dried over MgSO$_4$. The pure product was recovered as an oil in 75% yield

^{1}H-NMR (300 MHz, CDCl$_3$, 25 ^{0}C): δ = 7.45 (s, H$_o$, 1H), 7.34 (s, H$_m$, 1H), 2.77 (m,H$_{CH2}$, 4H), 1.29 (m,H$_{CH3}$, 6H),), 0.38 (s,H-$_{Si-CH3}$, 9H) ppm
^{13}C NMR (300 MHz, CD$_2$Cl$_2$, 25 ^{0}C): δ = 149.45 / 139.46 / 137.41 / 135.58 / 131.87 / 125.64 / 28.94 / 28.20 / 16.07 / 14.37 / 0.03 ppm
MS (ES) : *m/z* (%) = 287.2557 (100) [**17**] (calcd : 287.0694)

2,5-diethyl-4-trimethylsilylphenylboronic acid (18):
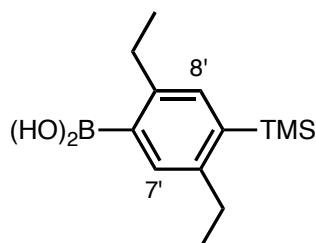
An oven-dried 50 mL three-necked flask was loaded under argon atmosphere with 500 mg (1.75 mmol) 2,5-diethyl-4-trimethylsilylbromobenzene **17**, 12 mL of ether and 3 mL of distillated THF. After cooling down the solution to -78 °C (acetone/CO$_2$ bath), 3.75 ml (1.4 M solution in hexane) of BuLi (5.25 mmol) were added drop by drop. The solution was then allowed to warm up to -10 °C then cooled down to -78 °C again. Now, 1.62 mL of triisopropylborate (7.02 mmol) were slowly added and the solution warmed up to room temperature and left under argon over night. 19 h after adding the triisopropylborate, 15 mL of water were added and the solution stirred for another 15 min before evaporation to dryness. The crude product was dissolved in dichloromethane and washed with water. The aqueous phase was extracted 3 times with 150 mL of dichloromethane. The organic solutions were collected and evaporated to dryness. By a quick column chromatography on silica with pentane/ethyl acetate as eluent (100/0 to 65/35), the pure product was obtained in 72% yield as a white powder.
^{1}H-NMR (300 MHz, CDCl$_3$, 25 ^{0}C): δ = 8.10 (s, H$_{7'}$, 1H), 7.41 (s, H$_{8'}$, 1H), [3,21 (m, 2H), 2.79 (m, 4H), -CH$_2$-] 1.31 (m, -CH$_3$-, 6H), 0.37 (s, -Si-CH$_3$, 9H)
^{13}C NMR (300 MHz, CD$_2$Cl$_2$, 25 ^{0}C): δ = 148.76 / 146.45 / 142.91 / 136.65 / 135.41 / 28.56 / 28.50 / 17.73 / 16.35 / 0.02 ppm
MS (ES) : *m/z* (%) = 301.17 (100) dimethoxyboronic ester derivative (MeOH used as a solvent for the spectrometry) + Na$^+$ (calcd : 301.18)

3,8-bis(4-(2,5-diethyl-4-iodophenyl)-2'-pyridyl)-4,7-phenanthroline **(19)**:
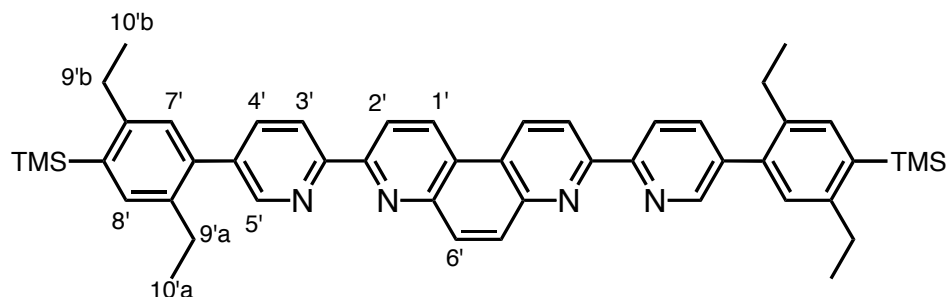
A 25 mL round bottom double-neck flask was loaded under argon atmosphere with 99,5 mg (0.202 mmol) of 3,8-bis(4-bromo-2'-pyridyl)-4,7-phenanthroline **7**, 215 mg of K_3PO_4, (1.011 mmol), and 10 ml of DMF, then degassed before 23 mg of $Pd(PPh_3)_4$ (0,202 mmol) were added. After another degassing, 150 mg of 2,5-diethyl-4-trimethylsilylphenylboronic acid **18** (0.606 mmol) was added and the solution purged with argon once more before heated to 120 °C. After 32 h, another 23 mg of catalyst were added and the reaction mixture left under argon at 120 °C for additional 18 hours. The solution was then poured into 150 mL of water and the precipitate collected by filtration. After column chromatography on alumina with pentane/ethyl acetate (100:0 to 70:30), the white solid product was obtained in 73% yield.

^{1}H-NMR (500 MHz, CD_2Cl_2, 25 ^{0}C): δ = 9.11 (d, J=8.82, $H_{1'}$, 2H) 8.84 (d, J=8.58 Hz, $H_{2'}$, 2H) 8.80 (dd, J_1 = 7.26 Hz, J_2 = 0.6 Hz, $H_{3'}$, 2H) 8.79 (dd, J_1 = 0.69 Hz, J_2 = 0.6 Hz, $H_{5'}$, 2H) 8.37 (s, $H_{6'}$, 2H) 7.93 (dd, J_1 = 8.34 Hz, J_2 = 2.01 Hz, $H_{4'}$, 2H) 7.47 (s, $H_{8'}$, 2H) 7.17 (s, $H_{7'}$, 2H) 2.87 (q, J = 7.53 Hz, $H_{9'b}$, 4H) 2.73 (q, J = 7.53 Hz, $H_{9'a}$, 4H) 1.33 (t, J = 7.50 Hz, $H_{10'b}$, 6H) 1.19 (t, J = 7.50 Hz, $H_{10'a}$, 6H) 0.41 (s, -$Si(CH_3)_3$, 18H) ppm

^{13}C NMR (500 MHz, CD_2Cl_2, 25 ^{0}C): 156.73 / 154.71 / 149.78 / 148.11 / 148.06 / 138.93 / 138.69 / 138.64 / 138.57 / 137.94 / 135.78 / 132.93 / 132.20 / 129.97 / 125.26 / 121.23 / 119.77 / 28.98 / 26.27 / 16.75 / 16.27 / 0.56 ppm

MS (ES): *m/z* (%) = 743,3961 (100) [**19** + H]$^+$ (calcd: 743.3960)

pseudo[3]rotaxane **(20)**:
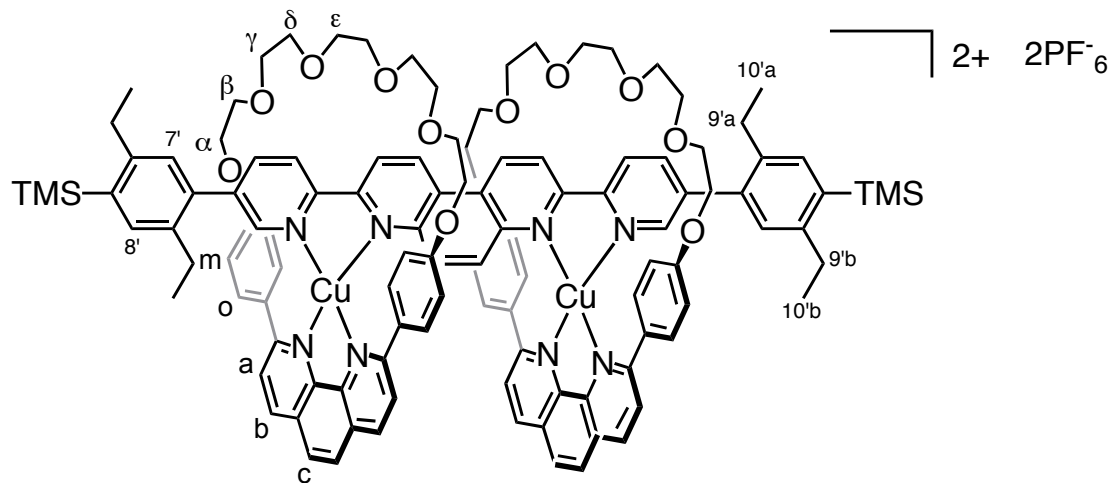
A 100 mL round-bottom flask was loaded with **m-30**, (46.58 mg, 0.081 mmol) and 5 mL freshly distilled and degassed CH_2Cl_2, then $[Cu(CH_3CN)_4]PF_6$, (31.30 mg, 0.084 mmol) in 5 mL degassed MeCN were added. After 1 h, the TMS-thread **19** in 5 mL CH_2Cl_2 was added to the now orange solution, which was then stirred at room temperature and under argon for 5 days. The solvent was then evaporated and the solid purified on a fast column (silica, MeOH 2%, CH_2Cl_2 98%). The brownish red product was obtained (40%).

¹H-NMR (300 MHz, CD_2Cl_2, MeOH-d_3, 25 ^{0}C): δ = 9.63 (d, J = 8.6 Hz, $H_{1'}$, 2H) 8.81 (d, J = 8.7 Hz, $H_{2'}$, 2H) 8.63 (d, J = 7.6 Hz, $H_{3'}$,2H) 8.60 (d, J = 8.4 Hz, H_b,4H) 8.07 (s, H_c, 4H) 8.0 (m, $H_{4'}$, $H_{5'}$, H_a, 8H) 7.46 (s, $H_{6'}$, 2H) 8.08 (s, $H_{8'}$, 2H), 7.27 (d, J_1=8.5 Hz, H_o, 8H) 6.96 (s, $H_{7'}$, 2H) 6.13 (d, J_1= 8.6 Hz, H_m, 8H) 3.83 (m, -O-CH_2-CH_2-O-, 40H) 2.79 (q, J_1= 7.6 Hz, $H_{9'b}$, 4H) 2.51 (q, J_1= 7.6 Hz, $H_{9'a}$, 4H) 1.24 (t, J_1= 7.6 Hz, $H_{10'b}$, 6H) 1.06 (t, J_1= 7.6 Hz, $H_{10'a}$, 6H) 0.32 (s,-Si(CH_3)$_3$, 18H) ppm

MS (maldi): *m/z* (%) = 2147.654 (100) $[\mathbf{20} - PF_6]^+$ (calcd: 2146.70)

3,8-bis(4-(2,5-diethyl-4-iodophenyl)-2'-pyridyl)-4,7-phenanthroline **(21)**:
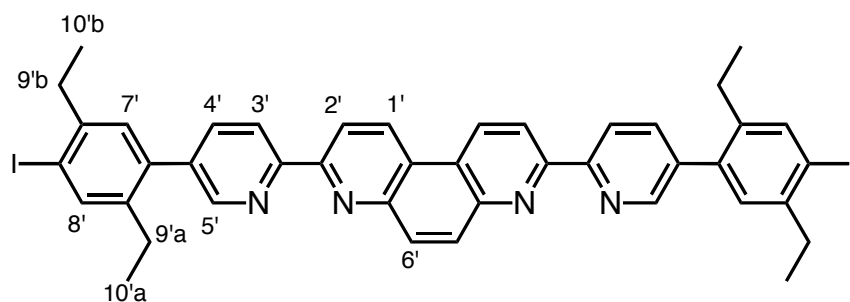
A three neck round bottom flask was loaded with 322 mg (4.3×10^{-4} mol) of TMS-TMS-thread **19** and 70 mL of freshly distilled CH_2Cl_2. After purging the solution with argon, it was cooled down to -10 °C. 19 mL of a 0,23 M solution of ICl (4.6×10^{-3} mol of ICl) in freshly distilled and degassed CH_2Cl_2 were added slowly and the solution allowed to warm up to room temperature and left for 15 h under argon. An orange precipitate has formed. The reaction was then quenched with $Na_2S_2O_5$ (stirred until the orange colour had disappeared). 50 mL of water were then added and the aqueous phase was extracted, with 3 x 150 mL of CH_2Cl_2. The combined organic layers were then washed with 3 x 50 mL of water. The white solid product was obtained quantitatively.

^{1}H-NMR (500 MHz, $CDCl_3$, 25 ^{0}C): δ = 9.13 (d, J=8.97 Hz, $H_{1'}$, 2H) 8.85 (d, J=8.58 Hz, $H_{2'}$, 2H) 8.81 (dd, J_1 = 9.75 Hz, J_2 = 0.6Hz, $H_{3'}$, 2H) 8.73 (dd, J_1 = 2.19, J_2 = 0.6Hz) Hz, $H_{5'}$, 2H) 8.39 (s, $H_{6'}$, 2H), 7.89 (dd, J_1 = 8.22 Hz, J_2 = 2.19 Hz, $H_{4'}$, 2H) 7.82 (s, $H_{8'}$, 2H) 7.12 (s, $H_{7'}$, 2H) 2.81 (q, J = 7.50 Hz, $H_{9'b}$, 4H) 2.63 (q, J = 7.50 Hz, $H_{9'a}$, 4H) 1.27 (t, J = 7.50 Hz, $H_{10'b}$, 6H) 1.16 (t, J = 7.50 Hz, $H_{10'a}$, 6H) ppm

^{13}C NMR (500 MHz, $CDCl_3$, 25 ^{0}C): 156.20 / 154.73 / 149.24 / 147.74 / 144.30 / 141.53 / 139.77 / 138.02 / 137.54 / 137.29 / 132.69 / 131.86 / 129.90 / 124.88 / 121.25 / 119.52 / 100.59 / 33.68 / 25.48 / 15.64 / 14.68 ppm

MS (ES): (*m/z* (%) =851.1119 (100) [**21** + H]$^+$ (calcd : 851.1102)

4-(tetrahydro-2H-pyran-2-yloxy)phenylboronic acid **(23)**:
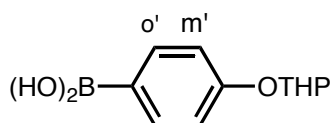
Commercially available 2-(4-Bromophenoxy)tetrahydro-2H-pyran, (5 g, 19,4 mmol), in 100 mL freshly distilled THF was cooled down to -78°C. 16,8 mL of a 1.5 M solution of BuLi in hexane (25.5 mmol) were then added, making sure the temperature stays below -70°C. After 15 min of stirring, triisopropyl borate, 7.30 g, (38.8 mmol) was slowly added and the mixture stirred for another hour at -78 °C. The solution was then allowed to warm up to room temperature before it was poured in 1L of a 1:1 mixture of H_2O/ Et_2O. A solution of HCl 0.1 M was then slowly added until pH = 8. The two layers were then separated and the aqueous layer extracted twice with Et_2O. The organic layers were dried over $MgSO_4$, filtered and the solvents evaporated to give compound **23** in 75% yield.

^{1}H-NMR (300 MHz, CD_2Cl_2, 25 ^{0}C): δ = 8.16 (d, J=8.8 Hz, $H_{o'}$, 2H), 7.16 (d, J=8.8 Hz, $H_{m'}$, 2H), [5.53 (t, J = 3.3 Hz, 1H), 3.93-3.58 (m, 1H), 2.05-1.56 (m, 6H), -OTHP)] ppm

OTHP-thread **(24)**:
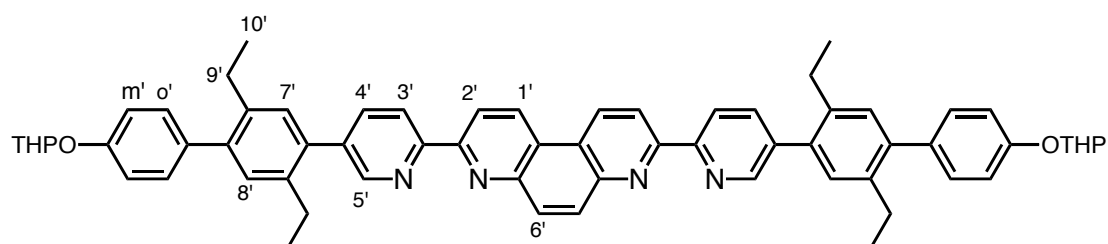
A two neck round bottom flask was loaded under argon atmosphere with 182 mg (0.214 mmol) of the iodo-thread **21**, 210 mg (0.944 mmol) of the 4-(tetrahydro-2H-pyran-2-yloxy)phenylboronic acid **23**, 226 mg (2,14 mmol) of Na_2CO_3, in solution in 24 mL of toluene, 8 mL of H_2O, and 4 mL of EtOH. After degassing the solution, 25 mg (2,14 x10^{-5} mol) of $Pd(PPh_3)_4$ were added and the mixture heated to 90 °C. After 5 h, the heating was stopped, and the solvents evaporated. The product was purified by column chromatography on alumina with pentane/ethyl acetate (100:0 to 50:50). The white product was obtained in 75% yield.

^{1}H-NMR (300 MHz, CD_2Cl_2, 25 ^{0}C): δ = 9.14 (d, J=8.70 Hz, $H_{1'}$, 2H) 8.88 (d, J=8.70 Hz, $H_{2'}$, 2H) 8.83 (d, J = 7.80 Hz, $H_{3'}$, 2H) 8.80 (d, J = 2,4 Hz, $H_{5'}$, 2H) 8.35 (s, $H_{6'}$, 2H) 7.96 (dd, J_1 = 8.40 Hz, J_2 = 2.40 Hz, $H_{4'}$, 2H) 7.32 (d, J = 8.70 Hz, $H_{o'}$, 4H), 7.24 (s, $H_{8'}$, 2H), 7.21 (s, $H_{7'}$, 2H) 7.12 (d, J = 8.7 Hz, $H_{m'}$, 4H) [5.46 (s, 1H), 3.95, 3.64 (m, 2H) –OTHP] 2.67 (m, $H_{9'}$, 8H), 1.87 (m, -OTHP, 6H) 1.14 (m, $H_{10'}$, 12H) ppm

^{13}C NMR (300 MHz, CD_2Cl_2, 25 ^{0}C): δ = 156.24 / 154.20 / 149.43 / 147.57 / 141.35 / 139.40 / 139.15 / 138.04 / 137.59 / 136.54 / 134.83 / 132.46 / 131.73 / 130.72 / 130.29 / 130.12 / 124.76 / 120.78 / 119.29 / 116.07 / 96.63 / 62.23 / 30.44 / 25.71 / 25.26 / 19.00 / 15.61 / 15.51 ppm

MS (Maldi-TOF): *m/z* (%) =951.511 (100) [**24** + H]$^+$ (calcd : 951.483)

phenol-thread **(25)**:
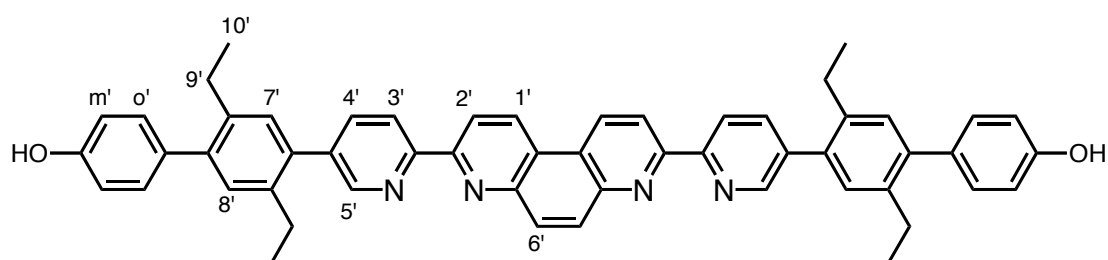
A 100mL round bottom flask was loaded under argon atmosphere with OTHP-thread **24,** which was dissolved in a minimum of CH_2Cl_2, then 50 ml of MeOH and 3 mL of concentrated HCl_{aq} (37%) were added. The mixture was heated to 80°C (reflux) for 4 h. The solvents were then evaporated and the remaining solid dissolved in 100 mL of CH_2Cl_2, before 150 mL of aqueous NaOH 1 M were added. By adding HCl_{aq} (37%) the solution was brought to pH = 7, then the aqueous layer is extracted with twice 100

mL CH_2Cl_2. The combined organic layers were then washed with twice 100 mL of H_2O and after evaporation of the solvent the pure product was obtained in 95% yield.

^{1}H-NMR (300 MHz, CD_2Cl_2, 25 ^{0}C): δ = 9.15 (d, J=8.7 Hz, $H_{1'}$, 2H) 8.89 (d, J=8.7 Hz, $H_{2'}$, 2H) 8.83 (dd, J_1 = 8.1 Hz, J_2 = 0.5 Hz, $H_{3'}$, 2H) 8.78 (dd, J_1 = 2,2 Hz, J_2 = 0.5 Hz, $H_{5'}$, 2H) 8.37 (s, $H_{6'}$, 2H) 7.96 (dd, J_1 = 8.1 Hz, J_2 = 2.2 Hz, $H_{4'}$, 2H) 7.27 (d, J = 8.6 Hz, $H_{o'}$, 4H) 7.23 (s, $H_{8'}$, 2H) 7.20 (s, $H_{7'}$, 2H) 6.93 (d, J = 8.6 Hz, $H_{m'}$, 4H) 2.68 (m, $H_{9'}$, 8H) [1.16 (t, J = 7.6 Hz, 6H) 1.13 (t, J = 7.6 Hz, 6H) $H_{10'}$] ppm

MS (ES): *m/z* (%) =783.3608 (100) $[\mathbf{25} + H]^+$ (calcd : 783.694)

Monoallyl triethyleneglycol **(27)**:
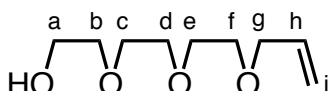
A 100mL round-bottom flask was loaded with 7.45 g (0.13 mol) crushed KOH, to which were added 20 g (0.13 mol) of triethyleneglycol. After a few minutes of stirring the mixture, the allylbromide 11.6 mL (0.13 mol) was added slowly. Then the solution was heated to 60 °C and stirred for 3 h. After letting the solution cool down to room temperature, 70 mL of water were added. The aqueous layer was then washed with 3 x 40 mL toluene and then extracted with 3 x 40 mL CH_2Cl_2. The dichloromethane layers were combined, dried over Na_2SO_4, which was then filtered of and after evaporating the solvents, the pure product was obtained in 32% yield.

^{1}H-NMR (300 MHz, $CDCl_3$, 25 ^{0}C): δ = 5.89 (m, H_h, 1H) 5.26-5.11 (m, H_i, 2H) 3.99 (m, H_g, 2H) 3.70-3.55 (m, H_a, H_b, H_c, H_d, H_e, H_f, 12H) ppm

mesylate derivative of the monoallyl triethyeneglycol 27 **(28)**:

A degassed solution of **27**, (8.04 g, 42 mmol) in 230 mL freshly distilled CH_2Cl_2 and in presence of 35 mL freshly distilled Et_3N was placed at -3°C. MsCl, 4 mL (52 mmol) were added while stirring the mixture. After 2 h, another 2.5 mL (32 mmol) of MsCl were added drop-wise and the solution then allowed to warm up to room temperature and left under further stirring over night. The solution was then washed with 4 x 100 mL H_2O; the remaining organic layer was then dried over Na_2SO_4. After column chromatography on alumina (CH_2Cl_2 / MeOH 98:2), the pure product was recovered as yellow oil in 88% yield.

^{1}H-NMR (300 MHz, $CDCl_3$, 25 ^{0}C): δ = 5.89 (m, H_h, 1H) 5.27-5.13 (m, H_i, 2H) 4.35 (m, H_a, 2H) 3.99 (m, H_g, 2H) 3.64-3.57 (m, H_b, H_c, H_d, H_e, H_f, 10H) 3.0 (s, CH_3SO_2-, 3H) ppm

bromo derivative of the monoallyl triethyeneglycol **(29)**:

A suspension of LiBr, (25.9 g, 299 mmol) in acetone was added to the mesyl adduct **27**, (10 g, 37.3 mmol). The mixture was stirred until the formed aggregates had disappeared; it was then heated to reflux (75 °C) for 17 h. The solvent was then evaporated and the solid residue dissolved in CH_2Cl_2 and washed with 150 mL H_2O. After washing the organic layer twice with 100 mL of water, it was dried over Na_2SO_4. After evaporating the solvent, the pure product was obtained as a yellow oil in 81% yield.

^{1}H-NMR (300 MHz, $CDCl_3$, 25 ^{0}C): δ = 5.86 (m, H_h, 1H) 5.27-5.11 (m, H_i, 2H) 3.99 (m, H_g, 2H) 3.79 (t, J= 6.3 Hz, H_a, 2H) 3.64-3.57 (m, H_c, H_d, H_e, H_f, 8H) 3.43 (t, J= 6.6Hz, H_b, 2H) ppm

polyethylenglycol-allyl thread **(30)**:
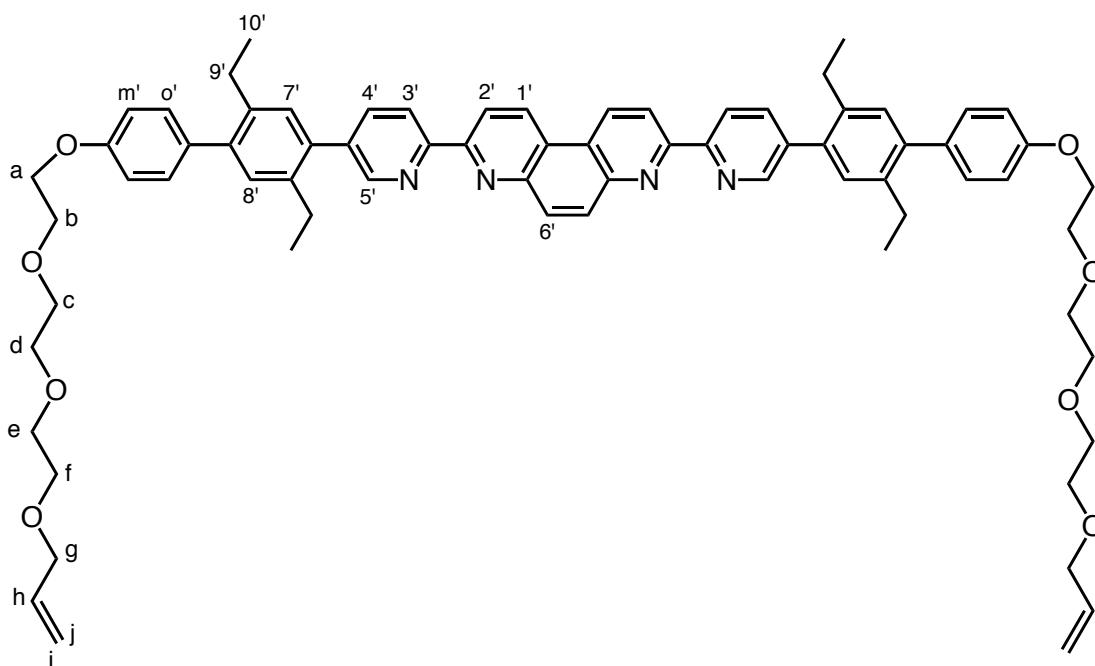
A round-bottom flask was loaded under argon atmosphere with the phenol-thread **25**, (80 mg, 1.02 x 10^{-4} mol), $CsCO_3$, (216 mg, 6.13 x 10^{-4} mol) and 8 mL of DMF. The solution was degassed and heated to 60 °C before the bromo-allypolyethylenglycol chaine **29** (206,8 mg, 8.17 x 10^{-4} mol) in 10 mL DMF is added drop-wise with an ampoule. After 24 h, solvents are evaporated before the remaining solid is redissolved in CH_2Cl_2 and washed twice with 100 mL H_2O. After additional washing with hexane, the pure white solid is obtained in 80% yield.

^{1}H-NMR (300 MHz, CD_2Cl_2, 25 ^{0}C): δ = 9.10 (d, J=8.9 Hz, $H_{1'}$, 2H) 8.86 (d, J=8.7 Hz, $H_{2'}$, 2H) 8.81 (d, J = 8.3 Hz, $H_{3'}$, 2H) 8.78 (dd, J_1 = 2,2 Hz, J_2 = 0.5 Hz, $H_{5'}$, 2H) 8.34 (s, $H_{6'}$, 2H) 7.93 (dd, J_1 = 8.2 Hz, J_2 = 2.3 Hz, $H_{4'}$, 2H) 7.31 (d, J = 8.7 Hz, $H_{o'}$,

4H) 7.24 (s, $H_{8'}$, 2H) 7.21 (s, $H_{7'}$, 2H) 7.01 (d, J = 8.5 Hz, $H_{m'}$, 4H) 5.93 (m, H_h, 2H) 5.32-5.24 (ddt, J_1 = 17.4 Hz, J_2 =1,9 Hz, J_3= 1,5 Hz, H_j, 2H) 5.19-5.14 (ddt, J_1 = 10.4 Hz, J_2 =1,7 Hz, J_3= 1,5 Hz, H_i, 2H) 4.18 (m, H_a, 4H) 4.00 (dt, J_1= 5.5 Hz, J_2= 1,5 Hz, H_g, 4H) 3.87 (m, H_b, 4H) 3.74-3.56 (m, H_c, H_d, H_e, H_f, 16H) 2.68 (m, $H_{9'}$, 8H) 1.15 (m, $H_{10'}$, 12H) ppm

MS (Maldi-TOF): *m/z* (%) =1127.508 (100) [**30** + H]$^+$ (calcd: 1127.59)

[4]pseudorotaxane **(31)**:
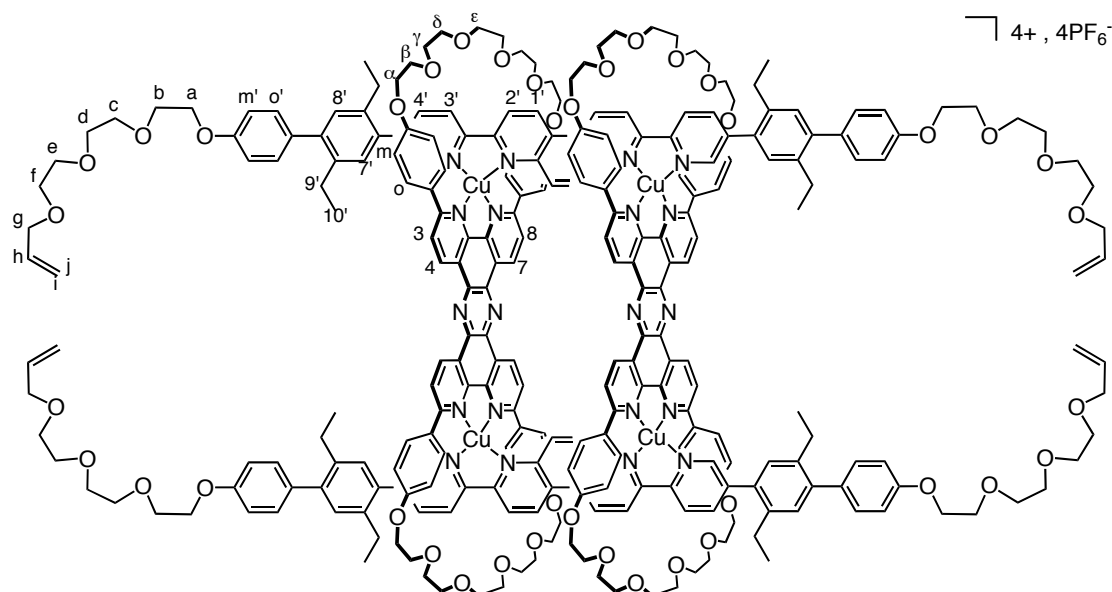
To a degassed suspension of **11** (80 mg, 6.91 x 10^{-5} mol) and **30** (78 mg, 6.91 x 10^{-5} mol, 1 eq.) in dry CH_2Cl_2 (50 mL), a solution of [Cu(MeCN)$_4$](PF$_6$) (52.0 mg, 13.95 x 10^{-5} mol, 2.02 eq.) in dry MeCN (25 mL) was added. The mixture turned immediately red but was reacted for further 7 days to complete threading of the bis-macrocycle. The crude is then filtered and evaporated to dryness giving **31** in 98% yield.

¹H-NMR (CD$_2$Cl$_2$, 500 MHz, COSY, ROESY, 25°C): δ = 10.03 (d, J = 8.3 Hz, H_4, H_7, 8H) 9.67 (d, J = 8.3 Hz, $H_{1'}$, 4H) 8.88 (d, J = 8.3 Hz, $H_{2'}$, 4H) 8.71 (d, J = 7.5 Hz, $H_{3'}$,4H) 8.27 (d, J = 8.6 Hz, H_3,H_8, 8H) 8.19 (s, $H_{5'}$, 4H) 8.14 (d, J = 7.5 Hz, $H_{4'}$, 4H) 7.56 (s, $H_{6'}$, 4H) 7.40 (d, J = 7.8 Hz, H_o, 8H) 7.23 (d, J = 7.8 Hz, $H_{o'}$, 8H) 7.17 (s, $H_{7'}$, 4H) 7.13 (s, $H_{8'}$, 4H) 6.96 (d, J = 8.5 Hz, $H_{m'}$, 8H) 6.20 (d, J = 7.8 Hz, H_m, 8H) 5,90 (m, J = 5.4, 10.1 and 17.0 Hz, H_h, 4H) 5.25 (d, J = 17.0 Hz, H_j, 4H,) 5.13 (d, J = 10.1 Hz, H_i, 4H) 4.18 (t, J = 5.1 Hz, H_a, 8H) 4.09-3.89 (m, $H_α$, $H_β$, $H_γ$, $H_δ$, $H_ε$, 80H) 3.88 (t, J = 5.1 Hz, H_b, 8H) 3.75-3.54 (m, H_c, H_d, H_e, H_f, H_g, 40H) 2.70-2.54 (2m, J = 7.0 Hz, $H_{9'}$, 16H) 1.14 (t, J = 7.0 Hz, $H_{10'}$, 24H) ppm

MS (ES): *m/z(%)* = 1655.755 (100) [**31**]$^{3+}$ (calcd: 1655.590)

[3]catenane **32**:
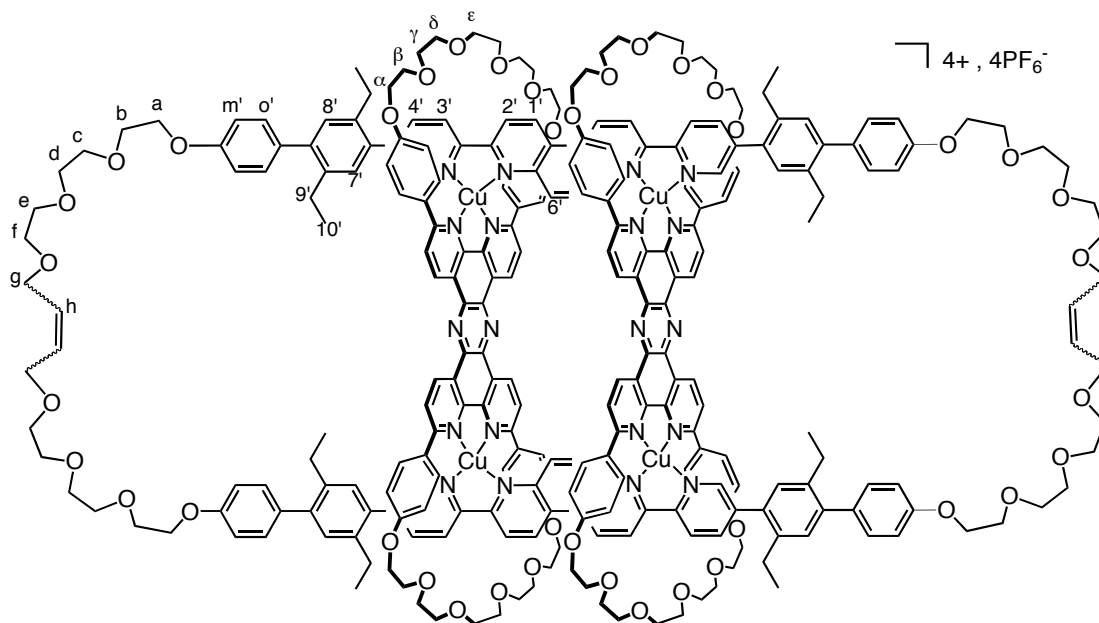
Compound **31**.4PF$_6$ (180 mg, 3.33 x 10^{-5} mol) and Grubbs' first generation catalyst RuCl$_2$(PCy$_3$)$_2$CHPh (10.0 mg, 10% per olefin) were dissolved in freshly distilled CH$_2$Cl$_2$ (3 mL so as to obtain a 10^{-3} M solution) and kept under argon. After 5 days of stirring at room temperature, the mixture is completely dry; another 10 mg of catalyst were added as well as CH$_2$Cl$_2$ (3 mL). The mixture was then stirred for further 5 days under argon, after which the material was precipitated with a saturated aqueous solution of KPF$_6$ and filtered. The crude product is filtered (150 g of alumina prepared in CH$_2$Cl$_2$/MeOH 0.5%, gradient elution from CH$_2$Cl$_2$/MeOH 0.5 to 1%) and then subjected to several consecutive chromatographies (100 g of silica prepared in CH$_2$Cl$_2$, gradient elution from CH$_2$Cl$_2$/MeOH 0 to 3%) to give impure **32**. (68 mg).

^{1}H-NMR (d^6-acetone, 500 MHz, COSY, ROESY, 25°C): δ = 10.34-10.10 (m, H$_4$,H$_7$, 4H) 8.91-8.80 (m, H$_{4'}$,H$_{7'}$, 4H) 8.37-8.31 (m, H$_{5'}$,H$_{6'}$, 4H) 8.16-8.07 (m, H$_3$,H$_8$, 8H) 7.75-7.66 (m, H$_{3'}$,H$_{8'}$, 4H) 7.99-7.76 (m, H$_{o'}$, 8H) 7.75-7.66 (m, H$_o$, 8H) 6.55-6.35 (m, H$_{m'}$, 8H) 6.20-6.14 (m, H$_m$, 8H) 5.74, 5.37, 5.16 (3m, H$_c$ E-E + E-Z + Z-Z, 4H) 3.89 (s, H$_\varepsilon$, 8H), 3.85-3.70 (m, H$_\delta$, H$_a$, E-E + E-Z + Z-Z, 16H) 3.68-3.65 (m, H$_\gamma$, 8H), 3.60-3.46 (m, H$_\alpha$, H$_\beta$, 16H) 2.40, 2.30, 2.18 (3m, H$_b$ E-E + E-Z + Z-Z, 8H)

MS (Maldi-TOF): *m/z* (%) = 5201.191 (100) [32 –PF$_6$]$^+$ (calcd: 5201.637)

Demetallated [3]catenane **33**:
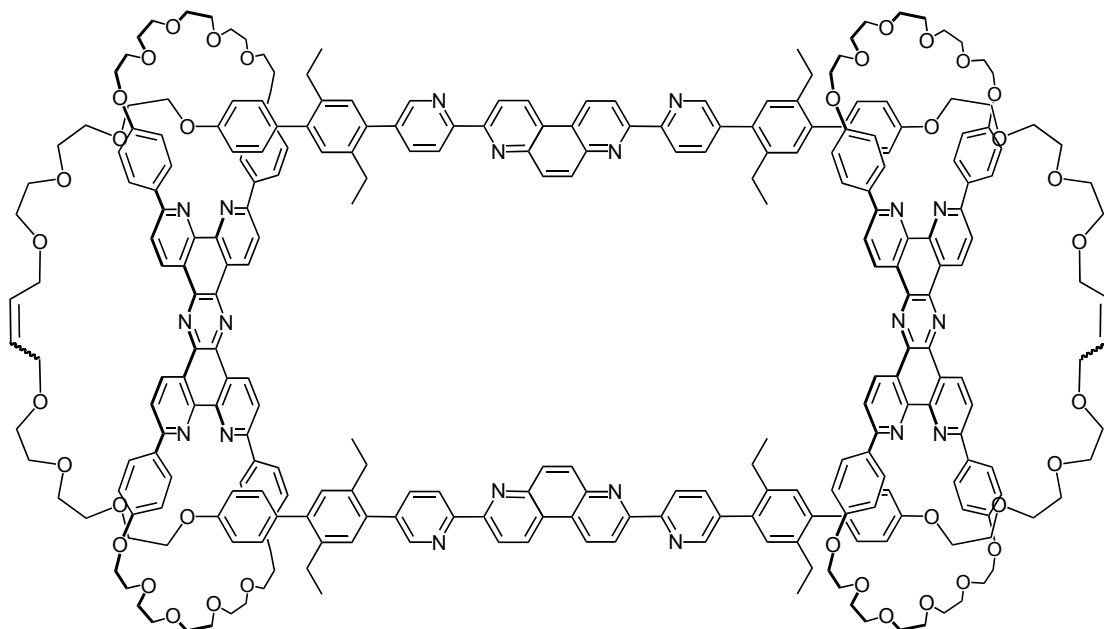
Impure compound **32** (68 mg, 1.22 x 10^{-5} mol) was dissolved in a 2:1:1 mixture of CH_2Cl_2/MeCN/H_2O (30 mL) and KCN (33 mg, 5.05 x 10^{-4} mol, ~100eq.) was added. The solution turned from brown to bright yellow within few minutes whereas a precipitate appeared. It was stirred for 1 hour and then the product was extracted with CH_2Cl_2 and water; organic layers were separated, filtered to eliminate the precipitate (namely, the bis-macrocycle) and evaporated to dryness. The yellow oily material (44 mg) is then adsorbed on preparative TLC (silica - 2 mm) and eluted 10 times with $CHCl_3$/MeOH 4%. The largest band that could be separated was collected and the support was extracted with boiling $CHCl_3$/MeOH 5%; after filtration, the organic solvent was removed under reduced pressure giving a bright yellow solid (3mg, impure).

^{1}H-NMR: impossible due to slow conformational changes.

HR ES-MS: m/z = 1505.3518 [**33** + 3H]$^{3+}$, (calcd: 1504.6827)
               m/z = 2257.5153 [**33** + 2H]$^{2+}$, (calcd: 2257.5200)

[4]pseudorotaxane **(35)** :
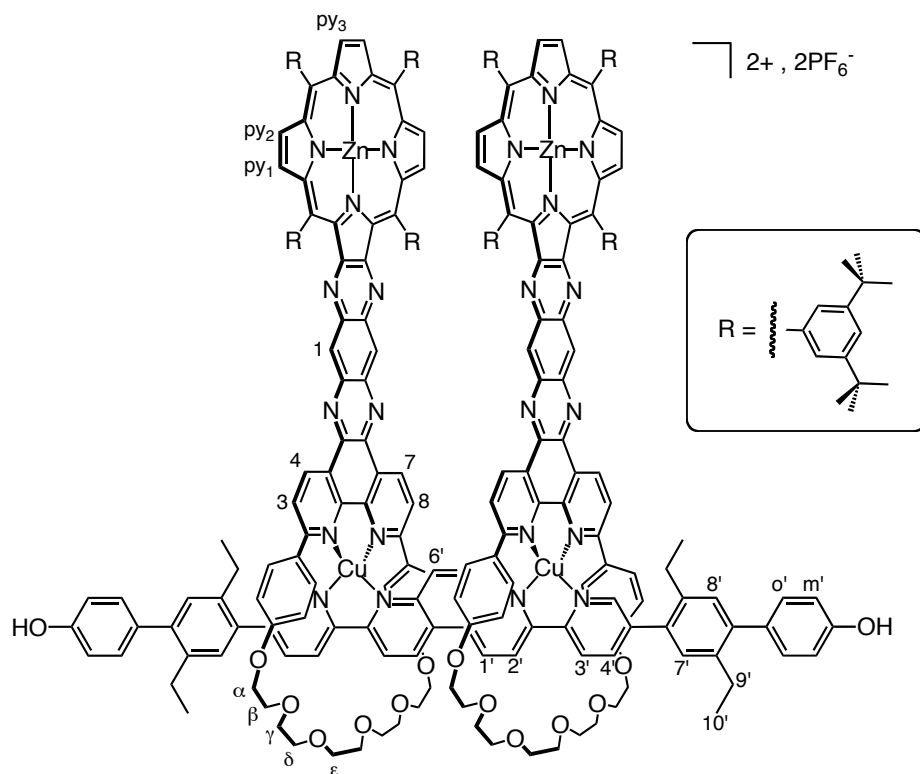
A 100 mL round bottom flask was loaded under argon atmosphere with the Zn-porphyrin macrocycle **34** (131.7 mg, 7.24 x 10^{-5} mol) and [Cu(MeCN)$_4$]PF$_6^-$ (28.05 mg, 7.53 x 10^{-5} mol) and 25 mL of freshly distilled and degassed CH$_2$Cl$_2$. After the addition of 25 mL of degassed MeCN, the mixture was stirred under argon and in absence of light for 1 h at room temperature. Then the phenol-thread **25** (28.3 mg, 3.62 x 10^{-5} mol) was added as well as another 25 mL of distilled and degassed CH$_2$Cl$_2$. After additional 3 days of stirring the solution under argon, at room temperature and in the absence of light, the solvents were evaporated and compound **35** obtained quantitatively.

^{1}H-NMR (CD$_2$Cl$_2$, 300 MHz, 25°C): δ = 9.99 (d, J = 8.3 Hz, H$_4$, H$_7$, 8H) 9.78 (d, J = 8.7 Hz, H$_{1'}$, 4H) 8.92 (s, H$_{py3}$, 4H) 8.91 (d, J = 8.3 Hz, H$_{2'}$, 4H) 8.78 (d, J = 4.7 Hz, H$_{py1}$, 4H) 8.76 (s, H$_1$, 4H) 8.73-8.69 (m, H$_{py2}$, H$_{3'}$, 6H) 8.22 (d, J = 8.2 Hz, H$_3$,H$_8$, 4H) 8.15 (d, J = 1.7 Hz, H$_{5'}$, 2H) 8.11 (dd, J$_1$ = 9.4Hz, J$_2$ = 1.7 Hz, H$_{4'}$, 2H) 7.97-7.77 (m, H-aromatic-R, 24H) 7.43 (d, J = 8.8 Hz, H$_o$, 8H) 7.17 (d, J = 8.5, H$_{o'}$, 4H) 7.16 (s, H$_{8'}$, 2H) 7.12 (s, H$_{7'}$, 2H) 6.87 (d, J = 8.5 Hz, H$_{m'}$, 4H) 6.24 (d, J = 8.6 Hz, H$_m$, 4H) 3.98-3.82 (m, H$_\alpha$, H$_\beta$, H$_\gamma$, H$_\delta$, H$_\varepsilon$, 40H) 2.61 (m, H$_{9'}$, 8H) 1.49 (s, ^{t}Bu$_1$, 36H) 1.45 (s, ^{t}Bu$_1$, 36H) 1.42 (s, ^{t}Bu$_2$, 36H) 1.17 (s, ^{t}Bu$_2$, 36H) 1.14 (m, H$_{10'}$, 12H) ppm

MS (Maldi-Tof): *m/z* (%) =4694.616 (100) [**35** – PF$_6^-$]$^+$ (calcd:4694.9918) ppm

α-[p-[Tris(p-tert-butylphenyl)methyl]phenoxy]-α'-bromo-p-xylene **(38)**:
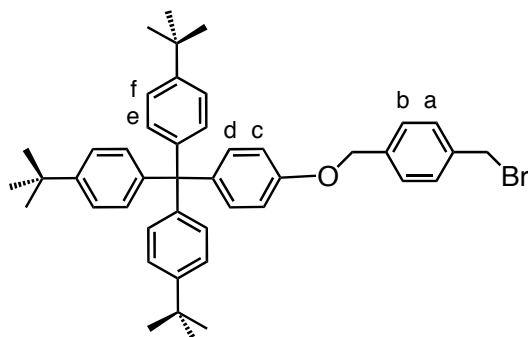
A 500mL round bottom flask was loaded under argon atmosphere with the phenolic stopper **37** (200 mg, 0.4 mmol), NaH (60% suspension in oil, 26 mg (43 mg), 1.0 mmol) in 120 mL freshly distilled THF. After stirring this mixture for 20 min, the αα'-dibromo-p-xylene (1.57 g, 5.9 mmol) was added as a solution in 120 mL THF. The reaction mixture was stirred under argon for 18h, then a few droplets of water were added to destroy the remaining NaH. The mixture was then filtered over celite, the solvents evaporated and the remaining compound dissolved again in Et_2O, which was then washed with NH_4Cl_{aq}, saturated $NaCl_{aq}$ and H_2O before the solvent was evaporated. After a silica gel column chromatography (pentane/ Et_2O, from 0% to 100%), the pure product was obtained as a white powder in 39% yield.

^{1}H-NMR (400 MHz, CD_2Cl_2, 25°C): δ = 7.41 (s, H_b, H_c, 4H) 7.28-7.14 (2d, J = 8.7 Hz, H_f, H_g, H_h 14H) 6.84 (d, J = 8.9Hz, H_c, 2H) 5.02 (s, H_d, 2H) 4.52 (s, H_a, 2H) 1.30 (s, -^{t}Bu, 27H) ppm

bromo-p-xylene thread **(40)**:
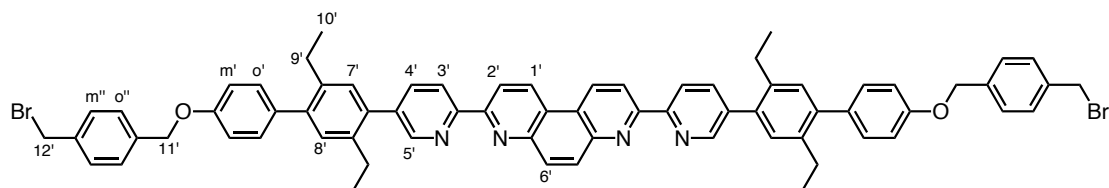
A 250 mL round-bottom flask as loaded under argon atmosphere with the phenol-thread **25** (200 mg, 2.55 x 10^{-4} mol), NaH (30.6 mg in oil suspension (60%) (51 mg), 1.28 mmol) in 80 mL freshly distilled THF. After 20 min of stirring under room temperature, αα'-dibromo-p-xylene (1.01g, 3.82 mmol) was added as a solution in 80 mL freshly distilled THF. The reaction mixture was then heated to 60 °C under argon for 17 h. 20 mg of NaH were added and the solution stirred at 60 °C under argon for another 2 days. The solvent was then evaporated and the remaining solid dissolved in CH_2Cl_2, the organic layer was washed twice with 100 mL of H_2O, then evaporated

and the remaining solid washed with 3 x 100 mL of Et$_2$O. The final white compound was obtained in 66% yield.

^{1}H-NMR (400 MHz, CD$_2$Cl$_2$, COESY, ROESY, 25 ^{0}C): δ = 9.13 (d, J = 8.8 Hz, H$_{1'}$, 2H) 8.87 (d, J = 8.8 Hz, H$_{2'}$, 2H) 8.82 (d, J$_1$ = 8.0 Hz, H$_{3'}$, 2H) 8.77 (d, J = 2,2 Hz, H$_{5'}$, 2H) 8.35 (s, H$_{6'}$, 2H) 7.94 (dd, J$_1$ = 8.1 Hz, J$_2$ = 2.2 Hz, H$_{4'}$, 2H) 7.46 (s, H$_{o''}$, H$_{m''}$, 8H) 7.32 (d, J = 8.6 Hz, H$_{o'}$, 4H) 7.24 (s, H$_{8'}$, 2H) 7.20 (s, H$_{7'}$, 2H) 7.06 (d, J = 8.6 Hz, H$_{m'}$, 4H) 5.13 (s, H$_{11'}$, 4H) 4.55 (s, H$_{12'}$, 4H) 2.68 (m, H$_{9'}$, 8H) 1.16 (m, H$_{10'}$, 12H) ppm

MS (MAldi-TOF): *m/z* (%) =1149.280 (100) [**40** + H]$^+$ (calcd : 1149.31)

Azide thread (**41**):
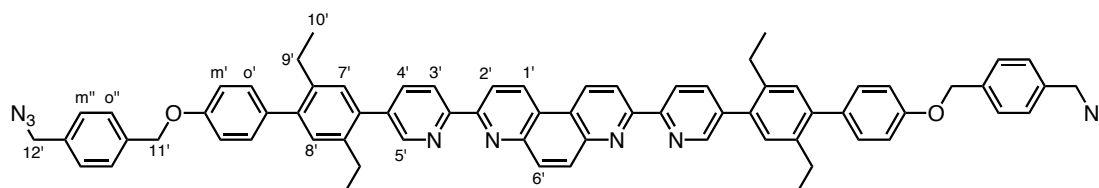
A Schlenk flask was loaded under argon atmosphere with bromo-p-xylene thread **40** (72 mg, 6.27 x 10^{-5} mol), NaN$_3$ (9.7 mg, 1.5 x 10^{-4} mol) and 5 mL of DMF. The reaction mixture was then heated to 80 °C and stirred for 20 h. The solvent was then evaporated and the remaining solid dissolved in CH$_2$Cl$_2$. This organic layer was then washed with H$_2$O. Alumina column chromatography (CH$_2$Cl$_2$ / MeOH 0-4%) afforded compound **41** in 60% yield.

^{1}H-NMR (400 MHz, CD$_2$Cl$_2$, COESY, ROESY, 25 ^{0}C): δ = 9.13 (d, J=8.8 Hz, H$_{1'}$, 2H) 8.88 (d, J = 8.8 Hz, H$_{2'}$, 2H) 8.83 (d, J$_1$ = 8.4 Hz, H$_{3'}$, 2H) 8.78 (d, J = 2,2 Hz, H$_{5'}$, 2H) 8.36 (s, H$_{6'}$, 2H) 7.95 (dd, J$_1$ = 8.2 Hz, J$_2$ = 2.2 Hz, H$_{4'}$, 2H) 7.53 (d, J = 8.1 Hz, H$_{o''}$, 4H) 7.39 (d, J = 8.1 Hz, H$_{m''}$, 4H) 7.33 (d, J = 8.7 Hz, H$_{o'}$, 4H) 7.25 (s, H$_{7'}$, 2H) 7.22 (s, H$_{8'}$, 2H) 7.08 (d, J = 8.6 Hz, H$_{m'}$, 4H) 5.15 (s, H$_{11'}$, 4H) 4.39 (s, H$_{12'}$, 4H) 2.68 (m, H$_{9'}$, 8H) 1.15 (m, H$_{10'}$, 12H) ppm

MS (MAldi-TOF): *m/z* (%) =1073.43 (100) [**41** + H]$^+$ (calcd : 1073.50)

[3]pseudorotaxane **(42)**:
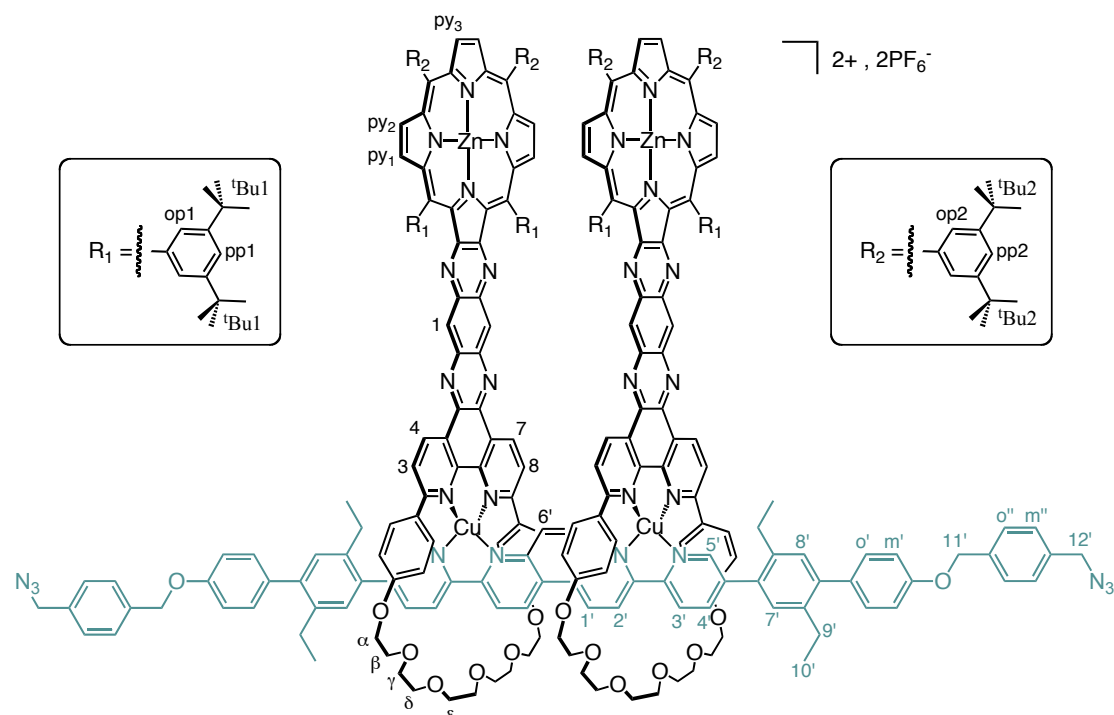
An oven dried 100 mL two-necked round bottom flask was loaded under argon with the Zn-porphyrin macrocycle **34** (135.6 mg, 7,45 x 10^{-5} mol) in solution in 25 mL freshly distilled and degassed CH_2Cl_2 and $[Cu(MeCN)_4]PF_6$ (28.90 mg, 7.75 x 10^{-5} mol) in 25 mL degassed MeCN. The mixture was stirred for one hour in absence of light at room temperature. Then azide thread **41** (40 mg, 3,72 x 10^{-5} mol) in 25 mL of freshly distilled and degassed CH_2Cl_2 was added *via* cannula. After 3 days of stirring under argon and in absence of light, the solvents were evaporated and the [3]pseudorotaxane **42** was obtained quantitatively.

^{1}H-NMR (500 MHz, CD_2Cl_2, COESY, ROESY, 25 ^{0}C): δ = 9.88 (d, J = 8.0 Hz, H_4,H_7, 4H) 9.77 (d, J = 8.8 Hz, $H_{1'}$, 2H) 8.91 (s, H_{py3}, 4H) 8.91 (d, J = 8.8 Hz, $H_{2'}$, 4H) 8.76 (d, J = 4.5 Hz, H_{py1}, 4H) 8.74 (s, H_1, 4H) 8.71 (d, J = 4.5 Hz, H_{py2}, 4H) 8.71 (d, J = 8.8 Hz, $H_{3'}$, 2H) 8.21 (d, J = 8.0 Hz, H_3,H_8, 4H) 8.13 (d, J = 8.8 Hz, $H_{4'}$, 4H) 8.08 (s, $H_{5'}$, 2H) 7.96 (bs, H_{op1}, 4H) 7.91 (bs, H_{op1}, 4H) 7.88 (bs, H_{pp2}, 4H) 7.83 (bs, H_{op2}, 4H) 7.78 (bs, H_{pp1}, 4H) 7.77 (bs, H_{op2}, 4H) 7.74 (s, $H_{6'}$, 2H) 7.45 (d, J = 8.3 Hz, $H_{o''}$, 4H) 7.42 (d, J = 8.3 Hz, H_o, 8H) 7.32 (d, J = 8.3 Hz, $H_{m''}$, 4H) 7.22 (d, J = 8.7 Hz, $H_{o'}$, 4H) 7.15 (s, $H_{8'}$, 2H) 7.11 (s, $H_{7'}$, 2H) 7.00 (d, J = 8.7 Hz, $H_{m'}$, 4H) 6.23 (d, J = 8.3 Hz, H_m, 8H) 5.09 (s, $H_{11'}$, 4H) 4.31 (s, $H_{12'}$, 4H) 4.02-3.75 (m, H_α, H_β, H_γ, H_δ, H_ε, 40H) 2.65-2.55 (2q, J = 6.8 Hz, $H_{9'}$, 8H) 1.48 (s, H_{tBu1}, 36H) 1.44 (s, H_{tBu1}, 36H) 1.41 (s, H_{tBu2}, 36H) 1.17 (s, H_{tBu2} 36H) 0.87 (t, J = 6.8 Hz, $H_{10'}$, 12H) ppm

MS *(ES)*: *m/z* (%) = 2418.543 (100) [**42**]$^{2+}$ (calcd 2418.579)

UV/vis: λ_{max} (ϵ in L.mol^{-1}.cm^{-1}) in dichloromethane: 438 (5.75 x 10^5), 535 (6.76 x 10^4), 705 (1.78 x 10^4)

Metallated [3]rotaxane **(44)**:
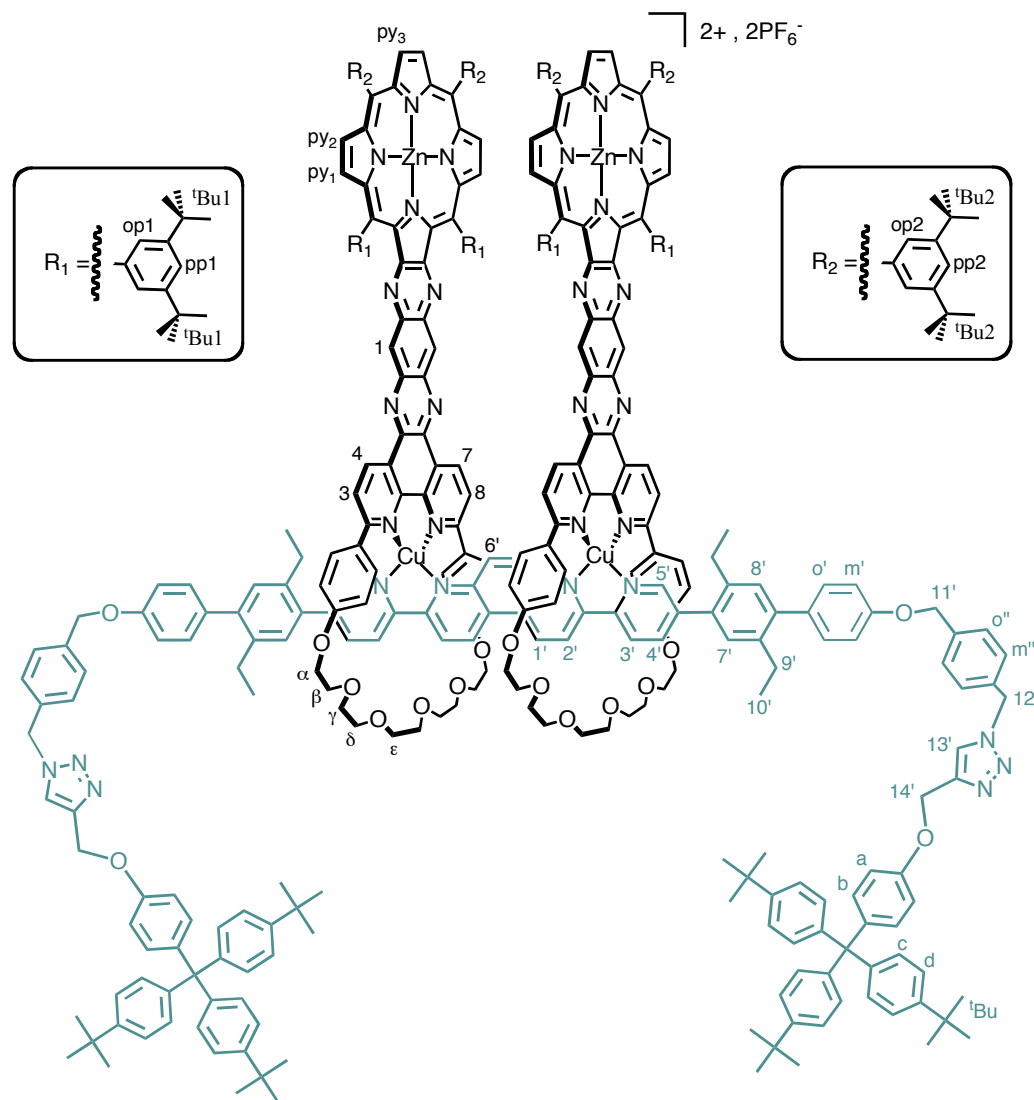
A 5 mL Schlenk flask was loaded under argon with [3]pseudorotaxane **42** (100 mg, 1.95 x 10^{-5}), alkyne stopper **43** (32 mg, 5.85 x 10^{-5} mol), Na$_2$CO$_3$ (1 mg, 0.97 x 10^{-5} mol) and [Cu(MeCN)$_4$]PF$_6$ (14.6mg, 3.92 x 10^{-5} mol). 1.8 mL of freshly distilled and degassed CH$_2$Cl$_2$ and 0.2 mL of degassed MeCN were added as solvents. The mixture was then left stirring, under argon, at room temperature and in the absence of light for 3 days. The solvents were then evaporated and the remaining solid dissolved again in CH$_2$Cl$_2$ and washed with H$_2$O. After several column chromatographies on silica (CH$_2$Cl$_2$/MeOH 99:1), the pure rotaxane **44** was obtained in 55% yield.

^{1}H-NMR: (500 MHz, CD$_2$Cl$_2$, COESY, ROESY, 25 ^{0}C): δ = 9.88 (d, J = 8.0 Hz, H$_4$,H$_7$, 4H) 9.75 (d, J = 9.0 Hz, H$_{1'}$, 2H) 8.90 (s, H$_{py3}$, 4H) 8.89 (d, H$_{2'}$, 2H) 8.69 (d, J = 8.7 Hz, H$_{3'}$, 2H) 8.78 (d, J = 4.4 Hz, H$_{py1}$, 4H) 8.67 (s, H$_1$, 4H) 8.63 (d, J = 4.4 Hz, H$_{py2}$, 4H) 8.21 (d, J = 8.0 Hz, H$_3$,H$_8$, 4H) 8.14 (bs, H$_{5'}$, 2H) 8.13 (d, J = 8.7 Hz, H$_{4'}$,

156

2H) 7.95 (t, H_{op1}, 4H) 7.90 (t, H_{op1}, 4H) 7.84 (bd, H_{pp2} + H_{op2}, 8H) 7.76 (bd, H_{op2} + H_{pp1}, 8H) 7.72 (bs, $H_{6'}$, 2H) 7.68 (s, $H_{13'}$, 2H) 7.43 (d, J = 8.3 Hz, $H_{o''}$, 4H) 7.40 (d, J = 8.3 Hz, H_o, 8H) 7.28 (d, J = 8.2 Hz, $H_{m''}$, 4H) 7.21 (d, J = 8.7 Hz, H_d, 12H) 7.19 (d, J = 8.9 Hz, $H_{o'}$, 4H) 7.13 (s, $H_{8'}$, 2H) 7.12 (d, J = 8.9 Hz, H_b, 4H) 7.08 (d, J = 8.7 Hz, H_c, 12H) 7.08 (s, $H_{7'}$, 2H) 6.97 (d, J = 8.9 Hz, $H_{m'}$, 4H) 6.80 (d, ^{3}J = 8.9 Hz, H_a, 4H) 6.21 (d, J = 8.3 Hz, H_m, 8H) 5.51 (s, $H_{12'}$, 4H) 5.07 (s, $H_{14'}$, 4H) 5.05 (s, $H_{11'}$, 4H) 3.98-3.73 (m, H_α, H_β, H_γ, H_δ, H_ε, 40H) 2.62-2.53 (2q, J = 7.3 Hz, $H_{9'}$, 8H) 1.46 (s, H_{tBu1}, 36H) 1.42 (s, H_{tBu1}, 36H) 1.39 (s, H_{tBu2}, 36H) 1.23 (s, H_{tBu}, 54H) 1.14 (s, H_{tBu2}, 36H) 1.12-1.07 (2t, J = 7.3 Hz, $H_{10'}$, 12H) ppm.

MS (ES): m/z (%) = 1975.2829 (100) $[44 + H]^{3+}$ (calcd 1975.2911) and 2961.9201 $[44]^{2+}$ (calcd 2961.9318)

UV/vis: λ_{max} (ε in L.mol^{-1}.cm^{-1}) in toluene: 440 (6.76 x 10^5), 536 (4.93 x 10^4)

Demetallated [3]rotaxane **(45)**:
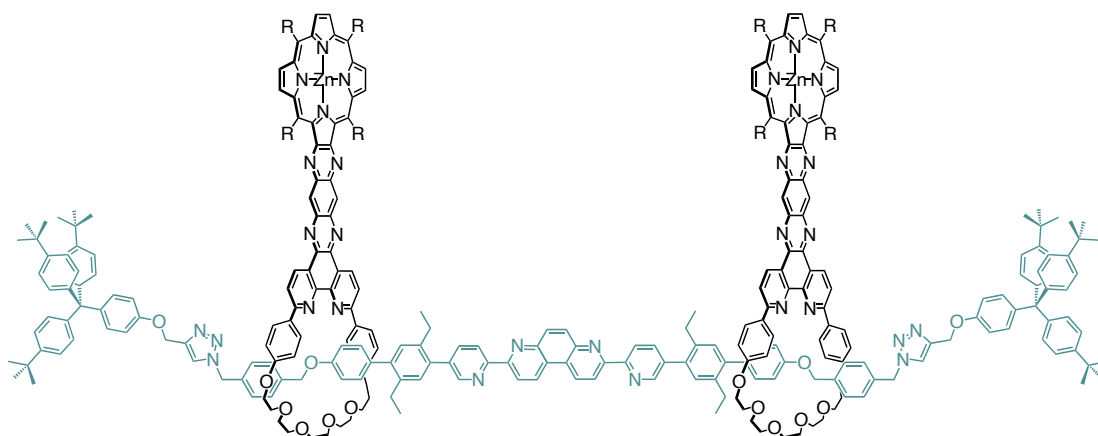
Metallated [3]rotaxane **44** (50 mg, 8.05 x 10^{-5} mol) was dissolved in a 2:1:1 mixture of CH$_2$Cl$_2$/MeCN/H$_2$O (30 mL). Then ~50 eq. KCN (26.2 mg, 4.02 x 10^{-3} mol) were added and the reaction mixture was vigorously stirred during 1 hour. The solution is then extracted with CH$_2$Cl$_2$ and water; the organic layers were separated and evaporated to dryness. The crude product is then filtered over silica (CH$_2$Cl$_2$/MeOH 99/1) to give demetallated rotaxane **45** in 95% yield.

^{1}H-NMR: impossible (even at low and high temperatures) due to slow conformational changes – *see* DOSY experiments.

MS (ES): m/z =

1933.6617	$[45+3H]^{3+}$	(calcd 1933.6770)
1940.9887	$[45+2H+Na]^{3+}$	(calcd 1941.0043)
1948.3159	$[45+H+2Na]^{3+}$	(calcd 1948.3316)
1450.5092	$[45+4H]^{4+}$	(calcd 1950.5096)
1455.7549	$[45+3H+Na]^{4+}$	(calcd 1455.7557)
1461.2512	$[45+2H+2Na]^{4+}$	(calcd 1461.2511)

UV/vis: λ_{max} (ε in L.mol^{-1}.cm^{-1}) in dichloromethane: 437 (5.01 x 10^5), 518 (6.92 x 10^4), 672 (1.70 x 10^4)

1,10-di-4-pyridyldecane "guest" **(46)**:
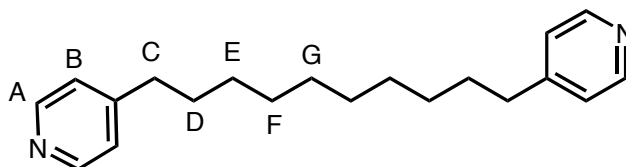
A 50 mL three-necked round bottom flask was loaded with picoline 2 g (21.4 mmol) and 10 mL of freshly distilled THF. The solution was then cooled down to -78°C (dry ice/acetone bath) and 14,6 mL of n-BuLi in hexane (1,6 mol/L, 23,5 mmol) were slowly added, keeping the temperature below -60°C. The orange solution was allowed to warm up to warm temperature. The now yellow solution is then heated up to 40°C for 40 min., 7 mL of distilled THF are added, and it is cooled down to -78°C again. The 1,8-dibromooctane is then added slowly to the solution, which is then allowed to warm up to room temperature. 15 mL of water are added and the organic and aqueous layers are separated. The aqueous layer is extracted with 3 x 25 mL of ET_2O and all the organic layers are combined, washed with 25mL of H_2O and dried on $MgSO_4$. After evaporating the solvents we obtain a yellow oil which solidifies once dried on the vacuum pump. After column chromatography on silica (DCM/MeOH , 99/1) the pure compound is obtained in 43% yield.

^{1}H-NMR (400 MHz, CD_2Cl_2, 25 ^{0}C): δ = 8.44 (d, J = 6.3 Hz, H_A, 4H) 7.09 (d, J = 6.3 Hz, H_B, 4H) 2.57 (t, J = 7.3 Hz, H_C, 4H) 1.60 (q, J = 7.4 Hz, H_D, 4H) 1.30 (m, H_E, H_F, H_G, 12H) ppm

^{13}C NMR (400 MHz, CD_2Cl_2, 25 ^{0}C): 149.46 / 123.72 / 35.03 / 30.23 / 29.35 / 29.25 / 29.05 ppm

MS (ES): *m/z* (%) = 297.2470 (100) [**46** + H]$^{+}$ (calcd: 297.2325)

UV/vis: λ_{max} (ε in L.mol^{-1}.cm^{-1}) in dichloromethane: 256 (3.8 x 10^{4})

*5,5 "-dibromoterpyridine **(48)** :*
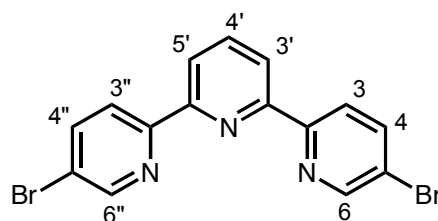
2,6 diiodopyridine **47** (1.92 g, 5.8 mmol) and 5-bromo 2-stannylpyridine **6** (3.72 g, 11.6 mmol) were dissolved in 100 mL of toluene. The solution was degassed (3 times vacuum/argon) and palladium triphenylphosphine (340 mg, 0.295 mmol, 5% mol)

was added. The solution was degassed once more and then brought to reflux (111°C) for 22h hours. After evaporation of the solvents, the crude product was purified by chromatography (alumina, pentane/ethyl acetate from 100/0 to 70/30 ratio). After additional recristalisation with dichloromethane and ethanol compound **48** was finally obtained pure in 50% yield.

^{1}H-NMR (300 MHz, CDCl$_3$, 25 ^{0}C): δ = 8.74 (dd, J$_1$ = 0.54 Hz, J$_2$ = 2.4 Hz, H$_{6-6"}$ 2H) 8.47 (dd, J$_1$ = 8.58 Hz, J$_2$ = 0.72 Hz, H$_{3-3"}$,2H) 8.41 (d, , J = 7.89 Hz, H$_{3'-5'}$, 2H) 7.96 (dd , J$_1$ = 8.4 Hz, J$_2$ = 2.37 Hz,H$_{4-4"}$, 2H) 7.93 (t, J = 7.68 Hz, H$_{4'}$, 1H) ppm

5-bromo, 5''-(4-methoxyphenyl)-terpyridine **(50)**:
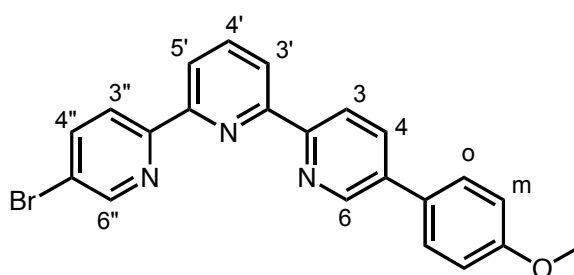
5,5″ dibromoterpyridine **48** (476 mg, 1.22 mmol), 4-methoxyphenylboronic acid **49** (185 mg, 1.22 mmol) and sodium carbonate (1.28 g, 12.22 mmol) were added with 60 ml of toluene to a 250 mL round bottomed two necked flask. 10 ml of ethanol were added to help dissolving the boronic acid. The solution was degassed (3 times vacuum/argon). After addition of 20 ml of water, the solution was degassed again before Palladium tetratriphenylposphine (71.4 mg, 5% mol) was added. After degassing a third time, this solution was brought to reflux and stirred under argon for 3h. Then the solvent was evaporated and the crude product was purified by column chromatography (alumina, pentane (100%) to ethyl acetate (100%). 188 mg of a white powder were obtained in 37% yield.

^{1}H-NMR (300 MHz, CDCl$_3$, 25 ^{0}C): δ = 8.92 (dd, J$_1$ = 1.65 Hz, J$_2$ = 0.9 Hz, H$_6$ 1H) 8.75 (dd, J$_1$ = 2.4 Hz, J$_2$ = 0.57 Hz, H$_{6"}$ 1H) 8.62 (dd, J$_1$ = 8.22 Hz, J$_2$ = 0.72 Hz, H$_3$ 1H) 8.55 (dd, J$_1$ = 8.58 Hz, J$_2$ = 0.72 Hz, H$_{3"}$ 1H) 8.49 (dd, J$_1$ = 7.86 Hz, J$_2$ = 1.08 Hz, H$_{3'}$ 1H) 8.42 (dd, J$_1$ = 7.68 Hz, J$_2$ = 0.9 Hz, H$_{5'}$ 1H) 8.01 (dd, J$_1$ = 8.43 Hz, J$_2$ = 2.4 Hz, H$_4$ 1H) 7.98 (dd, J$_1$ = 8.58 Hz, J$_2$ = 2.58 Hz, H$_{4"}$ 1H) 7.97 (t, J = 7.89 Hz, H$_{4'}$ 1H) 7.60 (d, J = 8.94 Hz, H$_o$, 2H) 7.04(d, J = 8.79 Hz, H$_m$, 2H) 3.89 (s, -O-CH$_3$, 3H) ppm

MS (ES): *m/z* (%) = 418.061 (100) [**50** + H]$^+$ (calcd: 418.055)

5-(4-trimethylsilylphenyl), 5"(4-methoxyphenyl)-terpyridine **(52)**:
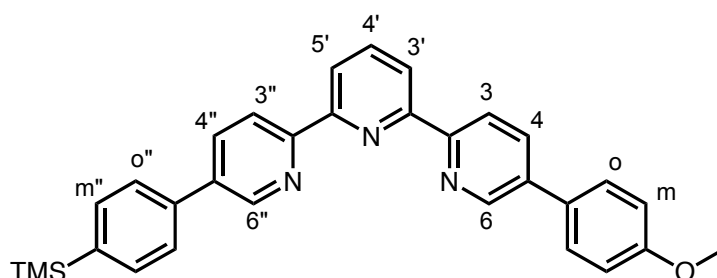
A solution of 5-bromo, 5"(4-methoxyphenyl)-terpyridine **50** (112 mg, 2.92 x 10^{-4} mol) trimethylsilyl)phenylboronic **51** (68 mg, 3.5 x 10^{-4} mol), sodium carbonate (309 mg, 2.92 x 10^{-3}), in toluene (60 mL), EtOH (10 ml) and water (20 mL) was degassed (3 times vacuum/argon) before palladium tetratriphenylphosphine (34 mg, 10% mol) was added. The solution was the heated to 120°c (reflux) under argon and stirred for 22h. After adding 17 mg of catalyst the solution was heated for another 3h, before evaporating the solvent. The crude product was filtered on alumina with ethyl acetate. Further purification was carried out by washing the product with pentane on millipore filter to finally obtain the pure product in 70% yield.

^{1}H-NMR (300 MHz, CDCl$_3$, 25 ^{0}C): δ = 8.97 (m, H$_{6"}$ 1H) 8.91 (m, H$_6$,1H) 8.72 (d, J = 8.49 Hz, H$_{3"}$, 1H) 8.69 (d, J = 8.49 Hz, H$_3$, 1H) 8.47 (d, J = 7.89 Hz, H$_{3'}$,H$_{5'}$, 2H) 8.08 (dd, J$_1$ = 8.25 Hz, J$_2$ = 2.4 Hz, H$_{4"}$, 1H) 8.03 (dd, J$_1$ = 8.25 Hz, J$_2$ = 2.4 Hz, H$_4$, 1H) 7.99(t, J = 7.86 Hz, H$_{4'}$, 1H) 7.67 (s, H$_{o"}$,H$_{m"}$, 4H) 7.61 (d, J = 8.97 Hz, H$_o$, 2H) 7.04 (d, J = 8.76 Hz, H$_m$ 2H) 3.89 (s,-O-CH$_3$, 3H) 0.37 (s, -Si-(CH$_3$)$_3$, 9H) ppm

MS (ES): *m/z* (%) = 488.204 (100) [**52**+ H]$^{+}$ (calcd: 488.215)

5(4-iodophenyl),5"(4-methoxyphenyl)-terpyridine **(53)** :
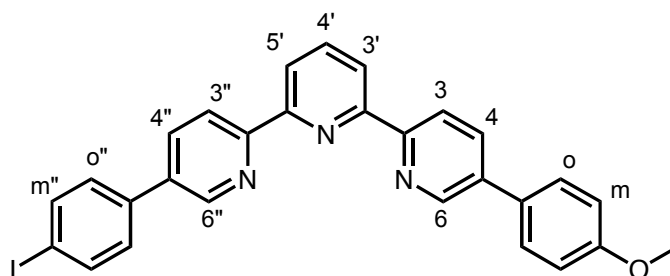
A solution of 5(4-trimethylsilylphenyl),5"(4-methoxyphenyl)-terpyridine **52** (45 mg, 9.24 x 10^{-5} mol) in 25 mL dichloromethane was degassed (3 times vacuum/argon) and cooled down to -10°C. 2 mL of a 0.23 M solution of ICl/CH$_2$Cl$_2$ were added and the solution allowed to warm up to room temperature. After 4h, the reaction was quenched by a saturated solution of Na$_2$S$_2$ O$_5$ (50 mL). After adding another 50 mL of water, the product was extracted with chloroform (2 x 100 mL). The organic layers

were collected and washed with water (150 mL). After evaporation of the solvents, terpyridine **53** was obtained in 84% yield.

^{1}H-NMR (300 MHz, CDCl$_3$, 25 ^{0}C): δ = 8.90 (m, H$_6$, H$_{6''}$ 2H) 8.70 (2dd, J$_1$ = 8.43 Hz, J$_2$ = 0.72 Hz, H$_3$, H$_{3''}$, 2H) 8.48 (m,H$_{3'}$,H$_{5'}$, 2H) 8.03 (m,H$_4$,H$_{4''}$, 2H) 7.99 (t, J = 7.86 Hz, H$_{4'}$,1H) 8.39(d, J = 8.94 Hz, H$_{m''}$, 2H) 7.61 (d, J = 8.94 Hz, H$_o$, 2H) 7.40 (d, J = 8.61 Hz, H$_{o''}$, 2H) 7.04 (d, J = 8.94 Hz, H$_m$ 2H) 3.89 (s,-O-CH$_3$, 3H) ppm
MS (ES): *m/z* (%) = 542.0823 (100) [**53**+ H]$^+$ (calcd: 542.0729)

5-(4-hexamethylstanyl), 5'' (4-methoxyphenyl)-terpyridine **(54)**:
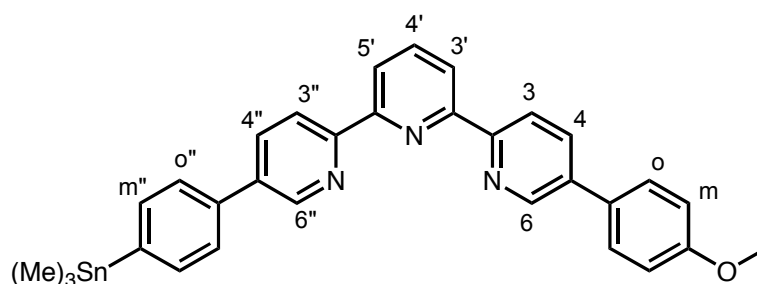
5-(4-iodophenyl),5''(4-methoxyphenyl)-terpyridine **53** (66 mg, 1.22x10^{-4} mol)   and hexamethylditin (90 mg, 2.75x10^{-4} mol) were dissolved in 14 mL of freshly distilled toluene. Then the solution was the degassed (3x vacuum/argon) and Pd(PPh$_3$)$_4$ (17 mg, 1.47x10^{-5} mol) was added. The solution was degassed once more and then heated up to 120°C for 6 h. After the first 2 and 4 hours, more catalyst was added, (+/- 5 mg). After another 6 hours reaction time, the solvent was evaporated and the crude product purified on a quick column (alumina, pentane/ethyl acetate). The white product **54** was recovered in 72% yield.
^{1}H-NMR (300 MHz, CDCl$_3$, 25 ^{0}C): δ = 8.94 (d, J = 1.54, H$_6$, 1H) δ = 8.91 (d, J = 1.54 Hz, H$_{6''}$, 1H) 8.71 (dd, J$_1$ = 8.46 Hz, J$_2$ = 0.72 Hz, H$_3$, 1H) 8.67 (dd, J$_1$ = 8.46 Hz, J$_2$ = 0.72 Hz, H$_{3''}$, 1H) 8.48 (d, J =7.86 Hz, H$_{3'}$,H$_{5'}$, 2H) 8.06 (dd, J$_1$ = 8.26 Hz, J$_2$ = 2.36 Hz, H$_4$, 1H) 8.03 (dd, J$_1$ = 8.26 Hz, J$_2$ = 2.36 Hz, H$_{4''}$, 1H) 7.99 (t, J = 7.82 Hz, H$_{4'}$,1H) 7.66 (s, H$_{m''}$, H$_{o''}$, 4H) 7.63 (d, J = 8.82 Hz, H$_o$, 2H) 7.05 (d, J = 8.79 Hz, H$_m$, 2H) 3.89 (s,-O-CH$_3$, 3H) ppm
MS (ES): *m/z* (%) = 580.146 (100) [**54** + H]$^+$ (calcd: 580.141)

stannyl-thread **(55)**:
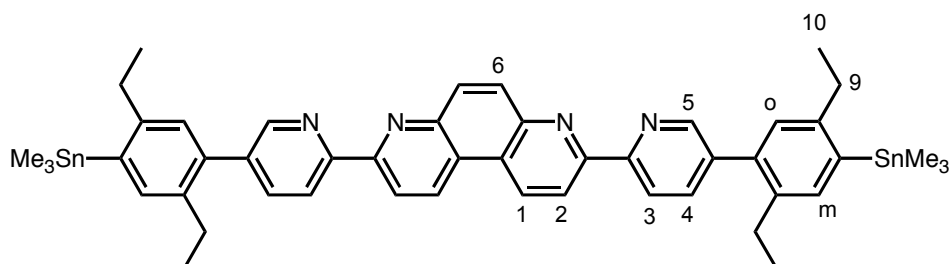
An oven-dried two-necked round-bottom flask was loaded under argon with iodo-thread **21** (85 mg, 6.8 x 10^{-5} mol) and hexamethylditin (148 mg, 4.2 x 10^{-4} mol) dissolved in 15 ml of toluene. The solution was then degassed and Pd(PPh$_3$)$_4$ (16 mg, 20 %) was added. After degassing the solution once more, the mixture was heated to 120°C and left under for 7 hours. A quick column chromatography on alumina (ethyl acetate / pentane 30:70) followed by a reprecipitation in Et$_2$O / MeOH gave the pure compound **55** in 60 % yield.

^{1}H-NMR (300 MHz, CDCl$_3$, 25 ^{0}C): δ = 9.11 (d, J = 8.9 Hz, H$_1$, 2H) δ = 8.85 (d, J = 8.4 Hz, H$_2$, 2H) 8.79 (dd, J$_1$ = 8.4 Hz, J$_2$ = 0.6 Hz, H$_3$, 2H) 8.72 (dd, J$_1$ = 2.2 Hz, J$_2$ = 0.6 Hz, H$_5$ 1H) 8.34 (2, H$_6$, 2H) 7.89 (dd, J$_1$ = 8.3 Hz, J$_2$ = 2.2 Hz, H$_4$, 2H) 7.40 (s, H$_m$, 2H) 7.16 (s, H$_o$, 2H) 2.71 and 2.66 (q, J = 7.7 Hz, H$_9$, 8H) 1.26 and 1.13 (t, J = 7.5 Hz, H$_{10}$, 12H)

MS (ES): *m/z* (%) = 925.2477 (100) [**55** + H]$^+$ (calcd: 925.2465)

Publications

Publications:

• *Nickel thiolate complexes as ligands for copper and zinc : Novel additions to a library of binding modes,* Johanna A.W. Verhagen, Christian Tock, Martin Lutz, Anthony L. Spek, and Elisabeth Bouwman, Eur. J. Inorg. Chem. 2006, 4800-4808

• *Copper(I)-induced threading of two bis-macrocycles on two rods : a cyclic[4]rotaxane,* Jean-Paul Collin, Julien Frey, Valérie Heitz, Efstathia Sakellariou, Jean-Pierre Sauvage and Christian Tock, New J. Chem. 2006, 30, 1386-1389

• *A [3]rotaxane acting as an adaptable receptor,* Julien Frey, Christian Tock, Jean-Paul Collin, Valérie Heitz, Jean-Pierre Sauvage (in press)

Presentations (conferences attended):

• Poster presentation at the *1ˢᵗ European Chemistry Congress* in Budapest (August 2006)

• Poster presentation at the *Reinhoudt workweek symposium* at the Institut de Science et d'Ingénierie Supramoléculaire (ISIS) in Strasburg (November 2005).

Discipline :   Chimie 42000 03

Présentée par : Tock Christian

Titre :   Multirotaxanes dynamiques
Vers une nano-presse pour mimer les chaperons moléculaires

Unité :   UMR: LC3 UMR7177

Nom :   LCOM, (Laboratoire de chimie organo-minérale)

Directeur de thèse :

Dr. Jean-Pierre Sauvage (D.R. CNRS)

Co-directeur de thèse :

Dr. Jean-Paul Collin (D.R. CNRS)

Localisation :   Laboratoire de Chimie Organo-Minérale
Institut Le Bel - 6ème Sud
4 rue Blaise Pascal
67070 STRASBOURG Cedex

en collaboration avec **Valérie Heitz** et **Julien Frey**

Introduction :

De nos jours, la nanotechnologie est un domaine en pleine expansion. Des chercheurs, dans le monde entier, ont relevé le défi de synthétiser des machines moléculaires. La nature a développé de nombreux dispositifs nanométriques effectuant des tâches spécifiques dans les organismes vivants et elle est souvent une excellente source d'inspiration. Bien évidemment nous sommes loin d'êtres capables de copier de tels systèmes très compliqués en les reproduisant en synthèse chimique. Mais on peut néanmoins essayer de copier et imiter certaines fonctions à l'aide de molécules plus simples.

Le sujet de thèse présenté ici est fondé sur de telles nanomachines naturelles : les chaperons moléculaires. Leur rôle dans les organismes est de capturer des protéines à l'intérieur d'une cavité et d'éviter ainsi leur agglomération. Les protéines ainsi isolées, peuvent alors se replier sur elles-mêmes afin d'atteindre leur structure tertiaire requise pour effectuer leurs tâches biologiques. Bien que l'information de la structure tertiaire soit inscrite dans la protéine même, les chaperons sont indispensables afin d'éviter les interactions entre les protéines. Une vision simplifiée permet de subdiviser l'activité des chaperons en trois parties : la capture, la compression et le relâchement des protéines.

Le système que nous proposons afin de modéliser ces fonctionnalités repose sur un axe à 4 stations coordinantes, deux bipyridines centrales et une terpyridines à chaque extrémité de l'axe (Figure 1). Sur cet axe seront enfilés des anneaux comportant une unité phénanthrolique qui sera liée aux bipyridines en présence de Cu(I) et aux terpyridines en présence de Cu(II). Effectivement, le complexe de Cu(I) est le plus stable sous forme tétracoordiné (donc 2 ligands bidentates) alors que le Cu(II) préfère des degrés de coordination plus élevés, 5 ou 6. (un ligand bidentate et un tridentate

par exemple). Une simple oxydation du Cu(I) en Cu(II) pourra nous permettre de déplacer les anneaux des unités bidentates centrales (position comprimé) vers les terpyridines tridentates externes (position relâchée). Le mouvement opposé se produira lors de la réduction de Cu(II) en Cu(I).
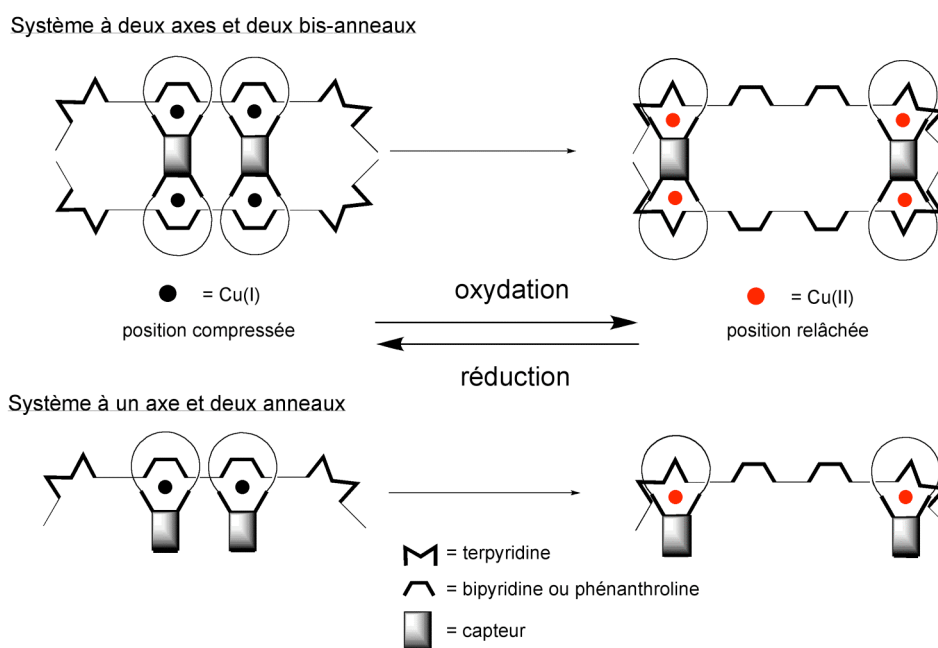
<u>Figure 1</u>

Afin d'assurer les fonctions simplifiées des chaperons, il est nécessaire d'adjoindre à ces anneaux des "capteurs", capables d'accueillir une molécule hôte. Un capteur possible est une porphyrine de Zn(II), qui comporte un cinquième site de coordination libre apical au niveau du Zn, ce site faisant office de point d'ancrage de la molécule hôte. Cette molécule intercalée entre deux porphyrines parallèles pourra alors être étirée ou compressée en oxydant ou en réduisant le Cu(I) ou le Cu(II) respectivement et en rapprochant ou en éloignant ainsi les deux anneaux sur l'axe. Une molécule hôte (invitée) rigide de taille adaptée à la position compressée sera, faute de flexibilité, éjectée lors d'un changement de distance entre les deux porphyrines. Les anneaux ou bis-anneaux présentés ici ont été synthétisés par Julien Frey dans le cadre d'une coopération interne au laboratoire.

Partie centrale, bis-bidentates

Dans une première étape, la partie centrale bis-bidentate, représentée en figure 2 a été synthétisée en 6 étapes. Une des caractéristiques importantes de cette molécule composée de cycles aromatiques est sa rigidité. Elle facilitera le glissement des anneaux sur l'axe et évitera des repliements conduisant à une gamme de positions possibles pour les anneaux. Cette rigidité de l'unité 4,7-phénathroline du milieu portant deux azotes du même côté assurera grâce à la complexation du Cu(I) une symétrie telle que les entités capteurs soient face à face.

R= TMS
R= OMe
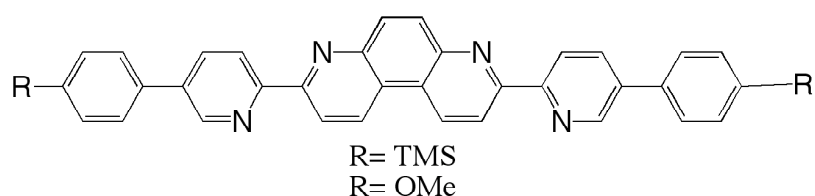
Figure 2

A partir de ce fragment, on a pu tester l'enfilage d'anneaux et de bis-anneaux sur la partie centrale de l'axe. L'obtention des pseudorotaxanes **1** et **2** représentés en figure 3, nous a démontré que les réactions d'enfilage étaient quantitatives.
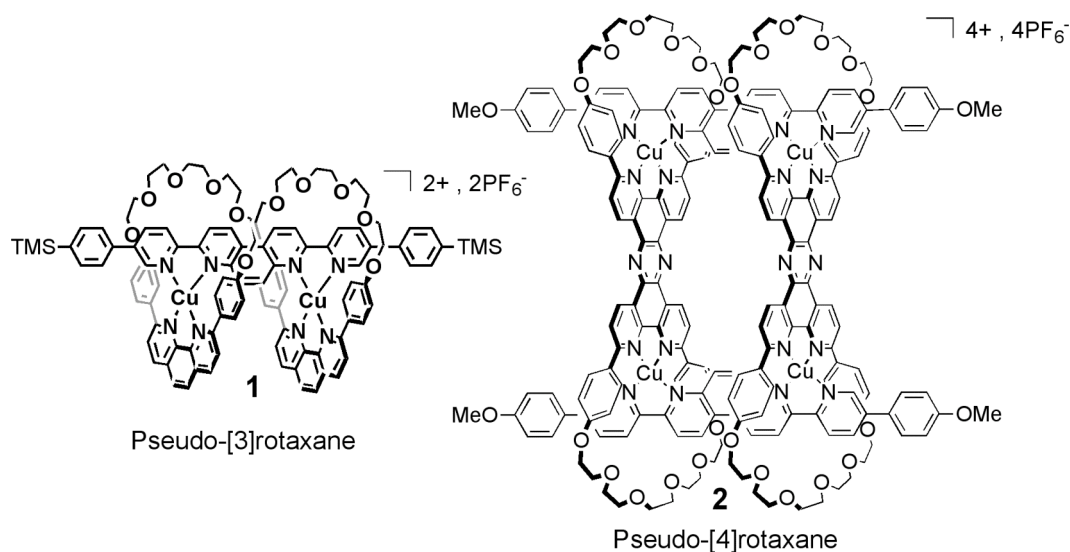
Figure 3

Pour passer d'un pseudo-rotaxane à un rotaxane, il faut faire en sorte que les anneaux ne puissent plus quitter l'axe, même si on démétalle les centres de coordination. Pour ce faire, des groupements suffisamment encombrants doivent être placés aux extrémités de l'axe. De tels bouchons permettront aux anneaux d'être assujettis aux axes par des liens purement mécaniques. Avant de fonctionnaliser l'axe aux extrémités soit par des bouchons, soit par les parties chélatantes tridentates, un problème majeur a du être résolu. En effet, l'insolubilité quasi totale de l'axe central a empêché toute réaction chimique de fonctionnalisation.

Ce problème a finalement été résolu en interposant deux groupements diéthyl-phénylène de part et d'autre de l'unité centrale. (Figure 4).
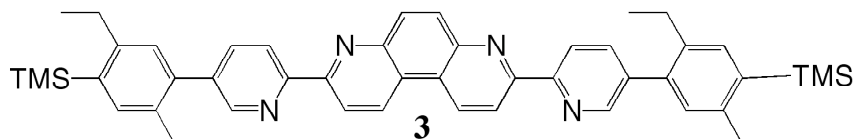
Figure 4

Les chaînes éthyles se sont avérées très efficaces pour augmenter considérablement la solubilité et des tests d'enfilage d'anneaux ont montré qu'ils n'empêchent pas les anneaux d'accéder aux stations bidentates centrales.

Rotaxanes

Cet axe moléculaire rendu ainsi soluble nous a permis de poursuivre les tentatives de bouchonnage. Dans un premier temps des réactions de Williamson entre un axe fonctionnalisé avec des phénols et des bouchons à terminaisons bromobenzyl furent un échec. La réaction de Williamson se faisant en milieu basique, les complexes de Cu(I) sont déstabilisés et les anneaux se désenfilent avant même que les bouchons soient greffés sur l'axe.
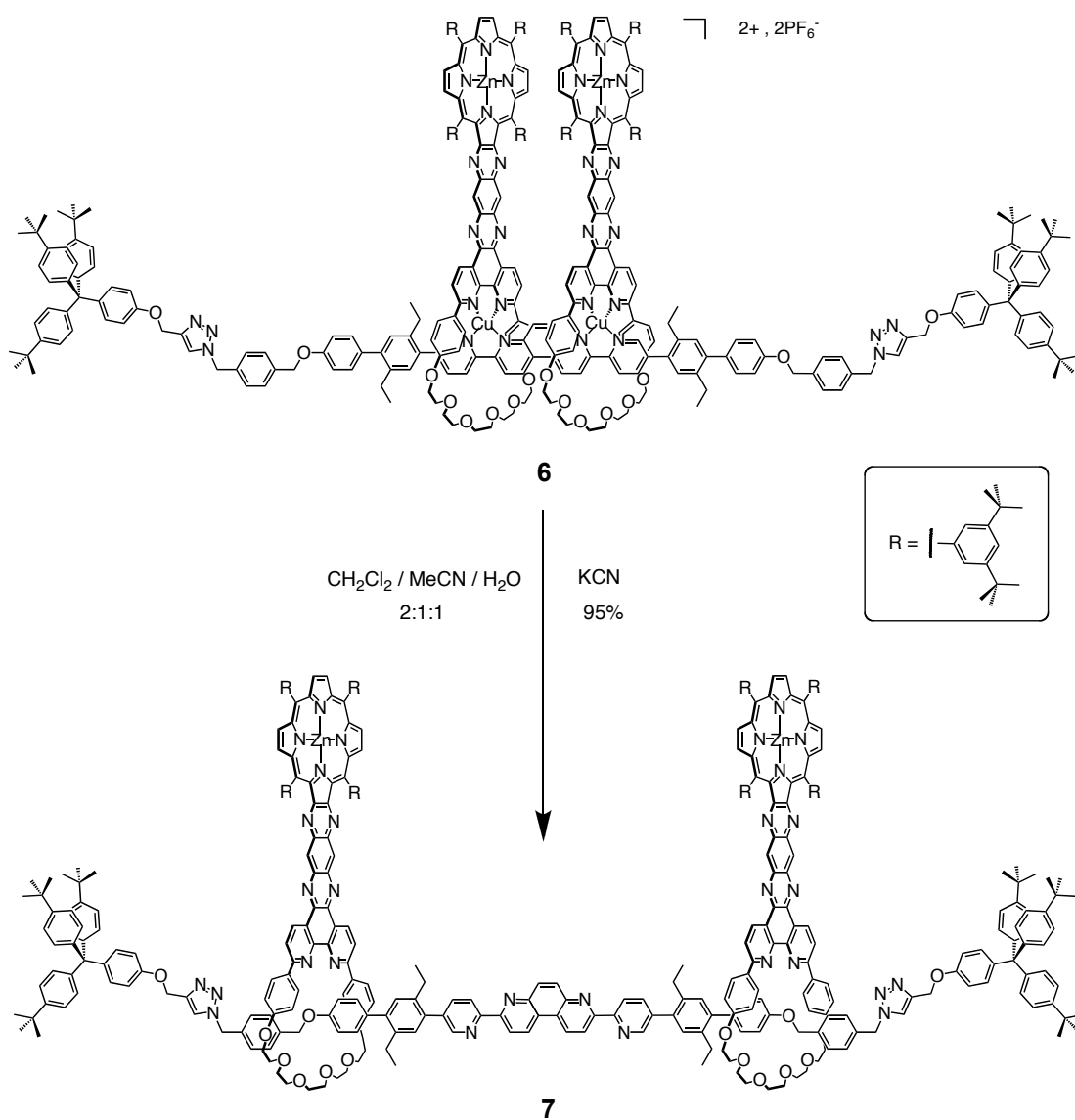
Figure 5

Une méthode chimique plus douce, la réaction de Huisgen a alors été choisie. Il s'agit d'une cycloaddition 1,3-dipolaire entre un alcyne et un azoture pour former un 1,2,3-triazole di-substitué. Ainsi nous avons synthétisé l'axe **4** à terminaisons azoture. Après enfilage des anneaux et réaction de Huisgen entre l'axe et les bouchons **5**, nous avons isolé et caractérisé le rotaxane mtallé **6** (figure 5) ainsi que la forme démétallé **7**. Ces deux systèmes ont été étudiés par ^{1}H-RMN (uniquement la molécule **6**), RMN-DOSY, CV, UV-vis et spéctrométrie de mass.

Ces deux molécules représentent un système de presse « simplifiée ». En effet le rotaxane métallé **6** peut être vu comme la situation comprimée de la presse et le rotaxane démétallé **7** représente une situation relaxée de la presse. Afin de tester ce système, une molécule invitée **8** a été synthétisée (figure 6). Elle comporte deux groupements pyridyls qui viendront se coordiner aux porphyrines de Zn(II). Ces deux ligands sont attachés en positions para par une chaîne alkyle C_{10}, qui est assez longue afin d'être comprimée et en même temps trop courte pour permettre à cette molécule invitée de se lier aux porphyrines autrement que par le mode interne - interne.

8
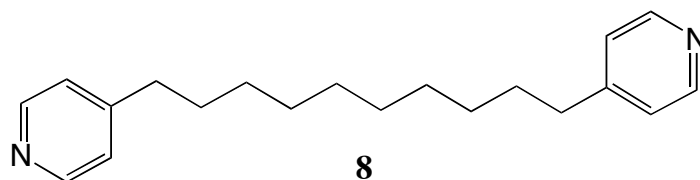
Figure 6

Les rotaxanes **6** et **7** ont ensuite étaient utilisés en combinaison avec la molécule invitée **8** aussi bien dans la chimie hôte – invité qu'en tant que presse (figure 7).

L'étude des interactions de **6** et **7** avec d'autres molécules invitées comme le DABCO, la 4,4'-bipyridine et le fullerène C60 sont actuellement en cours. Les constantes d'associations de tous ces complexes hôte – invité ont pu être déterminées par dosage UV-vis.
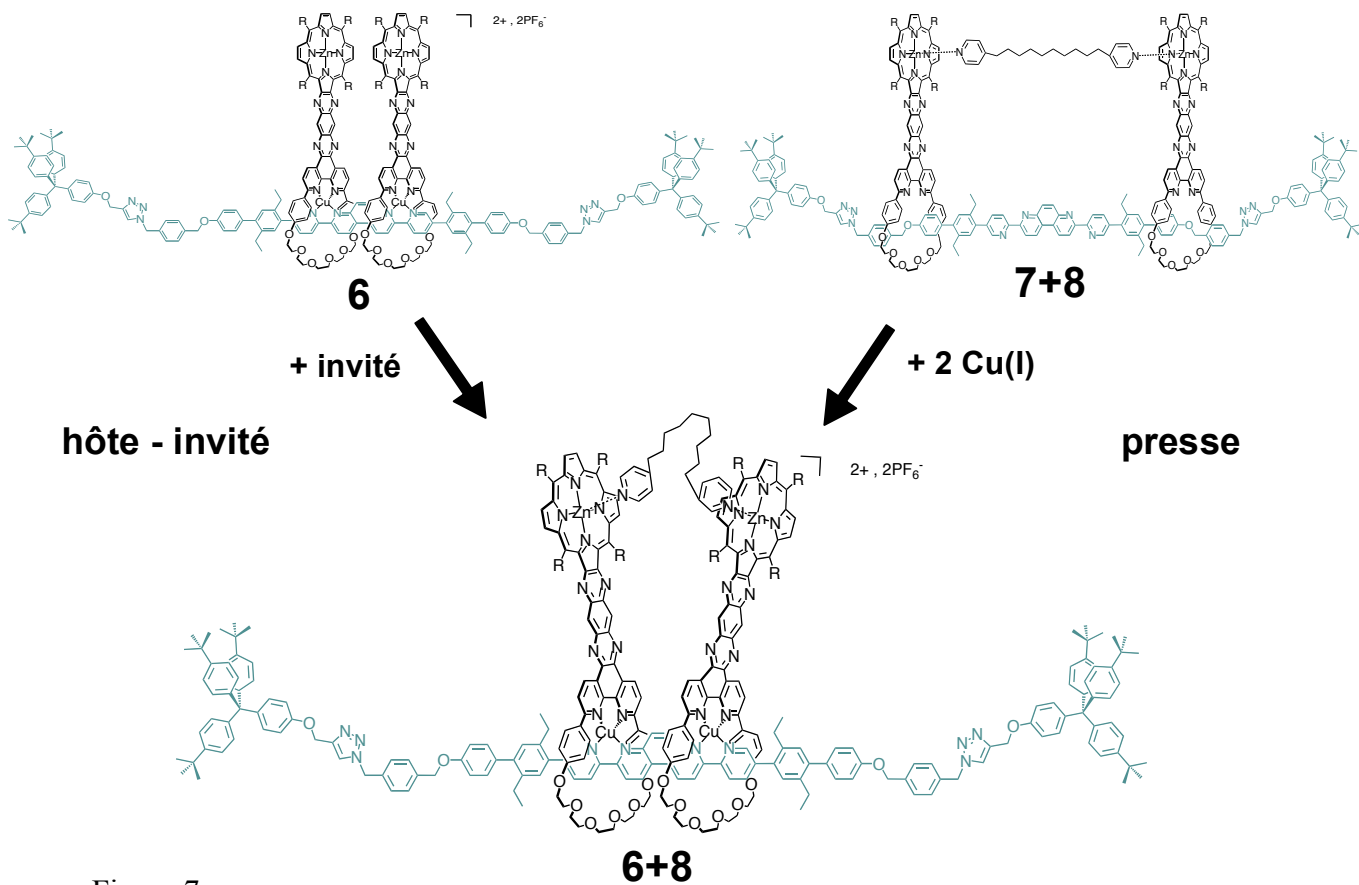
Figure 7

Caténane

Un caténane est une molécule constitué d'au moins deux anneaux entrelacés, et ainsi liés l'un à l'autre par des liens uniquement mécaniques. En partant de l'axe **9** qui est basé sur l'axe moléculaire **3** (figure 4), et des bis-anneaux déjà utilisés pour former de pseudorotaxane **2** (figure 3), nous avons pu synthétiser un tel caténane **10** (figure 8). Il s'agit d'un [3]-caténane comportant un grand anneau à 4 unités bidentates. Il a été formé après enfilage des 2 bis-anneaux sur deux axes moléculaires par Ring-Closing Metathesis (RCM) à l'aide d'un catalyseur de Grubbs de première génération.
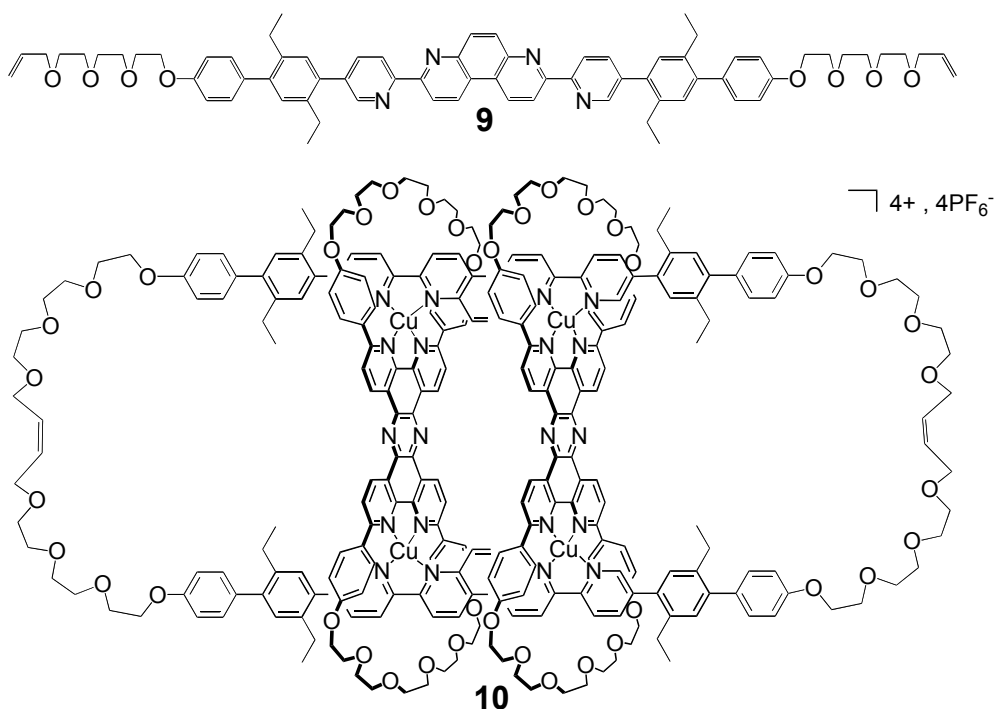
Ce caténane pourrait également servir de presse moléculaire en utilisant les interactions π-π des espaceurs entre les anneaux afin d'accueillir une molécule hôte. Cependant il constitue avant tout une nouvelle molécule à topologie non-triviale.

Axe à stations bi et tridentates

Nous avons essayé d'autre part de synthétiser un axe à deux stations bidentates centrales (bipyridines) et deux stations tridentates aux extrémités (terpyridines). À cet effet de nombreuses terpyridines représenteés en figure 9 ont été synthétisées. Jusqu'à ce jour, les tentatives de couplages avec l'axe central, soit par couplages de Suzuki ou de Stille, soit par réaction de Williamson ont conduit à des réactions partielles (bouchonnage à une seule extrémité) ou à des désenfilages des anneaux. D'autres

voies de synthèse, comme la formation d'amide ou d'ester sont actuellement étudiées afin de continuer ce projet.
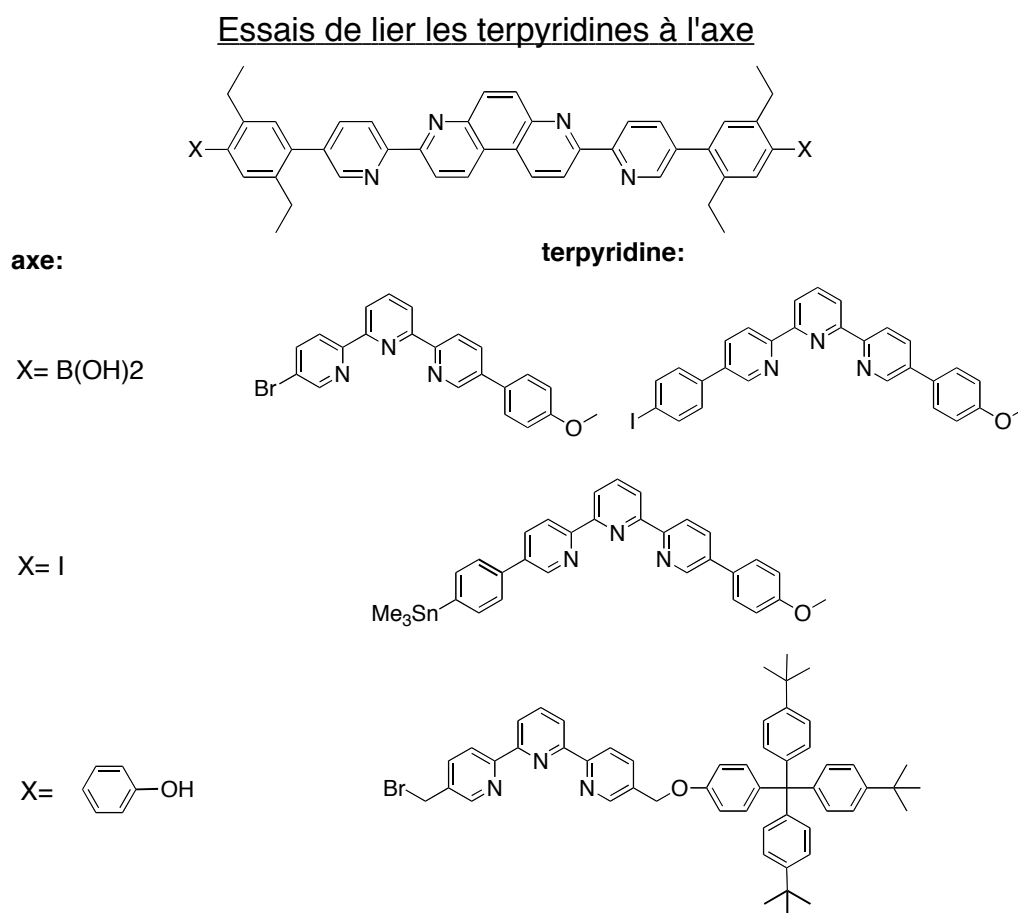
Figure 9

Conclusion

Nous avons synthétisé plusieurs axes à deux stations chélatantes, qui nous ont permis, en collaboration avec Julien Frey, d'obtenir des assemblages fonctionnellement et topologiquement intéressants. Des [3] et [4] rotaxanes et pseudo-rotaxanes ont pu être réalisés, ainsi qu'un [3] caténane basé sur deux bis-anneaux et deux axes bis-bidentates. Malheureusement l'axe à 4 stations n'a pas encore été synthétisé, mais nous restons confiant. Néanmoins, les rotaxanes **6** et **7** sont les prototypes d'une presse moléculaire qui a pu être exploitée en tant que telle en comprimant la molécule invitée **8**.

Index
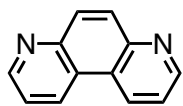
1
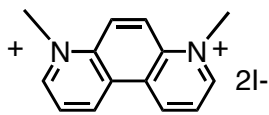
2
(CT 1)
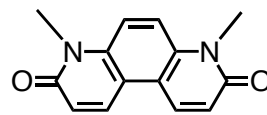
3
(CT 2)
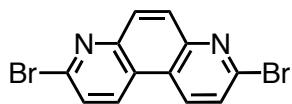
4
(CT 6)
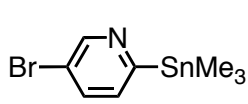
6
(CT 8)

7
(CT 9)

8
(CT 10)

9
(CT 23)

10
(CT 12)

12

13
(CT 24)

14
(CT 31)

16
(CT 45)

17
(CT 48)

18
(CT 49)

19
(CT 51)
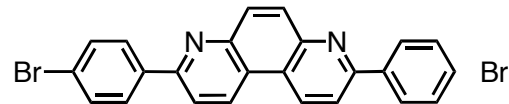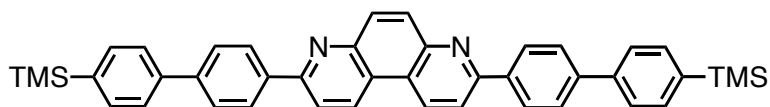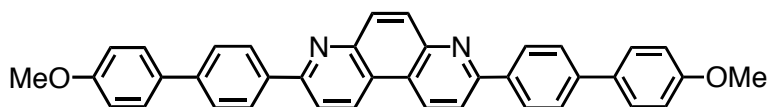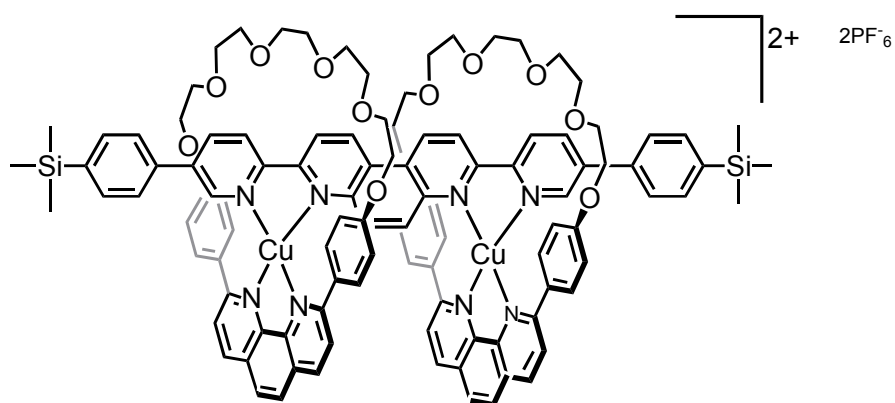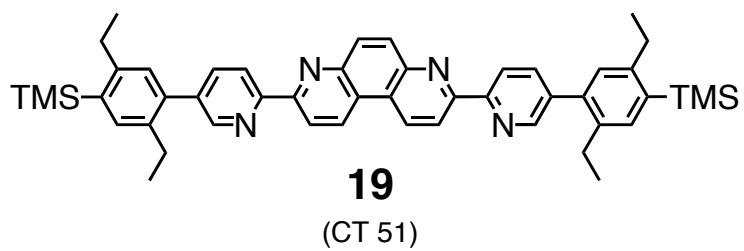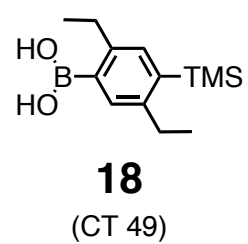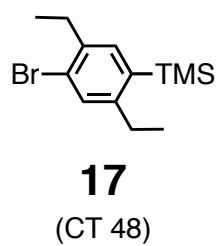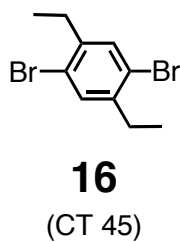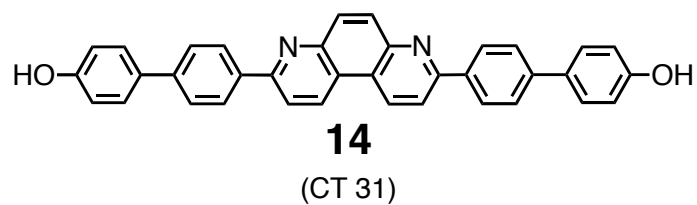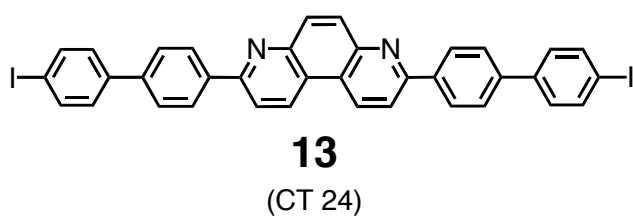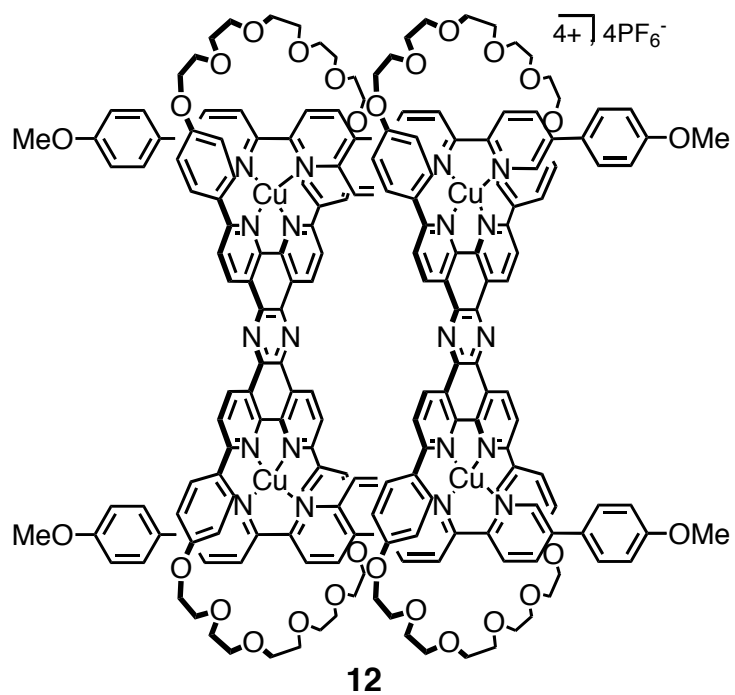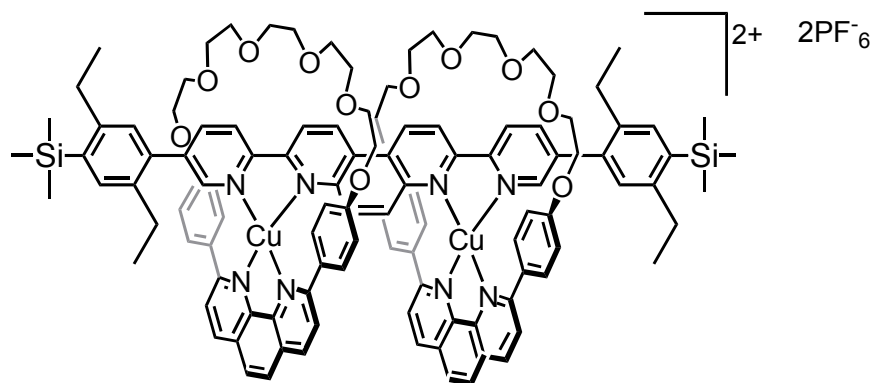
20

(CT 66)
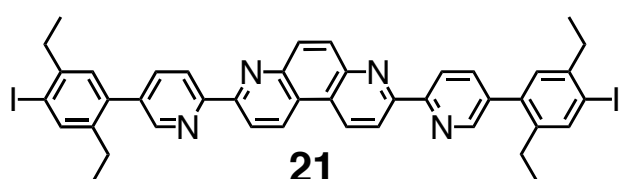
21

(CT 52)
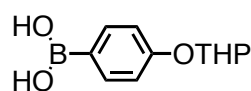
23

(CT 69)
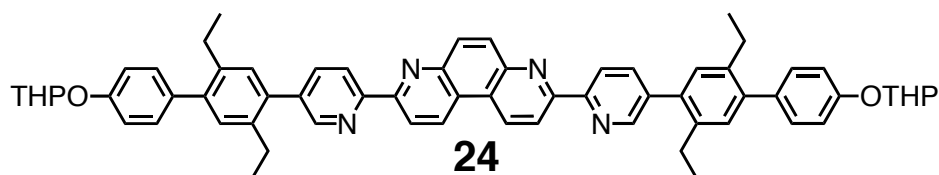
24

(CT 60)

25

(CT 62)

27

28

29

30

(CT 40)

177

31

32

(CT 71)

38

(CT 73)

40

(CT 75)

41

(CT 77)

2^+ , $2PF_6^-$

42

(CT 78)

179

44

(CT 79)

R =
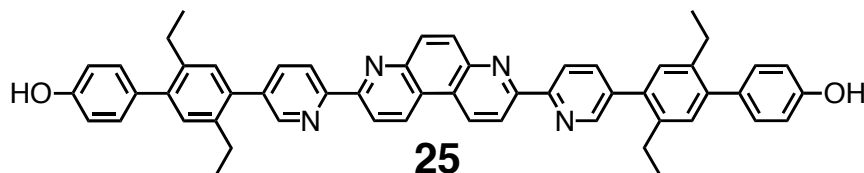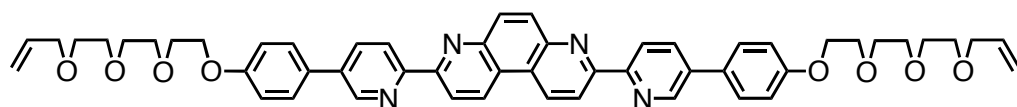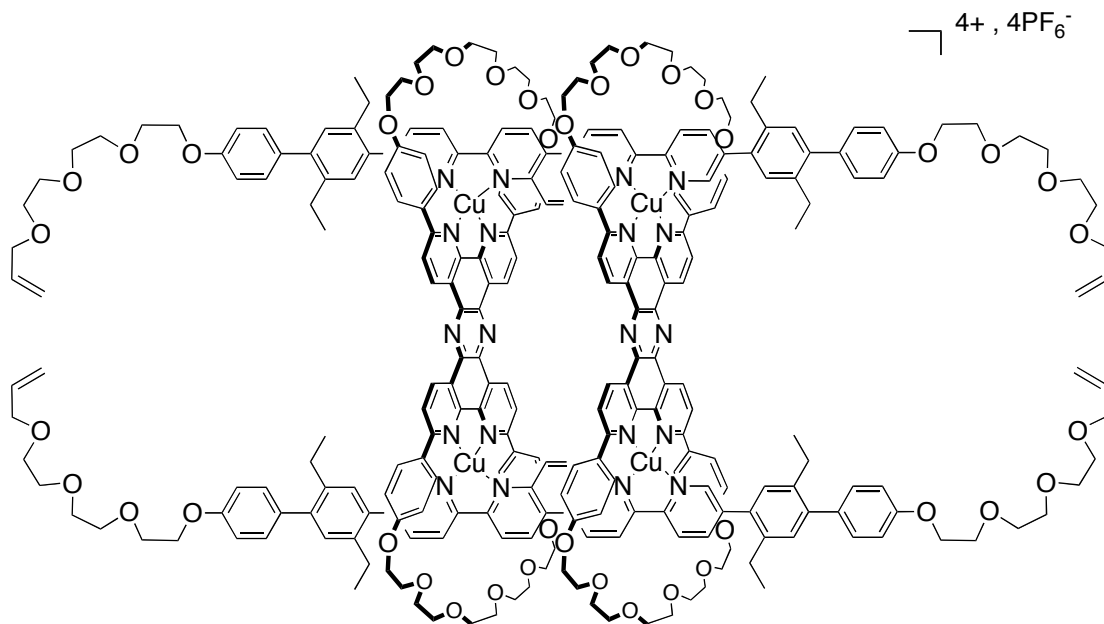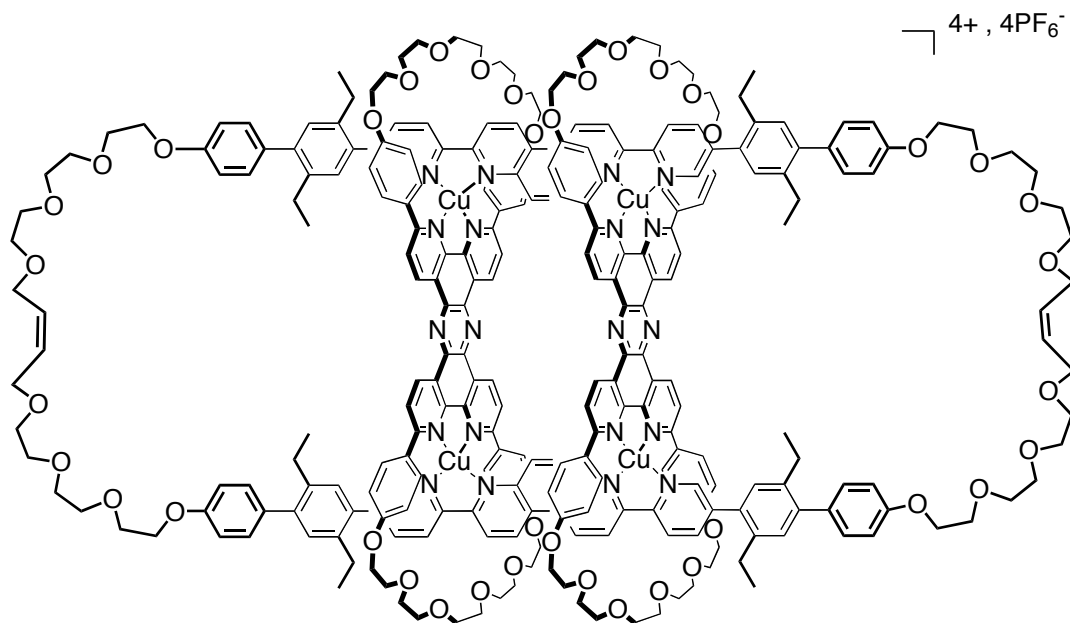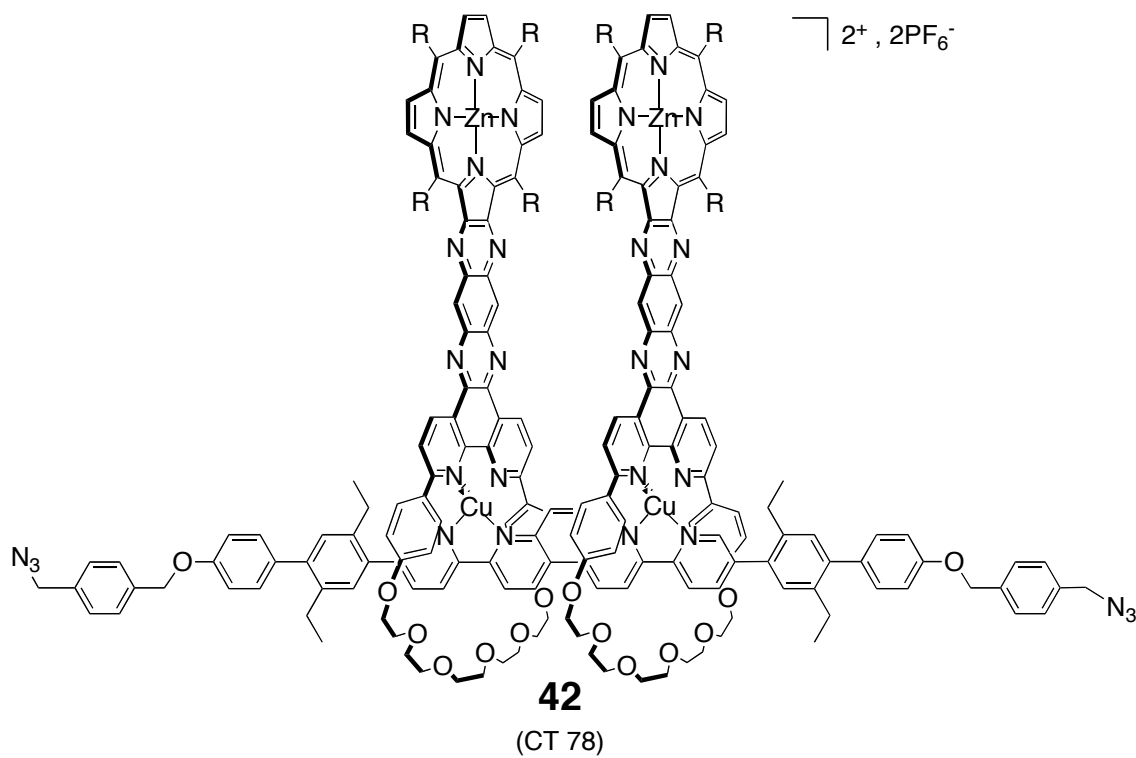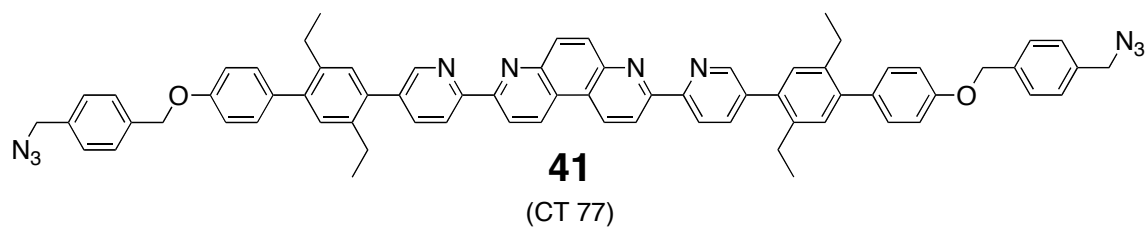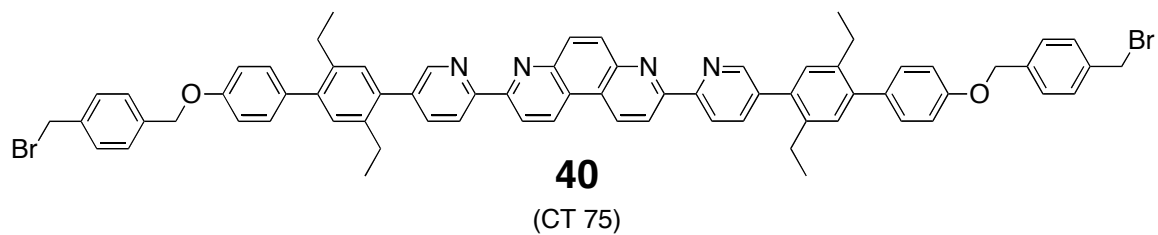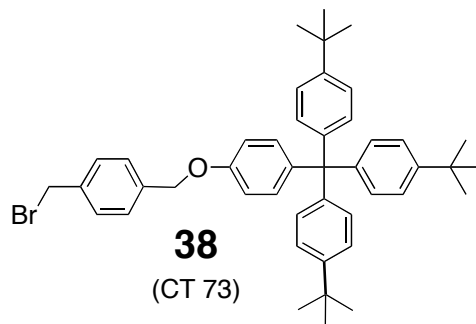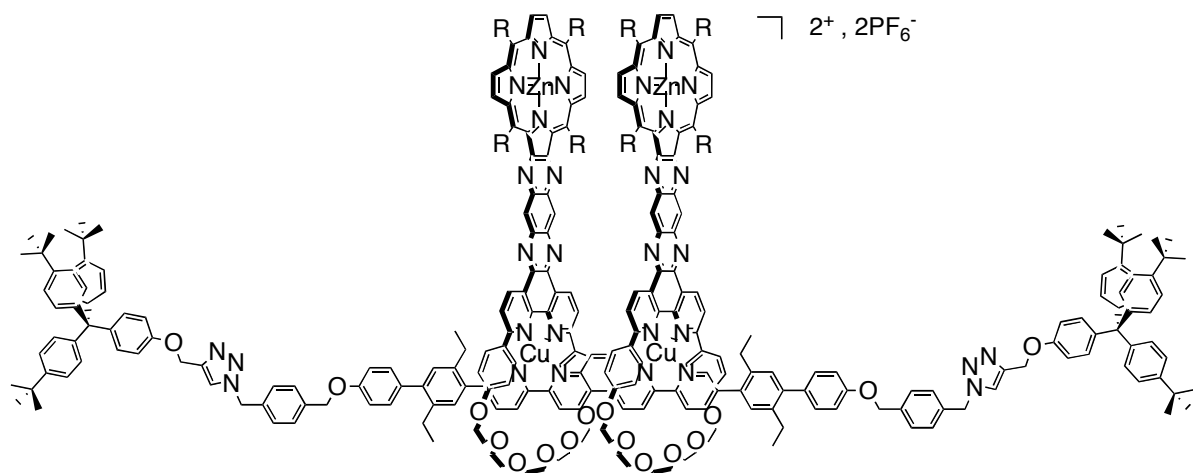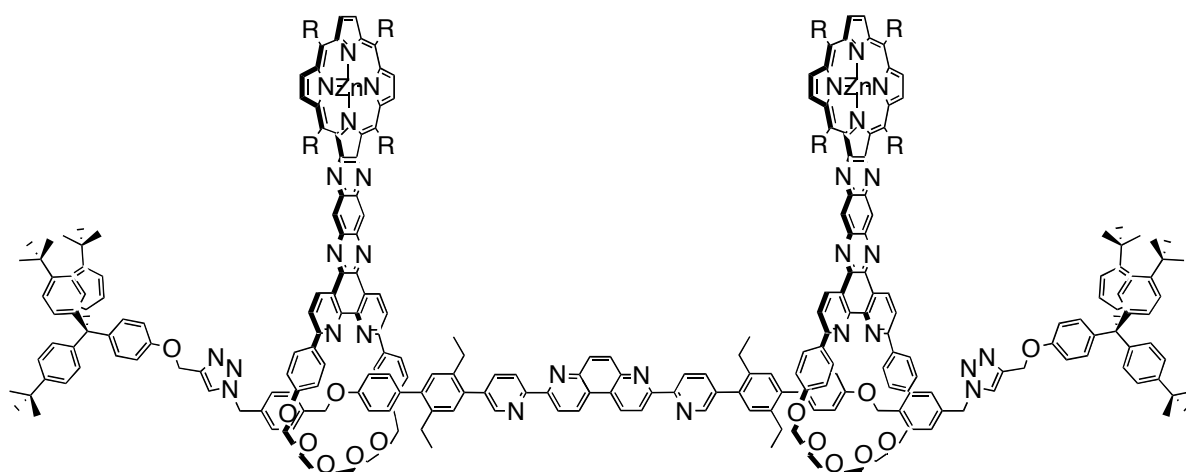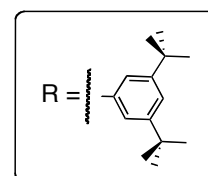
45
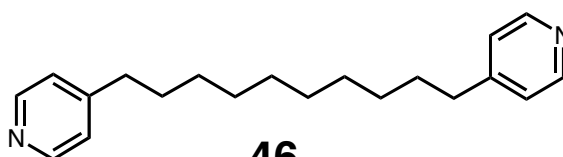
46

(CT 81)
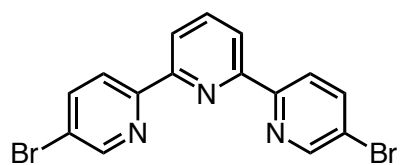
48

(CT 22)
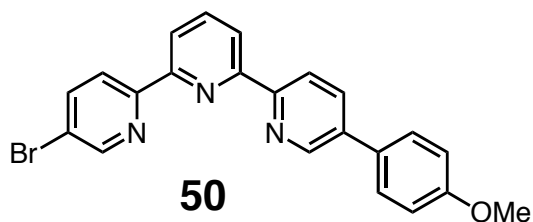
50

(CT 21)
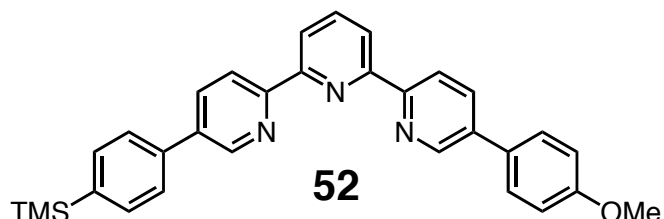
52

(CT 29)

53

(CT 36)

54

(CT 38)

55

(CT 53)